Developing a Person Guidance Module for Hospital Robots

By

Muhammad Kamrul Hasan

B.Sc., M.Sc.

This thesis is submitted in according with the requirements of
Dublin City University for the degree of
Doctor of Philosophy

Supervisor

Dr. Tamas Szecsi

School of Mechanical and Manufacturing Engineering
Faculty of Engineering and Computing
Dublin City University

September 2012

Declaration

I hereby certify that this material, which I now submit for assessment on the programme of study leading to the award of PhD in Engineering, is entirely my own work, that I have exercised reasonable care to ensure that the work is original, and does not to the best of my knowledge breach any law of copyright, and has not been taken from the work of others save and to the extent that such work has been cited and acknowledged within the text of my work.

Signed:
Muhammad Kamrul Hasan
ID No.: 54148294
Date: 10-10-2012

Abstract

This dissertation describes the design and implementation of the Person Guidance Module (PGM) that enables the IWARD (Intelligent Robot Swarm for attendance, Recognition, Cleaning and delivery) base robot to offer route guidance service to the patients or visitors inside the hospital arena. One of the common problems encountered in huge hospital buildings today is foreigners not being able to find their way around in the hospital. Although there are a variety of guide robots currently existing on the market and offering a wide range of guidance and related activities, they do not fit into the modular concept of the IWARD project. The PGM features a robust and foolproof non-hierarchical sensor fusion approach of an active RFID, stereovision and cricket mote sensor for guiding a patient to the X-ray room, or a visitor to a patient's ward in every possible scenario in a complex, dynamic and crowded hospital environment. Moreover, the speed of the robot can be adjusted automatically according to the pace of the follower for physical comfort using this system. Furthermore, the module performs these tasks in any unconstructed environment solely from a robot's onboard perceptual resources in order to limit the hardware installation costs and therefore the indoor setting support. Similar comprehensive solution in one single platform has remained elusive in existing literature. The finished module can be connected to any IWARD base robot using quick-change mechanical connections and standard electrical connections. The PGM module box is equipped with a Gumstix embedded computer for all module computing which is powered up automatically once the module box is inserted into the robot. In line with the general software architecture of the IWARD project, all software modules are developed as Orca2 components and cross-complied for Gumstix's XScale processor. To support standardized communication between different software components, Internet Communications Engine (Ice) has been used as middleware. Additionally, plug-and-play capabilities have been developed and incorporated so that swarm system is aware at all times of which robot is equipped with PGM. Finally, in several field trials in hospital environments, the person guidance module has shown its suitability for a challenging real-world application as well as the necessary user acceptance.

Publications Arising From This Work

Journal Paper

T. Szecsi, M. K. Hasan, K. A. Mamun, A. Islam, C. Griffin, M. Hoque. “Hospital Robot Development in the IWARD Project,” *VIMation Journal*, issue 1, pp.6-12, 2010.

Conference Papers

Mamun, K.A., Hasan, M.K.., Szecsi, T., (2010): Surveillance module, A Robotics Application in the Hospital environment. *In: Proceedings of 28th International Manufacturing Conference, Dublin, Ireland, pp. 272-279.*

Szecsi, T., Hasan, M.K., Mamun, K.A., Islam, A., Griffin, C., Hoque, M., (2010): Service Modules for Hospital Robots. *In T. Kennel, ed., Proceedings of the 12-th Mechatronics Forum Biennial International Conference (MECHATRONICS 2010), ETH, Zurich, Switzerland, pp. 108 - 113.*

Hasan, M.K., Hoque, M. Szecsi, T., (2010): Application of a Plug-and-play Guidance module for Hospital Robots. *In: Proceedings of International Conference on Industrial Engineering and Operations Management – IOEM ‘10, 9 – 10 January, 2010, Dhaka, Bangladesh.*

Hasan, M.K., Hoque, M., Cameron, L., Szecsi ,T., (2009): Developing a Delivery Module for Intelligent Hospital Robot Swarms. *In: D.T. Pham et al., eds., Proceedings of the 5-th Virtual International Conference on Intelligent Production Machines and Systems (IPROMS), Cardiff, UK, 6-17 July 2009, Elsevier Ltd., Oxford*

Hasan, M.K. and Szecsi ,T., (2008): Developing a patient guidance module for hospitals. *In: D.T. Pham et al., eds., Proceedings of the 4-th Virtual International Conference on Intelligent Production Machines and Systems (IPROMS), Cardiff, UK, 1-14 July 2008, Elsevier Ltd., Oxford*

Szecsi, T., Hasan, M.K., Mamun, M.K., Islam, A., Griffin, C., Hoque, M. (2008): Hospital Robot Module Development in the IWARD Project. *In: Proceedings of the 6th CIRP International Conference on Intelligent Computation in Manufacturing Engineering - CIRP ICME '08, 23-25 July 2008, Naples, Italy*

Acknowledgments

Numerous people helped me complete this work, directly and indirectly. First and foremost, I would like to thank Dr Tamas Szecsi for the excellent supervision and providing insight, knowledge and guidance with this work. I would also like to thank my family for their continued support throughout the course of my research, for celebrating my triumphs, encouraging me in defeat and for never asking demotivating questions like: “So, when are you finally going to get a job?” I wish to express my heartiest gratitude and profound in-debt to Professor M.S.J. Hashmi for guiding me during my life in Ireland. Whether he intended to or not, Dr Tarik Chowdhury acted as a big brother of sorts and is partly to blame for my decision to apply for this PhD in the first place. I would like to express my gratitude to Dr. Walid Smew for the good advice he provided in some DOE issues. I would also like to thank my colleague Dr Kabir Al Mamun. I would also like to offer my honest appreciation to Iffat Zehra Naqvi, for her time, effort and cooperation, volunteering in experiments and proof-reading most of this dissertation. A big thanks to my friend Dr. Arman Rahman, for the countless discussions he had with me on deep philosophical issues during our breaks from our busy research life in DCU. I would also like to thank Ciaran Molloy, Shakeel Qamar, Arefin A S M Shamsul, Dishant Issar and Nisha Sehrawat for proof-reading. I’m a big proponent of finding balance in life, and I have all my friends in Bangladesh, Ireland, Norway and many other countries to thank for helping me achieve that.

Contents

List of Figures

List of Tables

Chapter 1 Introduction

"Hospital staff shortages cause 500 deaths a year"

The Independent, UK[1]

"Shortage puts hospitals on critical list"

Irish Times[2]

1.1 Background

Healthcare systems around the world are in crisis due to shortage of healthcare professionals. The World Health Organization (WHO) estimated a shortage of almost 4.3 million health care staff in the year 2006, published in The World Health Report [3]. As Europe's population is ageing, the demand for healthcare professionals is increasing while the number of young healthcare workers is decreasing. The European Commission (EC) estimated that by 2020 there will be a dramatic shortage of approximately 1 million healthcare workers in the European Union (EU) [4]. The statistics are alarming and can have more serious consequences on healthcare unless counter measures are taken.

The School of Mechanical and Manufacturing Engineering at Dublin City University (DCU) teamed up with nine other European universities, research centres and hospitals from Germany, the United Kingdom (UK), Spain, France, Italy and Turkey, to develop a team of service robots that is capable of performing ward-related operational functionalities in hospitals. The project, called IWARD (Intelligent Robot Swarm for Attendance, Recognition, Cleaning and Delivery) was funded by the EC in the Sixth Framework Programme (FP6). The aim of IWARD project was not to replace hospital staff but to unburden them from time-consuming routine jobs so that they can spend more time with patients [5].

Although there are several service robots available in hospitals, most of these are single robots, developed for a single purpose with very restricted capabilities. These are very expensive systems and hospital personnel needs special training to programme such robots. Due to this there has not been a high demand for the already available expensive robots. The IWARD project is a combination of 'team approach 'and 'modular design approach' to develop a robot system supporting various functionalities of current and

future services for hospitals. This will enable highly efficient use of the robot resources and it is adaptable to dynamic shifts of requirements in a hospital [6]. Each IWARD robot contains a mobile, self-navigating platform and several service modules attached to it to perform their specific tasks. As an example, the cleaning modules help to maintain high hygiene levels, while the 'Delivery Module' assists in transporting medicine and documents (such as medical records or x-rays) between hospital departments and areas [7].

1.2 Objective of this thesis

This thesis is about the development of the Person Guidance Module (PGM), which is one of the five service modules installed on the IWARD mobile robot platforms. Guidance in a hospital is required especially by patients and visitors. In hospitals it is a common problem for foreigners to find their way to a certain location [8]. The PGM will enable the IWARD base robot to offer route guidance service to the patients or visitors inside the hospital arena. Once it is attached to the IWARD base robot, it can guide a person or visitor between pre-defined locations in the hospital. For example, a patient can be guided to the X-ray room, or a visitor to a patient's ward.

The speed of the robot while guiding needs to be adjusted automatically according to the pace of the person as the normal walking speed of people can vary widely. Moreover, in a hospital environment patients with various physical abilities may require guiding assistance from the robot. Different patients can follow a moving robot with different speed. Setting one robot speed for all patients, therefore, is not the optimum solution. Also, a person may be temporarily hindered from following the robot due to obstacles, people and other robots in the hospital. In order to ensure that a person is able to follow the robot, speed control of the robot is necessary. The speed control is based on continuously measuring the distance between the moving robot and follower. If the person is lagging far behind the robot the latter may slow down or start waiting for the patient. This simulates a 'virtual elastic band' between the robot and the follower. The robot should be able to measure distances regardless of the orientation of the follower relative to the robot [9].There is a variety of guidance robots like Xavier [10], Rhino [11], Minerva [12], Nursebot [13] and RoboVie [14] etc. currently on the market as shown in Figure 1-1.

XAVIER [10]

RHINO [11]

MINERVA [12]

ROBOVIE[14]

NURSEBOT[13]

Figure 1-1: Existing guide robots.

Although those robots can perform a wide range of guidance and related activities, they do not fit into the modular concept of the IWARD project. These robots are standalone devices and cannot be coupled with other service modules. Their price is considerably out of line with the budget constraints of the project. In order to minimise the cost of such a system and to make it affordable to hospitals, the IWARD robot swarm heavily relies on low-cost, standard components and plug-and-play sensors. As opposed to the large individual robots that are currently available in some hospitals, the robot swarm is based on smaller robots. This will cause less interference with persons and objects in the hospital [15].

1.3 Guidance Scenario

The PGM starts to work when an authorised staff member (nurse, doctor, or receptionist) calls a robot for guidance. Different input devices like voice adoption, keyboard, personal digital assistant (PDA), and touch screen are used to call the robot, specifying the start and end locations. The robot management system selects a suitable robot and sends it to the start point. When an emitter tag is placed on the person to be guided then the robot identifies the signal from the emitter tag. The person's identification (ID) is linked to this tag and the robot only guides a person with this tag. The robot moves towards the final destination; the person follows the robot with a 'virtual elastic band'. PGM continuously measures the distance between the robot and the follower so that the speed of the robot can be adjusted automatically according to the pace of the follower. If the person is lost for a certain time period the robot raises an event and informs the appropriate system and/or personnel. For the person guidance module sensors are required for the tasks involving the identification of the person and speed control of the robot [9, 15].

1.4 Structure of this Dissertation

The remainder of this dissertation is organised in the following manner. Chapter Two describes the overall IWARD system architecture. Chapter Three focuses on the existing solutions from various disciplines and evaluates feasible solutions for the PGM modules. Chapter Four analyses in detail all the sensors which seem feasible for the PGM. Chapter Five contains details of how all the module-hardware were installed in the PGM box. Chapter Six summarises the software development process for PGM

which is in line with the general software architecture of the IWARD project. Chapter Seven discusses the results from the real world deployment. Finally, Chapter Eight concludes the thesis by summarising the major contributions of the thesis and recommending the future work. Furthermore, the appendices present some implementation details and test results. The reader is encouraged to make use of the Glossary while reading the thesis. For further interest, it is recommended to view the video of the robot on www.iward.eu

Chapter 2 System Architecture

2.1 Introduction

In order to enhance robotic services in hospitals, IWARD brings out two new concepts and combines them together:

- The service robots act as a team.
- Each robot has a modular design.

The following is an overview of the IWARD architecture.

2.2 Team Approach

In IWARD several robots work together as a team to perform various tasks that occur in a hospital. The concept of team approach is very cost effective as it allows a highly efficient use of the robot resources. Optimised task planning and scheduling can be achieved by such an approach. Furthermore, having several robots co-operating with each other can provide a fully integrated robot system. The benefit of such an integrated system is that different user interfaces for different tasks can be integrated into one single user interface that can give full control on the operations of the system. All robots of the IWARD system follow the rules of the team while sharing their perceptions and information with the system. This will provide support to the system in deciding which robot is most suitable to perform a given task at any given time [5-7, 16, 17].

2.3 Modular Design Approach

The IWARD robots were developed by applying modular design principles. Figure 2-1 depicts a prototype robot. Each IWARD robot comprises of an inexpensive base platform that can have several service modules plugged and unplugged while the robot is running (hot-plug mechanism). The base robot provides only sensors and actors needed for safe and reliable navigation; for any other application purposes a module with its specific sensors and actors needs to be attached. For the first prototype, five service modules for the robot platforms are supported. These are cleaning, delivery, patient guidance, patient condition monitoring and surveillance. The guidance module is already discussed in Chapter 1. Details of the other service modules are given below.

2.3.1 Cleaning Module

In order to maintain a high level of hygiene, the cleaning module participates in cleaning the hospital floor in the wards, corridors and other rooms. It supports two major types of cleaning tasks: scheduled cleaning and spot cleaning. Scheduled cleaning is performed according to the pre-defined schedule. Spot cleaning can be ordered in case of any incidents for eg. a spillage that is recognised by a nurse or any other members of staff [18].

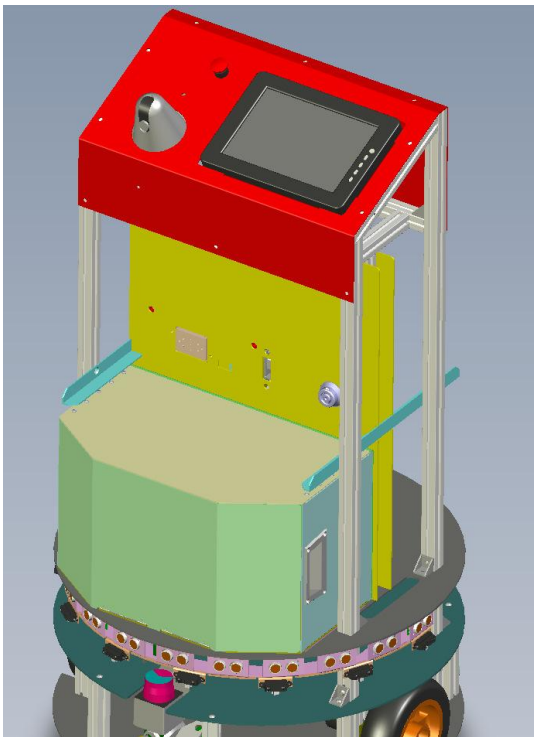

Figure 2-1: Modules in IWARD are implemented as “drawers” [19].

2.3.2 Delivery Module

The Delivery module is comprised of a delivery box with secure access control system. This is used for delivering medical supplies and other materials to patients, and medical documentation (X-rays, patient’s files) to doctors and nurses. The access control system ensures that only authorised personnel can gain access to the box [18].

2.3.3 Condition Monitoring Module

This module serves several tasks such as remote collection of data from patients related to their condition, virtual consultation between patients and doctors, and situation recognition. It remotely measures patients’ body temperature, heart rate, respiration

effort rate, body position and acceleration. If necessary it can inform a doctor or nurse that the patient requires medical attention. It provides virtual consultation services between a doctor and patient in order to communicate remotely with each other. In the situation recognition scenarios it can recognise if a patient is lying on the floor and warns the nurses [18].

2.3.4 Surveillance Module

This module constantly monitors hospital temperature and humidity. It can also detect if any smoke/fire occurs inside the hospital building. If any emergency situation arises it alerts the corresponding staff member. Additionally, it can detect any potential intruder entering the building [18].

A quick-fix mechanism is provided for attaching and detaching these modules on the base robot on demand. Nurses without any prior knowledge of robotics can easily insert and remove the modules from the base robot. As a result of such modular design, robot configuration becomes very flexible and it can be adapted according to the requirements of the hospital. Additionally, if any sensor fails only that certain module needs to be taken out for troubleshooting without hampering the general operation of the system. Moreover, future service modules can be added as developed. Plug and play technology is used the moment any module is connected; the application software recognises the module and enables the corresponding software for the module. More details about the IWARD service modules can be found in [5-8, 18, 20].

2.4 Robot Base

There are three robot bases developed for the IWARD project. Two of them are based on the Pioneer 3-DX platform and one is a purpose-built robot (left in Figure 2-2) developed by IWARD partner Newcastle University. All of them have an aluminium alloy frame superstructure into which rectangular-shaped boxes (modules) can be easily slot in like a drawer. These boxes define the shape of the robot's 'body'. The robot base platform provides only sensors and actors that are required for safe and reliable navigation of the robot. Person's safety is a major concern as these robots will operate in crowded environment. All robots are equipped with a front and rear facing sonar array and a laser sensor for obstacle avoidance. Furthermore, an active bumper is mounted on each of these base robots which trigger an emergency stop if any collisions

occur. These robot bases can reach a speed of up to 1.6 meters per second and carry a payload of up to 23 kg. Also, each base robot has a touch screen for Human-Robot Interface (HRI) and an Internet protocol (IP) camera. Service modules can access the IP camera, if required [6, 21].

Figure 2-2: IWARD Robot Team [6].

2.5 Human-Robot Interface

Although each IWARD robot is autonomous in performing their scheduled tasks, they also interact with health care staff. Team approach in IWARD provides a fully integrated robot system and such approach is beneficial for integrating different user interfaces for different tasks into one common human robot interface as shown in Figure 2-3. The users (nurses, doctors and auxiliaries) are not expected to programme the robots; they can only give them high-level task-oriented commands. Access authorisations are managed by the robot software. As typical users constantly change their location within the ward or hospital, it is not viable to only provide control interface to a fixed computer terminal. All robots are equipped with touch screen and sound for direct HRI.

Additionally, users can access the robots through PDA or mobile phone. For ease of use, IWARD provides a common look and feel for every visual interface [5, 6, 17]. More details about the algorithm used for IWARD HRI can be found in [22].

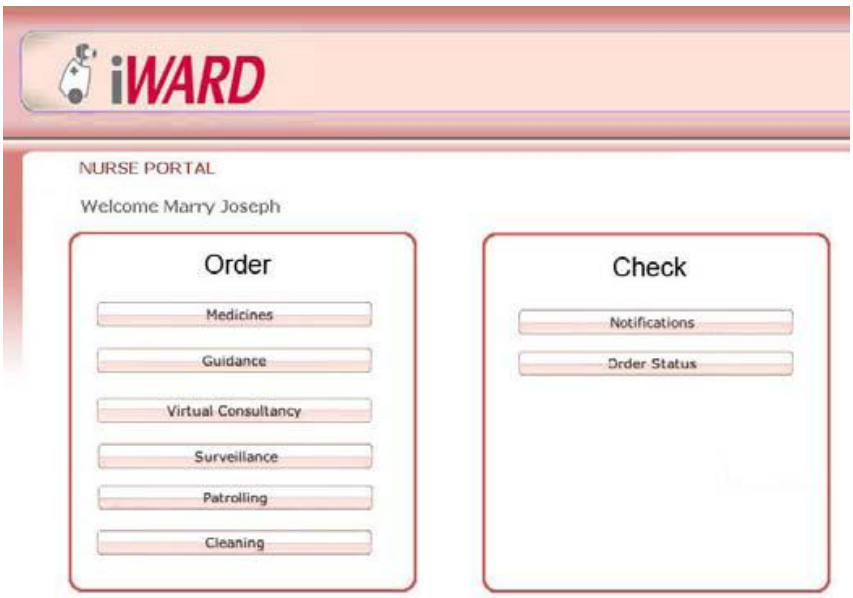

Figure 2-3: Graphical User Interface (GUI) for order selection [6].

2.6 Mission Handling

Instead of a centralised remote control system, each robot in the IWARD system is fully qualified to be self-organised. This ensures a failsafe operation in any condition, which includes potential breakdown of any device of the system. The team approach among IWARD robots is implemented through a distributed planning, scheduling and decision finding mechanism. Each IWARD robot is connected over Wi-Fi and acts as a peer in a network via a communication server. Figure 2-4 presents IWARD mission handling approach.

When a user request a service (known as mission within the IWARD system), the mission is transferred to the temporary team controller. The controller broadcasts the mission among all peer connected robots to initiate the negotiation process. At this stage, all robots calculate the penalty for scheduling the incoming mission and forward the result to the controller [16]. Such calculation is based upon the robot's configuration, existing queue of tasks, position, power level as well as start and due time preferences and the importance of the mission [6]. Finally, the controller assigns the mission to the robot with the lowest penalty.

IWARD introduces a "Shared Knowledge" approach that is accessible by each peer. Within the shared knowledge all relevant information, such as the status of a mission,

configuration and position of each robot is updated on a regular basis. A benefit of such an approach is that, if a peer gets disconnected from the network, the mission can be continued by another peer.

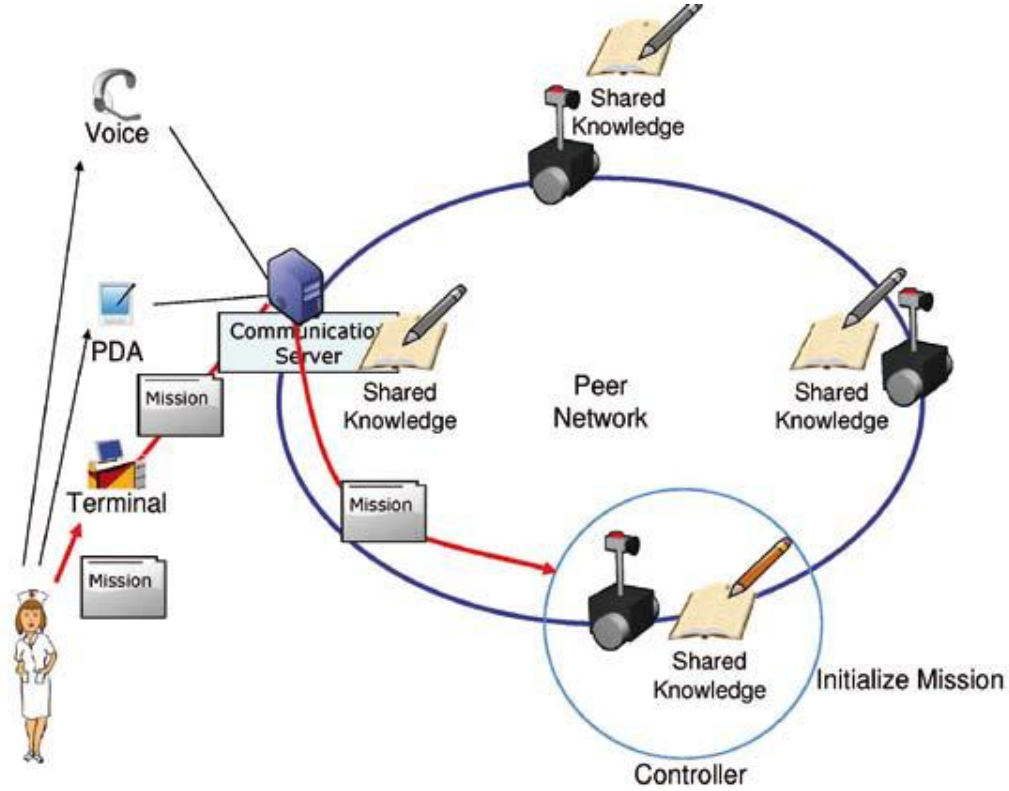

Figure 2-4: IWARD Mission Handling Approach [6].

To prevent single point failure, the role of the controller is not fixed to a certain peer. In case of a failure of the current controller, it can be taken over by another peer. That's why the team controller is called the 'temporary team controller' in IWARD. Most of the IWARD missions can be handled by a single robot. However, missions like virtual consultancy and regular cleaning require multiple robots. Details about the algorithm used for distributed scheduling and planning for IWARD can be found in several publications [6, 16, 20, 23].

2.7 Software Architecture

Considering the fact that most robotic development tools are based on Linux, this is the selected Operating System for IWARD (in order to simplify development between different project partners, Ubuntu Linux was used). Several software architectures and frameworks for the robotics domain had been developed by the community in the past

years. For IWARD, only source packages unencumbered by licensing costs and available for free download are considered. The software for the IWARD project is component-based, and has been developed using the Orca framework. Orca is an open-source framework for developing component-based robotic systems [24]. Currently the second version is being used and named as Orca2. It supports Linux and all components which are currently in the Orca repository, are written in C++. The software architecture for IWARD is shown in Figure 2-5.

All IWARD software modules are logically located above the hardware abstraction layer, and are developed as Orca2 components. The design of the Orca2 framework is conceptually simple. It considers a system as a set of components which run asynchronously, communicating with one another over a set of well-defined interfaces. Each component has a set of interfaces it provides and a set of interfaces it requires. The fundamental purpose of the framework is to provide the means for defining and implementing the interface [25].

The Orca2 framework promotes decentralisation of software development by the adoption of a Component-Based Software Engineering approach. Advantages of such component based frameworks are as follows:

- **Modularity:** The software engineering benefits of having a modular system with controlled, explicit dependencies only.
- **Replaceability:** The ability to build flexible systems in which individual components can be developed independently and replaced.
- **Reusability:** The ability to build more reliable systems by incorporating components which have been tested across multiple projects.

2.7.1 Sequence of Operation

As soon as the service modules are added to the base robot, the embedded computer (Gumstix) inside the module boots up and the module gets registered in the robot's 'Hardware Manager'. The hardware manager keeps track of the status of the robot's hardware and makes it accessible for other components. It is also responsible for providing access to the attached modules and handling the register/unregister process.

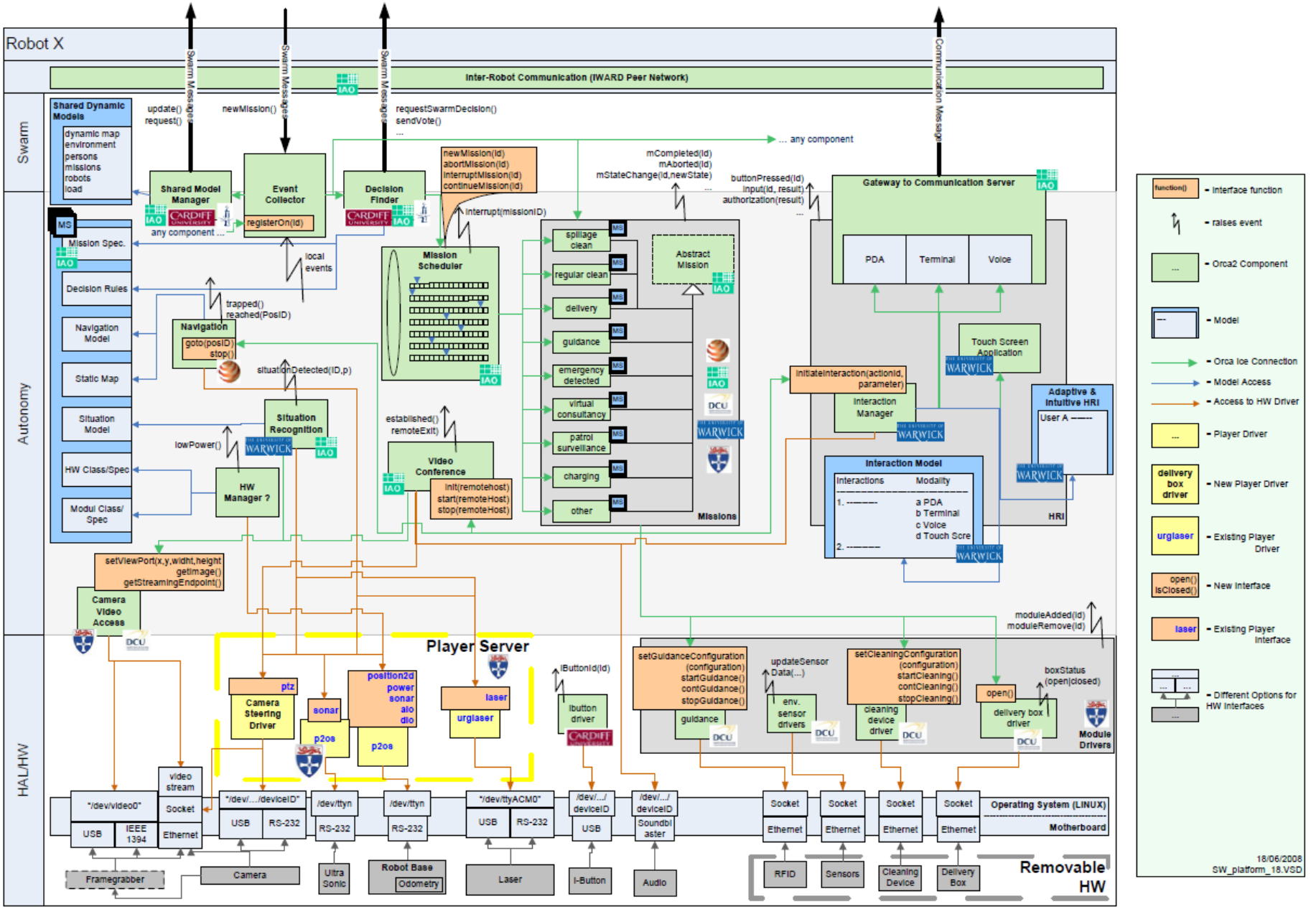

Figure 2-5: IWARD Software Architecture [19].

The ‘Shared Knowledge’ of the whole system gets updated periodically. Thus, the system become aware of which module is available for which robot. Each module provides interfaces so that other software components can communicate with the module. The plugged module waits to receive an order from the ‘Mission Controller’ and as soon as it gets the order, it starts executing its main software.

The operation can be terminated by the module itself or it can be interrupted by the ‘Mission Controller’. In either case, the module software enters a standby mode and waits for new instructions. The software components can communicate amongst themselves, for example to provide data for other components through the Orca middleware software. Primarily, the ‘Hardware Manager’ and ‘Mission Controller’ communicate with the module software (the latter running on the module’s embedded computer). For registering and deregistering the module from the robot base, each module component accesses the interface provided by the ‘Hardware Manager’.

Similarly, the ‘Mission Controller’ (running on the robot base computer) can access the module interface to initiate the execution/termination of the module programme and request information from them. Any external component that needs to access the module components directly needs to request the address of the module from the ‘Hardware Manager’. More details about the Software development can be found on Chapter 6.

2.8 Chapter Summary

This chapter described the overall architecture of the IWARD system. The development of the guidance module has to follow this general architecture (both in terms of hardware and software). The next chapter describes the literature survey.

Chapter 3 Literature Survey

3.1 Introduction

The notion of guide robots is not novel. A myriad of tour-guide robots have been reported throughout various literary journals, with common deployment taking place across various hospitals [26], care centers [27], museums [28], exhibitions[29], trade fairs [30], office buildings [31], campuses [32] and shopping malls [33] etc. Primarily, these robots help visitors by guiding them to their destination. As a result of the aforementioned efforts, guide robot technology has become an important element in the delivery of intelligent robotic services.

An ideal tour guide robot should detect a potential user in a busy, crowded public place and guide them to their destination while maintaining a distance sufficient to ensure safety while adapting its speed according to the pace of the follower for physical comfort. For such successful operation, human detection, identification, tracking and localisation are essential prerequisites. However, performing these tasks in an unconstructed environment solely from a robot's onboard sensor is challenging. Unfortunately, a comprehensive solution in one single platform has remained elusive in existing literature. The goal of the PGM is to accomplish this task while relying on cheap, simple, light weight plug-and-play sensors.

The goal of this chapter is to summarise existing solutions from various disciplines and to select a suitable solution for the PGM modules. The remainder of the chapter is organised as follows. Section 2 provides an overview of existing noteworthy guide robots. The importance of personal distance in human-robot interaction and the necessity of speed adaptation during the guiding process are discussed in section 3. There are many existing options for human sensing in the mobile arena. Section 4 is apportioned into an assessment of existing human sensing approaches and further subdivided into the examination of uninstrumented and instrumented approaches, single-modality versus multimodal sensor fusion. Due to the expansive vista of this field, the scope of this segment will seek to focus on sensor systems, presence detection, identification and localisation of the human form while excluding non-human objects. A

summary of findings and a discussion are presented in section 5. Section 6 concludes the chapter.

3.2 Notable Existing Guide Robots

To the best of the author's knowledge, the first mobile tour-guide robot, named 'Polly', was developed during 1994 by Horswill [34]. Polly used vision to give primitive tours of the seventh floor of the MIT AI Laboratory. Polly guided visitors with a speed between 0.75 and 1 m/s. To distinguish a visitor from the normal occupant, it relied on the fact that the normal occupants were probably sick of it and would therefore leave it alone, whereas interested visitors would stand directly in front of it. It detected people's leg through its vision systems in order to offer tours to visitors.

Probably, the first successful tour guide robot was 'Rhino' [11] operated for six days in May 1997 in the Deutsches Museum Bonn, followed by 'Minerva' [35] which was installed for a total of 14 days in the Smithsonian's National Museum of American History, during August/September of 1998. Rhino and Minerva found people by comparing a map with their range measurements extracted from laser range finders, sonar and active infrared sensors. Such a system can only detect whether a person is present in its surroundings but cannot distinguish whether or not this person is facing the robot, as an expression of his will to interact with the robot [36]. Both of these robots' maximum speeds were limited to 70 cm/s during opening hours. They did not consider any kind of motion coordination with the followers and assumed that people were following them, during the tour. Additionally both were equipped with on-board computers and auxiliary off-board workstations to ease computational loads [37].

Rhino and Minerva have been the precursors to a series of tour-guide robots in various public places, developed by different universities and research centres around the globe, such as 'Jinny' from Korea Institute of Science and Technology [38], 'Blacky' from University of Madrid [30], 'Rackham' from LAAS-CNRS Robotics and Artificial Intelligence group [39], 'Robovie' from ATR Intelligent Robotics and Communication Laboratories [40], 'Atlas' from University of Essex [41] and 'Minnie' from Royal Institute of Technology, Stockholm [31] etc.

In order to keep a track of the follower while guiding them, Imai et al. [42] adopted an infrared (IR) identification system for their tour guide robot named, 'ITAKO'. The system consisted of several IR readers fixed on the ceiling at various locations and IR badges were attached on both the user and the mobile robot. The user's badge was attached to a mobile PC which the user would carry during the guidance operation. The central server updated the locations of the mobile robot and the user during the tour. There is no information about whether they adopted any speed adaptation technique during operation.

Jin et al. [26] developed a guide robot named 'GRGP' (Guide Robot for Guests and Patients) for use in hospitals. In addition to the guiding task, it performed delivery and intruder monitoring operations as well. They used PIR (Passive Infra-Red) sensors to detect human body but did not disclose any information on speed adaptation. PIR can only detect human presence but it cannot authenticate the person.

'Jinny' developed by Kim et al. [38] for the National Science Museum of Korea had different types of motion algorithms for different scenarios, but neither of these was concerned with the follower, nor did they consider tracking the follower during guidance.

Martin et al. [36] used an omnidirectional camera for their office guide robot, to make sure that the user followed their robot while guiding. They developed a multi person tracking system in order to recognise the actual user among other people. At first the system would detect skin colour and employ a condensation sampling algorithm to track the positions of an unknown number of persons around its surroundings. Then it differentiated people using face detection. The tracker needed more time to detect the correct number of people as the number of people in field of view could increase. Moreover, if the distance between the user and robot grew over 1.5 m, the face of the user would become very small in the omnidirectional images and the tracking system would fail, hence the robot would stop and ask the user to come closer.

A tour guide robot, 'RoboX' [29] has been developed at the Autonomous Systems Lab. It tracks visitors through its multimodal tracking system, consisting of a laser, a motion

detector and a camera. The laser scanner data is fed to a motion detector indicating where in the robot's vicinity there is movement. Then the colour images from the camera are used to identify skin colour and subsequently human faces. There is no identification process while guiding a visitor. Eleven RoboX robots were guiding visitors during the 5 months of the Robotics exhibition at Expo.02. RoboX has recently been commercialised by BlueBotics.

Another tour guide robot is 'ATLAS', developed by Bellotto and Hu [41]. They combined visual and laser range information to detect and track visitors. Human legs were extracted from a laser scan and, at the same time, faces were detected from the camera's image. With this system, their robot could only approach a visitor prior to guiding. They did not disclose any information whether they track the visitor or adapt speed during guiding.

Pacchierotti et al. [31]developed an office tour guide robot named 'Minnie'. It waits for visitors in front of the elevator and offers assistance to go to any office on the floor. While the system offers assistance in locating the appropriate office that a visitor wants to reach, it engages in a passing behaviour to allow free passage for other persons that it may encounter. They used an on-board laser scanner for detecting and tracking people.

Several "Robovie" humanoid series robots from the ATR robotics lab were tested as guide robots in exhibitions [40], museums [43] and shopping complexes [44, 45]. Koide et al. [40] constructed an exhibition room with a ubiquitous sensor. The 'Robovie' retrieved the recorded information from the interaction corpus to guide visitors to preferred exhibited contents. Both wearable and stationary ubiquitous sensors consisted of IR-trackers, light-emitting diode (LED)-tags, video cameras and microphones. All of these components were attached to the visitors, guides, the robots, and potential focal points such as posters in the room. By using the LED-based tag system (IR tracker and LED tags), the system identifies the objects that each camera captures. In other words, it enables the system to identify the focus of attention of each visitor. Shiomi et al. [43] investigated whether Radio-frequency identification (RFID) tags and readers could be used for Robovie to guide visitors in Osaka Science Museum. During the two month field trial, visitors wore a RFID tag while looking around the museum's exhibits. They

used four Robovie series humanoid robots for interaction with visitors in guidance and giving explanations. Information obtained from the RFID tags was used to direct the robot's interaction with the visitors. They installed twenty RFID tag readers, which included the two equipped on the Robovies, three IR sensors and four video cameras. All sensor data was sent to a central server at a base through an Ethernet network. The active type RFID tag reader on Robovie enables it to easily identify the individuals around it and is also unaffected by the occurrence of occlusions. The distance between the tag reader and an RFID tag can also be roughly estimated. But they did not consider any speed adaptation while guiding at this trial period. Later, Sviestins [46] et al. tried to establish a hypothesis about how to maintain the relationship between walking speed and relative position while people are walking with Robovie . During this experiment they only used a laser range sensor to retrieve and track human and robot positions. However, they concluded that not all subjects in their experiments displayed speed-position relationships consistent with their hypothesis. Glas et al. [45] used multiple Robovie series robots to provide route guidance and shop recommendations to customers in a shopping mall. They installed multiple SICK LMS-200 laser range finders (LRF) around the environment's perimeter at a height of 85 cm and used particle filters to track the location of each person in the scanning area based on the combined torso-level scan data from all LRFs. Tracking accuracy was +/- 6 cm. Recently Kanda et al. [44] developed another shopping guide robot using Robovie to provide root guidance. Their system detects a person with floor sensors to initiate interaction and identifies individuals with RFID tags. They installed 16 floor sensors around the robot covering a 2 m by 2 m area. For person identification, they attached a passive type reader to the robot's chest. As a passive RFID system has limited reading distance, the user has to place the tag on the reader to identify him/herself. Moreover, ubiquitous sensors cover only a small area (2 m by 2 m), implying that the robot cannot actually guide the user from one place to another, instead, it explains a route to the user with utterances and gestures by standing within its limited operational area.

Another interactive robot-guide is 'Rackham'. It was developed by Clodic et al. [39] and since its development, it has been used in several places and exhibitions. It has a pan-tilt camera, with face detection module to find people to interact with. As soon as a person is detected, it offers to guide them to the different exhibits. It then leads them to the spot of their choice and introduces the different exhibits to them. From the direction

and the size of the face, it can estimate the 3D position of the detected person with sufficient accuracy (about 10 cm for the height and 20 cm for the range) within a range of about three meters.

Gross et al. developed a series of interactive shopping guide robots to be used in shopping centres or home improvement stores. 'TOOMAS' [33] is their latest version of the guide robot. Earlier versions of this robot were 'Shopbot' [47] and 'PERSES' [48]. TOOMAS autonomously navigated through the market for potential users, intuitively interacting with them, offering its services, guiding the customers to the products of their choice and accompanying them during the whole purchase. They combined vision with distance measuring sensors for user detection and tracking. There is an omnidirectional camera mounted on the top of the head, which can be panned around 360^{o} to allow it to face the user during interaction. The robot is also equipped with a set of 24 sonar sensors at the bottom to cover 360^{o} around the robot for obstacle detection, map building, localisation and person tracking. Furthermore, a laser range finder is mounted on its front, at a height of 35 cm, covering 270^{o}. From a group of people, the robot selects the person with the smallest distance from itself. Also, if any person from the group is facing the robot, the robot will interpret that as interest in its assistance. During the guided tour, the robot continuously observes the user to check if he/she is still following it. They developed a probabilistic approach for detection and tracking of (potential) users in the local vicinity of the robot. The main sources of information are the images from the frontal and panoramic cameras and the occupancy map of the local environment. It integrates all the range information from sonar and laser. The maximum driving speed is up to 1.4 m/s. The speed of the robot during the customer-guiding process is controlled according to the speed of the follower. In their field trial, 16.3% of the time the robot did not reach their targets due to reasons such as blocked hallways (by a group of customers) or other dynamic obstacles. Also, the robots sometimes lost their position hypotheses due to unusable measurements, for example in over-crowded hallways. Currently, they are working on further developing their person tracker module to allow detecting humans as potential users at distances greater than 2-3 m.

An EU-FP6 funded museum tour guide robot is 'Indigo' [49] which was developed by Vogiatzis et al. Their system can track two people using a single laser range finder

mounted on a mobile robot [50]. Although speed adaptation was proposed as a goal, no paper regarding this goal has yet been published [51].

Table 3-1: Overview of some existing Guide Robots ('-'denote No and '√' denote Yes).

Name	Tracking	Authenticate Tracking	Speed Adaptation	Only relying on board Sensors
RHINO [11]	-	-	-	-
Minerva [35]	-	-	-	-
ITAKO [42]	√	√	-	-
GRGP	√	-	-	√
Jinny. [38]	-	-	-	√
ATLAS [41]	√	-	-	√
RoboX[29]	√	-	-	√
Minnie [31]	√	-	√	√
Robovie [40, 43-45]	√	√	-	-
Reckham[39]	√	-	√	√
Toomas[33]	√	-	√	-
Indigo[49]	√	-	√	√
IWARD	√	√	√	√

Industry giants have already stepped into this market. Unfortunately, much of their technology is proprietary. 'TPR-Robina' from Toyota is in operation for escorting visitors around the various displays of Toyota Kaikan Exhibition Hall in Toyota City, Japan since august 2007 [52]. Similarly, Fujisu developed a tour guide robot named 'Enon', which is currently in operation in the Kyotaro Nishimura museum [53].

Earlier versions of tour guide robots such as Polly [34], Rhino [11], Minerva [35] and Jinny [38] etc. did not consider tracking the follower during the guidance operation. It was automatically assumed that the person was following them during the process. Developers of Urbano [54], Blacky [30], Buttler [55] and Bryn Mawr [32] did not publish any results on how they tackled this task. It can be assumed that they did not implement this important feature in their system. On the contrary, although GRGP [26], ATLAS [41], RoboX [29], Minnie [31], Reckham [39], TOOMAS [33] and Indigo [49] considered tracking the follower using different sensors (laser, camera, PIR or a combination of them) they could not robustly distinguish the follower from other persons. On the other hand, ITAKO [42] and Robovie [40, 43-45] could identify the follower but speed adaptation with the follower to provide a more comfortable and socially acceptable guidance operation was not one of their functions. Only a few of the

robots such as Minnie [31] and TOOMAS [33] considered speed adaptation with the pace of the follower but surprisingly they did not have any authentication module.

Table 3-1 presents an overview of some existing guide robots. The challenge of the PGM is to combine all these features into one platform. Additionally, Rhino, Minerva, ITAKO, Robovie and TOOMAS relied on their on board and off board sensors for performing their operations. On the contrary, the goal of PGM is to use only the on board sensors for its guidance task to minimise cost. Finally, most of these guide robots do not fit into the modular concept of the IWARD project. These robots are standalone devices and cannot be coupled with other service modules. Their price is considerably out of line with the budget constraints of the project. In order to minimise the cost of such a system and to make it affordable to hospitals, the IWARD robot swarm heavily relies on low-cost, standard components and plug-and-play sensors. As opposed to the large individual robots that are currently available in the literature, the robot swarm is based on smaller robots. This should cause less interference with persons and objects in the hospital.

3.3 Distance and Speed adaptation in Human-Robot Interaction

Distance between human and a robot is important [56-58]. The robot should always maintain an appropriate distance from the human for safety and physical comfort [59]. It is necessary that a virtual space should be created in order to prevent the robot from invading the user's personal space. Anthropologist Edward T. Hall presented one of the most widely used person-person interaction model in the 1960s, referred to as 'Proxemics'. Proxemics is the study of set measurable distances between people as they interact. In Proxemics literatures, [56] the space around a person is divided into four zones: (i) Intimate (ii) Personal (iii) Social (iv) Public. The proposed personal space by Edward T. Hall is shown in Figure 3-1.

Intimate distance

This ranges up to 45 cm from the body and is used for interaction with a lover or a close friend. The activities that may occur within this space might include physical contact such as embracing, touching or whispering.

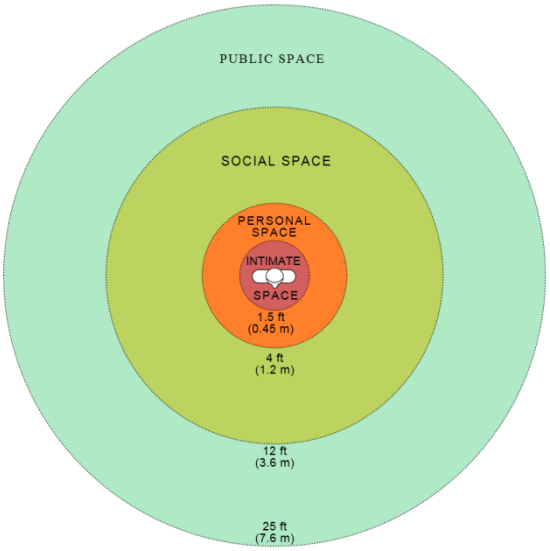

Figure 3-1: Personal space by Edward T. Hall [60].

Personal distance

This ranges from 0.45 m to 1.2 m and is used amongst good friends, family members or for organised interactions such as queuing.

Social distance

The interaction ranges here from 1.2 m to 3.5 m. This range is used for interactions among acquaintances.

Public distance

It extends beyond 3.5 m and is used for public speaking.

Proxemics theory can be applied for the interaction between people and robots operating in public spaces. Several user studies and experiments [61, 62] have been conducted to establish and/or verify these spatial distance zones from the viewpoint of human-robot interaction. In a typical guiding operation, the robot should maintain this spatial relation with the follower so that the follower feels safe and comfortable. Hall also notes that the distance between interactors may vary by culture, gender, status, age, familiarity, relationship, pose, etc. [63]. That's why in order to grant the human more flexibility during guiding; speed adaptation is required while maintaining this Proxemics theory.

In a hospital environment, patients with very different physical abilities may require guiding assistance from the robot. Different patients can follow a moving robot at different speeds. Setting one robot speed for all patients, therefore, is not the optimum solution. Also, a patient may be temporarily hindered from following the robot due to

obstacles such as other people and robots in the hospital. In order to ensure that the patient is able to follow the robot, speed control of the robot is necessary. However, much research on an adaptation mechanism for a robot during guiding has not been conducted previously [46].

Gockley et al. [58] founded that the direction following behaviour has been more human like and natural than the path following behaviour for a mobile robot to follow a human. Mitsunaga et al [64] showed that their Robovie-II robot could adjust its distance by reading discomfort signals that were subconsciously emitted by the human**.** From a case study in human-human walking interaction, Sviestins et al. [46] tried to establish a hypothesis about how to maintain the relationship between walking speed and relative position while people are walking with robots. They have conducted an experiment with a humanoid robot, Robovie-IV, to verify this hypothesis. Panday and Alami [65] proposed a probability model based framework for the Rackham tour guide robot so that during the guiding process, the person may switch from one side of the robot to another, or he may speed up, slow down or even temporarily stop and in response, the robot does not show any reactive behaviour apart from that of adaptation in its speed, if required. They equipped the robot with a front and back laser and camera pair at its top and at hand. For the reliable human tracking and activity detection, a motion capture system has been installed in the environment. The project is still ongoing and has not yet been implemented. It is expensive to have laser on both sides of the robot. Moreover, additional external motion sensors make it unsuitable for mobile robots to operate in unconstructed environments.

All the above researches are based on laser-based person tracking and operate on single person scenarios. These approaches are very expensive from the computational perspective and do not work if there is no line of sight between the follower and the robot. Moreover, laser-based tracking systems cannot distinguish a follower from others.

3.4 Existing Human Sensing Approaches

There are numerous options available for sensing: presence, count, location, track and identity of human. To describe all of them is an impossible task. The goal in this section

is to expose and organise the existing literature rather than to detail the exact algorithms that they employ. Existing sensing approaches can be classified as instrumented and uninstrumented. Instrumented approaches require each person to carry an attractor device on them and uninstrumented approaches are those that do not rely on any carried device.

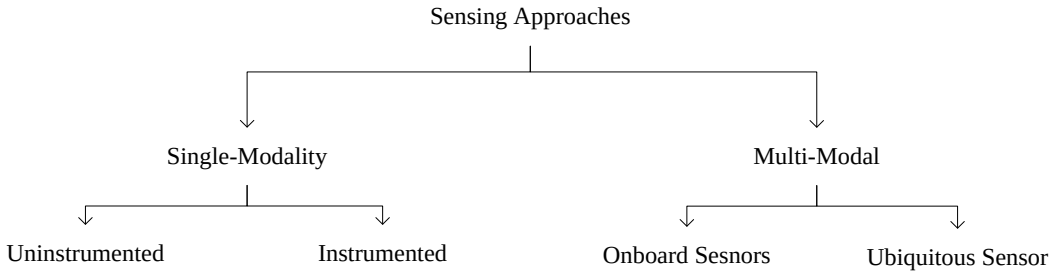

Figure 3-2: Classification of existing human sensing approaches [66].

They can be further classified by single modality and multimodal approaches. In single modality approaches, only one type of sensor is utilised to perform the human sensing task, whereas multimodal approaches typically combine several sensors to perform the task. Classification of existing approaches is described in Figure 3-2.

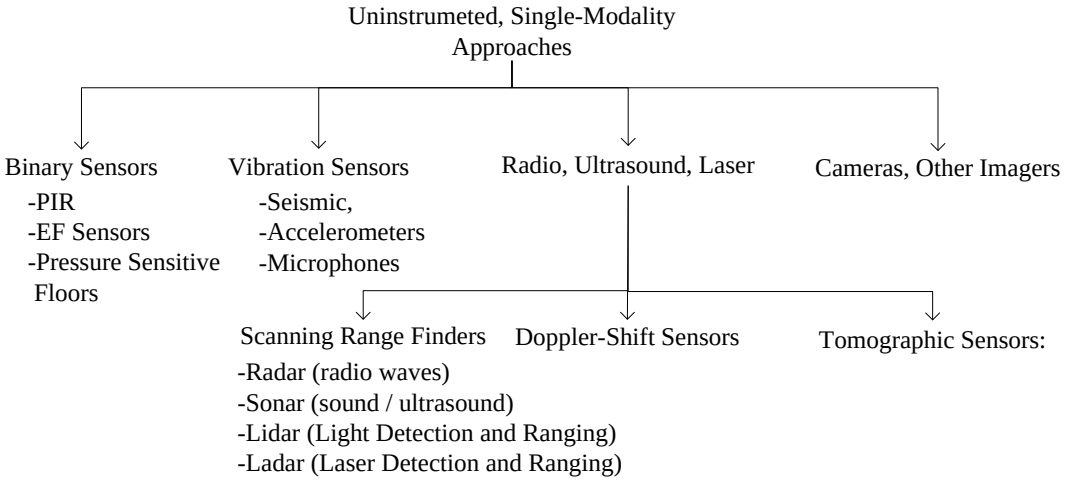

Figure 3-3: Classification of Uninstrumented, Single-Modality Approaches [66].

3.4.1 Uninstrumented, Single-Modality Approaches for Human Sensing

An overview of uninstrumented, single-modality sensing approaches is presented here. These types of solutions dominate in literature and in real-world deployments. These

approaches can be further classified as ‘Binary Sensors’, ‘Vibration Sensors’, ‘Radio, Ultrasound and Laser’ and ‘Computer Vision’. Classification is presented in Figure 3-3.

3.4.1.1 Binary Sensors

A variety of binary sensors are available. Examples include PIR, break beams, contact sensors, binary Doppler-shift sensors, electric field (EF) sensors and pressure-sensitive floor tiles. Binary sensors simply return 1 if they detect human presence within their range; otherwise they return 0. A single binary sensor is capable of detecting nothing more than presence. In contrast, with an aid of a high-density network and data-inference tools, binary sensors can count, localise and track objects. In contrast with other conventional localisation and tracking techniques, binary sensor based localisation is cheaper and does not require the processing of large amounts of data [66-70].

The disadvantages of this approach are:

- Accuracy depends on node density and sensing range [71].
- Only works in constructed environments.
- Suffers from tracking ambiguities; if two people cross paths their relative identities will be lost and cannot be recovered [66].

Passive Infrared

PIR sensors are sensitive to human body temperature changes and are widely used in home, office, or factory environments for person detection. PIR motion detectors are cheap and have a reasonable range (up to 10 m) [72]. It can be modulated via Fresnel lenses. Processing infrared data is much easier than processing acoustic or video data. Moreover, they can work in the dark whereas vision based systems typically cannot [73]. Several researchers [72, 74-79] have developed PIR-based tracking by placing sensors on the ceiling upon maintaining a strictly geometric formulation. As the readings from the infrared sensors are rough, they have implemented data-inference tools such as Particle [75], Kalman [77] or extended Kalman filtering [79]. But their accuracy and performance of tracking is highly dependent on the number of sensors and the size of their sensing areas [72, 76]. PIR sensors cannot detect stationary people thus the system can be fooled very easily. Moreover, they cannot distinguish between

multiple people. Thus this type of system is limited to single person scenarios and the system assumes that people are always moving. Shankar et al. [80] developed a cluster of sensors with eight piezoelectric detectors and modulated their visibility with the Fresnel lens in such a way that each detector's visible space is divided into distinct zones. When a human walks across the field of view of one lens array, the sensors generate a binary signal sequence that contains gait information as well as location information of the walker. Using several of these multi-PIR sensor nodes placed on walls, the authors show that it is possible to detect and localise a moving person. Later, other researchers [79, 81-85] investigated the pattern hidden in this binary signal sequence, to identify one person from others. One of the essential criteria for this process is the orientation of the sensor; it has to be known in advance to calculate the direction of motion and angular velocity which is not a feasible solution for a mobile robot as it is always in motion [80]. Moreover, human walking motion is not very distinctive [81]. IR radiation from the human body depends on the type of clothing that the walker wears and weather situations (wind, rain, snow, etc.) influence the recognition rate as well [84]. Indeed, gait is not very distinctive and much of the work on gait analysis has been conducted using video cameras, processing large amounts of data to extract the identity of the person in a computationally expensive way [81]. Thus this approach is restricted to only a small group of people in a constructed area whose patterns are already registered within the system [79].

Pressure Sensitive Floors

Pinkston et al. [86] developed a dance floor with a large number of Force Sensing Resistors (FSRs) to track the precise position of a person and his velocity and pressure information. The Nintendo Power Pad is based on similar technology. Murakita et al. [87] used pressure sensors underneath floor tiles to track a person. He used Markov Chain Monte Carlo method (MCMC) as the tracking algorithm. The system can neatly track a person who walks alone. Addlesee [88] et al. and Orr et al. [89] both used footstep force profiles for identifying people. They created user footstep models with hidden Markov models (HMMs) and compared unknown identity footsteps against the stored HMMs. Orr et al. also showed that recognition accuracy is not affected by the different footwear. Middleton et al [90] used floor sensors for gait recognition. They measure stride length, stride cadence, and heel to toe ratio for person identification. Although high-resolution sensor floors improve the identification precision, until now

these approaches work only amongst small groups of people. Moreover, constructing hospital floor with pressure sensitive tiles is not a convenient solution. Furthermore, like other binary sensors, floor sensors require a high network density to provide precise locations.

Electric Field Sensors

An EF sensor measures the changes of AC signal between a capacitor plate and a receiver plate due to human presence. SenseFloor and SenseFloorMats are based on similar technology [91]. Henry et al. [92] developed a human tracking system using EF sensors and a matrix of conductive floor tiles. As the human stands on tiles, a current flow to the grounded tiles increases compared to the empty floor. In contrast, Valtonen et al. [93] did not measure the current flow from the transmitting electrode to the ground, but used a transmitter-receiver configuration for tracking the moving person. EF sensors are simple, cheap, durable and penetrable over non-conducting objects like furniture or walls. But altering a hospital floor environment is not a feasible solution. Moreover, their sizes are larger than that of other systems.

3.4.1.2 Vibration Sensors

The modality of vibration sensors includes seismic sensors, accelerometers, microphones etc. Pakhomov et al. [94] and Audette et al. [95] developed footstep-based person detection using seismic sensors like “geophone”. Although detection range is quite high (up to 20 m) by Pakhomov et al. and up to 38 m by Audette et al., all these are outdoor based applications. For indoor applications, Diermaier et al. [96] used microelectromechanical systems (MEMS) accelerometers for indoor room level localisation. Other researchers have worked on acoustic source localisation. Potamitis et al. [97] used multiple microphone arrays to estimate positions and velocities of a moving speaker based on time delay of arrivals (TDOAs). Compared to radio, ultrasound, cameras, etc., vibration and acoustic sensors require simpler signal processing steps. Unfortunately acoustic and vibration systems are not suitable for crowded environments. Signal interference from multiple people known as the ‘cocktail party problem’ limits this system to a single person scenario.

3.4.1.3 Radio, Ultrasound and Laser

Scanning Range Finders

Range-finder sensors calculate distance by measuring either time or energy of the response signal. Depending on the medium that these devices use they can be divided as:

- Radar (radio waves)
- Sonar (sound / ultrasound)
- Lidar (Light Detection and Ranging)
- Ladar (Laser Detection and Ranging)

Zetik et al.[98] used Ultra Wideband (UWB) radar which works through-the-wall to locate a person indoor. He developed an adaptive background subtraction technique to differentiate electromagnetic waves scattered from a person from other objects. Although the system accuracy is within 40 cm and it can work through walls, it only detects one person in a static scenario. Chang et al. [99] used UWB radars to detect people based on their scatter signature. Later they extended their approach to detect for multiple people as well. But it only works outdoors.

Ultrasonic transducers or sonar units are widely used for tracking the position of mobile robots in indoor scenarios. The robot is generally equipped with a sonar transducer that transmits an ultrasonic wave at periodic intervals and then waits for the corresponding echo to determine the distance to an object in front of the robot. But they cannot distinguish a person from an obstacle. Wan and Paul [100] presented tag-free indoor tracking using wall-mounted ultrasonic sensors with an accuracy of 0.5 m. Multiple sonar modules were positioned throughout a given room. The active ultrasonic transducers captured analogue echoes and a number of signal processing steps were then used to remove background clutter in order to determine a person's position and velocity. Their system is only a prototype and the testing was performed in a 6×5 m^2 laboratory. It cannot track and distinguish when there are multiple people in the scenario.

In mobile robotics, two-dimensional laser range finders have been widely used for navigation, obstacle avoidance, and person detection and tracking purposes. Laser range finders are insensitive to lighting conditions and require less data processing time.

Rhino [11], Minerva [35], Tourbot [101], Grace [58], Minnie [31] and Indigo [49] for example, use a laser range finder based on detecting people in the robot's surroundings. A common approach is to extract legs as local minima from the range image. The robots, Grace [58], Minnie [31] and Indigo [49] are a few examples of such systems. However, two-dimensional laser data is not sufficient for accurate tracking in cluttered and crowded environments, due to occlusions among multiple people. To address this problem, several researchers [49, 102-109] used Bayesian filtering such as Kalman filter and particle filter to track multiple people. Another option is to mount lasers at different heights on the mobile robot to extract a single "Person sized" convex pattern [110, 111] or use multilayered laser scanners [102-104] on the mobile robot and detect different body parts of a person, like legs and torso simultaneously. Another approach [45, 45, 107, 112, 113] for tracking multiple people is to install multiple laser range finders in different locations to reduce occlusion; however this limits the detection to only over a certain constructed area and thus is not suitable for a mobile robot. Although less used, 3D laser range finders are now commercially available [114] and are very promising. 2D-Lasers represent a slice of the environment whereas 3D laser range sensors offer far more comprehensive information so that the whole body of a person can be detected. A few researchers [115, 116] successfully tracked a person using 3D laser range data and explicitly adapted to the occlusion problem. In spite of recent improvements, however, the line of sight imaging requirement and a high resource utilisation, such as time, memory and CPU in real time applications are the disadvantages of laser based tracking systems [117]. In dynamic and cluttered environments like hospitals, the reliability of such entirely laser-based systems is not sufficient for the PGM.

Doppler-Shift Sensors

Like PIR, Doppler sensors serve as motion sensors. They can also provide the speed measurement. Doppler-shift sensors operate on the principle that if a body is in motion in a direction towards or away from the transmitter, the received wave is shifted in frequency from the transmitted wave by an amount proportional to the velocity of the object [118].

When a human walks, the swinging movements of his arms and legs induce frequency modulation on the returned signal and generate sidebands about the Doppler frequency, known as micro-Doppler signatures. Several researchers [119-126] have been working

to characterise the micro-Doppler radar signature of the human gait. Radar signals have certain advantages over other sensors as they are insensitive to lighting conditions and can penetrate walls [121]. Kalgaonkar and Raj [127] used micro-Doppler sonar for gait-based person identification. They analysed the spectral signatures of individual walkers and employed a Bayesian classifier to identify an individual among 30 subjects with 90% success rate. However, all these tests were carried out in a regulated laboratory environment in a single person scenario. If multiple people walk with similar speed their Doppler signatures interfere with each other. Doppler sensors are suitable for solely person detection and not for counting or identification.

Scanning or triangulation techniques can also be used to localise multiple people using Doppler sensors. Lin and Ling [128] developed a prototype system with Doppler radars consisting of three antenna elements and four integrated receivers for tracking multiple people in a three-dimensional space. Kubo et al. [129] used particle filters to estimate human location with multiple microwave Doppler sensors placed at four corners of the room. However, all these techniques can only localise multiple people if they walk at different speeds; otherwise their Doppler signatures interfere with each other.

Recently Ultra-wideband (UWB) Doppler radars for detection and positioning of human beings in a complex environment became popular, as they are immune to multi-path interference. Moreover, due to wide frequency spectrum, they can pass through the wall [130]. There are several commercially available UWB Doppler radars for person detection and localisations through walls such as prism 200 [131], PulsON 220[132] and Xaver 800 [133]. All these products were developed using an array of radars, which transmit UWB pulses, and then measure echoes to estimate a range and bearings. Although these devices are very accurate at close distance, noise increases at larger distances due to monostatic radar scattering losses and large bandwidths [134]. At present these are mainly being used by the military, police, special forces or fire and rescue communities.

Tomographic Sensors

The technique of tomography has long been used for medical imaging to provide two-dimensional cross-sectional images of a three-dimensional object from a set of narrow

X-ray views of an object over the full 360° of direction [135]. The principles of tomography are applicable to radar as well. Radio Tomographic Imaging (RTI) is an emerging technology and several researchers [136, 137] demonstrated tomographic imaging with Ultra-narrowband (UNB) radars for people detection, counting, localisation and tracking. UNB radar signals permit a substantial reduction in thermal noise power compared to UWB based systems, which in turn improves the overall detection performance. Wilson and Patwari [134] used 'Radio Tomographic Imaging' to track targets that move within a wireless network consisting of 28 narrowband transmitters and receivers operating at 2.4 GHz. RTI-based human sensing researches are still in their development stage and require a considerable amount of investment for equipment and setup. Moreover they cannot be used to identify a person. They can only provide current images of the location of people and their movements.

3.4.1.4 Cameras, Other Imagers

Compared to other approaches, computer vision approach has been widely used by almost every mobile robot developer for human sensing as they are inexpensive, offer high spatial resolution, and provide a large amount of information regarding objects in a scene, including size, shape, colour, texture, and so on. On the contrary, this large breadth of information from images and videos produces an overwhelming number of false positive detection, which in turn causes most of the vision-based human sensing methods to be more challenging. Detecting a person in an image is difficult, as human body is highly articulated [138]. Additionally, varying human appearance (e.g. different clothing, sizes, aspect ratio etc.) and unconstructed environments further complicate the task [139]. Counting and localisation are more trivial once the system can successfully detect a person in the frame [66].

Presence

Background subtraction (also known as background differencing) techniques [140] are widely used as a person detection method for video security applications [141]. They work under the assumption that a background scene is either static or slowly changing. Several background subtraction methods can be found in literature, such as [142-144]. Although the surveillance applications or human-machine interfaces where the cameras are static allow the use of background subtraction techniques for quick detection of non-background objects, it cannot be applied in PGM as both the robot and the person are in

motion. Background subtraction techniques tend to fail in scenarios where the background varies. Object segmentation and pattern matching are other two methods for person detection. The segmentation process does not require subtracting the background from the image. Rather, a person's shape can be extracted directly from the image. The GrabCut algorithm, developed by Rother et al. [145], is one such method. In pattern matching, the input image convolves with sample images of the candidate's object. Mostly these comparisons are done in other feature spaces such as SIFT (scale-invariant feature transform) [146] and HoG (histograms of oriented gradients) [147] . Several mathematical tools are employed to classify the object later on. Among them, PCA (Principal Component Analysis) [148], support vector machines [147], AdaBoost classifiers [149], and neural networks [150] are well known.

Stereo-based person detection provides more robust results than monocular approaches [151]. Some researchers [152-154] successfully applied foreground segmentation on disparity maps to differentiate people from the background scenery. Moreover, stereo-based approaches can provide information about the person's distance from the stereo head. The downside is that stereo-based approaches require significant CPU resources.

Beyond the visible spectrum, thermal imagers are also applied by a few researchers [155, 156] to differentiate people from background through their temperature. Humans have a distinctive thermal profile with respect to inanimate objects [139]. Bertozzi et al [157] used a stereo pair of thermal imagers to detect a person. Cielniak et al. [155] used thermal vision for human detection and colour images for capturing the appearance of a person. Although commercially available [158], these sensors are very expensive. Moreover, in crowds, it is impossible to identify a given person from their thermal profile [66].

Motion information can be used for detecting a person. Interframe motion (i.e. subtracting consecutive frames pixel wise) and optical flow (i.e. measuring the motion vector of each pixel over a number of frames) have been used for foreground segmentation, primarily in the general context of moving human detection. Motion based approaches require less processing and provide less false detection compared to background subtraction or pattern matching approaches. Unfortunately, it can only be applied to moving people.

Tracking

Tracking is the process of estimating the trajectory of an object (or multiple objects) in the image plane over time as it moves around a scene [159]. Among all uninstrumented modalities, cameras and imaging sensors are by far the most superior in tracking. This is due to their ability to capture a large breadth of information (colours, height, width, shape, speed etc) and several specialized image features (SIFT and HoG). Numerous approaches for object tracking have been proposed in the literature. Most tracking algorithms work on the Bayesian principle to determine the a posteriori probabilities of all possible tracks. Classical approaches to this include multiple hypothesis tracking (MHT) [160], joint-probabilistic data association filter (JPDAF) [161], and recently, particle filters (also known as Sequential Monte Carlo methods) [162], have been popular. However, the core difference between them is the way they implement the appearance model and handle the combinatorial explosion of the track space [66]. Accurate tracking in crowded environments, in the presence of clutter and occlusions is still an open research problem.

Identification

There are two ways a camera can be used to identify people, namely, face and gait recognition. One of the first face recognition methods was based on eigenfaces developed by Turk and Pentland's [148]. Their approach used PCA to create a face-space. Each face was interpreted as a subset of its eigenvalues. The recognition worked by projecting faces onto a feature space, which was created from sample data. However, this was a holistic approach (used the whole face region as a raw input) and not robust to occlusions or unexpected variations in facial expressions. Although Wiskott et al. [163] showed 99% success rate using PCA-based methods, its rates largely depended on the same-person images in the training set, and on the similarity between the training and testing sets [66]. Moreover, these rates dropped dramatically as facial expressions changed, rotated, or the lighting varied. For training sets with only a single image per person, one of the most successful systems is the Elastic Bunch Graph Matching (EBGM) developed by Wiskott et al. [163]. Local features (eyes, nose, mouth, etc) are first extracted and then these local features are represented by Gabor wavelet coefficients for different scales and rotations based on fixed wavelet bases. Then the recognition is done using a graph similarity measure. Although this approach is more

robust than the holistic approach, it is still not reliable or accurate enough. For example, most eye localization techniques fail if the eye is closed.

Most of the vision base gait recognition methods [164-166] are based on the person's exact silhouette and failed if the person wore different clothing or carried a backpack or when the environment was highly cluttered.

3.4.2 Instrumented, Single-Modality Approaches for Human Sensing

In instrumented approaches the person has to carry wearable devices that openly announce its presence. The unique advantage of these approaches is that they can perform near perfect person detection, tracking and identification. The main challenge in these approaches is localisation [66]. Depending on the way the sensor is distributed, instrumented approaches can be further divided as ‘Absolute location’ and ‘Relative location’ approaches. Absolute location approaches use external readers/sensors placed on several places throughout the environment, whereas relative location approaches are based on on-board sensors.

3.4.2.1 Absolute Location approach

Satellite-based Global positioning systems (GPS) are widely used for tracking users outdoor. However, GPS does not fit well in indoor environments, as satellite signals cannot penetrate buildings [167]. Most of the outdoor-based localization solutions are not feasible in indoor environments. Indoor localization is challenging due to no line of sight, multipath effect and noise interference [168]. Various obstacles such as walls, equipment or human being can influence the electromagnetic waves and degrade the accuracy of positioning [167]. Bearing these shortcomings, in the past 15 years, various commercial and research oriented indoor positioning systems have become available for tracking humans in real time.

Indoor GPS is similar to outdoor methods, consisting of pseudo satellites and the receivers can achieve high localisation accuracy. But they are too complex and expensive and require line-of-sight [117, 169]. As shown in Figure 3-4, there are two main steps in any absolute indoor localization process: measuring the signal and

position calculation. In the first step, some signals are transmitted between the target node (attached to people) and a number of reference nodes (placed at known locations). Signal properties such as TOA (Time of Arrival), TDOA (Time difference of Arrival), RSS (Received Signal Strength), and AOA (Angle of Arrival) are extracted during this stage. In the next stage, the sensor forwards these extracted parameters to the base station (PC) to process the received data. Based on these extracted signal parameters and the known coordinates of the reference nodes, the base station employs some positioning techniques such as mapping (fingerprinting) or geometric approaches (trilateration or triangulation techniques) to calculate the physical position (i.e. coordinates) of the target.

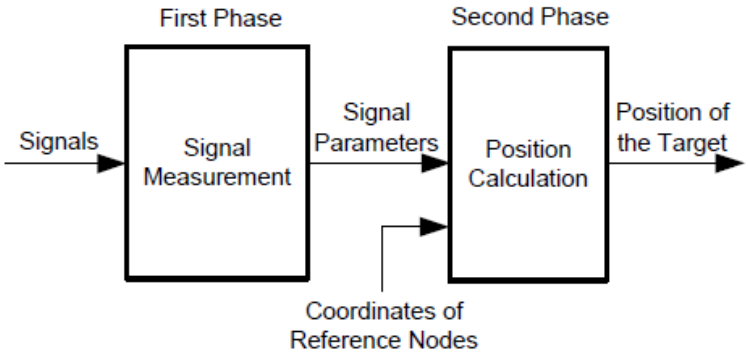

Figure 3-4: Two-phase localisation [168].

These techniques may be used separately or jointly. In addition, optimisation-based statistical techniques are also employed to filter the measurement noise and improve location accuracy. Along with the signal measurement method and positioning algorithm, signal technology that the localisation system is using, has a high impact on the accuracy of the positioning system. Different companies, research centres and universities have developed a number of wireless technologies such as IR, ultrasound (US), radio frequency (RF), electromagnetic waves, vision-based analysis and audible sound. Features of some common wireless localization techniques are given in Table 3-1. Each system has its advantages and its drawbacks. Usually, there is a trade-off between the price and the performance. [168, 170]

IR-based Systems

Several IR based products are available for identifying locations of objects. IR-tags periodically transmit their identification codes by emitting infrared light to readers

installed throughout the facility [171]. IR signal attenuation is relatively high, requiring close proximity between transmitter and receiver [172]. IR waves cannot penetrate opaque materials thus the system fails when the user's clothes cover an IR tag. Despite the fact that the IR emitters are cheap, the whole system using camera array and connected via wires is expensive compared to the coverage area. Moreover, fluorescent light and sunlight interfere with IR signals. This can be resolved by using optical and electronic filters to reject the disturbance from the light sources, which again raise the cost of the positioning system**.** Active Badge [173], Firefly [174], and OPTOTRAK [175] are examples of some IR based positioning systems. Such systems are utilised for inventory management where the degree of accuracy needed is at the room level [168].

RF-based Systems

Based on the use of radio waves from low frequencies to high frequencies, there are many mobile objects identification, location and tracking techniques that have been developed. RF is superior in terms of range, scalability, deployment, and maintenance over IR based localisation systems. Radio waves can penetrate walls and human bodies thus they can cover a larger area than indoor localisation systems. They are remarkably fast, for example, LANDMARK [176] systems can read RF tags in less than a 100 milliseconds. Besides, an RF system can uniquely identify people or objects tracked in the system. Triangulation and fingerprinting techniques are widely used in RF-based positioning systems. Based on this technology, RFID, WLAN (Wireless Local Area Network), Bluetooth, Wireless sensor networks, UWB are created. Table 3-2 presents some features of common wireless localization techniques. A WLAN-based positioning system reuses the existing WLAN infrastructures, which lower the cost of indoor localisation. TOA jointly with UWB technology offers higher accuracy among all these technologies. Due to short pulse duration (less than 1 nano second) it can filter the reflected signals from the original signal [167, 168, 177, 178].

US-based Systems

US-based positioning is relatively simple, cheaper and requires less signal processing as compared to other technologies. It has lower accuracy (several centimetres) than IR (several millimetres). Reflected US signals and other noise sources in indoor like jangling metal objects, crisp packets, etc degrade the accuracy of US based positioning systems[167]. Usually US is combined with RF technology to fulfil the synchronisation

requirement, which in turn adds further cost to the final system. Active Bat [179] and Cricket [180] are very well known US-based localisation technologies.

Table 3-2: Features of some common Wireless localization Techniques.

System	Network	Method	Accuracy	Overall Evaluation (A: Advantage; Disadvantage)
WhereNet [181]	RFID	TDOA	2 m to 3 m	A: Unique Identification, small lightweight tag D: Need Numerous infrastructure components
Compass [182]	WLAN	Fingerprint	1.65 m out of 312 m2	A: Reuse the existing WLAN, consider the orientation impact of the user D: Only consider single user.
Topaz [183]	Bluetooth	Not Available	2 m to 3 m	A: Multi-Person Tracking D: Expensive, Slow update rates (10s-30s)
Ubisense [184]	UWB	TDOA and AOA Triangulation	10 cm	A: No line-of-sight required, no multipath distortion, less interference, high penetration ability, large coverage area, high accuracy D: Expensive
Active Badge [173]	IR	RSS	Room level	A: Address privacy D: influenced by fluorescent light and sunlight
Firefly [174]	IR	Not Available	3.0 mm	A: High level accuracy; D: coverage area is limited to 7m.
Optotrak [175]	IR	Not Available	0.1 mm to 0.5 mm	A: High accuracy; D: Limited by line-of-sight requirement.
IRIS_LPS [185]	IR	Triangulation	16 cm out of 100 m2	A: Larger covered area D: Subject to interference from florescent light and sunlight
Active Bat [179]	US	Multilateration	3 cm out of 1000 m2	A: Cover large area, High Accuracy D: Expensive, Subject to reflections of obstacles;
Sonitor [183, 186]	US	Not Available	Room level	A: Energy-efficient, No line of sight required D: Low level accuracy
Cricket [180]	US,RF	TOA Triangulation	10 cm	A: Address privacy; low cost. D: More energy consumption
Motion –Star [187]	Magnetic	Not Available	1 cm	A: High accuracy, No line-of-sight required D:Low range(3m)
TRIP [188]	Vision	Not Available	6 cm	A:Inexpensive D:Line of sight required, Low range(3m)
Beep [189]	Audio	TOA Triangulation	0.4 m	A: Cheap D: Influenced by other sound sources

Magnetic Positioning System

Magnetic positioning systems use magnetic signals and offer high accuracy and do not require line-of sight. MotionStar wireless [187] is developed by Ascension Technology. It provides precise body motion tracking by measuring wirelessly numerous sensors mounted on different parts of a person. This is used by various applications, such as

animation, biomechanics, virtual reality, etc. The magnetic-based positioning systems can offer higher accuracy (1 cm) and support multi-position tracking. However, the limited coverage range (3 m) is a drawback for magnetic positioning systems. Moreover, presence of metal objects in the environment affects the MotionStar positioning system [167].

Audible Sound Positioning System

Audio sound emitted by the mobile phone or PDA can be used for indoor positioning. Beep [189] is an example of cheap positioning solution using audible sound technology. Audible sound does not have high penetration ability, so the scope of an infrastructure component is within a single room. Additionally, transmitting audible sound is a kind of noise to indoor environments, where people would not like to hear audible sound made by the positioning services.

Vision-based Positioning System

Vision based Indoor positioning is inexpensive which involves mounting multiple cameras at different viewpoints to get images containing the target object and to estimate its location using various image processing algorithms [190, 191].The TRIP [188] system employs computer vision techniques to track printable 2D circular bar code tags on users and devices. Compared to untagged vision based location systems [190, 192], the processing demands of TRIP are low. However, the performance of vision-based localisation is very sensitive to the camera characteristics such as blur, noise and frame rate. Moreover, it requires direct line of sight between the camera and the tag. CyberCode [193] is another similar vision-based tracking system [117, 188].

3.4.2.2 Relative Location approaches

The relative position between the mobile robot and the person/mobile object can be estimated without stationary external sensors fixed at known positions in the environment. The mobile robot could thus sense a human target for detecting, identifying and localising in order to guide them from one place to another based solely on the sensors placed on mobile robot. This is challenging as both the mobile robot and the human are in motion.

Infrared Emitter

Ohya et al [194, 195] used infrared LED in order to develop a human escorting mobile robot. They designed a light emitting device with two infrared LEDs fixed on a stick. The device is carried by a person on his waist perpendicular to the ground. Two LEDs flash on an interval and the robot's on board camera captures the image of this device and calculates the distance from the human. It can also appreciate the direction taken by the device by determining the distance between the lights and the central vertical axis of the image. In order to keep the device in the field of vision of the camera, the camera rotates, and because the orientation of the light emitting device rotates in the image, the LEDs are always kept in the centre of the image. It only works while the distance between robot and the LEDs is within 0 to 3 m. Due to the nature of infrared signals, line of sight is mandatory at all times between the robot and the device. If an obstacle is found, the robot stops until it is removed. Moreover, it is difficult to synchronise the successive image capture exactly when the LEDs are on and off [196].

Gigliotta et al. [196] used an IR emitter for a person-following mobile robot. They developed an infrared sensor-emitter device based on the IR beacon .The emitter device consists of four infrared emitters and is placed on a target person. The receiver device, which includes four infrared receivers, is orientated in the four cardinal directions on the mobile robot. It computes the intensity of the received signal, and returns the relative direction of the emitter (up to a distance of about 6 m). The robot can locate and follow a human target moving in a domestic environment. Due to IR characteristics, it only works while the robot and the target person are in line of sight.

Ultrasonic Transponder

Ohya et al [197, 198] used ultrasonic sensors to estimate the position of a specific person by the mobile robot. The ultrasonic sensor on the mobile robot has one transmitter and three receivers and tracks the person carrying an ultrasonic transponder. The distance between the robot and the tracked transponder is calculated from the inclination angle and difference of time of flight at two receivers on the mobile platform. To recognise a specific person among other objects, they have separated the ultrasonic waves emitted by the robot from the ones emitted by the transponder carried by the object. The robot transmits an ultrasonic pulse A and the object which has a transponder transmits another ultrasonic pulse B after detecting pulse A while pulse A is

returned by the reflection at an obstacle. Nuñez et al. [199] used similar US sensor arrangement as Ohya et al. [197, 198] to develop their Electronic Luggage Follower (ELF) that follows the user.

RF-based approaches

RFID is very promising due to the no contact and non-line-of-sight nature of this technology. The robot equipped with a single active RFID reader can easily identify an RF tag instrumented person using the RF signal transmitted from the tag, but a single RFID reader cannot provide accurate location information. GPS systems use the flight time of RF signals to approximate the distance between GPS satellites and the GPS receiver [200]. RF based distance calculation is based on TOA and it is really impractical at short ranges. The TOA technique requires very fast processors with extremely accurate clocks. GPS works in a similar fashion to this but only because the signals are travelling quite a large distance from satellite to receiver. It takes 300 nanoseconds for a signal to traverse 100 m (approx.). There are neither any processors or clocks in embedded controllers that can run fast enough to time the signal, including all associated instruction clock cycles for taking a measurement as well as intervening operating system clock cycles, nor any methodology that calibrates the origination time of the transmission per tag without having substantial impact on the anti-collision properties of multi- RFID. The reason GPS works is because the signal takes up to 30 microseconds to arrive from satellites, well within the clocking capabilities of high powered embedded controllers which would account for the high cost of GPS units [201].

One of the solutions is based on RF signal strength (RSS) analysis. Theoretically, the RF signal strength is inversely proportional to the square root of the distance. The distance can be calculated from the signal strength [202], but radio propagation in indoor environments is subject to numerous problems such as severe multipath, rare line-of sight path, absorption, diffraction, and reflection. The wave strength is reduced not only by the distance, but also the scattering and reflection of the wave [202]. This makes it difficult to measure signals precisely. Benkic et al. carried out an experiment and proved that RSS is, in fact, a poor distance estimator when using wireless sensor networks in buildings due to reflection, scattering and other physical properties that have an extreme impact on RSS measurement [203]. For these reasons, despite all the

promise surrounding RFID, it is still not possible to locate an RFID tag from a single RFID reader, particularly in cluttered or dynamically changing environments. A single RFID reader can only detect if the tag is in its range. RFID systems are still developing. Accurate distance estimation of an RF Tag from a single RFID reader is still a hot topic in the academic arena, particularly in cluttered or dynamically changing environments.

The RFID Radar [204] from Trolley Scan can provide an accurate position of the transponder using only a single reader. RFID Radar operates on 870 MHz with a bandwidth of 10 kHz. The principle is based on both TOA and AOA methods and consists of a single reader and an array of antennas. When a transponder enters the area covered by the emitting antenna, it sends its ID. The signal is then transmitted by the transponder and is received by two receiving antennas. Based on the time difference between the two received signals and the range data, it computes the angle and the distance information. This system has some disadvantages. Before starting the measurement session, the receiver itself must be calibrated for every site in order to compensate the influence of antennas, cables and receiver positions. Moreover the receiver and antenna system needs to be placed in a static position. Thus it is not suitable for the PGM mobile platform [205].

Kim et al. [202] designed a prototype of a 3-axis orthogonal array antenna to determine the direction of a tag by comparing the measured signal strength in each axis of the antenna. The antenna consists of three loop antennas of the same geometry and characteristics. The distance from the reader antenna to the tag can be determined by the phase shift of electromagnetic signals received from the transponder at each antenna. Their proposed system is still in its simulation phase. Currently, experiments are under way for validation beyond simulation.

Kim et al. [206-209] later developed a prototype system that could guide an RFID based mobile robot to a transponder position. This system consists of a 315MHz RFID reader that reads the tag data simultaneously and picks up the direction of the transponder using the received signal strength pattern. At the initial stage [206], in order to find the AOA of the signal, they attached a loop antenna onto the pan head of the mobile robot. This system could sense only the stationary transponder, because it was required to repeat the scanning of the environment to estimate the direction of arrival (DOA) of the

signal. The robot therefore could not detect changes in its surroundings while moving. To cope with this problem they later substituted the single antenna with a dual directional antenna to estimate the DOA of signals from various transponders by using the ratio of the received strengths between the two antennas [207]. The dual directional antenna system consists of two identical loop antennas perpendicularly positioned to each other having a 90^{o} phase difference. It finds the DOA of signals by the ratio of the signal strength between two antennas without scanning the environment. Since the system can detect changes in the DOA of the transmitted signal in real time, it can monitor the changes in target transponder locations while keeping the robot moving around. The reader was able to track any target moving unpredictably by rotating the dual-directional antenna to keep the ratio of the received signal strengths at the crossover point. The results of the experimental tests showed that the accuracy was within a reasonable range in an obstacle-free environment. However, in real environments, RF signals were easily distorted by obstacles that reflected and/or scattered the transmitting signal. This resulted in incorrect direction finding and the robot lost its way to the target in a cluttered environment. To cope with this problem, [208] the direction correction algorithm is proposed to triangulate the location of the transponder with the most recent three DOA estimates. However, in their latest paper [208] they concluded that the success rate of their system does not reach a satisfactory level to be used in commercial mobile robots.

Kanda et al [210] developed a humanoid teaching robot using “Robovie” and utilised the RFID tag for person identification. In this system, a tag periodically broadcasts its ID at 303 MHz, which is received by the reader attached to the top of the robot. In order to identify persons and separate them into participant and observer categories according to their distance, the reader has eight steps of attenuation to reduce the maximum gain of the receiver by 12.4 % with each step. As the attenuation parameter setting is increased, the readable area decreases, but with high attenuation, the readable area for the tag system becomes oversensitive to the noise radiated by the robot itself. According to Halls theory they used a distance of less than 1.2 m which is “conversational,” and a distance from 1.2 m to 3.5 m which is “social.” The attenuation parameter was frequently changed to categorise the participant. However, the time needed to detect a person was a little bit slow and the delay is about 10 seconds. Similarly, Hori et al. [211] proposed a method to estimate the position of an RFID tag by changing the

transmission power of the RFID reader. The transmission power of the RFID reader can be changed by three steps: Long-Range, Middle-Range, and Short-Range. First the robot searches for the presence of tags by the Long-Range at a certain position. Second, if the robot detects the presence of tags, it repeats the search by the Middle-Range and the Short-Range at the same position, i.e. the robot searches for the positions of tags within the long-range in detail. The robots and tags need to be in static position during this estimation. This is not a practical solution for person tracking by a mobile robot during the guidance operation as both of them are in motion.

Dead Reckoning

The Dead Reckoning (DR) process estimates one's current position from inertial measurements, such as speed or acceleration. The most widely used sensors for this purpose are Inertial Measurement Units (IMU) containing accelerometers, gyroscopes and magnetometers. The main basis of dead reckoning is that if one's location at time t is known, then their location at $t+i$.e. Δt can be inferred by integrating his velocity or twice integrating his acceleration, during the time interval Δt. However, since the new positions are estimated entirely from the previous positions, accumulated measurement errors grow over time. This causes the location estimation to quickly diverge from the real one. Dorota et al. employed a technique called zero-velocity updates (ZUPTs) [212] to mitigate these cumulative errors and later several researchers employed this technique. Basically, the solution is to mount the IMU on the foot and whenever the IMU detects that the shoe is touching the ground it assumes that the true velocity and acceleration of that foot is zero. Therefore, if at that moment the velocity inference is set to 0 m/s, then the errors accumulated from the integration of the acceleration component will be effectively discarded [66]. With this technique Ojeda and Borenstein [213] could infer a person's actual path with an error rate of 2%. Rather than simply setting the velocity to zero, Foxlin [214] entered the ZUPT information as a pseudo measurement in an extended Kalman filter and reduced the error to 0.2%. DR with foot-mounted IMU is a more viable method for motion inference compared to IMU sensors mounted in other locations such as mobile phones inside a person's pocket [66].

3.4.3 Sensor Fusion Approaches for Human Sensing

Multi-modal Sensor Fusion approaches integrate multiple sensors to combine their advantage while cancelling out their disadvantages as much as possible. These multi-

modal approaches on a system may give impressive results and can provide effective solutions to problems of occlusion and sensor errors. Considering the vast literature of this vain, the author excludes sensor fusion over distributed networks as the IWARD prerequisite is to rely on onboard sensors for operating in any unconstructed environment [66, 215-217].

3.4.3.1 Sensor Fusion over unconstructed environment

Cameras and Microphones

Several researchers integrated audio and video information to enable robots to choose and track a desired person. First they localised sound sources and then localised human faces for accurately selecting desired faces. These fusion approaches enable more precise speaker tracking than by sound alone. Additionally, in some instances, visual ambiguities (when a person moves too fast, for instance) are resolved by audio fusion [66]. This approach is especially useful for scenarios like face-to-face interaction [218]. For sound source localization, conventional methods require a microphone array, which usually consists of eight microphones. Nakadai et al. developed a system to localise multiple sound sources only using two microphones [219, 220] and fuse them with face detection data. Moreover, to classify multiple faces, they extracted the skin-colour. They have implemented this on their humanoid robot SIG-2. To cope with a loud noise and/or a dynamically changed environment Kim et al. [221] developed a probability based method to integrate audio and video information for SIG-2. The robot can recreate the colour feature whenever the illumination or background conditions change. They claim their system was able to track humans while dealing with various background noises, such as music played from audio components or voice signals generated by a TV or radio.

Camera and Laser Range-Finder

Similar to the speaker localization approach, where camera based face detection results are enhanced through microphones, many researchers [222-224] detected people by fusing face detection systems with laser range data to track a human. The legs of a person are extracted from laser range data while faces are detected in camera images. These authors were able to localise people around their robots even when their faces were not visible. Brooks and Williams [223] used a Kalman filter to fuse two sensors which was proved to be optimal for linear systems in case of Gaussian distributions.

Belloto [222] used an unscented Kalman filter (UKF) which performed well when the system was not linear.

Camera, Laser and Microphone

The combination of lasers with visual and additional auditory cues can be found in the BIRON [225] and ROKY [215] robots. BIRON detects people by using the laser-range-finder for detecting leg-profiles and combines this information with visual and auditory cues. The sensors providing input data are two microphones for sound source localisation, a pan-tilt camera for face and torso recognition, and a laser range finder for leg detection. Based on the colour of the clothes worn by the human, the torso is tracked with an adaptive colour segmentation approach. The torso helps to track a person when other cues are not available, e.g., due to visual occlusion of the legs. The drawback of these types of hierarchical approaches is the sequential integration of the sensory cues. These systems typically fail if the laser range finder yields no information [48, 218].

Rocky Lin et al. [215] incorporated similar sensory systems to detect and track multiple targets simultaneously for their mobile robot, Roky. The whole system is integrated and controlled with an agent-oriented robot control (ARC) architecture to handle the multi-modal information fusion. Their speaker direction estimation system consists of an eight-channel digital microphone array platform and an automatic DOA estimation system. A webcam is mounted on a pan-tilt platform for face detection and tracking. A laser scanner is installed in the lower-front side of the robot for human detection and obstacle avoidance. Although these three onboard sensory modules have different characteristics, their hypothesis is that these three sources of information will seldom malfunction at the same time and can complement each other.

Camera and Sonar

Wilhelm et al [217] developed an interactive mobile shopping assistant PERESES. The robot actively contacted potential users and guided them as needed through the market area. The system consisted of an omnidirectional and a frontal camera and sonar sensors. They deployed a two step solution. The first step consisted of the omnidirectional camera and sonar systems to provide a fast rough estimation of the potential user. In the second step, a high resolution image was checked for the presence of a face. In detail, during the first step the robot analysed its complete surroundings

using the omnidirectional camera. The camera provided a low resolution panoramic image with a 360◦ field of view. The panoramic image was automatically white balanced to cope with varying illumination conditions. At the same time the robots were equipped with two layers of sonar sensors with 24 sonars to measure the distance in every direction around the robot. They employed a condensation algorithm for fusing sonar and vision data. In the second step, the robot's active vision head consisting of a high resolution camera was turned to look towards this estimated position of the user's face. The active vision head looked continuously in the direction of the salient region. Thus, a high resolution image was grabbed and analysed with a face detector.

Camera, Sonar and Laser

The HOROS [226] robot is an extension of the PERESES robot. HOROS integrated the omnidirectional and frontal camera, the sonar sensors and the laser-range-finder. They kept the same sensor arrangement and hypothesis for the sonar rings & the omnidirectional camera and added a laser range finder to it to implement leg hypothesis for more robust tracking and guiding. Muller et al. later [48] claimed that the introduction of a motion model for interaction partners did improve the tracking robustness of PERSES in difficult environments.

Camera, Microphone and PIR

Sekmen [73] used the sound source localisation and PIR motion detection systems to provide the face-tracker system with candidate regions for finding a face from their robot named ISAC. The pan and tilt vision system locates a face from stereo images. The motion detector configuration consists of five PIR motion detectors that are placed in such a way that they can cover a large area. As the human walks in, the motion detectors can detect the body and turn the camera and initiate the tracking system. Furthermore, two small microphones are attached on the upper part of ISAC to localise the talker.

Camera, Laser and US

Itoh et al. [227] developed a person following mobile robot which follows a target subject while tracking one's back. They combined a stereo camera, a laser range sensor and ultrasonic sensors for performing this operation. They distinguished the specific person from the disparity image and colour distribution matching by a stereo camera.

Pan-Tilt function is added to the stereo camera to extend the view range of a robot. Sixteen ultrasonic sensors are attached around the torso of the robot, and the existence of an object can be recognized for all the directions by the measurement range scale 0.15 m to 10 m. Furthermore, in order to acquire surrounding information and the distance information to an exact object for the cognition of an obstacle, a laser range finder is attached ahead of the robot. They did not provide any quantitative analysis to assess the accuracy of their system nor their sensor aggregation method. Moreover, it is difficult to detect a specific person form the back when two of them having the same coloured shirt.

Vision and RFID

Jia et al. [138] used an Active RFID System and stereovision for human recognition. An RFID Reader attached with three antennas was installed on a mobile robot. Their proposed method first calculates the probability where a human with the ID tag exists, using Bayes rule, and then determines the region of interest (ROI) for stereo camera processing in order to get the accurate position and orientation of the human. The stereo image is then processed to recognise the human body pattern using the Hu moment invariants. An advantage of their method is that it does not need to process all images, thus reduces the number of images to be processed and the processing time hence enabling quick detection. Moreover, the Hu moment invariants' recognition method is insensitive to the variations in position, size and orientation. Their system can actually only distinguish the tagged human from other tagged obstacles such as tables, chairs etc. Furthermore, the maximum communication distance of RFID systems is only about 3.5 m.

German et al. [228] have fused the vision and RFID data for their person following robot named Rackham. They equipped their robot with an RFID reader, connected to an array of 8 directive antennas to detect the passive tags worn by the customer and a camera mounted on a pan-tilt unit. 8 antennas were aimed radially at different angles from its centre to detect tags in a 360° view field. A particle filter was used to fuse the azimuth measurements from the antenna array with the detections from the camera by simply rejecting all particles that do not fall within the detected azimuth range. From the experiment the fusion approach significantly outperformed the vision-only solution: the visual systems succeeded in 12% of the missions while more than 85% of them were

successfully performed using the multimodal counterpart. But as they use Passive RFID tags their range is limited within 0.5 m only.

3.4.3.2 Sensor Fusion over constructed environment

Several researchers [40, 217, 229-231] take the advantage of multisensory sensor fusion approaches in order to detect, count, localise, track, and identify people in a constructed environment. These systems require installing ubiquitous sensors which limits their operation only to a certain area. For a busy and crowded hospital environment it is not practical to use this type of solution. Additionally, others combined RFID with GPS [232], IMU [233], PIR [234] and Floor sensor [235] . Some combined Laser with GPS [236] and ID badge [237]. Kim et al. [238] and Li et al. [239] combined PIR with US. Furthermore, just to cite an example, Teixeira et al.[240] utilised vision with accelerometer.

3.5 Discussion

Instrumented approaches are more suitable than uninstrumented ones, especially for the purpose of identity-detection. For PGM, the IWARD robot can take the advantage of numerous commercial and research oriented indoor positioning systems that are available to identify, track and localise humans in real time. IR [175], US [179] and vision-based [185] positioning systems require line of sight between the tag and the reader. In an Audible Sound Positioning System, [189] sound can be interfered by other sound noises in the dynamic changing and crowded public place. Although Magnetic positioning systems do not require line-of sight they have a limited coverage range (3 m).

RF based positioning systems seem the obvious choice as they do not require line of sight and they can cover larger area than any other systems. Although, a WLAN-based positioning system reuses the existing WLAN infrastructures, which lowers the cost of indoor localisation, their accuracy is only 1.65 m out of a 312 m^2 area [167]. Similarly the Bluetooth based Topaz is very expensive and accuracy lies between 2 m to 3 m. An active-type RFID based absolute localisation system such as WhereNet [181] based on TDOA has only 2 m to 3 m accuracy. Thus, with this accuracy alone, the robot cannot approach the target person and continue its guide operation. Ubisense [184] uses TOA jointly with UWB technology and offers higher accuracy among all these technologies.

However, they are very expensive. Unfortunately, all these existing systems that provide absolute positioning information are often not a practical solution for mobile robotics since they typically rely upon pre-installed and calibrated environmental infrastructures. It might not be acceptable to retrofit the whole hospital area with external sensors. Absolute Location systems require a complex infrastructure of beacon nodes, which can be expensive and cumbersome to install and manage. Additionally, the number of stations and the interval between the stations affect the accuracy.

Rather than structuring the environment with external sensors, the best solution would be a simple plug & play solution using only the robot's on-board sensors. Hence, relative location technologies that do not require structuring the environment are economically more viable options for the PGM. Absolute location systems might be useful for robot navigation but in the IWARD project the navigation module has been developed by one of its other research partners. Relative location between the robot and the follower is sufficient for the PGM to estimate the follower position during the guidance operation to synchronise its speed accordingly. Surprisingly, research on the development of relative location systems based on infrared and/or radio sensors/emitters is a rather unexplored area. Infrared Emitter [194, 195] or Ultrasonic Transponder [199] have been tested by a few researchers on this purpose, unfortunately they only work in line of sight situations. Another system called Cricket [180] developed by MIT is very promising as it has a centimetre level accuracy. It uses the difference of arrival times between the RF signal and the ultrasonic pulse and can be used both as absolute and relative positioning. However, in such systems the optical line of sight is still required for transmitting the ultrasonic pulse.

As discussed, RFID is very promising due to the no contact and non-line-of-sight nature of this technology. The robot equipped with an active RFID reader can easily identify an RF tag instrumented person using the RF signal transmitted from the tag, but RFID does not usually support localisation. Additionally, radio propagation in indoor environment is subject to numerous problems such as severe multipath, rare line-of sight (LOS) path, absorption, diffraction, and reflection due to the presence of obstacles and people. For these reasons, despite all the promise surrounding RFID, it is still not possible to locate an RFID tag from a single RFID reader, particularly in cluttered or dynamically changing environments. A single RFID reader can only detect if the tag is

in its range. Kanda et al [210] continuously changed the transmission power of the reader to coarsely estimate the tags' position from the on-board RFID reader, which is worthy to note here. Unfortunately, the time needed to detect a person was relatively slow in their system. The delay is about 10 seconds. With such latency, the mobile robot might have significantly changed its position since the measurement took place. If the robot is travelling at 1 m/s and the localisation algorithm takes 5 seconds to complete from the time the ranging measurements were taken, the robot might be 5 m off from its intended position [172].

For uninstrumented scenarios, a camera is the best modality for human sensing. Cameras are inexpensive, and are the most field-tested solutions and widely used in mobile robots for person detecting, tracking and identification. Most solutions track people and identify them from faces [29, 39, 41]. Such systems assume that people coarsely face the robot. These approaches cannot be applied for a mobile robot which has to deal with moving people with faces that are not always perceivable [218]. Others extended the approach to skin colour [29, 36] or the full or upper human body detection. Some complementary approaches combine person detection and recognition [241, 242] in order to distinguish the targeted person from others. Stereo-based person detection provides more robust results than monocular approaches [151]. Some researchers [152-154] successfully applied foreground segmentation on disparity maps to differentiate people from the background scenery. Moreover, stereo-based approaches can provide information about the person's distance from the stereo head [139]. The field-of-view of conventional cameras is usually not more than 60 degrees, which means that a larger field-of-view can only be obtained through pan motion as implemented by [39]. Others [36, 47, 48] used an omnidirectional camera. Nevertheless, despite many advances, their performances heavily depend on the lighting conditions, viewing angle, distance to persons, and variability of humans' appearance in video streams. Detecting people across multiple image frames as well as robustly identifying them solely with visual features is still a topic of much research in computer vision. Moreover, in real environments, such as crowded hospitals, this solution is not practically feasible to implement, because occlusions frequently arise due to the existence of many people [228].

Scanning range-finders and Doppler-shift sensors hold second choice among uninstrumented sensing approaches. They are insensitive to lighting and require less processing power when compared to vision. The UWB radar [98]; [99] works through-the-wall but it can only detect static people. Laser and sonar approaches still require line of sight. Moreover, leg detection in a 2D scan does not provide robust features for discriminating the different persons in the robot's vicinity, while the detector fails when one leg occludes the other. Similarly, if multiple people walk with similar speed, their Doppler signatures interfere with each other. Recently UWB Doppler radars for detection and positioning of human beings in a complex environment became popular as they are immune against multi-path interference. But they are very expensive and cannot distinguish a certain person among others.

For resource-constrained scenarios, simple binary sensors are preferable. But they can only detect people and nothing else. It will require retrofitting the hospital environment, which is not a practical solution. Moreover, PIR cannot detect stationary people and floor tiles and EF sensors are difficult to install and interpret. Furthermore, all binary sensors require a high network density to provide accurate locations. Finally, binary sensor based person identification approaches [79, 81-85, 90, 243] only work among a small group of people over a constructed laboratory environment.

Despite the advances in the field, truly robust human-sensing is still practically an unrealised goal. Not any single module can robustly perform people detection, tracking, identification or localisation at the same time from a mobile platform. Multiperson tracking is still challenging in the real world, crowded environment such as hospitals, office buildings or in airports. People are easily lost, and tracks are often terminated or, even worse, incorrectly extended in the face of ambiguities [66].

The solution to overcome this issue for the PGM is sensor fusion. Sensor fusion approaches build upon the use of multiple sensors or sensing modalities in an attempt to combine their advantages while cancelling out their disadvantages as much as possible. These multi-modal sensing approaches have proven to be reliable and suitable for real-world applications. Multi-sensory systems increase the fault tolerance, reliability, robustness and precision of human sensing capability for mobile robots [66, 229, 235].

As discussed in section 3.4.3.2**,** sensor fusion over constructed environments is not a practical solution for the IWARD robot. Consequently, numerous guide robots considered multimodal sensor fusion for human sensing relying on onboard sensors. Typical approaches use cameras for face detection and microphones for sound source localisation. Speech-based user tracking is not suitable as single users typically don't speak along their paths, and background noise is significantly higher than the voice of a person in a distance of several meters [33]. Others combined cameras with: lasers [222-224]; sonar [217]; laser and sonar [48, 226]; laser and microphone [215, 225], microphone and PIR [73]; laser and US [227]. The major drawback of most of these hierarchical approaches is the sequential integration of the sensory cues. These systems typically fail if the laser range finder yields no information. Besides, for a mobile robot which has to deal with moving people, faces will not always be perceivable, hence verification could fail too. Moreover, unfortunately, not the least of them is overcome line-of-sight requirements in indoor environments [48].

Integration of Cricket, Stereovision and Active RFID modality should be an ideal solution for the IWARD PGM. Apart from person detection and tracking, stereo can provide distance information. Active RFID systems have a higher range than the passive ones and can perform accurate person identification and coarse localisation. Although similar combinations were employed in [228], their robots did not perform similar guiding tasks that the IWARD system required. In [228], vision and RFID data were fused for their person following robot. The person following robot has somewhat an opposite function than a person guiding robot where the robot follows a human instead of the human following the robot. Also they used passive RFID whose range is limited to only within 0.5 m and they used hierarchical approaches for sensory data integration. These systems typically fail if the RFID yields no information. Cricket sensors provide centimetre level distance accuracy when they are at line of sight. Feasibility of this sensor can be more rigorously scrutinized to find out whether it can be used as a third modality to be added with the other two choices.

3.6 Conclusion

- From Table 3-1, it should be clear that although there exist a multiplicity of guidance robots in today's market, performing a gamut of guidance and related activities none combine human sensing: detection, tracking and identification

capacities with the implementation of speed adaptation measures in one unified platform.

- Stable human sensing in unconstructed environments which rely solely on onboard sensors is a challenging endeavour but stands as a fundamental pre requisite for the IWARD robots in providing smooth patient and/or visitor guidance in a dynamic and crowded hospital arena.
- Guidance robots should not simply drive towards a goal and expect the person to follow them; rather, they should maintain constant awareness and verification to ensure the subject guided from the point of origin is indeed the same subject delivered to the intended destination.
- From the perspective of safety and physical comfort, the robot should always maintain an appropriate distance from the human and adapt its speed during guidance tasks.
- Existing guide robots do not fit into the modular concept of the IWARD project. These robots are standalone devices and cannot be coupled with other service modules.
- Price of existing guide robots is substantially at odds with the current and potentially future budget constraints of the project.
- In order to minimise the cost of such a system and to make it affordable to hospitals, the IWARD robot swarm relies heavily on relatively small, lightweight, low-cost, standardised components and plug-and-play sensors. In further contrast to large individual robots currently available in some hospitals, the robot swarm is based on smaller robots. This size reduction alone should result in less interference with persons and objects in a crowded hospital environment.
- Stereovision, Cricket and Active RFID represent the best modality across the board for uninstrumented and instrumented scenarios. The ideal solution would be a fail-safe non-hierarchical sensor fusion approach so that they can complement each other.
- If the IWARD project is successful and performs according to expectations it will represent a significant success in the field of Service Robotics research.

Chapter 4 Sensor Testing

4.1 Introduction

Based on the conclusions of the literature survey, it is obvious that in order to develop a reliable and robust system, a multisensor arrangement is necessary. To deal with all possible guiding scenarios, a combination of RFID, vision and direct distance measurement seems to be the best solution.

This chapter describes all the sensors that seem feasible for the PGM in details. Each of these sensors has undergone several tests under various scenarios at different indoor locations to analyse their performance. Section 4.2 describes the reason behind choosing the sensors. Section 4.3 deals with experiments of the cricket sensors developed by MIT. Section 4.4 describes Active RFID System from Wavetrend Ltd. Section 4.5 examines the stereo vision system. Section 4.6 presents the multisensory experiments and finally 4.7 draws the conclusions.

4.2 Sensor Selection

The cricket sensor developed by Massachusetts Institute of Technology (MIT) [180] is very promising as it has a centimetre level accuracy. The only real downside of this sensor is that it requires optical line of sight between the beacon and the receiver. A robust Design of Experiment (DOE) analysis has been performed for the Cricket sensor in section 4.3. All the possible factors which might arise in the PGM scenario were considered.

RFID is very promising due to the no-contact and non-line-of-sight nature of this technology. However, it is not possible to determine the distance of an RFID tag form the RFID reader exactly. A single RFID reader can only detect if the tag is in its range. In section 4.4 several approaches were investigated to find its suitability as PGM sensor.

Stereo-based approaches can provide information about the person's distance from the stereo head and it is widely used in mobile robots for person detection, tracking and identification. However, with their many advantages their performances heavily depend

on the lighting conditions, viewing angle, distance to persons, and variability of humans' appearance in video streams. Detecting people across multiple image frames as well as robustly identifying them solely with visual features is still a topic of much research in computer vision. Section 4.5 describes the development of a stereo head for IWARD and its experimental results.

From the literature survey in Chapter 3 it is evident that not any single modality is robust enough to fulfil the entire requirement of PGM. In order to provide a fail-safe patient guidance solution, a Multi-modal Sensor Fusion approach is ideal. In Section 4.6, experiments were carried out while all three of the above sensors ran synchronously.

4.3 Cricket Mote

The Cricket transceiver, as shown in the left side of Figure 4-1, is developed by MIT. It is based on TDOA of RF and US signals to compute distances. It can be configured as either beacon or listener. Its maximum range is about 10 m when the listener and the beacon are facing each other and there are no obstacles between them. The theoretical distance accuracy of the Cricket hardware is on the order of 1 cm at a distance of up to 3.5 m, and 2 cm in the rest of the 10 m range [244].

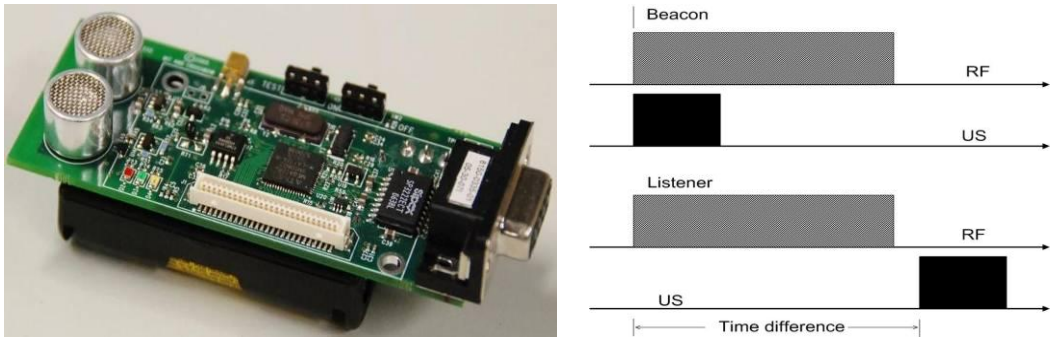

Figure 4-1: A Cricket hardware unit (left) [180]; Cricket principle for distance calculation (right) [245].

The Cricket beacon and listener hardware is identical. Each cricket dimension is: 20 cm × 5 cm × 2 cm. The Cricket hardware unit consist of a CC1000 RF transceiver, an Atmega 128L microcontroller and other related hardware for generating and receiving US signals and interfacing with the host device. The RF transceiver is configured to operate at 433 MHz and it sends and receives data at a rate of 19.2 kilobits/s. Both the

US transmitter and receiver are open-air type piezo-electric devices which operate at 40 KHz. Beacons periodically transmit a narrow ultrasonic pulse, followed by a RF message containing beacon ID, coordinates, space ID and measured ambient temperature. As RF (speed of light) travels about 10^6 times faster than ultrasound (speed of sound), a listener attached to the host device (e.g., mobile handheld, portable laptop, sensor, etc.) receives RF message first, followed by the US signal. The listener measures the time difference δT between the start of the RF message and the arrival of the US signal and compute the distance d to the beacon from:

$$\partial T = \frac{d}{v_u} - \frac{d}{v_r} \tag{4.1}$$

In normal room temperature and humidity, the speed of sound $v_u \cong 344$ m/s, and speed of light $v_r \cong 3 \times 10^8$ m/s. As $v_r >> v_u$

$$d \cong \delta T \,.\, v_u \tag{4.2}$$

The Cricket's distance measurement accuracy is subjected to the accurate measurement of the time interval δT and the accurate estimation of speed of sound. Accurate measurement of δT depends on various factors such as the RF bit rate, ultrasonic sensors and the detection circuits, and the timer resolution. On the other hand, the speed of sound in air depends on ambient temperature, humidity and atmospheric pressure. Indoor air contains varying amounts of water vapour with non-zero humidity. The speed of sound is less sensitive to relative humidity and atmospheric pressure. At 25^0C and 101.325 kPa, the speed of sound changes by only about 0.5% as the relative humidity changes from 0% to 100%. At 25^0C and 50% relative humidity, the speed of sound changes by only about 0.6% as the atmospheric pressure changes from 101.325 kPa to 30 kPa.

On the contrary, speed of sound is relatively more sensitive to temperature compared to humidity and atmospheric pressure variations. The speed of sound changes at approx. 0.18% per degree C. Indoor temperature can easily vary by even 10^0C within the same room. The Cricket hardware consists of a pre-calibrated thermistor-type temperature sensor to measure the ambient temperature with an accuracy of $\pm 1^0$C to compensate for variations in the speed of sound with temperature.

Lacking line of sight path between the beacon and the listener causes errors in cricket distance measurements. Due to no line of sight, the sound may reach the listener after bending over an edge (refraction) or after reflecting off of some object. These cause the sound to travel a longer distance than the Euclidean distance between the beacon and the listener. Priyantha [246] performed Cricket distance measurement performance test in a controlled environment to prevent outlier distance measurement due to reflected ultrasonic signal. From their experiment they concluded that the absolute measurement error increases with the beacon to listener distance. This is because increasing the distance causes the received US signal strength at the receiver to drop. This in turn causes the detection circuits to take a longer time to detect the signal, resulting in an increased positive error. Cricket has a ranging accuracy of about 0.5% when the beacon and the listener are 2 m apart and are facing each other and the ranging performance degrades as the separation increases and when they do not face each other.

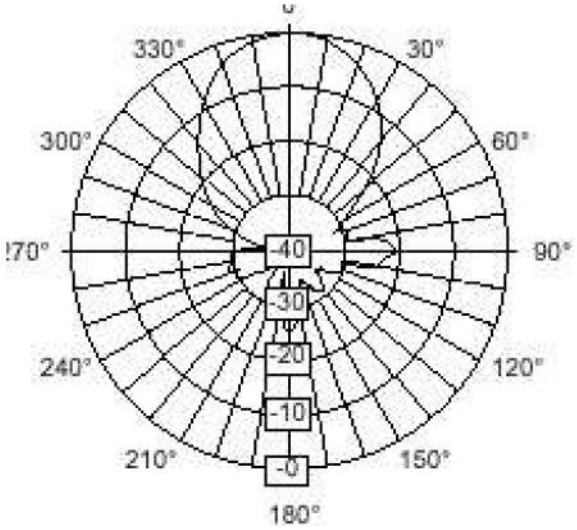

Figure 4-2: The radiation pattern of the Cricket ultrasonic transducer on a plane along its axis in (r, θ) polar coordinates. The r represents the signal strength (sensitivity) in dB and the θ represents the offset from the Z axis of the transducer [246].

The radiation pattern of a Cricket's US transducer is shown in Figure 4-2. From the pattern it is clear that with increasing θ, the received signal strength at the listener decreases and results in increased error. In the range (-40^o, 40^o), the error is under 5 cm. As the angle increases the ultrasonic signal at the listener becomes weaker to detect. At $\theta = 90^o$, there are no data points [244, 246]. Although the current implementation of Cricket has a physical form factor that is amenable to be used as a distance measurement sensor in the PGM, its accuracy needs to be analysed more robustly in real indoor environments. Priyantha's test result was carried out in a controlled environment.

Hence, it does not provide enough information whether it will be feasible for the IWARD project. In the IWARD patient guidance scenario, the robot needs to perform its guidance task in a crowded hospital environment. Common ultrasonic sources in a hospital environment such as certain faulty fluorescent lamps, jangling keys, air conditioners, and air conditioning ducts may deteriorate the cricket's system performance. Cricket's US receiver is a physical resonator that resonates at 40 KHz. Any loud noise in the environment, such as a banging door, can cause the receiver to resonate at 40 KHz and to generate ultrasonic noise. The orientation and decoration of the hospital environment such as corridors, reception area or in a patient ward etc. may differ and change from place to place and time to time. The line of sight path between the beacon and the listener may not be maintained during guiding. It is unknown how a follower carrying a beacon would orient himself toward the listener (on the robot). Moreover, during obstacle avoidance, cornering etc. the beacon and receiver would certainly disorient from each other which may cause the sound to reach the listener after reflection and/or refraction. This would result in the sound to travel a longer distance than the Euclidean distance between the beacon and the listener. Furthermore, different followers, having different physical heights, will also force the beacon to be placed vertically higher or lower relative to the listener.

To investigate the significant factors that have considerable effects on cricket distance performance measurement in real indoor environment, Design of Experiment (DOE) can be used. It is a powerful tool to establish functional relationships between independent and dependent variable in any experiment [247].

4.3.1 DOE for Cricket Distance Measurement Performance

Conventionally, experimentation has been done in an unorganised one factor- at-a-time manner. This method is inefficient and very often yields misleading results. In order to investigate the effect of various factors on cricket's performance, DOE has been used.

4.3.2 General 3^k Design

A three level experiment with k number of factors is addressed as a 3^k factorial design. These levels are usually referred as low, intermediate and high levels and numerically

expressed as 0, 1, and 2. The reason that the three-level designs are used in Cricket DoE is to model possible curvature in the response function and to handle the case of nominal factors at 3 levels. A third level for a continuous factor facilitates investigation of a quadratic relationship between the response and each of the factors [248]. Unfavourably, the size of the designs increases rapidly with k. For example, a 3^3 has 27 runs, the 3^4 has 81, and the 3^5 has 243 and so on.

4.3.3 Software Selection for DoE

For DoE, Design-Expert software (version 8) from Stat-Ease Inc was used [249]. The Design-Expert program offers various factorial design selection options. Factorials designs are useful for screening significant factors to sequentially model and refine a process. For cricket DOE analysis, 'General Factorial Design' is selected as it allows having factors that each has a different number of levels. It creates an experiment that includes all possible combinations of all factor levels of choice. Although a general factorial design primarily deals with categoric factors (can either be specified as nominal or ordinal), it also allows converting truly continuous factors from categorical to numerical. Hence, it is possible to generate response surface graphs that provide a better perspective of the system making the results easier to interpret and understand [250].

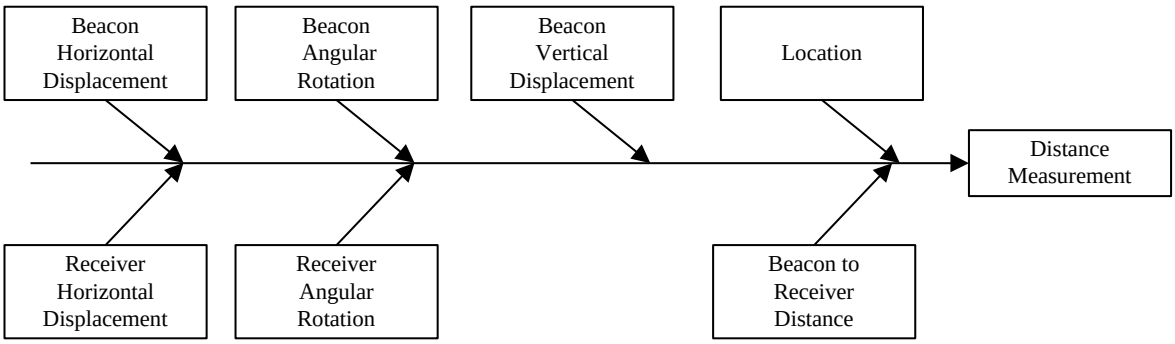

Figure 4-3: Fishbone diagram for DOE.

4.3.4 Factors and Levels Selection for DOE

There are several factors that might influence the Cricket distance estimation performance. Initial brainstormed factors are shown as fishbone diagram in Figure 4-3.

4.3.4.1 Beacon-to-Receiver Distance

From the literature [244, 246] it is clear that when the beacon and the receiver are at line of sight, measurement error increases with the beacon to listener distance. In the initial testing at several indoor locations, the cricket's maximum range was recorded up to 8 m. Noticeably, distance readings after 7 m onward are very infrequent. The received US signal at the receiver drops around this range. For the PGM, follower distance information up to 6 m is sufficient. Hence, to be in line with the PGM requirement and for the sake of frequent data mining, the maximum range of the Distance factor (beacon to reader distance) was kept at 6 m. The lower level of the 'Distance' factor was kept at 2 m to avoid transformation of responses data (For details see the Transformation Section in 4.3.7.2). As the beacon/receiver moves from the receiver/beacon horizontally (See Figure 4-4) the accuracy of Cricket's distance estimation drops as the sound requires to travel a longer distance than the Euclidean distance between the beacon and the listener. Due to such horizontal displacement, accuracy drops at higher rate at lower beacon-to-receiver distance compared to large beacon-to-receiver distance. For an example, from the initial testing it was revealed that at 1 m Euclidean distance and 1.5 m horizontal displacement the Cricket system outputs 1.91 m to the host device and the accuracy becomes only 9%. In another test, at 1 m Euclidean distance and line of sight between the receiver and the beacon the accuracy recorded was 100%. Thus the ratio of minimum and maximum responses becomes 11.11, which is greater than 10. Design Expert software requires transformation of responses data if the ratio is higher than 10. To avoid such transformation the low level for distance was selected as 2 m.

4.3.4.2 Beacon and Receiver's Horizontal Displacement

The term 'Horizontal Displacement' in this thesis means how far the receiver and beacon can be horizontally away from each other. This could have a significant effect on cricket distance measurement. During the guidance operation, the robot containing the cricket receiver would be positioned left or right (e.g. while cornering, avoiding obstacles). In this thesis such displacement is termed as 'Receiver Horizontal Displacement' (Figure 4-4 left). On the other hand, how followers equipped with a cricket beacon would orient themselves toward the robot is unpredictable. Such displacement is termed as 'Beacon Horizontal Displacement' (Figure 4-4 right). To select an acceptable limit for these horizontal displacement factors, an initial test was carried out.

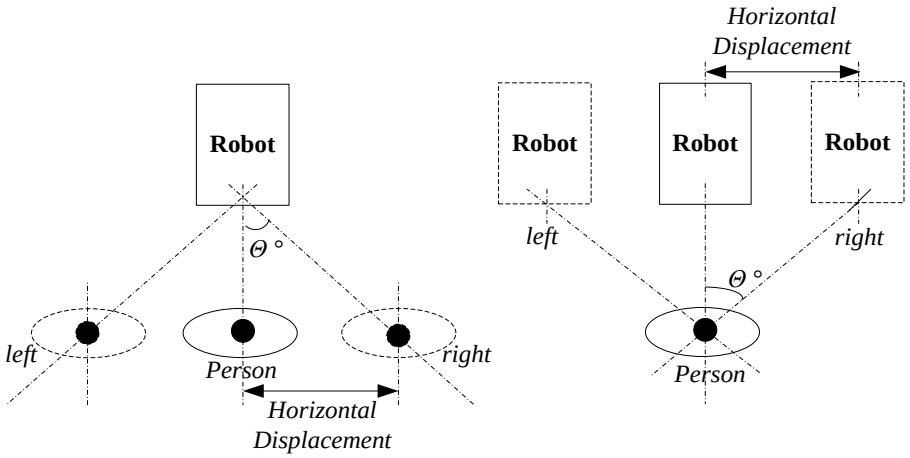

Figure 4-4: Horizontal displacement of beacon (left) and receiver (right).

The goal was to observe the maximum horizontal ranges. In this experiment the receiver was placed on a fixed position and the beacon position was horizontally moved at every 1 m beacon-to-receiver Euclidean distance up to 8 m. The recorded data are presented in Table 4-1.

Table 4-1: Results from 'Horizontal Range' test.

Distance(cm)	Horizontal Range (cm)	Reading (cm)	Accuracy (%)
100.00	150.00	185.50	14.50
200.00	225.00	312.00	44.00
300.00	240.00	394.00	68.66
400.00	235.00	473.00	81.75
500.00	270.00	574.50	85.10
600.00	217.00	639.50	93.41
700.00	200.00	728.00	96.00

Accuracy was calculated as follows:

$$Accuracy = \left[\left\{1 - \frac{|(Distnace - Reading)|}{Distnace}\right\}\right] \times 100 \quad (4.3)$$

As the beacon was shifted horizontally towards the left, the listener frequently reported distance readings up to 1.5 m from the Euclidean point at 1 m. After this range the readings were irregular. The maximum horizontal range (270 cm) was recorded at 5 m Euclidean distance. The horizontal range decreases as the Euclidean distance increases. From the accuracy column in Table 4-1, it can be observed that accuracy is worst at lower distances at its maximum horizontal displacement range. For frequent data mining the highest level of both beacon and receiver horizontal displacement factor was kept at 150 cm throughout the DOE. Figure 4-5 is showing the selected range (dark rectangle) for the DOE analysis.

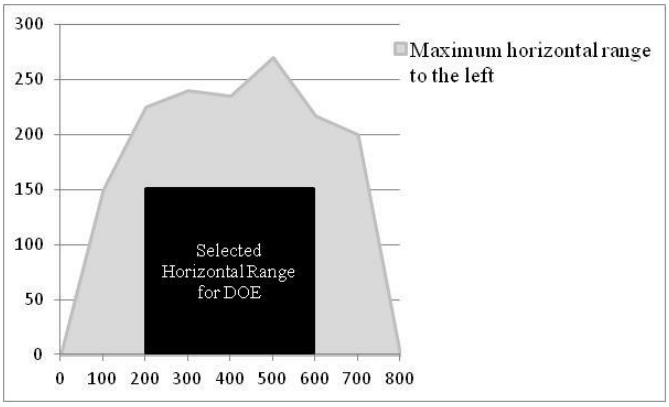

Figure 4-5: Graph showing the selected range (dark rectangle) for DOE. In the graph the x-axis represents the beacon-to-reader Euclidean distance (cm) and the y-axis is the horizontal range from the Euclidean point (cm).

4.3.4.3 Beacon and Receiver's Angular Displacement

It is obvious that during the guidance operation both beacon and receiver might rotate clockwise and/or anticlockwise from their line of sight position and it is unpredictable in a similar way to 'Horizontal Displacement'.

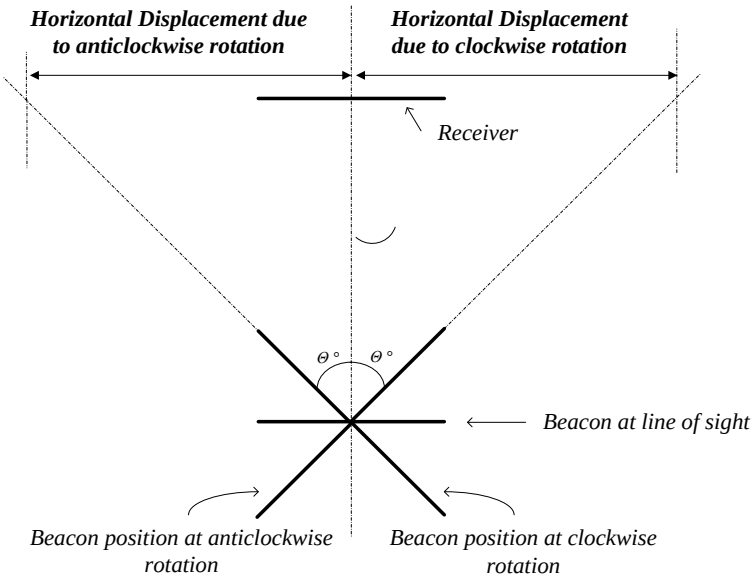

Figure 4-6: Angular rotation of beacon with respect to receiver.

Theoretically, conducting experiments with such angular rotation factors are similar to 'Horizontal Displacement'. When a beacon moves horizontally from a receiver, it also results in an angular displacement with respect to the receiver (Figure 4-6). Hence, to

avoid increasing the number of experiments, this angular displacement factor is discarded for the Cricket DOE analysis.

4.3.4.4 Vertical Displacement of the Beacon

The receiver would be placed on the robot at a constant height from the floor during the guidance operation. On the contrary, beacon position will vary depending on where it will be placed on the follower. The ideal place to equip a person with a beacon would be at their waist as it can be easily hooked with their belt or trouser.

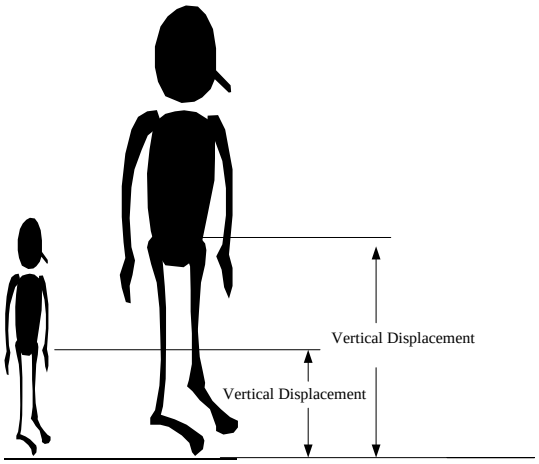

Figure 4-7: Showing Vertical displacement of the Beacon.

For the DoE analysis, the receiver will be at 60 cm above the floor. As different people have different physical heights, it is not possible to keep the beacon position vertically at the same height as the receiver. The difference in vertical heights is termed as vertical displacement in this thesis (Figure 4-7). Typically human height is twice of their waist height [251]. Thus a beacon, placed at 60 cm from the floor similar to the receiver vertical height, would mean the person's height is approximately 120 cm. For "Vertical Displacement" factor, the low level was selected as 60 cm. For mid level and high level, the beacon was placed at 80cm and 100 cm above from the floor to represent 160 cm and 200 cm height of the follower respectively.

4.3.4.5 Location

Location is an important qualitative factor that needs to be considered in Cricket DoE analysis. Environmental factors such as temperature, humidity, and atmospheric pressure cause errors in velocity of sound-based distance measurements. Though it is

possible to minimise errors by measuring these factors directly, the errors cannot be eliminated completely.

Figure 4-8: Corridor at DCU Computing Department.

Indoor RF and US signal propagation characteristics differ from place to place. Cricket operates at 433 MHz for transmitting location information. RF ranges rely on what types of antenna is used and what kind of obstacles is there in between a beacon and listeners. Indoor RF propagation is a well-researched topic. RF signal strength has no well-defined correlation with the distance between the RF transmitter and the receiver due to the reflection and attenuation of RF signals by metallic objects. Cricket US signals operate at 40 kHz. Unlike RF signals, they cannot penetrate physical objects such as walls and can be easily reflected off from such hard surfaces resulting listeners to receive a given ultrasonic transmission from multiple paths. To simulate different hospital environments, all experiments were carried out in two completely different indoor areas. The goal is to see how Cricket's distance measurement accuracy varies as the indoor environment varies.

The first DoE experiment was carried out in the corridor of DCU's computing building (Figure 4-8). It is 230 cm wide and one side has concrete wall and the other side has a thick glass wall. The second location is the large and wide reception arena of the DCU engineering building (Figure 4-9). The final selected factors and their levels for DOE analysis are presented in Table 4-2.

Figure 4-9: Wide reception area at DCU engineering building

Table 4-2: Factors and their levels for DOE. All units are in centimetres.

Factors	**Levels**		
	Low	Intermediate	High
Receiver Horizontal Displacement	0	75	150
Beacon Horizontal Displacement	0	75	150
Beacon Vertical Displacement	60	80	100
Beacon to Receiver Distance	200	400	600

4.3.5 Design Summary

Two general full factorial DOE analysis were carried out for two different locations. Although location itself can be used as a qualitative factor in general factorial design, it was omitted intentionally to reduce the number of runs. For example, two 4 factor and 3 level experiments require, $3^4 + 3^4 = 81 + 81 = 162$ runs. Whereas five factors (including location as a factor) would require**,** $3^5 = 243$ complete runs. A summary of the DOE studies investigated in this research is summarised in Table 4-3.

Table 4-3: Summary of DOE studies.

Experiment type	Description	Factors	Responses
3^4 Full-Factorial Design	4 factors	Receiver Horizontal Displacement	Accuracy
	3 levels	Beacon Horizontal displacement	
	1 response	Beacon Vertical Displacement	
	81experiments	Beacon to Receiver Distance	

4.3.6 Experimental Set up

The listener was placed on a cart as shown in the left side of Figure 4-10. The laptop running on Linux was attached to it through a USB to RS232 converter. Software for continuously retrieving distance from the cricket listener was developed for this experiment. The beacon was attached to a stand (Figure 4-10, right) and its vertical position was changed according to the requirements.

Figure 4-10: Experiment set up in the corridor. The listener is placed on a cart (left) and the beacon is attached to a stand (right).

4.3.7 Accuracy Model for Corridor

4.3.7.1 Response Data

Experiments were carried out in randomised order to 'average out' extraneous factors that may be present. This technique is called 'randomisation' [247, 252]. At each

combination of settings provided by the DOE software, the Cricket distance measurements were noted and the accuracy was calculated. If there were several readings for one setting, they were averaged. The first 10 responses are shown in Table 4-4. Complete data sheets are attached in Appendix A. The summary of Corridor DOE is presented in Table 4-5. When the beacon and the listener were at 2 m distance, the maximum accuracy was recorded as 100% and the minimum accuracy was 71.25% with an average of 90.55 %. At this distance range, the standard deviation of response data was found 10.2 cm.

Table 4-4: First 10-Response data in Corridor DOE analysis.

Select	Std	Run	Factor 1 A:Receiver Horizontal Displace... cm	Factor 2 B:Beacon Horizontal Displ... cm	Factor 3 C:Beacon Vertical Displac... cm	Factor 4 D:Distance cm	Response 1 Accuracy %
	45	1	150.00	150.00	80.00	400.00	99.125
	70	2	0.00	150.00	80.00	600.00	97.3333
	10	3	0.00	0.00	80.00	200.00	100
	5	4	75.00	75.00	60.00	200.00	100
	58	5	0.00	75.00	60.00	600.00	99.6667
	66	6	150.00	0.00	80.00	600.00	96.9167
	32	7	75.00	75.00	60.00	400.00	99.125
	71	8	75.00	150.00	80.00	600.00	99.75
	42	9	150.00	75.00	80.00	400.00	99
	76	10	0.00	75.00	100.00	600.00	99.9167

At 4 m distance range, maximum and minimum accuracies were recorded respectively as 99.75% and 92.73%. Average accuracy at this range was founded as 97.92% with a standard deviation of 2.55 cm. It is noticeable that accuracy is increasing and standard deviation of responses is decreasing with increasing the beacon-to-listener distance.

Table 4-5: Design summary for corridor area.

Factor	Name	Units	Type	Subtype	Minimum	Maximum	Coded	Values	Mean	Std. Dev.	
A	R.H.D	cm	Numeric	Continuous	0	150	-1.000=0.00	1.000=150.	75	61.23724	
B	B.H.D	cm	Numeric	Continuous	0	150	-1.000=0.00	1.000=150.	75	61.23724	
C	B.V.D	cm	Numeric	Continuous	60	100	-1.000=60.00	1.000=100.	80	16.32993	
D	Distance	cm	Numeric	Continuous	200	600	-1.000=200.00	1.000=600.	400	163.2993	
Respons	**Name**	**Units**	**Obs**	**Analysis**	**Minimum**	**Maximum**	**Mean**	**Std. Dev.**	**Ratio**	**Trans**	**Model**
Y1	Accuracy	%	81	Polynomial	71.25	100	95.81864444	7.113386	1.4	None	RCubic

Design Summary				
Study Type	Response Surface		**Runs**	81
Design Type	D-optimal	Best	**Blocks**	No Blocks
Design Model	2FI		**Build Time (ms)**	1.25963

Finally at 6 m distance range, maximum accuracy was recorded as 100% and minimum was 96.92%. Like in the previous result, the average accuracy responses increased to 98.98% with and standard deviation was found as 1.12 cm.

4.3.7.2 Analysing the Results

Transformation

Response data ranges from 71.25 to 100 and the ratio of maximum to minimum response is 1.40351 (Figure 4-11). A ratio greater than 10 usually indicates that a transformation is required. For ratios less than 3 the power transmission has little effect.

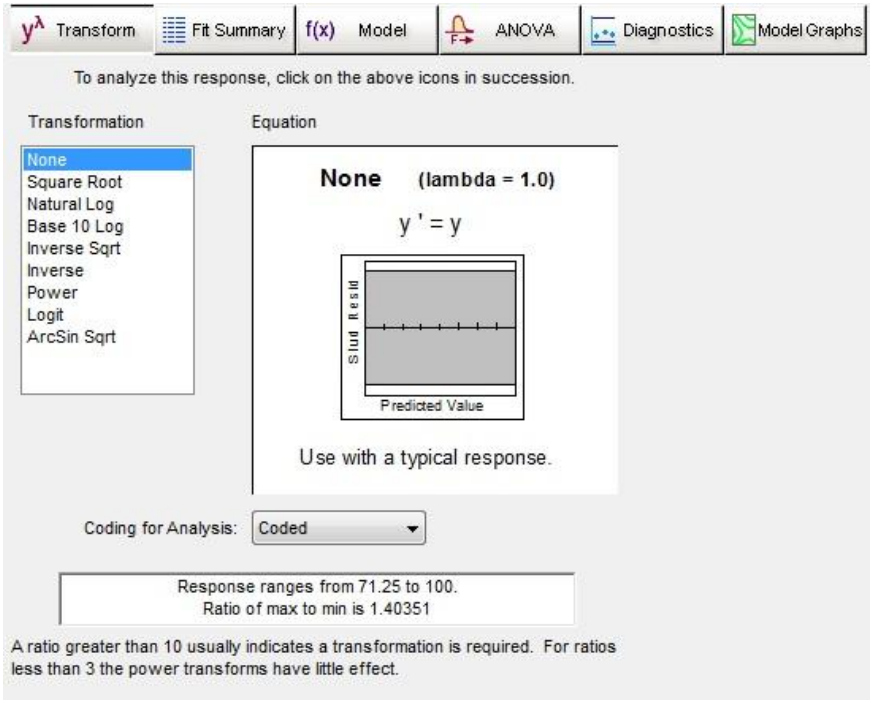

Figure 4-11: No transformation was selected for Corridor accuracy Model.

As the ratio of maximum and minimum responses of the corridor experiment is only 1.4, no transformation was performed which means that the responses were directly proportional to the factors imputed.

Effects

Design-Expert provides a model screen (Figure 4-12) containing all of the terms for a polynomial. All the main effects of the selected variables and any interaction effects were initially selected manually to fit a linear model. To eliminate negligible terms from the model, an automatic ‘stepwise regression’ was performed, which was supported by

the Design-Expert. It is very useful at the early stages of model building when it is not very clear which terms are really important [247]. Finally after stepwise regression Design Expert automatically selects all the necessary terms to make the model hierarchical (See Figure 4-12).

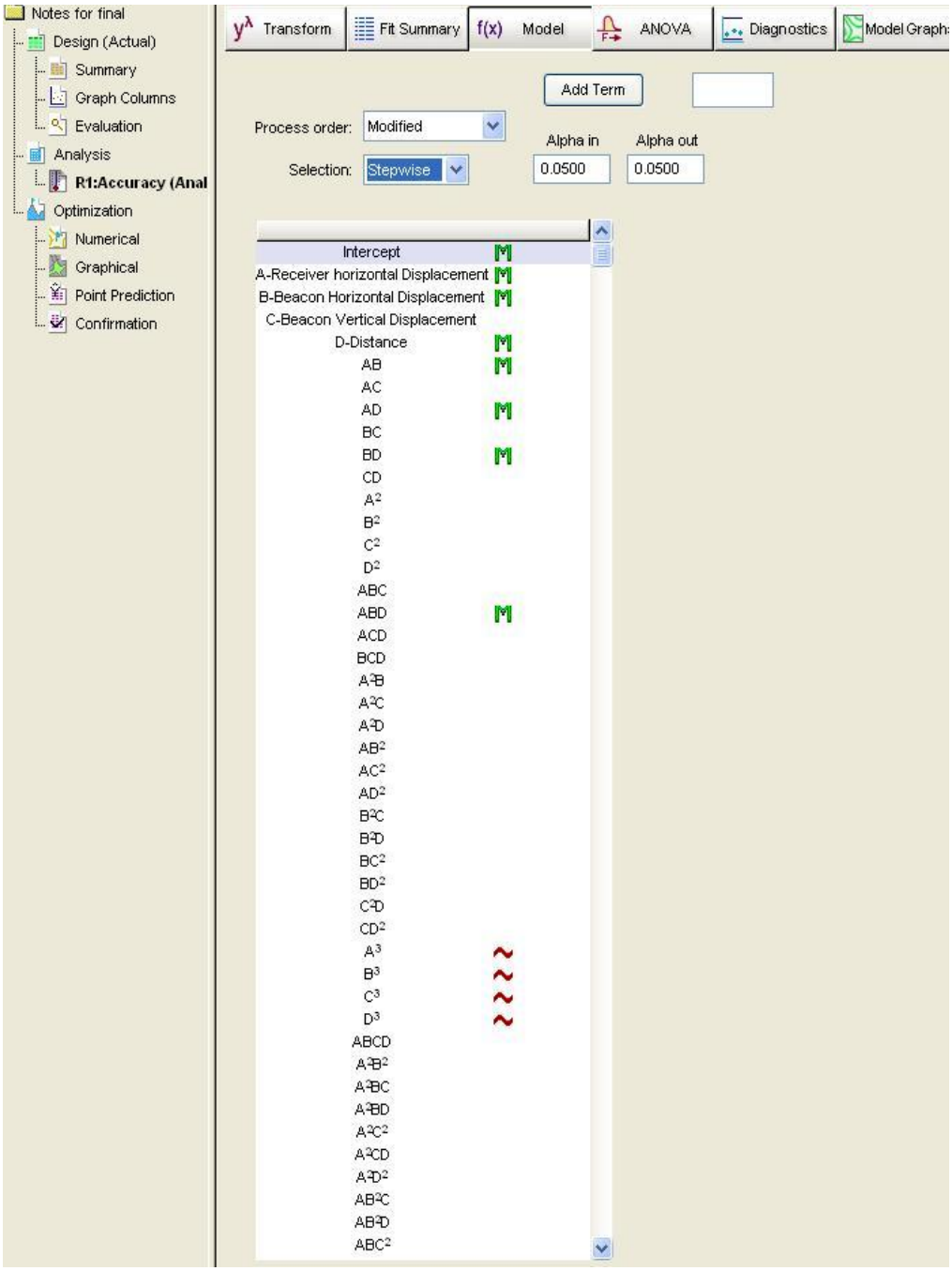

Figure 4-12: Model screen for Corridor Accuracy Model (M-means model).

ANOVA

The analysis of variance (ANOVA) table for the corridor accuracy model is given in Table 4-6. The Model F-value of 32.23 implies that the model is significant. There is

only a 0.01% chance that a "Model F-Value" this large could occur due to noise. Values of "Prob > F" less than 0.0500 indicate that the model terms are significant. Here, 'Prob' stands for probability. In this case D, AB, ABD are significant model terms. From this ANOVA table it is clear that among all the factors that influence cricket distance measurement accuracy, Distance (D) is the most significant.

Table 4-6: ANOVA table for the Corridor Accuracy Model

Analysis of variance table [Partial sum of squares - Type III]						
	Sum of		Mean	F	p-value	
Source	Squares	df	Square	Value	Prob > F	
Model	**3058.486**	**7**	**436.9265**	**32.23294119**	**< 0.0001**	significant
A-Receiver Horizontal Displacement	0.976094	1	0.976094	0.07200837	0.7892	
B-Beacon Horizontal Displacement	4.046107	1	4.046107	0.2984894	0.5865	
D-Distance	962.1195	1	962.1195	70.97747909	< 0.0001	
AB	1210.962	1	1210.962	89.33510445	< 0.0001	
AD	0.15802	1	0.15802	0.011657414	0.9143	
BD	0.169277	1	0.169277	0.012487931	0.9113	
ABD	880.0543	1	880.0543	64.92336168	< 0.0001	

Although not significant but from the ANOVA table it can be noted that in a corridor the Receiver Horizontal Displacement (A) factor has a greater influence than the Beacon Horizontal Displacement (B). Within 60 cm to 100 cm levels, Vertical Displacement (C) has no significant effect on accuracy. Finally among all the interactions, AB and then ABD are the most significant.

Table 4-7: R-Squared values for Corridor Accuracy Model

Std. Dev.	3.681749472	**R-Squared**	0.755550828
Mean	95.81864444	**Adj. R-Squared**	0.732110497
C.V. %	3.842414484	**Pred. R-Squared**	0.680808792
PRESS	1292.092713	**Adeq. Precision**	21.08374627

The R-Squared values are shown in Table 4-7. The Predicted R-squared (Pred R-Squared) of 0.6808 is in reasonable agreement with the Adjusted R-Squared (Adj R-Squared) of 0.7321. "Adeq Precision" measures the signal to noise ratio. A ratio greater than 4 is desirable. Here the ratio of 21.084 indicates an adequate signal. This model can be used to navigate the design space.

Equation

The final mathematical model for accuracy is given in in terms of coded factors:

Accuracy =

+95.82
-0.13 * A
+0.27 * B
+4.22 * D
+5.80 * A * B
-0.066 * A * D
-0.069 * B * D
-6.06 * A * B * D (4.4)

Validation

To validate the above model, a separate validation experiment was carried out. In validation it is recommended not to use the combination of factors that already had been used while generating the model [247]. Values for A, B and D settings are generated based on the Random number table [253]. Results are shown in Table 4-8.

Table 4-8: Validation Result for Corridor Model

Settings			**Actual accuracy**	**Expected accuracy**	**Difference**
A	B	D			
cm	cm	cm	%	%	
75	56	450	98.88	105.63	6.75
93	56	350	99.28	102.4	3.12
112	93	600	98.41	88.95	9.46
112	93	500	98.2	91.1	7.1
75	150	250	93.5	95.86	2.36

Initially all the readings were taken from the listener and actual accuracy was calculated. The expected accuracy was then calculated using the equation provided by the DOE model (Equation 4.3). The average actual accuracy of 97.6 % is very close to the average expected accuracy of 96.8%. The maximum difference was recorded at the third setting which is only 9.46 cm.

Diagnostics

Normal Plot of Residuals

From Figure 4-13, it is clear that the residual points follow a straight line indicating that residuals follow a normal distribution. Though some moderate scatters exist on the graph, there is no definite pattern like an "S-shaped" curve.

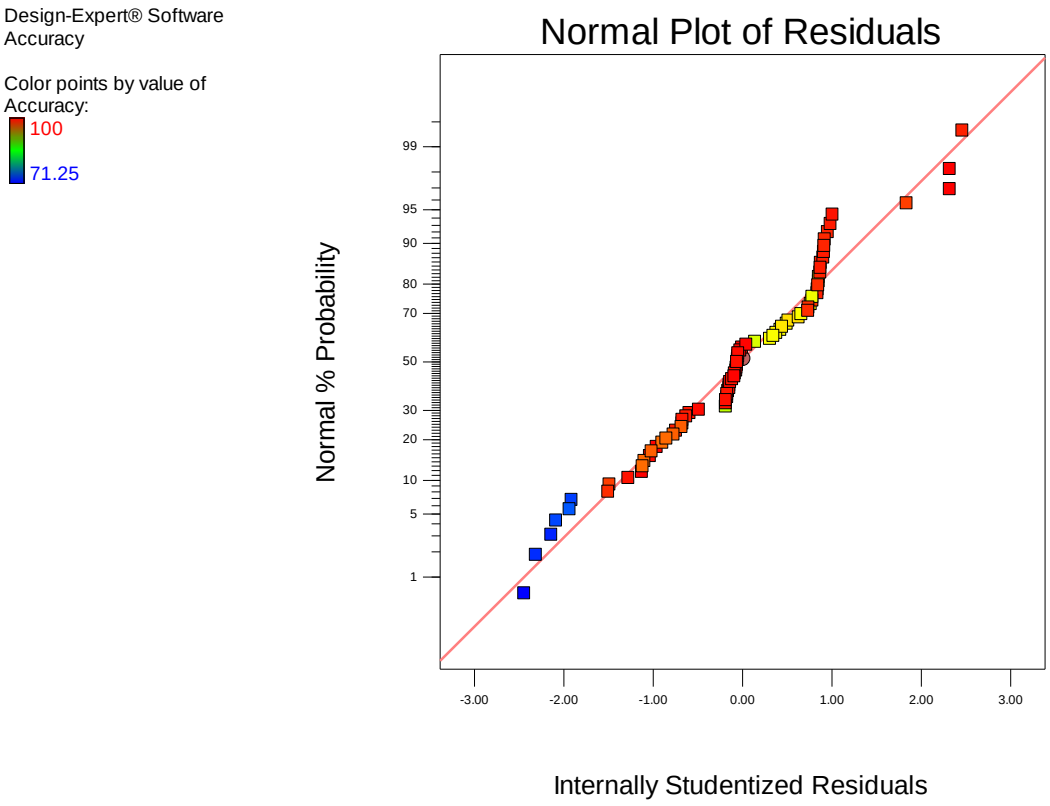

Figure 4-13: Normal probability plot for the Corridor experiment.

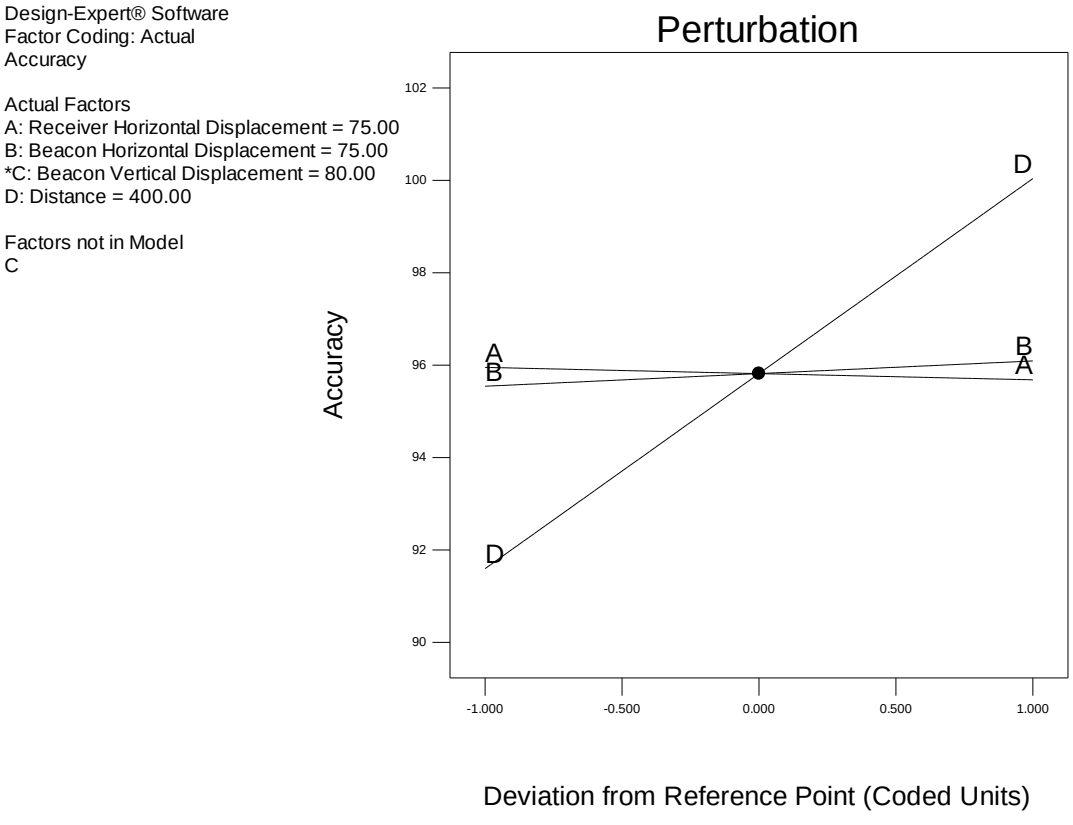

Figure 4-14: Perturbation Plot for the Corridor Model.

Model Graphs

Perturbation Plot

The perturbation plot helps to compare the effect of all the factors at a particular point in the design space [250]. The response is plotted by changing only one factor over its range while holding all the other factors constant. By default, Design-Expert sets the reference point at the midpoint of all the factors. From the graph (Figure 4-14), it is obvious that the accuracy is highly sensitive to the beacon-to-reader distance (D). Accuracy increases as D increases. At lowest level of D (2 m), accuracy is below 92% and as D increases from 2 m to 4 m (middle point) the accuracy rises to 96%. As the distance increases further, the accuracy increases sharply and it reaches near 100% at maximum D level (6 m). This result is contradictory to Parthia's result (See Section 4.3) where accuracy decreases as the beacon to reader distance increases. This may happen because all the experiments were carried out at line of sight condition in Parthia's test. But in this experiment the beacon and receiver were not always set at line of sight. They were moved horizontally and vertically from the line of sight position depending on the DOE settings. From the ANOVA table it is clear that due to this type of experiment settings there is a significant effect of A and B and their interaction on cricket's overall distance accuracy. The effect of factor A and B are not very significance to the responses (Figure 4-14). Accuracy decreases slightly as factor A increases. In contrast, accuracy increases slightly as factor B increases.

AB-interaction

The two-dimensional representation of the responses across A and B is presented in Figure 4-15. Although the A and B factors are individually not so significant, (See Table 4-5), the AB-interaction has a significant effect on accuracy. When the beacon and the receiver are both at their low level settings (0, 0) accuracy is very high. This is because under these circumstances they are at line of sight condition. If the beacon position is held constant at 0 cm (low level of A) and the receiver position is changed horizontally, the accuracy gradually drops. At high level of A (150 cm), accuracy drops up to as low as 90% (Figure 4-15). Similar effect can be observed on B as well. However, changes of both A and B by the same quantity, i.e. they are still at line of sight, results in higher accuracy. The projection of the AB-contour plot (3D surface graph) is shown in Figure 4-16.

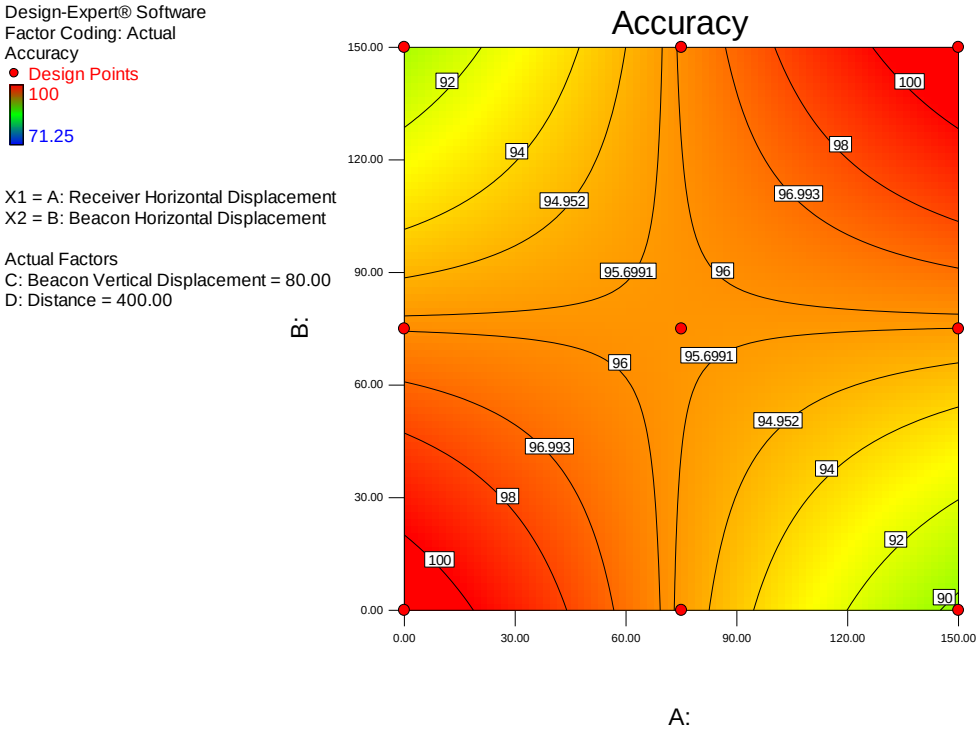

Figure 4-15: Contour Graph of AB-interaction in the Corridor Experiment

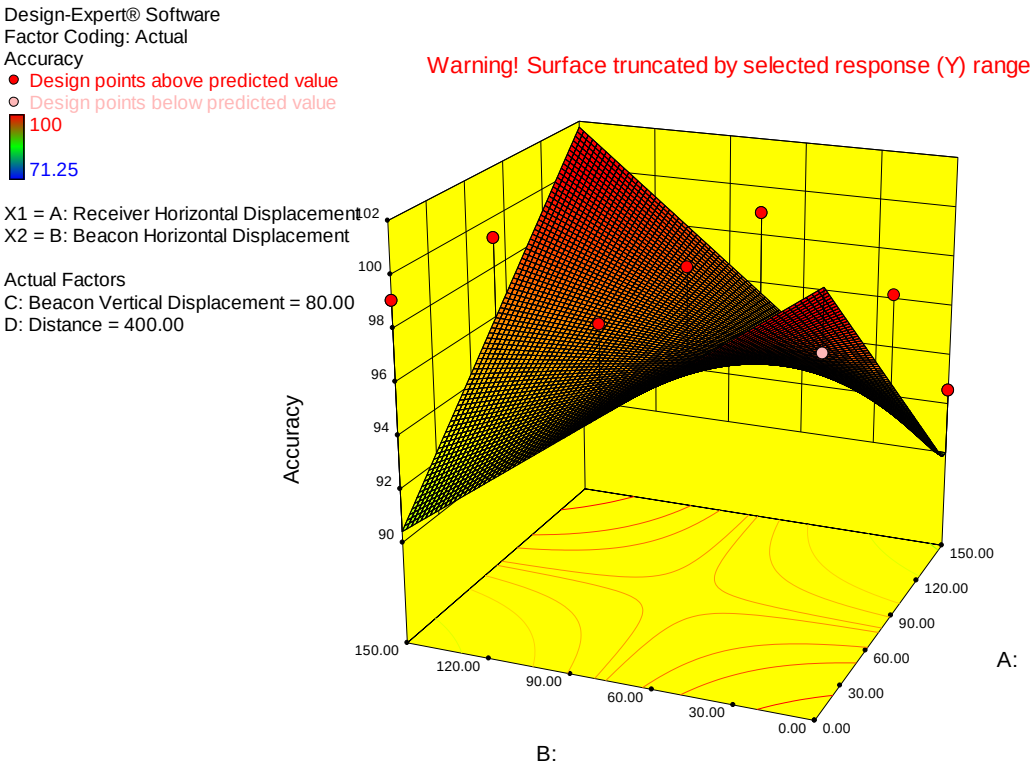

Figure 4-16: 3D surface graph of AB-interaction in the Corridor experiment

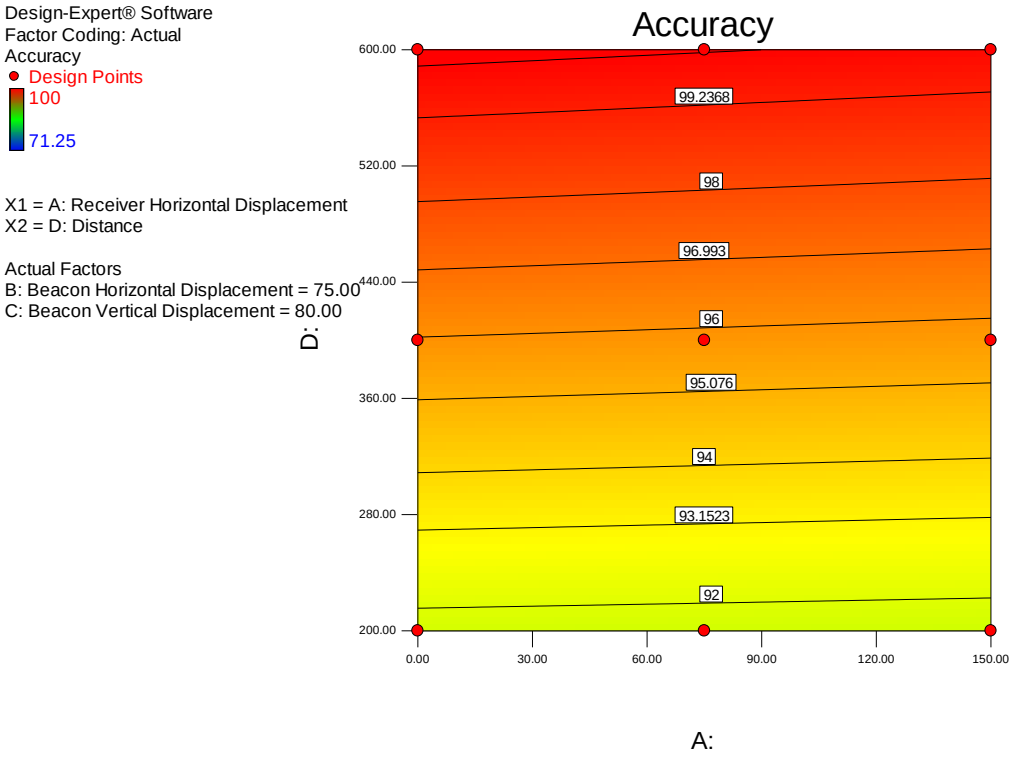

Figure 4-17 : AD-contour graph for Corridor

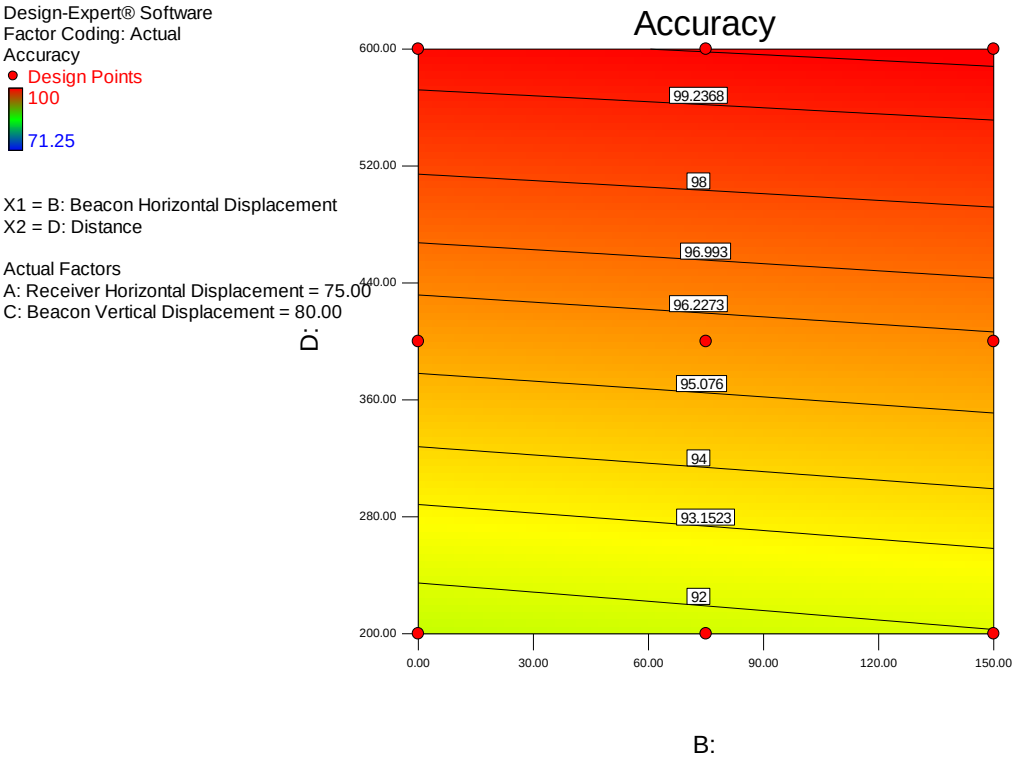

Figure 4-18: BD- contour graph for Corridor

ABD-Interaction

From the ANOVA (Table 4-6) and Perturbation Plot (Figure 4-14) it is clear that AD and BD interactions are less significant but ABD-interaction has large affect on overall accuracy. This is partly because the AB-interaction contributes largely on the ABD interaction. The contour plot of AD and BD- interactions are shown in Figure 4-17 and Figure 4-18. From both figures it can be seen that accuracy increases as the distance increases. The effect of moving a receiver or a beacon horizontally on accuracy is not clearly visible from these two interaction figures.

4.3.8 Accuracy Model for the Reception Area

4.3.8.1 Response Data

Similarly to the previous experiment in the corridor, this experiment was carried out in randomised order in the reception area in the DCU engineering building. Cricket's distance data were collected at each combination of the settings provided by the DOE software. The full data sheets are shown in Appendix A. At 2 metre beacon to reader distance, the response data ranges from 100% to 71.25% with an average value of 89.33% and a standard deviation of 10.1 cm. At 4 m distance, the average accuracy response increased to 95.39% with a standard deviation of 5.32 cm. When the beacon and the listener distance was at 6 m, the responses vary only from 99.5% to 89.75%. Furthermore, average accuracy became 97.05% and the standard deviation was only 3.42 cm.

4.3.8.2 Analysing the Results

Transformation

In the reception area the responses ranges from 71.25 to 100 and the ratio of maximum to minimum is 1.40351. Hence, like in the previous DOE, no transformation was required**.**

Effects

Like in the previous experiment, all the main effects of the selected variables and any interaction effects were initially selected manually to fit a linear model. To eliminate negligible terms from the model, an automatic 'stepwise regression' was performed. Finally after stepwise regression, Design Expert automatically selects all the necessary

terms to make the model hierarchical. All the selected terms are identical to the previous corridor model as shown in Figure 4-12.

ANOVA

From ANOVA in Table 4-9, the Model F-value of 34.60 implies that the model is significant. Like in the previous experiment in the corridor, in this case D, AB, ABD are significant model terms as well. R-Squared values are shown in Table 4-10.

Table 4-9: ANOVA table for the Reception area.

Analysis of variance table [Partial sum of squares - Type III]						
	Sum of		Mean	F	p-value	
Source	Squares	df	Square	Value	Prob > F	
Model	3352.273967	7	478.8962809	34.59933837	< 0.0001	significant
A-Receiver Horizontal Displacement	6.980411574	1	6.980411574	0.504321356	0.4799	
B-Beacon Horizontal Displacement	1.729856019	1	1.729856019	0.124978782	0.7247	
D-Distance	639.5305042	1	639.5305042	46.2048531	< 0.0001	
AB	2239.103534	1	2239.103534	161.7709385	< 0.0001	
AD	0.185617361	1	0.185617361	0.013410499	0.9081	
BD	0.236034028	1	0.236034028	0.017053006	0.8965	
ABD	464.5080094	1	464.5080094	33.55981333	< 0.0001	

Table 4-10: R-Squared values for Reception Accuracy Model

Std. Dev.	3.720376	**R-Squared**	0.768398
Mean	94.20475	**Adj. R-Squared**	0.746189
C.V. %	3.949244	**Pred. R-Squared**	0.702884
PRESS	1296.222	**Adeq. Precision**	21.75373

The "Pred R-Squared" of 0.7029 is in reasonable agreement with the "Adj R-Squared" of 0.7462. "Adeq Precision" of 21.754 indicates an adequate signal. This model can be used to navigate the design space.

Equation

The final mathematical model for accuracy is given in Equation 4.4 in terms of coded factors:

$$\begin{aligned} \text{Accuracy} = {} & +94.20 \\ & -0.36 * A \\ & +0.18 * B \\ & +3.44 * D \\ & +7.89 * A * B \\ & +0.072 * A * D \\ & +0.081 * B * D \\ & -4.40 * A * B * D \end{aligned} \qquad (4.5)$$

Validation

To validate the above model, a separate validation experiment was carried out in a similar way to the corridor DOE validation. Values for A, B and D settings were kept as in the corridor validation test. Results are shown in Table 4-11.

Table 4-11: Validation Result for the Corridor Model

Settings			**Actual accuracy**	**Expected accuracy**	**Difference**
A	B	D			
cm	cm	cm	%	%	
75	56	450	95.5	105.63	10.13
93	56	350	94.22	102.4	8.18
112	93	600	99.41	88.95	10.46
112	93	500	97.2	91.1	6.1
75	150	250	91.5	95.86	4.36

From the validation results it can be concluded that the accuracy model developed for corridor is very accurate. The difference between the actual accuracy and expected accuracy are very small.

Diagnostics

Normal Plot of Residuals

Figure 4-19, represents the normal probability of residuals. From here it is clear that the residual points follow a straight line, indicating that the residuals follow a normal distribution. Though some moderate scatters exist on the graph, there is no definite pattern like an "S-shaped" curve.

Model Graphs

Perturbation Plot

From the perturbation plot (Figure 4-20) for the reception experiment it can be seen that accuracy is highly sensitive to the beacon to reader distance in the reception area. The effect is similar to the corridor experiment. Accuracy increases as the beacon to reader distance (D) increases. At the lowest level of D (2 m), accuracy is below 92% and as D increases from 2m to 4m the accuracy becomes 94%. With an increase of distance, accuracy increases sharply and it reaches close to 98% at 6 m distance.

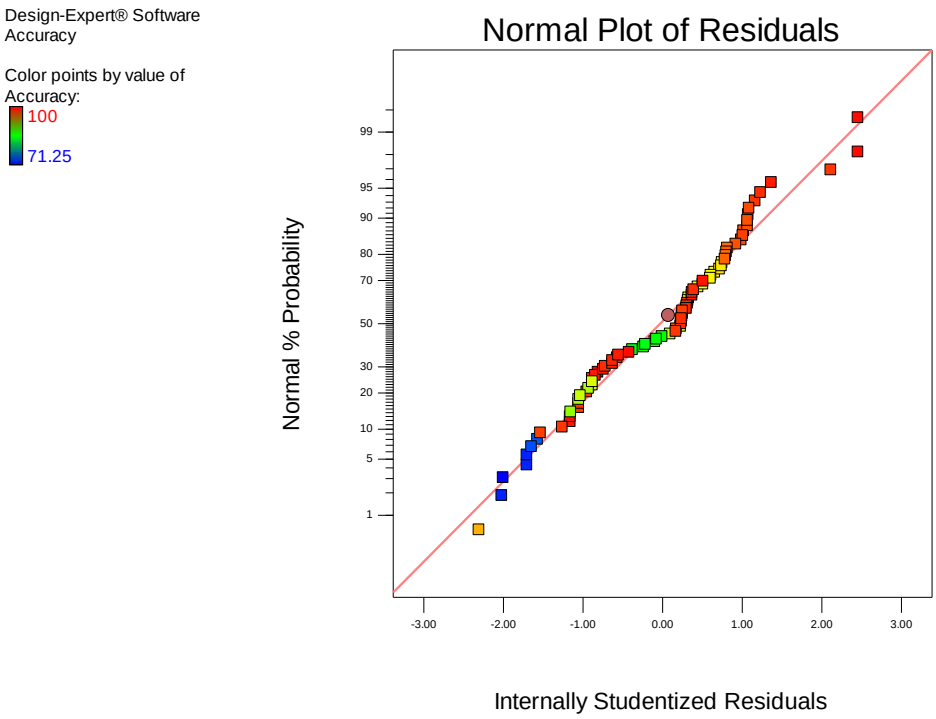

Figure 4-19: Normal probability plot for the Reception experiment.

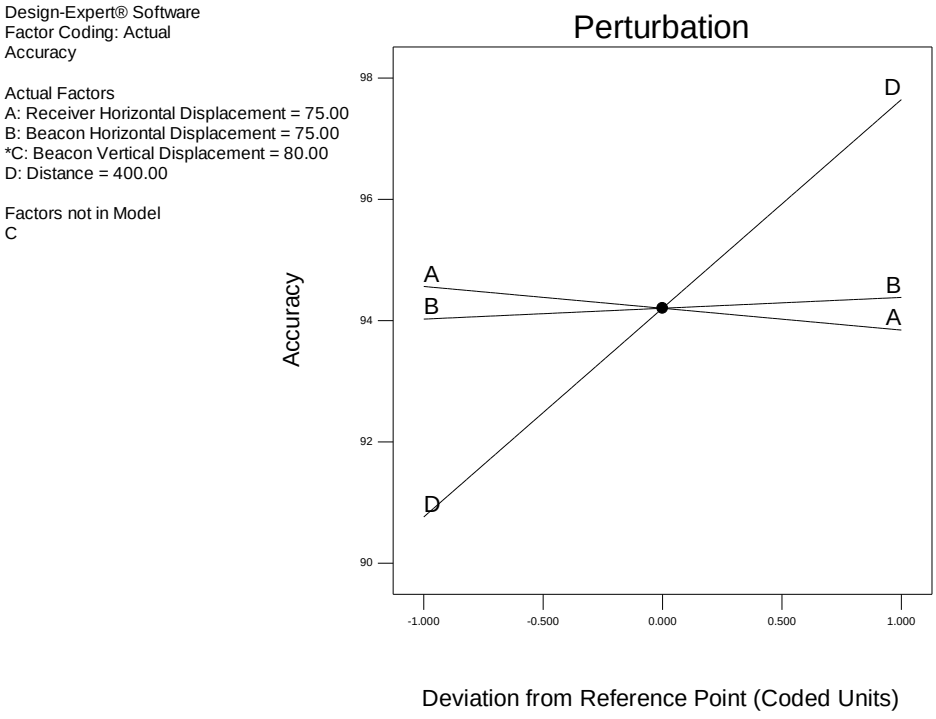

Figure 4-20: Perturbation Plot for the Reception area experiment

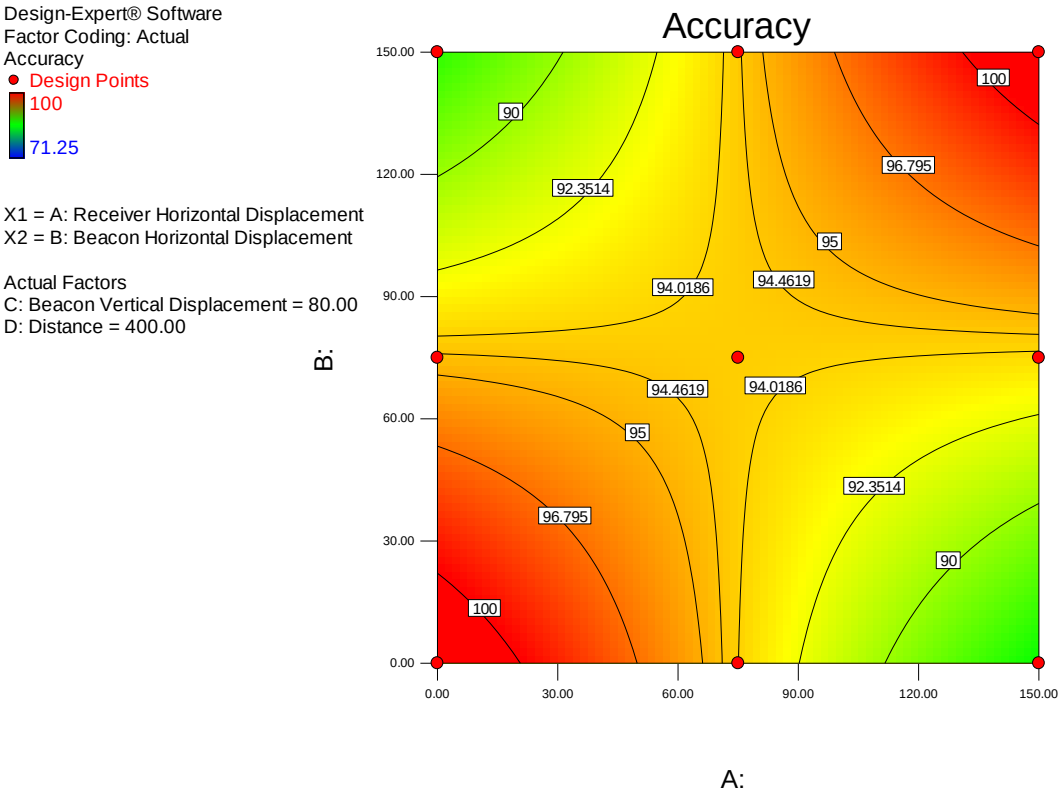

Figure 4-21: Contour Graph of AB-interaction in the Reception Area

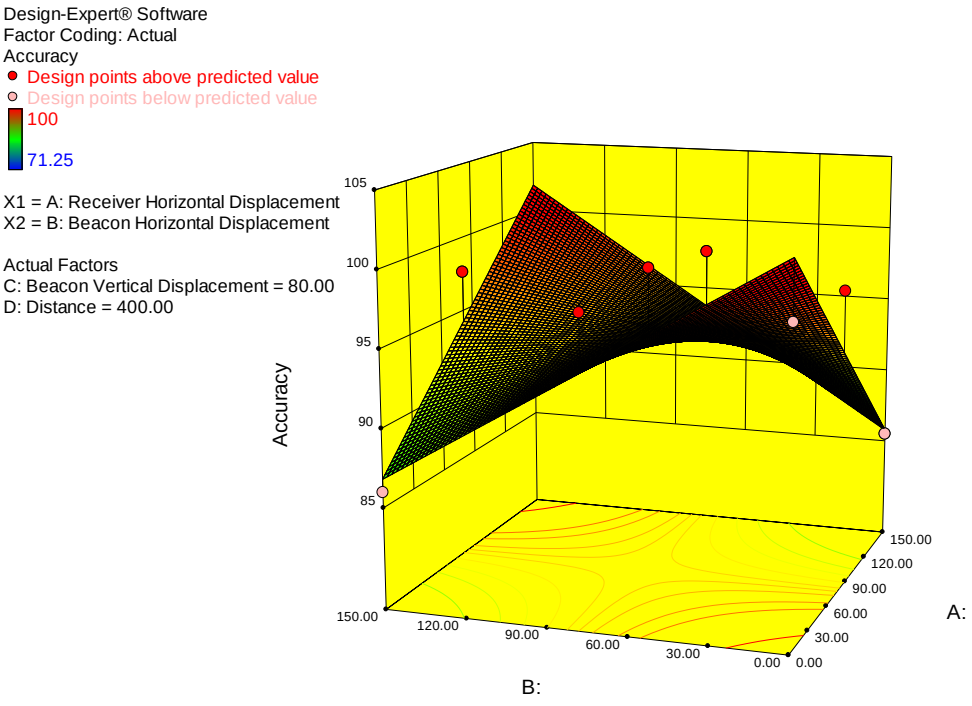

Figure 4-22: 3D surface graph of AB-interaction in the Reception area

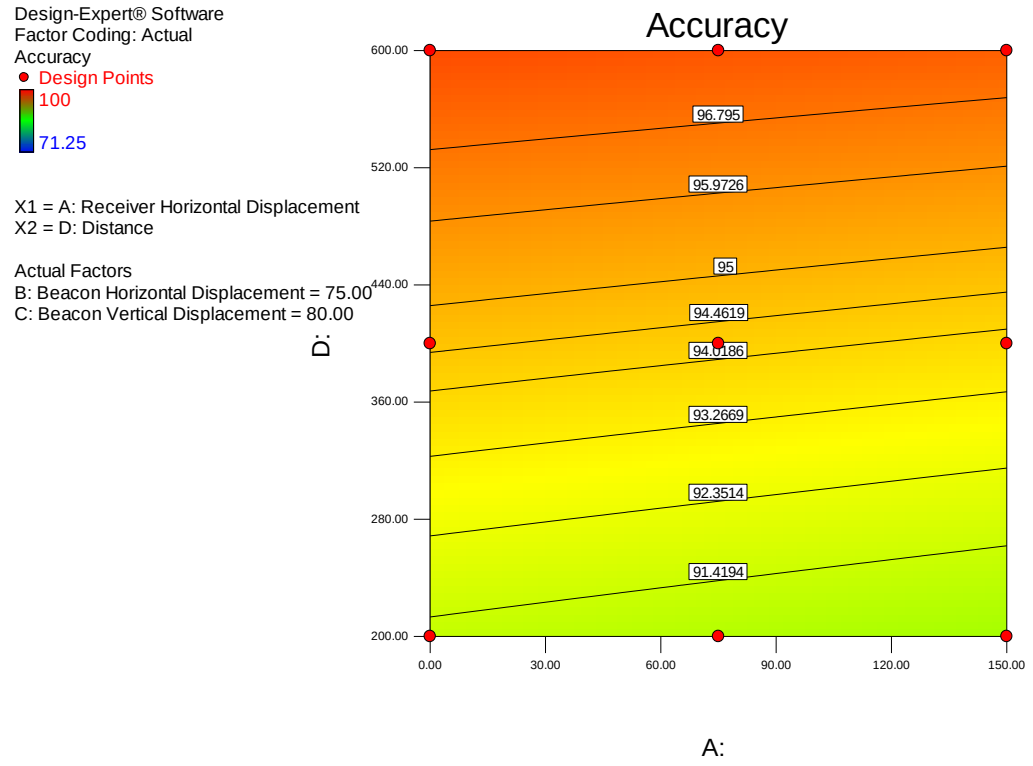

Figure 4-23: Contour plot of AD-interaction in the Corridor.

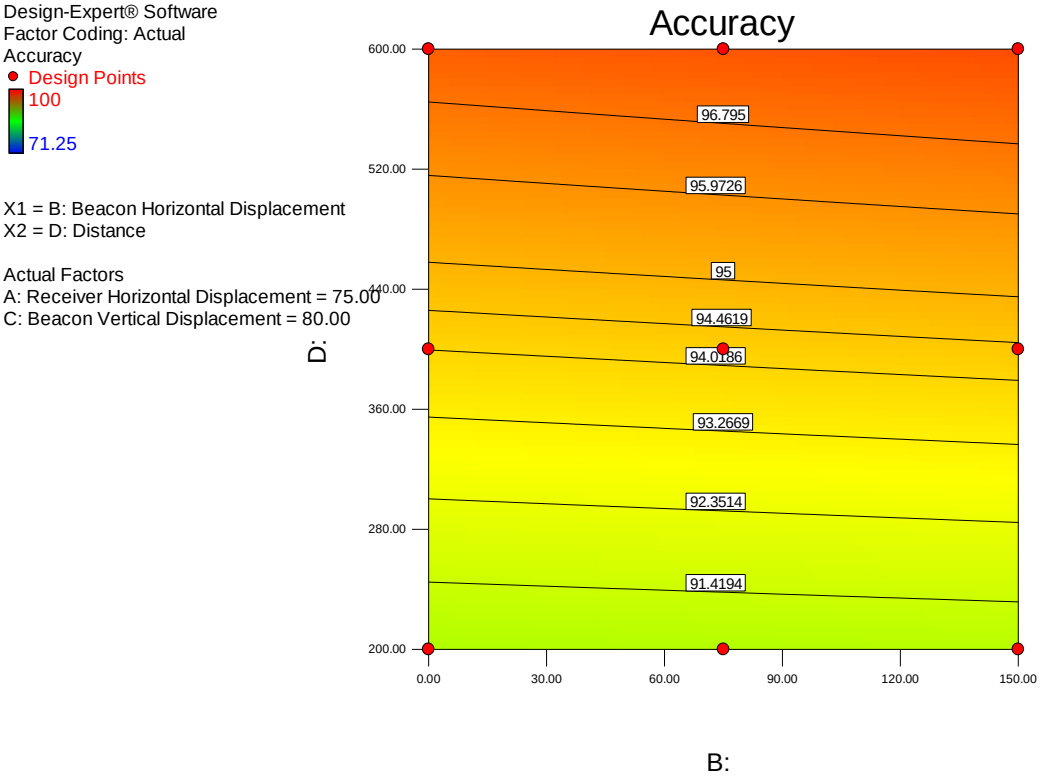

Figure 4-24: Contour plot of BD-interaction in the Corridor.

AB-interaction

The contour graph and 3D surface graph for the AB-interaction in the reception area is shown in Figure 4-21and Figure 4-22 respectively. Similarly to the previous experiment in the corridor, the AB-interaction has a significant effect on the responses. When the beacon and the receiver are at (0, 0) position the accuracy is higher. If the beacon stays at '0' position and the receiver moves horizontally, the accuracy drops up to as low as 90%. Similar effect can be seen if the receiver moves and the beacon stays at the same point as their horizontal displacement increases.

ABD-Interaction

The ABD-interaction has a large affect on Accuracy (See Table 4-9). The contour plot of the AD and BD interactions are shown in Figure 4-23 and Figure 4-24 respectively.

4.3.9 Summary of findings from the Cricket experiments

From these two DOE analyses, it is clear that the vertical displacement is not an important factor in both locations. A follower carrying a beacon can be as small as 120 cm or 2 m in height. The beacon can be placed at waist height or at shoulder height depending on the follower's choice and/or feasibility. The overall vertical displacement's affect on cricket's distance accuracy is negligible.

At line of sight condition between the beacon and reader, the cricket system can measure distances up to 8 meters. It has around one centimetre accuracy up to 3.5 meters, and 2 cm in the rest of the 8 m [244]. From the initial experiment in the DCU corridor and reception areas, it was revealed that distance readings are not very frequent as soon as the beacon to receiver distance reaches more than 7 m.

Accuracy deteriorates as the beacon/receiver moves horizontally from each other. This trend was similar in both the corridor and reception area. If the beacon moves horizontally from the receiver, at lower distance it affects significantly on accuracy but as the distance increases this effect become less significant. Similar result was observed for the receiver's horizontal displacement as well. From the overall DOE analysis, this phenomenon is similar in both the corridor and receiver experiment. Location does not

play any significant role on distance reading as their response patterns are similar in both experiments.

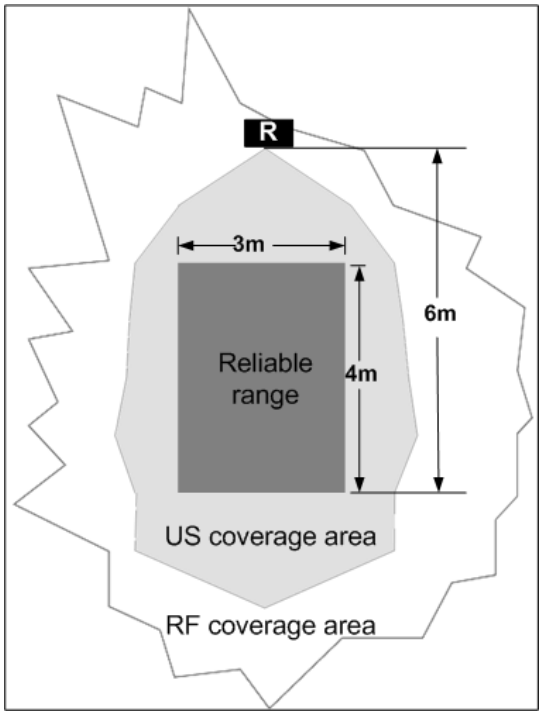

Figure 4-25: Reliable Area for Cricket distance accuracy; R means Receiver.

The Cricket sensor is very reliable for distance measurement up to 6 meters. Distance readings are reliable even though the beacon and receiver move horizontally from each other up to 1.5 m left or right in most of the normal indoors locations. In the corridor area the lowest accuracy of 71.25% was found when the receiver was 1.5 m horizontally away from the beacon. Similar accuracy was observed in the reception area at 2 m distance and 1.5 m horizontal displacement of the receiver from the beacon. Thus it can be concluded that cricket measurements are reliable enough for the IWARD PGM as long as the distance between them are within 2 to 6 m and horizontal displacements are in between 0 to 1.5 m left or right to each other. The reliable area in front of the receiver is shown as a dark rectangle in the middle of Figure 4-25. Although indoor propagation of RF and US is not predictable, it can be assumed that the RF range is higher than the US range [246].

The overall accuracy of cricket's distance readings up to the 6 m range is suitable enough for the PGM to make a decision whether the patient is within its range while guiding. At lower beacon to reader distance (0 to 2 m), the accuracy drops at much

higher rate if the sensors move horizontally from each other. This should not be a major concern for the PGM. As the follower is still in the normal speed zone, the listener would report this type of reading at smaller distances. For instance, at 1 m distance and 1.5 m horizontal displacement if the listener reports 185 cm distance readings then the robot would not act chaotically as these erroneous distance readings are still in the normal speed range of the Robot (0 to 3m).

The major drawback of cricket is its US sensor as it cannot penetrate an opaque material. If there are any obstacles or a person in between the robot and the follower, then the PGM would fail to decide where the follower is. This is because the listener would not report any distance information. This would result in stopping the robot unnecessarily even though the follower is within its range. Moreover, some lighting fixtures (mostly fluorescent tubes that are about to die) may produce noise in the ultrasonic range that interferes with Cricket and cause distance measurements to fluctuate rapidly. Furthermore, although Cricket does not require line-of-sight for distance ranging, objects in the environment may deflect signals and cause a systematic error in distance ranging [244].

Although the RF part of the beacon would still report to the listener of its presence, it can only confirm that the beacon is somewhere within the 30 m (maximum) range. Only this information is not sufficient for the PGM for adapting the robot's speed in the guidance operation. The RF range depends on the RF transmission powers which can be modulated. Unfortunately, the MIT Cricket Mote transmits RF at its default transmission range, which is not configurable for the end user. Therefore, a standalone Cricket sensor is not enough to be used as a distance measurement sensor in the PGM.

4.4 RFID

Radio frequency identification, or RFID, uses radio waves to automatically identify and to track an object. RFID systems comprise of two main elements: a data-carrying device (or tag or transponder) and a reader (or transceiver). Commonly an RFID tag stores a serial number on an electronic microchip that identifies an attached person or object and this microchip is attached to an antenna (as shown in Figure 4-26) which enables the chip to transmit the identification information to the reader. The reader then decodes the signals and passes the information to a middleware (PC, robot control system, etc.). The middleware can be linked to other systems or networks that require the information for further analysis [254, 255].

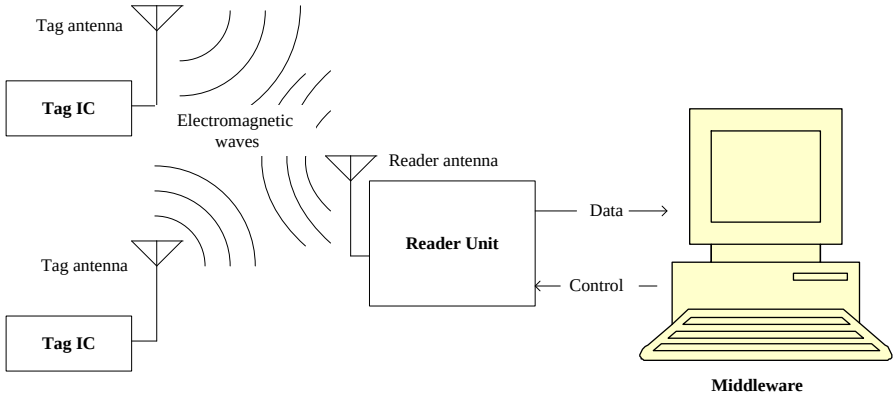

Figure 4-26: Overview of a Generic RFID system.

Reader

The reader, as a scanning device, sends out electromagnetic waves through its antennas and the tag antenna is tuned to receive these waves. In a nutshell, a reader consists of a radio frequency module (transmitter and receiver), a control unit and an antenna. Readers are also fitted with an additional interface (RS 232, RS 485, USB etc.) to enable them to forward the received data to another system (PC, handheld device, robot control system, etc.). The supply of power to the tag and the data exchange between the tag and the reader are normally achieved using magnetic or electromagnetic fields [254].

RFID Tags

An important feature of RFID systems is the power supply to the tag. Tags are mainly classified as passive and active. Passive tags do not have their own power supply and all

power required for the operation of a passive tag is drawn from the electrical/magnetic field of the reader. Passive tags are only activated when they are within the interrogation zone of a reader. Power supply to an inductively coupled transponder is shown in Figure 4-27. Although passive tags are cheap, smaller in size and have long lifetime, they have short communication range.

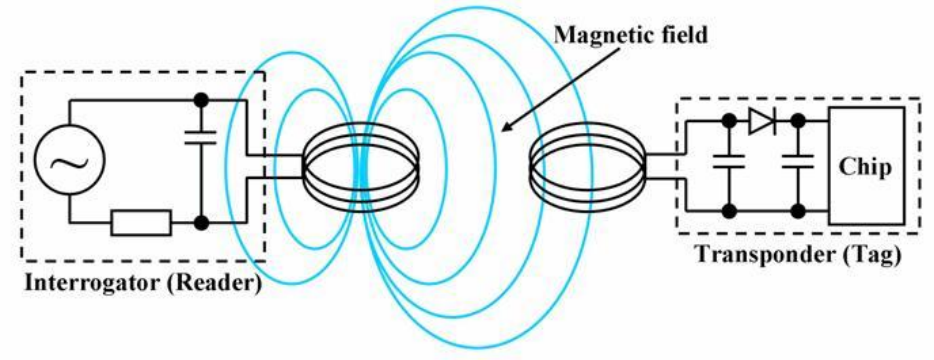

Figure 4-27: Power supply to an inductively coupled transponder [254]

Conversely, active tags incorporate a battery, which supplies all or part of the power for the operation of a microchip. This allows them to have a longer communication range, larger data storage capability, the ability to record and store sensor data, operate on higher frequencies, and function independently of the reader. However, the battery also makes them expensive and larger in size [254, 256]. The summary of major differences between active and passive tags is given in Table 4-12.

Table 4-12: Distinction between Active and Passive Tags [256].

	Active RFID	**Passive RFID**
Battery	Yes	No
Range	Long range (from a few meters to 100 meters)	Short range (from a few centimetres to 5 metres
Frequency	Operate at higher frequencies: 315-433MHz, 2.4 GHz, & 5.8 GHz	Operate at lower frequencies:125-134 KHz, 13.56 MHz, & 860-960 MHz
Size	Large	Small
Cost	Expensive–tags cost from €20 to €100	Cheap–cost of tags is typically in eurocents
Lifetime	Limited by the life time of the battery	Unlimited

Within these different types of tags, different suppliers offer a wide range of different alternative configurations to fulfil requirements. Range, accuracy, longevity, size and attachment criteria determine the options. Additionally, some tags are Read Only (RO); these are tags which are pre-programmed by the suppliers and cannot be changed. Others are Write Once- Read Many (WORM) tag types. The most flexible and

expensive tags can be reprogrammed and rewritten many times; these tags are defined as Read-Write (RW). RW tags might also be a security concern. It might be possible for competitors to reprogram the tags in a way that does not benefit an organisation. Tags are also divided into generations and classes based on their characteristics. As an example, a Generation 2, Class 3 tag is a semi-passive or battery-assisted tag [257].

Frequency, Range and Coupling

Operating frequency and the resulting range are important characteristics of any RFID system. The operating frequency of an RFID system is the frequency at which the reader transmits. A tag's transmission frequency is normally disregarded as in most cases it is the same as the reader transmission frequency [254].

Table 4-13: Summary of characteristics of RFID Frequencies [254, 255, 257].

Frequency		**Key Characteristics**
Low Frequency (LF)	30–300 kHz	• Low data transfer rate • Perform well around metals, liquids, dirt, snow and mud • Very short range and it reads just beyond actual contact
High Frequency (HF)	3–30 MHz	• Low data transfer rate • Poor performance around metals or liquids • Reading range limited to around 30 cm
Ultra High Frequency (UHF)	300 MHz–1 GHz	• Faster data transfer rate • Susceptible to environment involving liquid and metal • Longer read range than HF(>3m) and can be up to 100m when used with active tags
Microwave	>1 GHz	• Fastest data transfer rate among all • Poor performance around liquid and metal • Read range is similar to UHF

The different frequencies of RFID systems can be classified into the four basic ranges, LF (low frequency, 30 – 300 KHz), HF (high frequency, 3 – 30MHz), UHF (ultra high frequency, 300 MHz – 1 GHz) and microwave frequency (>1 GHz). The choice of frequency to use is important because radio waves behave differently at different frequencies. The summary of characteristics of different RFID frequencies is given in Table 4-13. Prior knowledge of how different frequencies react with different materials, their range and more importantly the nature of the application that they are going to be used for, need to be considered so that the right frequency is selected for the right application. Some materials are RF-opaque; they block, scatter and reflect RF waves. Other materials are defined as RF-absorbent, and they absorb the energy and allow only

parts of it to pass through. The exact environment where they are used and the materials that are in that area directly determines the efficiency of the signals that are transmitted [257].

For the physical coupling of tags and the readers, electric, magnetic and electromagnetic fields are used. According to their range, RFID systems can be further classified as close-coupling (0 – 1 cm), remote-coupling (0 – 1 m), and long-range (>1 m) systems [254]. Close coupling systems have ranges up to 1 cm hence for their operation the tag must either be inserted into the reader or positioned upon a surface provided for this purpose. Close coupling systems are coupled using both electric and magnetic fields and can theoretically be operated at any desired frequency between DC and 30 MHz because the operation of the transponder does not rely upon the radiation of fields. Close coupling systems are primarily used in applications that are subject to strict security requirements, but do not require a large range. Systems with write and read ranges of up to 1m are known by the collective term of remote coupling systems. Almost all remote coupled systems are based upon an inductive (magnetic) coupling between reader and transponder. Both close and remote coupling (operates on LF and HF) have small ranges (<1 m) and they are not feasible to be used in the PGM and will not be further discusses in this section [254].

Long-range RFID systems have ranges above 1 m and operate using electromagnetic waves in the UHF and microwave range. UHF and MF use backscattering techniques to communicate with the reader, which is similar to radar techniques. In addition, there are also long-range systems using surface acoustic wave transponders in the microwave range. The UHF tag uses the range from 300 MHz to 1 GHz and Microwave frequencies use the frequency area above 1 GHz. Typical ranges of 3 m can now be achieved using passive (battery-free) backscatter transponders, while ranges of 15 m and above can even be achieved using active (battery-supported) backscatter transponders. The battery of an active transponder, however, never provides the power for data transmission between transponder and reader, but serves exclusively to supply the microchip and for the retention of stored data. The power of the electromagnetic field received from the reader is the only power used for the data transmission between transponder and reader [254, 257].

UHF has faster data transfer rate than LF and HF. Parts of the spectrum in UHF perform badly in the presence of metals or liquids, but there are areas in this field that are not severely affected by the materials. The use of the UHF range is not accepted worldwide. Europe uses 868 MHz, whereas the US uses 915 MHz for the UHF applications. Japan does not allow the use of the UHF frequency for RFID applications [258]. To determine frequencies that are available to use, the user must check with local authorities to find out if they are allowed to use them [257].

Microwave frequencies use the frequency area above 1 GHz. They work both with passive and active tags and have the fastest data transfer rate between the tag and the reader of all frequency types. The tags in a microwave system can be very small, as the antenna needed to collect the signals can be short. Microwaves perform poorly when metals or liquids are present in the environment of the system [254, 257].

Reader Antenna

Attached to the reader, the RFID antenna transmits electromagnetic waves from the reader's transmitter and receives replied electromagnetic waves from the tags. Once a frequency range is determined, it is time to choose an antenna that best fits the application. Directivity, gain and polarisation are important parameters for determining antenna type and how to install it. Directivity influences in which direction signals are transmitted and received. Gain controls how energy is focused within the direction, and polarisation describes the orientation of the waves that are transmitted [257]. Antennas come in all sorts of sizes and shapes. There are two basic types of antennas, including linear and circular. Linear antennas transmit in vertical or horizontal straight lines that allow for long range but the signals transmitted are narrow. Hence, to be successful they must be aimed precisely at the tags. The straight lines are also better able to penetrate RF-absorbent materials. Circular antennas emit RF in circular patterns, thus tolerating multiple tag orientations and supporting more general RFID purposes. Read ranges for circular antennas may be shorter than linear antennas, however, the ranges are wider than those of linear antennas [259].

4.4.1 RFID System Selection Criteria for the PGM

Passive RFID technology is inherently constrained due to its short range. The range limitations require that a tag reader be placed in close proximity in order to read it. The

PGM needs to detect a follower from at least 6m distance. Due to its long range capability, an active RFID system is a perfect solution for the PGM. Active RFID works on UHF and MF band and both of them have similar long reading ranges (up to 100 m). Their higher carrier frequency allows for a much faster read rate of the tag information, thus allowing the transmission of higher amounts of data. This is beneficial as the PGM needs to detect a follower continuously at very fast rate while guiding. Unfortunately, compared to UHF, the performance of MF is very poor when exposed to metals or liquids [257]. An active RFID system operating on acceptable UHF band (at least acceptable within the EU) should be an automatic choice when selecting an RFID system for the PGM. The communication between tag and reader used in UHF systems is by electrical field instead of the magnetic coupling used by LF and HF systems. The antennas required by UHF systems can also be smaller than the antennas used for LF and HF systems, resulting in higher efficiency.

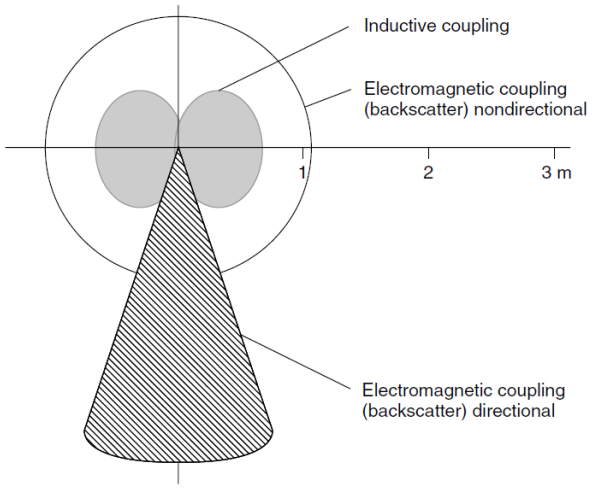

Figure 4-28: Comparison of the relative interrogation zones of different RF systems [254]

Circular antennas would provide the follower more flexibility as during a guidance operation they can orient themselves in whatever way they want with respect to the robot. The follower can walk side by side or behind or in front of the robot. Comparison of the relative interrogation zones of different systems is shown in Figure 4-28.

4.4.2 Active RFID kit

Active tags and readers (receivers) can give an RSSI (Received Signal Strength Indication) value that can be indicative of the spacing between the patient and the robot.

However, it is necessary to investigate how to adjust the power levels and receive antenna gain to control the signal strength within the span of range (2 - 6 m).

Figure 4-29: L-RX201 Active reader with attached AN200 Stub Antenna [260]

A Patient just turning around may affect the RSSI value since his position and the orientation of the tag he is carrying will affect the relative signal strength. The application software on the robot's platform will have to meter the gradient of change in signal strength and adjust its speed algorithm accordingly [9].

Figure 4-30: Wavetrend active tags family [260]

Based on the considerations above, the Wavetrend L-RX201 Reader (Figure 4-29) is selected for the PGM. It detects and decodes RFID signals from Wavetrend's range of active RFID tags (See Figure 4-30). The L-RX201 RFID Reader is a 433MHz receiver that is rated to -103 dBm sensitivity at 700 kHz bandwidth. It connects to a PC via the

Serial RS232 protocol and can transfer data at a speed of 9600 kbps to 115200 kbps. The 433 MHz-ISM-band is acceptable within the EU [261]. Its compact size (98 mm x 60 mm x 20 mm), minimal weight (58 gm) and potential to be powered through a battery (DC 6-16V) fulfil the essential prerequisites for any sensor to be installed on a mobile robot.

The L-RX201 reader incorporates a BNC connector to allow for attachment of an external antenna to extend the reader's range. The use of adequate connectors is also critical for RFID systems working in the UHF band. The transmission line used to connect a UHF reader to its antenna is very critical. The most effective approach to improve the performance of the system is to minimise the length of the transmission line between the output of the reader and its antenna. The BNC connector does not result in significant performance degradation in UHF applications. Moreover, BNC connectors are safe, efficient and quickly accessible. They minimise the risk of accidentally disconnecting other close-by connectors. Typical read ranges of Wavetrend Tags with various Wavetrend antennas are shown in Table 4-14. Distances may vary depending on the ambient RF environment. The following tests were conducted in free air.

Table 4-14: Typical read ranges based on antenna type [260]

Antenna	**Minimum Range (m)**	**Maximum. Range (m)**
None	0.2	7
L-AN200	1	30
L-AN100	3	35
L-AN300	3	100

Considering the characteristics of all antennas, the L-AN200 433 MHz Wavetrend antenna stub antenna (See Figure 4-29) is selected for the PGM. This compact antenna connects directly to RX201 type readers. It has an omnidirectional reception pattern around the vertical axis with null points being at the extreme ends of the stub [262]. Such an omnidirectional radiation pattern facilitates detecting tags in any orientation relative to the antenna and is designed for both indoor and outdoor use. The resulting 30 m operational range of the L-RX201 reader and the L-AN200 antenna would be sufficient for the IWARD PGM scenario.

The Wavetrend RFID tag generates electronic data and transmits it through a radio signal with a default transmission interval of 1.5 s. The Wavetrend RFID readers pick

up this signal and measure the Relative Signal Strength (RSS) and forward the data through a serial port to the processing software. Wavetrend provides windows platforms-supported demo application software to capture, aggregate, filter, store and display the received data. This software has a graphical user interface to display received signal strength indicator (RSSI) values of each detected tag and refresh the results periodically. RSSI is a measure of signal power over distance and obstacles in the signals path and is an indication of signal quality [263]. Since the IWARD system operates on the Linux platform, new device drivers and application software were developed by the author. All Wavetrend series tags come in two different flavours. One comes with the mercury switch to detect tag movement and the other comes without the mercury switch. The mercury switch flips when the tag moves. When the switch is triggered, a custom integer field is incremented on the tags internal memory. This field is included with every data packet sent. The software compares the current integer with the previous integer and if there is a change, it is shown in the application software.

4.4.3 Calculate distance using RSSI value

In an effort to relate the RSSI value to distance, several tests were carried out under different circumstances. Although RSSI is a bad estimator for distance calculation [264], an initial test is required before discarding the idea of using the RSSI value.

Table 4-15: List of Wavetrend Tag ID for experiments

Tag ID	Tag Type
124	Small Asset Tag (TG801)
66	Small Asset Tag (TG801-MS)
194	Domino Tag (TG100)
193	Domino Tag (TG100-MS)
47	Asset Tag (TG800)
187	Asset Tag (TG800-MS)
82	Wrist Tag (TG1800)

The first test was carried out in a wide room-the room located at the basement floor in the DCU engineering building (See Figure 4-32), and the readings were taken at 1m intervals over a range of 1 m to 8 m. Table 4-15 is showing the list of all Wavetrend Tag ID's that were used for these experiments. In the table 'MS' stands for mercury switch.

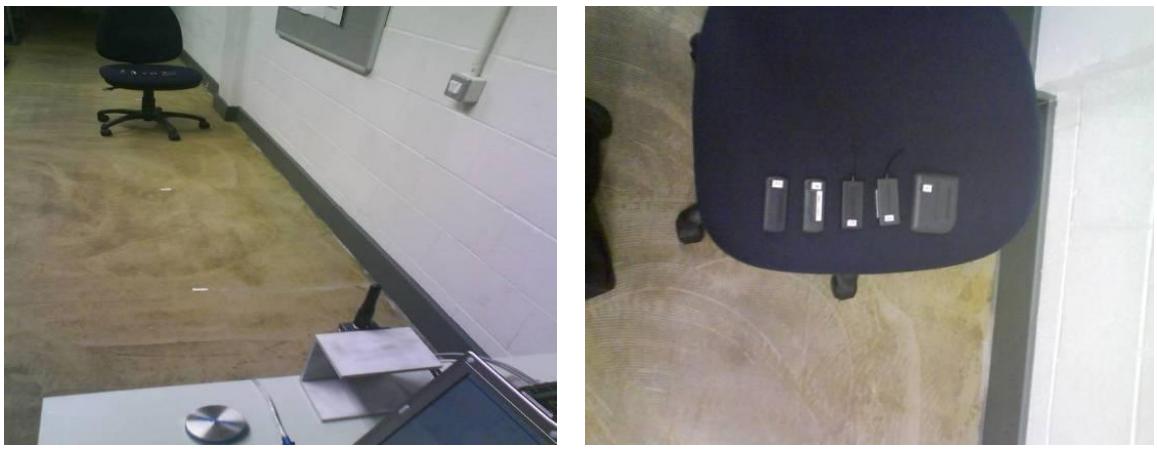

Figure 4-31: RFID Tag Reader Experiment set up.

Figure 4-32: Wide area (left) and Narrow corridor (right) for the RFID experiments.

4.4.3.1 Experiment in the Wide Area

Figure 4-33 shows the results of moving the tags further away from the tag reader. The reliability of the results obtained in the graph can be debated upon because the graph displays unexpected results. The action of moving the tag away from the tag reader should result in a noticeable linear decrease in the signal strength but the graph shows that the signal strength stayed in the same range and in some cases, the detection increased after a decrease, which again shouldn't happen, some tags disappeared and were not detected at further distances.

In order to get results from this experiment, it was decided to concentrate on the frequency of detection while moving away from the tag reader. Figure 4-34, shows the experimental effects on the detection frequency of moving the tags away from the tag reader. The reliability of the results can again be questioned because the graph does not

show the expected decrease pattern for the frequency and as in the previous signal strength experiment, the graph showed an increase after a decrease.

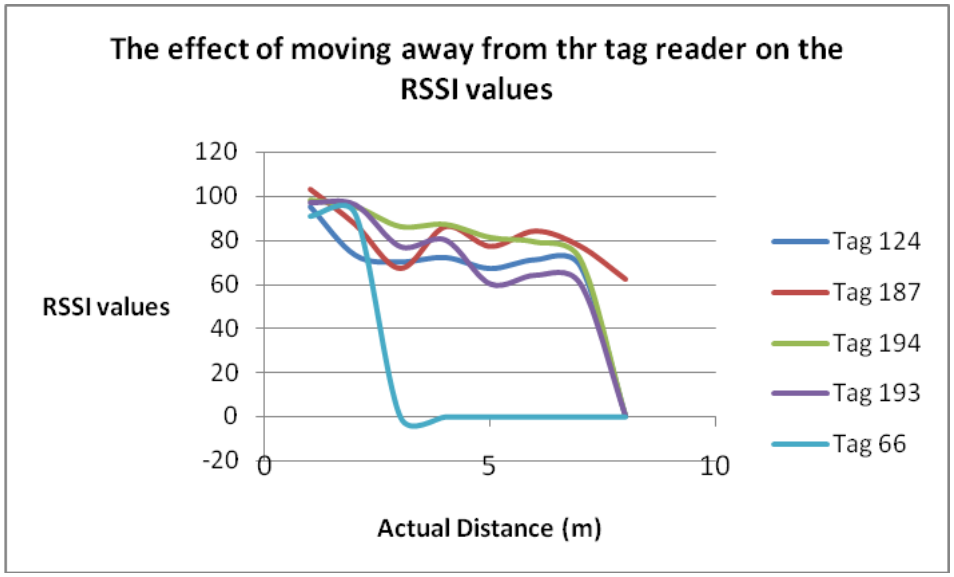

Figure 4-33: The effect of moving different tags away from the tag reader on the signal strength; the tags were placed at 1 m up to 8 m at 1 m intervals.

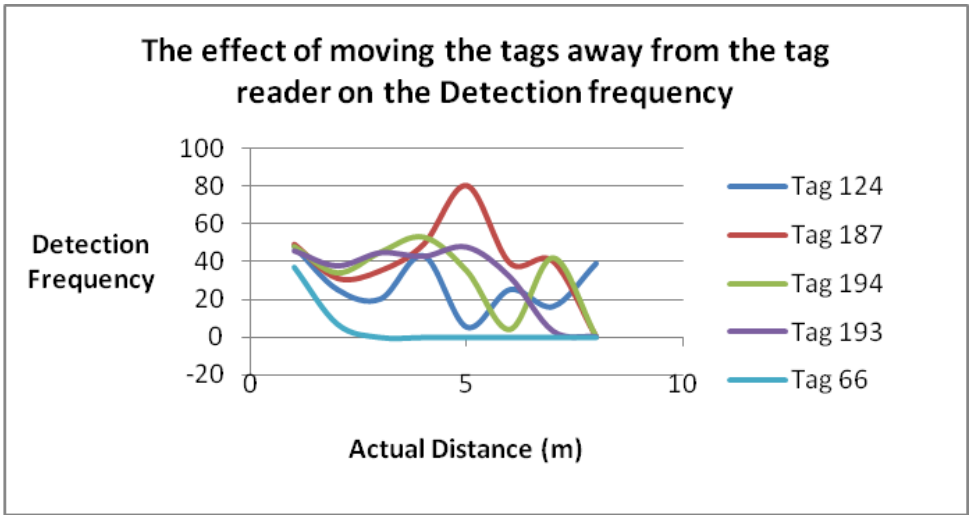

Figure 4-34: The effect of moving different tags away from the tag reader on the detection frequency; the tags were placed at 1 m up to 8 m at 1 m intervals.

4.4.3.2 Experiment in the narrow Corridor

Except for the location being changed to a narrow corridor, the set up for this experiment is similar to the previous experiment. Figure 4-35 shows the results obtained; they were again not as expected, the strength range was similar to the previous results but the detection of some tags was better in this experiment. Again, this data was unreliable, thus the detection frequency test was carried out again. The results are

shown in Figure 4-36, which again are unreliable because the detection frequency does not show any pattern in its behaviour, it is random.

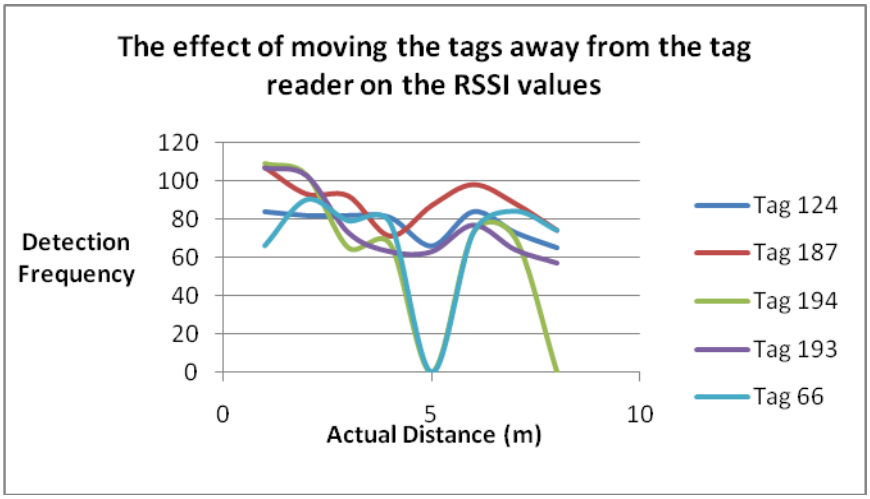

Figure 4-35:The effect of moving different tags away from the tag reader on the signal strength; the tags were placed at 1m up to 8 m at 1 m intervals.

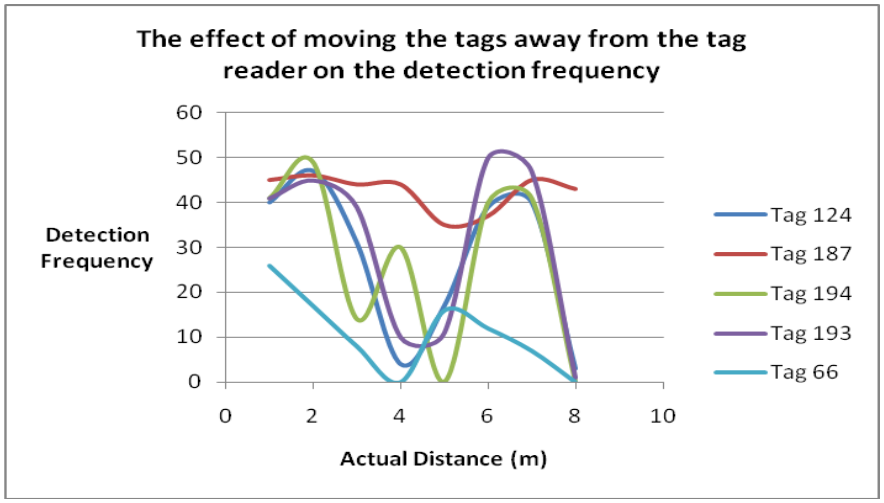

Figure 4-36: The effect of moving different tags away from the tag reader on the detection frequency; the tags were placed at 1m up to 8 m at 1 m intervals.

From both experiments it can be concluded that the results do not follow any pattern, but it was also noticeable that the results obtained from carrying out the experiments in a narrow corridor were better than the results from the wide room. The reason is that in narrower environments, the signal reflections against the walls increase as shorter distances are required for the signal to reach the wall and be reflected. Reducing the signal travelling distance increases the signal strength which will consequently result in better detection. Also, it was obvious that the detection of the tags differed from one tag

to another. In the first experiment, at 1m and 2m distances, all the tags were detected. Tags 124, 187, 193, and 194 were detected from the 3 m to 7 m distance range and only Tag 187 was detected at 8 m. In the second experiment at 1 m to 3 m, all tags were detected by the reader. Tags 124, 187,193 and 194 were detected at 4 m. At 5 m, Tags 124, 187, 193 and 66 were detected. Surprisingly at 6 m and 7 m all tags were detected again. Finally in 8 m range only Tags 124 and 187 were detected.

4.4.4 Alternative approach

From the above two experiments it is clear that RSSI is a poor estimator of Tag distance. Even two tags of the same type provide different results. In the previous test, both tags and readers were kept in stationary positions. Still the results did not correspond to any specific pattern. In the PGM scenario, the RFID readers are attached to a mobile robot and tags are attached to the followers who are always in motion as well. There is a high level of mobility in this scenario, so the RSSI-distance result is expected to be worse than that currently obtained at static conditions.

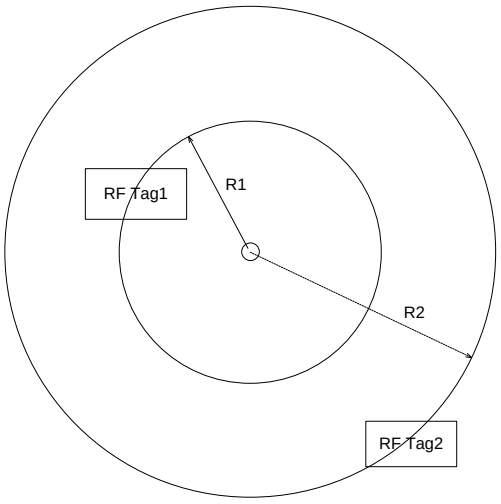

Figure 4-37: Distance calculation technique using two tags.

The RSSI varies significantly depending on the spatial configuration of line of sight impediments from tag to reader. Furthermore it also varies based on the continuous wave (CW) configuration or modulation technique utilised by the manufacturer. Additionally, objects to which the tag is mounted and the orientation of the tag to the reader depending on antenna configurations will dramatically impact the RSSI output [9].

Active RFID systems seem applicable only to detect whether the tags are in their range and certainly are not reliable to calculate the exact distance using RSSI values. Hence an alternative approach needs to be searched out so that RF can be used to measure the distance of a follower reliably. There are several types of active tags. Each type has a certain range. The idea is based on having two different range tags added together and worn by the follower. The technique is shown in Figure 4-37. For an example, 'Tag 1' which has approximately a range of 3 m and 'Tag 2' which has approximately a range of 6 m. If the system detects both 'Tag 1' and 'Tag 2' then the PGM will consider that the patient is within 3 m range. If it detects 'Tag 2' but not 'Tag 1' then it is in between 2 - 6 m. Finally, if neither tag is detected then the patient is out of range and eventually the PGM requests the robot to stop and wait for the patient to come within its range. Unfortunately, the read range of all types of the Wavetrend family tags is higher than the desired 6 and 3 m of the PGM requirement. The lowest range of 8 m was found with the TG 100 type tag.

4.4.5 Experiment with Multiple Readers in Proximity Mode

The L-RX201 reader also works as proximity or close range model without antenna. This type of setting is typically used in an environment where the tag has to be very close in range to the reader. Two different readers without antennas were used to find the range for each tag in the next experiment in the narrow corridor environment; the results were divided into 'reader 1' results and 'reader 2' results. Removing the antenna limited the detection range according to the user's specifications. Both readers were set to detect at a high gain command (via software). As mentioned earlier, this approach was necessary to get reliable results for the RFID active tag reader, which could not be obtained using the readers with the antennas. The results obtained from the two readers were arranged in Table 4-16. This experiment concentrated on the tag detection.

Despite the fact that the two readers were identical, they both yielded different results. Among TG 801 type tags, Tag ID 66 was not detected at all and Tag 124 was detected only up to 2 m. In the TG 100 series tags, Tag ID 193 was not detected at all by both of the readers while Tag ID 194 was detected up to 3 m range by 'reader 2' and up to 2 m by 'reader 1'. The TG 800 wrist type tag (Tag ID 82) was detected up to 3 m by 'reader 2' and up to 2 m by 'reader 1'. The results were very inconsistent.

Table 4-16: Detected tags results of two readers; tags were placed at 1m up to 8m at 1 m intervals. The tags labelled with (•) in the table were the tags that the readers could detect in the shown ranges.

Distance	Reader	Tag ID						
		66	124	193	194	82	47	187
1 m	Reader 1		•		•	•	•	•
	Reader 2		•		•	•	•	•
2 m	Reader 1				•	•	•	•
	Reader 2				•	•	•	•
3 m	Reader 1						•	
	Reader 2				•	•	•	
4 m	Reader 1						•	
	Reader 2						•	
5 m	Reader 1						•	
	Reader 2						•	•
6 m	Reader 1							
	Reader 2						•	•
7 m	Reader 1							
	Reader 2							•
8 m	Reader 1							
	Reader 2							•

Even two similar type readers output different results for the same tag and similar type of tags perform differently for the same reader. TG 800 type tags (187 and 47) have the highest range. Tag ID 47 was detected by both readers up to 5 m. Tag ID 187 was not detected by both readers at the 3 and 4 m range. But it pops up again at the 5, 6, 7 and 8 m range by ‘reader 2’.

‘MS’ type tags (ones with mercury switch) behave more irregularly. For example Tag ID 66 and Tag ID 193 were not detected at all during this experiment. Tag ID 187 was missing at the 3 m and 4 m range and again popped up at the 7 m and 8 m rage. The presence of mercury near the RF tags might cause some interference with the signal.

4.4.6 Tuning the tag range through shielding

As calculating distances using RSSI failed and from the last experiment it was not possible to find a reliable RF tag that works exactly within the specific range (3m and 6 metre range), it was necessary to seek an alternative solution. The antenna resonant circuit of the inductively coupled tags can be heavily tuned by using a metal surface in its immediate surroundings. In the simplest case it is sufficient to wrap a household aluminium foil around the tag. This will also dampen the reader’s magnetic field due to eddy-current loss in the metal foil. It will reflect the electromagnetic field of a UHF

backscatter system and efficiently keeps it away from the tag. For passive tags it will not even be supply with sufficient power to operate the chip [265]. There is a difference between RF shielding and magnetic shielding. RF shielding is used to block high frequency (100 kHz and above) fields. Typically copper, aluminium, galvanized steel, or conductive rubber, plastic, or paints are utilised for this purpose. These materials work by means of their high conductivity. On the hand magnetic shields use their high permeability to attract magnetic fields. RF shielding has little or no magnetic permeability. However, with properly engineered and constructed magnetic-shield alloys can be served as both RF and magnetic shields [266].

For the PGM, the idea is to wrap the Wavetrend tags in such a way that tags correspond exactly in the 3 m and 6 m ranges. Shielding effectiveness depends on shield material, geometry, frequency and where the field reduction is measured. A current is induced in the surface of the conductive shield material due to the incident electric and magnetic shield. Shields manage these currents and reduce the incident fields (that penetrate the conductive material) by utilising reflection, absorption (attenuation) and internal reflection (see Figure 4-38).

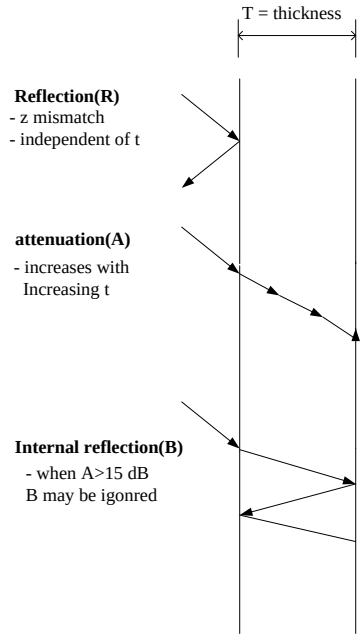

Figure 4-38: Shielding mechanisms. The material is of thickness T, and z is the impedance [267]

As the electromagnetic wave is transmitted into the shield, absorption losses (attenuation) occur due to the exponential decrease of the field amplitude. Absorption

losses (attenuation) occur from the exponential decrease of the field amplitude as an electromagnetic wave is transmitted into the shield. Absorption increases with the increase of the shield thickness. In general, for a given material, skin depth varies inversely with frequency. Reflection is independent of reflector thickness for electric fields and plane waves. Electric fields and plane waves are normally reflected from the first surface (air-shield interface) of the shield. But magnetic fields are transmitted into the shield and reflected from the second interface (shield-air interface). Losses due to reflection are high if the characteristic impedance of the shield is low and/or the wave impedance is high.

Internal reflection losses result from the multiple reflections within a shield material. For thin shields and magnetic fields, internal reflections are high but for electric fields and plane wave it can be ignored. The shielding effectiveness (SE) of a material is the function of the losses resulting from absorption (A), reflection(R) and internal reflection (B).

$$SE = A+R+B\ (db) = 10 \log_{10} (W_i / W_t)\ dB \quad (4.6)$$

Where W_i is the incident power density and W_t is the transmitted power density. For electric field strength, the equation becomes:

$$SE = 20 \log_{10} (E_i / E_t)\ dB \quad (4.7)$$

Here, E_i is the incident power density of electric field and E_t is the transmitted power power of electric field. For magnetic-field intensity, E in Equation 4.6 is replaced with magnetic H field or magnetic B field. Paris and Yan provide a qualitative description of SE as shown in Table 4-17. SE depends on the material used and its thickness. A thicker material produces greater values of SE [267].

Table 4-17: Interpretation of Field Reduction Values [267].

Attenuation (dB)	**Qualitative Description**
0-10	Negligible shielding
10-30	Minimum significant shielding
30-60	Average shielding
60-90	Above average shielding
90-120	Excellent shielding
>120	Superior shielding

4.4.6.1 RF shield Experiment

Shields can be constructed using single or multiple layers of shielding material. A shielding material exhibits a frequency dependent nature in its shielding effectiveness.

A shield does not always have to be a continuous solid material. Perforated solid sheet can be used to achieve the desired level of attenuation [267].

For the PGM, the idea is to wrap Wavetrend 433 MHz tags with a single and/or multiple layers of aluminium foil in such a way that their ranges can be controlled. The ideal solution would be to wrap tags in such a way that they correspond to 3 m and 6 m range in every possible location. It is unknown how thick and/or how many layers of aluminium foil is required for this purpose. For experimental purposes, two TG 800 type tags were wrapped with a 16 micron aluminium foil in several arrangements and after each experiment their range and RSSI value were observed at different locations. The experiment was carried out in similar locations as the cricket experiment. The first experiment was carried out in the corridor of the DCU computing building and another in the reception area in the DCU engineering building. For systematically wrapping a TG 800 tag, it is divided horizontally and vertically in four grids in each direction (see Figure 4-39).

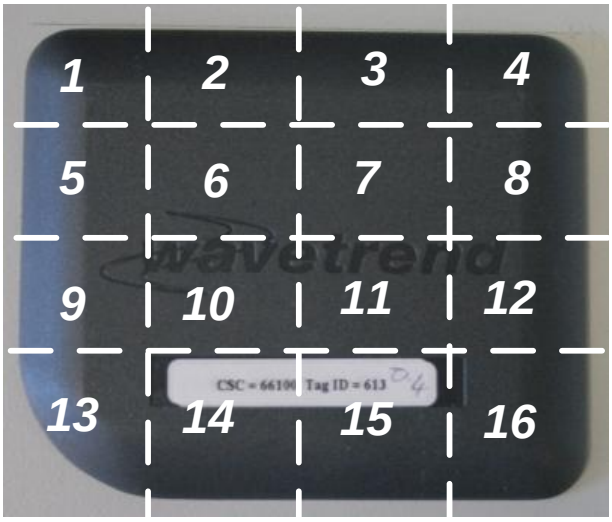

Figure 4-39: TG 800 Tag divided into 4 x 4 grid for wrapping

Altogether, 21 different wrapping styles were used as shown in Figure 4-40. In the first experiments tags were used without wrapping them, and the next one with full wrapping. There was no detection while the tags were fully wrapped. For example, wrapping style 3- Grid 1, 2, 3 and 4 were fully covered with aluminium foil both on front and back of the tags. For wrapping style 10- grid 1 to 4 and 4, 8, 12 and 16 were wrapped completely and moreover grid 4 had two layers of foil. The LRX-201 Reader can be set as Low and High gain mode. Experiments were carried out in both modes.


No wrapping


Full wrapping


Wrapping style 1


Wrapping style 2


Wrapping style 3


Wrapping style 4

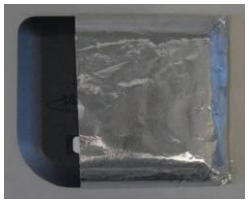
Wrapping style 5


Wrapping style 6


Wrapping style 7


Wrapping style 8


Wrapping style 9


Wrapping style 10


Wrapping style 11

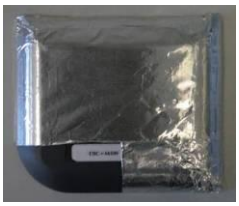
Wrapping style 12

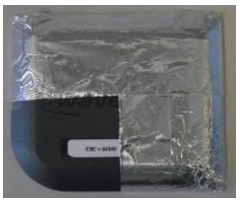
Wrapping style 13


Wrapping style 14


Wrapping style 15


Wrapping style 16


Wrapping style 17


Wrapping style 18


Wrapping style 19

Figure 4-40: Different tag wrapping styles.

4.4.6.2 Experimental Result

Tags were not detected in both the corridor and reception area when they were fully wrapped with foil. This phenomenon was consistent both in high gain and low gain mode. Aluminium foil completely blocks RF signal when the tags are fully covered. Figure 4-41 presents the detected range graph for Tag ID 068. The horizontal axis presents the distance range and the vertical axis is set for different wrapping styles. In the figure, a red dotted line means the tag is not detected, and a black continuous line means the tag is detected. When the tags were open (not wrapped) they were detected uniformly within 1- 8 m but as soon as they were fully wrapped no tags were detected at any distance. With wrapping style 1, the tag was only detected at 1 m range. Surprisingly, with wrapping style 2, the tag was first detected at 1 m and then it suddenly disappeared and reappeared at 2 to 5 m range. Only style 15 was found with uniform tag detection within the 0 to 4 m range.

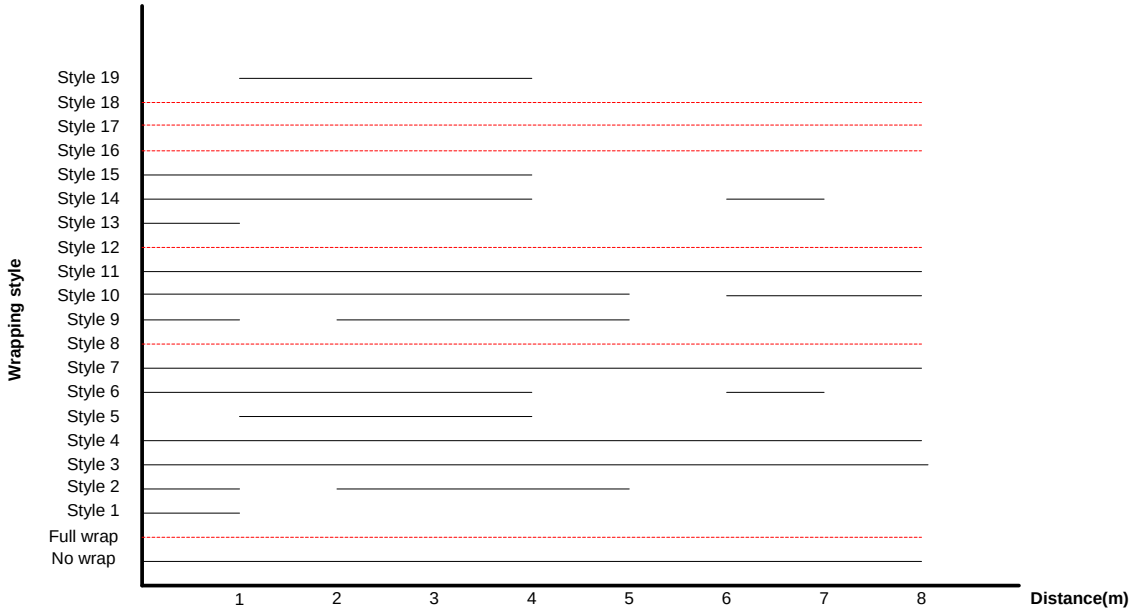

Figure 4-41: Detection Range Graph of Tag ID 068 for different warping style in corridor (low gain mode).

For both the corridor and reception area, no uniform wrapping style was found while the reader was set at Low gain mode. For both Tag ID 068 and Tag ID 631 this phenomenon was somewhat similar. All graphs are attached in Appendix B. In high gain there are a number of wrapping styles which show the tags can be detected uniformly over a certain range. Figure 4-42 presents the experimental findings for several wrapping styles that can be used to tune the RFID range.

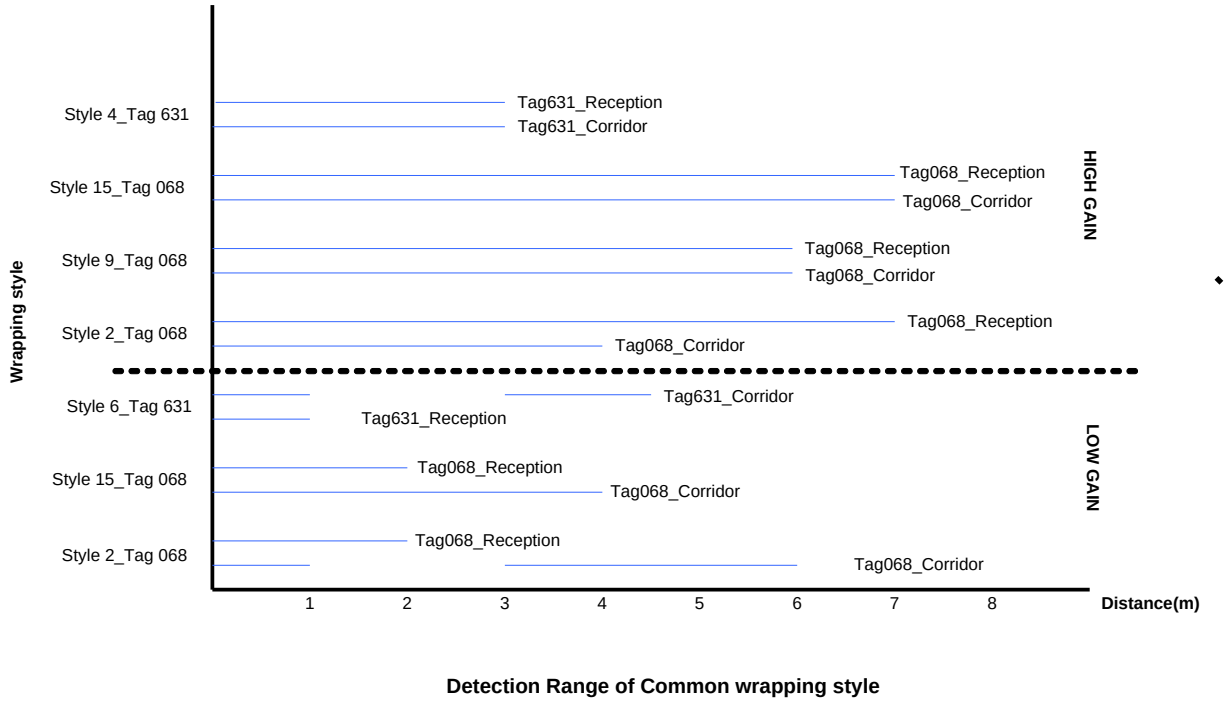

Figure 4-42: Comparison of possible usable wrapping styles and their range.

For example, if wrapping style 9 is used for Tag ID 068, it will be uniformly detected from 0 to 6 m range in both the corridor and reception area. Similarly, wrapping style 4 can be used for Tag ID 631 for 0 to 3 m range.

4.4.7 Summary of findings from the Experiments with RFID

Although RFID can identify a tagged person wirelessly, it is clear from the RFID experiment that the RSSI value cannot be used for distance calculation. It is possible to tune the range through RF shielding. Before implementing it on an actual robot, the shield needs to be carefully calibrated as RF varies due to several factors. It is possible that the results obtained from the above experiments will be different if the experimental location is changed or if there is a presence of multiple people in the scenario. RFID can robustly detect whether a person is present within a specific region but it is not reliable enough to be used solely as a PGM sensor.

4.5 Stereovision

Analogous to human vision, Stereovision is a technique aimed at inferring image depth from two or more cameras. Figure 4-43 shows the difference between a single and stereo pair. In the figure, both real points P and Q project into the same point (p ≡q). This occurs for each point along the same line of sight which is useful for optical illusions. With two (or more) cameras we can infer depth by means of triangulation provided that corresponding (homologous) points in the two images are found.

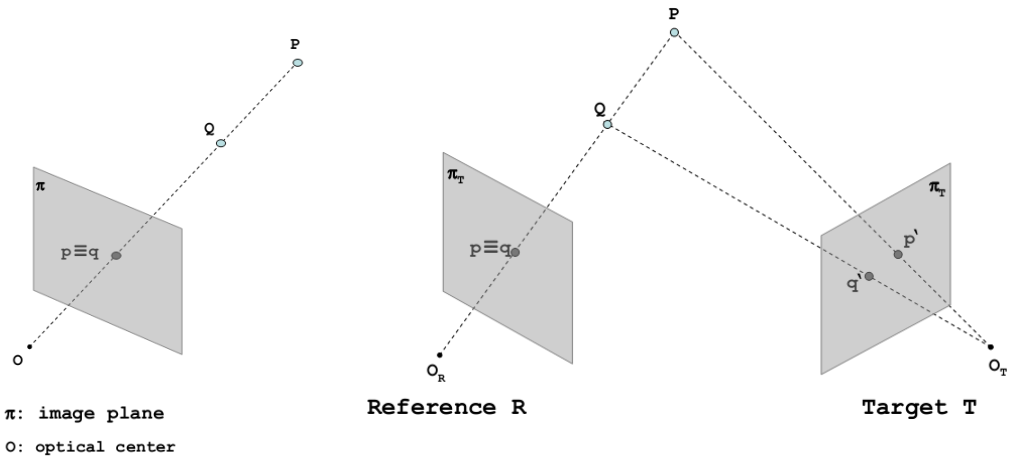

Figure 4-43: Single camera (left) and Stereo camera (right) [268].

An overview of a stereo system is presented in Figure 4-44 . In practice, stereo imaging involves four steps when using two cameras.

- Mathematically remove radial and tangential lens distortion; this is called undistortion. The outputs of this step are undistorted images.
- Adjust for the angles and distances between cameras, a process called rectification. The outputs of this step are images that are row-aligned and rectified.
- Find the same features in the left and right camera views, a process known as correspondence. The output of this step is a disparity map, where the disparities are the differences in x-coordinates on the image planes of the same feature viewed in the left and right cameras: $x_l - x_r$.
- If we know the geometric arrangement of the cameras, then we can turn the disparity map into distances by triangulation. This step is called reprojection, and the output is a depth map [141].

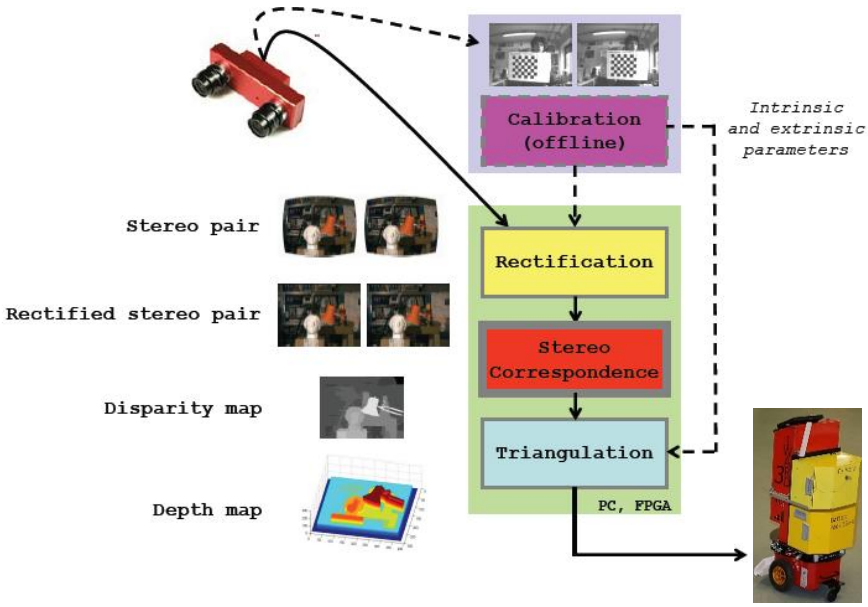

Figure 4-44: Overview of a Stereo Vision system [268].

4.5.1 A simple Stereo System

Figure 4-45 shows the top view of a stereo system composed of two perfectly undistorted and aligned pinhole cameras that are a known distance apart (T), and with equal focal lengths $f_l = f_r$.

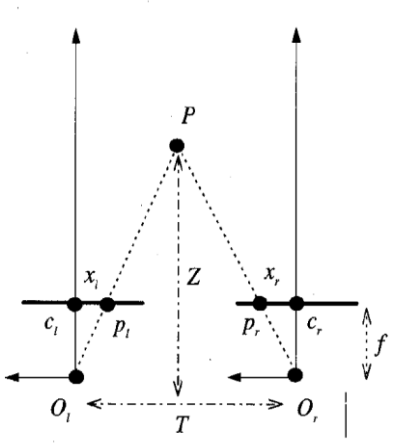

Figure 4-45: A simple stereo system with a perfectly undistorted, aligned stereo rig [269].

The image planes (I_l , I_r) are coplanar and the optical axes (O_l c_l , O_r c_r) are exactly parallel. The first assumption is that the actual principal points, c_l and c_l, have been calibrated to have the same pixel coordinates in their respective left and right images. The second assumption is that two camera's are frontal parallel; every pixel of one camera aligns exactly with the corresponding row in the other camera. The last assumption is that a single point P in the physical world can be viewed in the projection

points of p_l and p_r for the left and right camera respectively. Let x_l and x_r be the horizontal coordinates of p_l and p_r. The depth Z can be estimated from the disparity of corresponding points. The principal rays of the imagers begin at the centres of projection O_l and O_r and extend through the principal points of the two image planes at c_l and c_r. In such a simplified case, disparity can be defined by $d = x_l - x_r$. The distance between P and the baseline T is Z. From the similar triangles (p_l, P, p_r) and (O_l, P, O_r) –

$$\frac{T + x_l - x_r}{Z - f} = \frac{T}{Z} \tag{4.8}$$

Solving (4.8) for Z,

$$Z = f\frac{T}{d} \tag{4.9}$$

From (4.9), depth is inversely proportional to disparity.

4.5.2 The parameters of stereo system

As shown in (Figure 4-45) depth depends on the focal length f, and the stereo baseline T; the coordinates x_l and x_r are referred to as the principal points, c_l and c_r. The quantities of f, T, c_l ,c_r are the parameters of the stereo system, and finding their values is the stereo calibration problem. Stereo calibration is required to find these values. There are two kinds of parameters to be calibrated in a general stereo system and they are intrinsic and extrinsic parameters. The intrinsic parameters characterise the transformation mapping an image point from camera to pixel coordinates in each camera. The extrinsic parameters describe the relative positions and orientations of the two cameras. Stereo calibration is discussed in section- 4.5.4.

4.5.3 The Correspondence Problem

From a computational stand point, solving the correspondence is a challenge. Correspondence consists of determining which item in the left image corresponds to which item in the right image. Thanks to epipolar geometry, the search space for corresponding points can be narrowed from 2D to 1D.

4.5.3.1 Epipolar Geometry

The geometry of stereo is known as epipolar geometry, as shown in Figure 4-46. Figure 4-46 shows two pinhole cameras, their projection centers O_l and O_r, and image planes Π_l

and Π_r. The point P in the physical world has a projection onto each of the projective planes which are labelled as p_l and p_r .

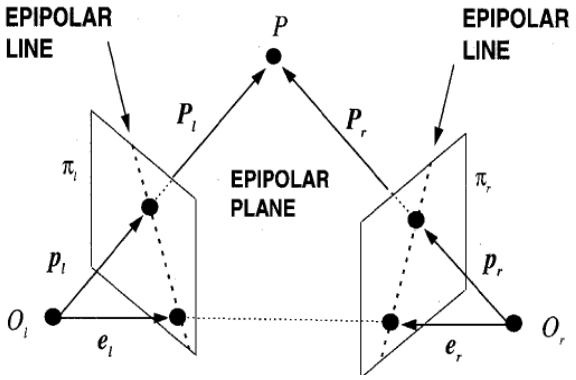

Figure 4-46: The epipolar geometry. [269]

An epipole e_l (resp. e_r) on image plane Π_l (resp. Π_r) is defined as the image of the centre of projection of the other camera O_r (resp. O_l). The plane in space formed by the actual viewed point P and the two epipoles e_l and e_r (or, equivalently, through the two centres of projection O_r and O_l) is called the epipolar plane, and the lines p_le_l and p_re_r (from the points of projection to the corresponding epipolar points) are called the epipolar lines. If the projection point p_l is known, the epipolar line p_re_r is known and the point P projects into the right image, onto a point p_r which must lie on this particular epipolar line. Thus each point observed in one image must be observed in the other image on a known epipolar line. This is known as the epipolar constraint.

In the stereo vision process, searching for corresponding points can be computationally expensive, but thanks to the Epipolar geometry the search space can be narrowed down as much as possible. Once the epipolar geometry of the stereo rig is known, due to epipolar constraints, the two-dimensional search for matching features across two imagers become a one-dimensional search along the epipolar lines. Apart from huge computational savings, it allows the rejection of points that could otherwise lead to spurious correspondences.[141, 269]

4.5.3.2 The Essential and Fundamental Matrix

Prior to the computation of epipolar lines, the Essential matrix E and the fundamental matrix F need to be calculated. The essential matrix contains information about the translation T and rotation R that relate (as shown in Figure 4-47) the location of the

second camera relative to the first in global coordinates. On the other hand, F contains the same information as E along with information about the intrinsics of both cameras. More details can be found in [269].

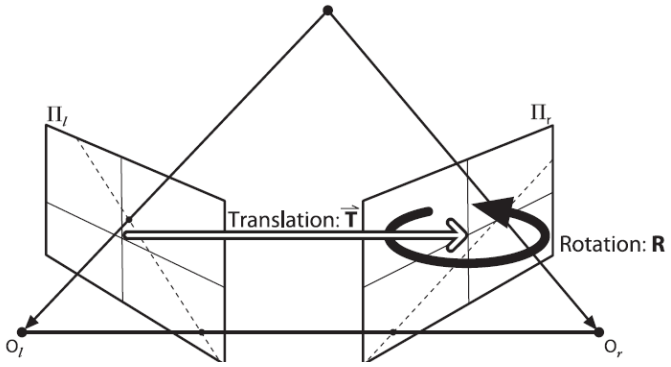

Figure 4-47: Essential matrix E [141]

4.5.4 Stereo Calibration

Stereo calibration is the process of computing the geometrical relationship between two cameras in space [141]. Stereo calibration depends on finding the rotation matrix R and the translation vector T between the two cameras, as depicted in Figure 4-47.

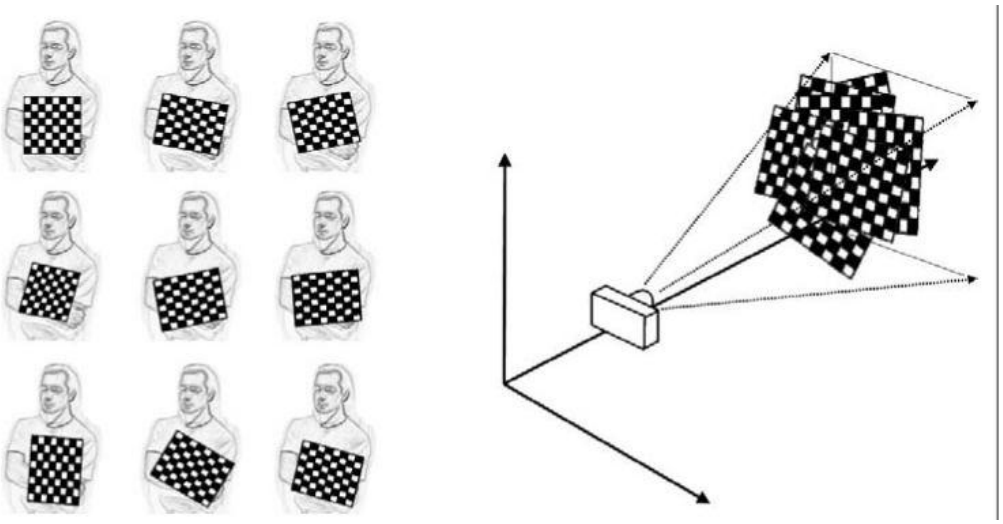

Figure 4-48: Images of a chessboard being held at various orientations [141]

The stereo calibration procedure aims at finding:

- Intrinsic parameters of the two cameras (focal length, image centre, parameters of lens distortion, etc)
- Extrinsic parameters (R and T that align the two cameras)

Calibration is carried out by acquiring and processing more than ten stereo pairs of a

known pattern (typically a checkerboard) as shown in Figure 4-48. More details about stereo calibration can be found in [141, 269]

4.5.5 Stereo Rectification

Stereo rectification is the process of "correcting" the individual images so that they appear as if they had been taken by two cameras with row-aligned image planes [141]. It is easier to compute stereo disparity when the image planes are exactly co-planner as shown in Figure 4-45.

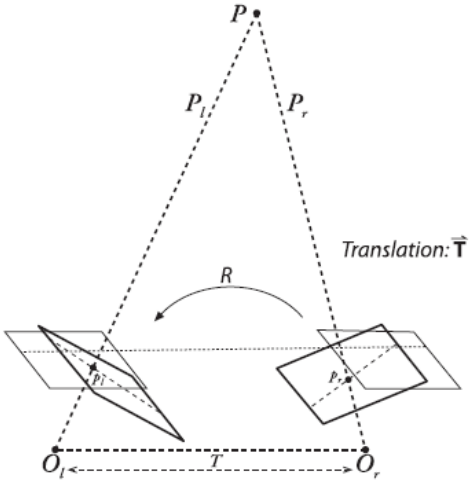

Figure 4-49: Rectification of a stereo pair.[141]

In the real world, rarely do any stereo systems have exactly co planner, row aligned imaging planes. Using the information from the stereo calibration step, it is possible to mathematically align the cameras into a frontal parallel configuration. The goal of the stereo rectification process is shown in Figure 4-49.

There are many methods to compute rectification terms. Of them Hartley's and Bouguet's algorithms are popular. The result of the process of aligning the two image planes will be eight terms, four each for the left and the right cameras. For each camera, there is a distortion vector, a rotation matrix, and the rectified and unrectified camera matrices. Hartley's algorithm [270] can yield uncalibrated stereo using just the fundamental matrix. It can be used to derive structure from motion recorded by a single camera. On the contrary, Bouguet's algorithm [141] uses the rotation and translation parameters from two calibrated cameras. Hartley's algorithm may produce more distorted images than Bouguet's calibrated algorithm. More details about stereo rectification can be found in [141, 269].

4.5.6 Stereo Correspondence

As discussed earlier, stereo aims at finding homologous points in the stereo pair. Given the disparity map, the baseline and the Focal length (calibration), the triangulation computes the position of the correspondence in the 3D space. Similar to the algorithm developed by Kurt Konolige [271], OpenCV[272] uses a fast and effective block-matching stereo algorithm which works by using small "sum of absolute difference" (SAD) windows to find matching points between the left and right stereo rectified images. The block-matching stereo correspondence algorithm has three stages which only work for undistorted, rectified stereo image pairs:

1. Prefiltering to normalise image brightness and enhance texture.
2. Correspondence search along horizontal epipolar lines using an SAD window.
3. Postfiltering to eliminate bad correspondence matches [141].

The software details are discussed in Chapter 6 and more details about the OpenCV stereo correspondence can be found in [141].

4.5.7 Stereo Rig

Several stereo rigs are commercially available in the market but they are very expensive. To check the feasibility of distance calculation by stereovision for the PGM, it was decided to build an experimental stereo rig using cheap webcams.

Figure 4-50: Phillips web camera, Model: PCVC840K

The Philips PCVC840K ToUcam PRO II webcam (Figure 4-50) is a small 1.2 Megapixels colour camera with a USB interface. This camera has a 1 Lux illumination sensitivity which makes it a good camera for in-house and low lighting environments.

Its maximum frame rate is 60 fps and its exposure rate can be set manually. Two PCVC840K ToUcam PROII cameras, as shown in Figure 4-48, were used for building the IWARD experimental stereo rig. Although it did not have a pan/tilt/zoom mechanism, it was good enough for experimenting with various imaging techniques. The horizontal and vertical field-of-view (FOV) of this camera are shown in Figure 4-51.

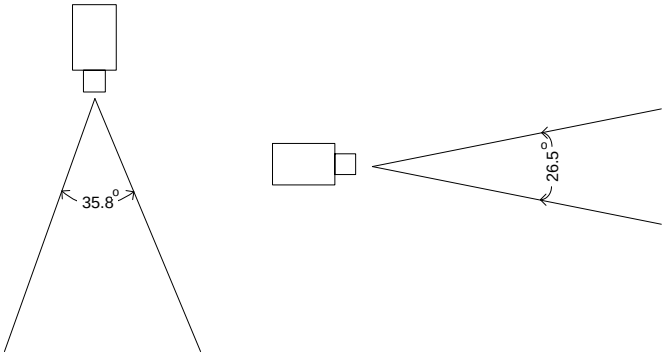

Figure 4-51: Horizontal (left) and vertical (right) FOV of Philips ToUcam

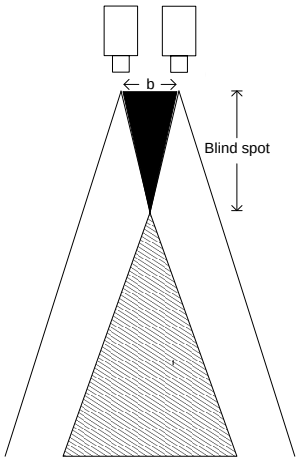

Figure 4-52: Stereo field of view (FOV).

They were measured using a small rig. For the stereo rig, only the 3-D information in the hatched area can be computed (as shown in Figure 4-52), which is simultaneously observed by both cameras, and a blind spot (indicated in solid black) exists between the two cameras. This blind spot can be reduced by decreasing the distance ‘b’ between two cameras. The stereo rig designed for the experiment is shown in Figure 4-53. The base length b, between the two cameras can decrease or increase.

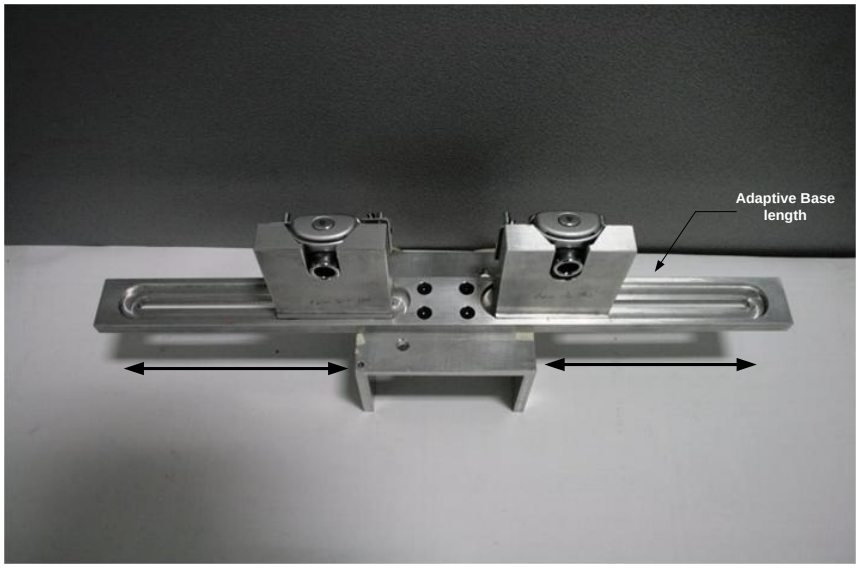

Figure 4-53: Stereo Rig with adaptable base length.

4.5.8 Experiment and Results

The experiment was carried out to find the accuracy of the stereo rig that was developed. Two cameras were placed 150 mm apart and stereo calibration was performed. The experimental setup is shown in Figure 4-54 (left). The objective was to find the distance of a badge worn by a person as shown in Figure 4-54 (right).

Figure 4-54: Stereo Experiment setup (left), a person with a concentric badge (right)

At each meter interval, the distance reading from the stereo software was noted. The software algorithm is presented in Chapter 6. The distance measurement was taken

when a person wearing a circular badge was standing in front of the stereo rig (shown in Figure 4-55). The results are presented in Table 4-18 .

Figure 4-55: A person wearing concentric badge in front of the stereo rig

Table 4-18: Stereo experiment result sheet

Real distance (mm)	**Stereo vision distance (mm)**					
	Ex.No.1	**Ex.No.2**	**Ex.No.3**	**Ex.No.4**	**Ex.No.5**	**Avg.**
100	128	128	126	122	125	125.8
200	209	212	211	213	209	210.8
300	290	290	303	292	289	292.8
350	356	355	355	361	361	357.6

For 1m distance, the average values were recorded as 125.8 mm with a standard deviation of 2.5. The average error was recorded as 25.8%. At a 2 m distance, the average error was only 5.1% and the standard deviation was 3.2. For 3 m, the accuracy increased up to 97.6%. The maximum range was recorded at 3.5 m with an accuracy of 97.82 %. After 3.5 m, the stereo rig could not detect the badge anymore. This was due to the limited resolution of the camera; at longer distances the pixels in the frame representing the badge are too few for stereo vision calculations.

4.5.9 Summary of findings from the Stereo Vision experiments

The above results show that distance calculation using the stereo rig is fairly accurate. Although the maximum range is only 3.5 m (using the low-cost webcams), it is possible to increase it by using a better quality camera. The horizontal and vertical FOV of the stereo rig also can be extended by implementing a pan and tilt mechanism.

4.6 Sensor Fusion

Sensor fusion is also known as (multi-sensor) data fusion. This is a process of combining sensory data in such a way that the resulting information is relatively better than the resulting information produced by the individual sources [273].

In recent years, multisensor data fusion has received significant attention for mobile robotics. As discussed in Chapter 3, sensor fusion approaches build upon the use of multiple sensors or sensing modalities in an attempt to combine their advantages while cancelling out their disadvantages. In systems where high integrity and reliability of measurement is needed, the information provided by a single sensor is not sufficient [274]. In these cases, combining the results of multiple sensors can provide more accurate information than using a single sensor. Stereovision as discussed in section 4.5 is an example of sensor fusion.

From the experiments conducted earlier in this chapter with RFID, stereo vision and cricket, it is clear that none of the single sensors can robustly detect a follower in every possible scenario. The PGM can take the advantage of the sensor fusion approach to resolve this issue. In this section, experiments were carried out while all three sensors: Cricket, RFID and Stereovision were running synchronously in parallel. The goal was to observe how these sensing modalities perform while they are running in parallel. Results from this experiment will give an idea how to develop a sensor fusion algorithm for the PGM.

4.6.1 Experimental setup

In this section, experiments were carried out while all three sensors: Cricket, RFID and stereovision were running synchronously in parallel. For such operation, a special multi threaded application was developed using a C++ programme on Ubuntu Linux platform. The main goal was to collect all incoming data synchronously while a person followed a robot at different conditions. A mobile rig was attached to the RFID reader, Cricket receiver and Stereovision cameras as shown in Figure 4-56 (left). A person was decorated with all the required sensors as shown in Figure 4-56 (right).

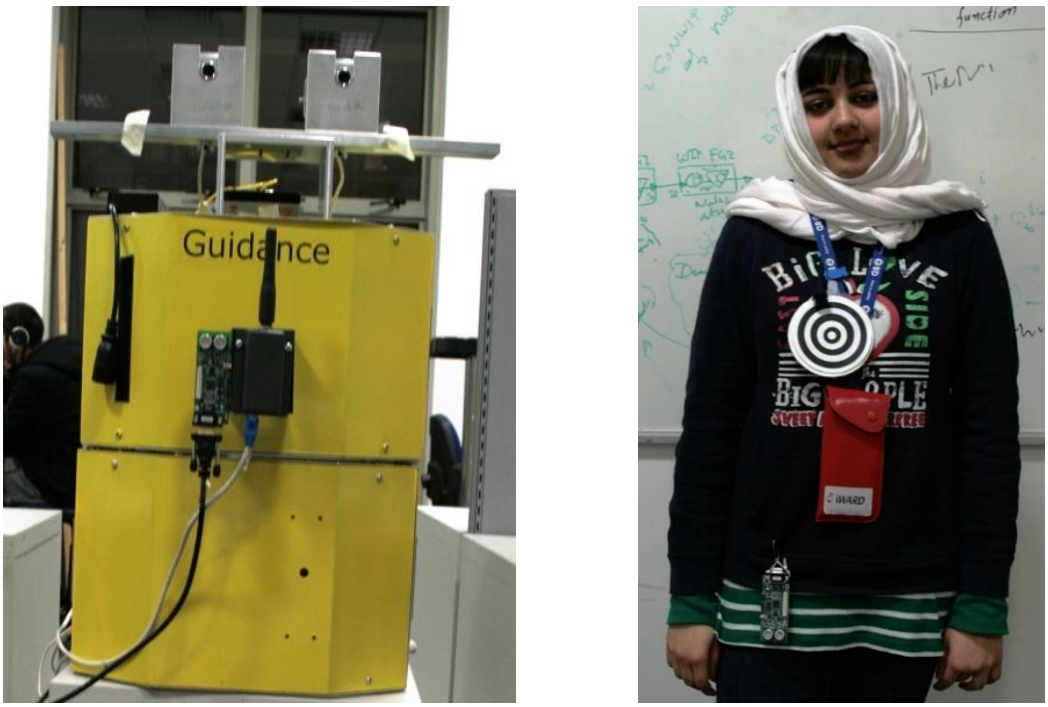

Figure 4-56: Arrangement of sensors for multisensory experiment (left). A person decorated with sensors (right).

Experiments were carried out in a corridor of the DCU computing building as shown in Figure 4-57. In the first experiment, the distance between the follower and the mobile rig was 2 m. The distance was then increased by 1m intervals up to a total distance of 8 m and the same experimental procedure was followed. The last experiment was carried out while the mobile rig was passing a corner as shown in Figure 4-58. All collected data is presented in Table 4-19.

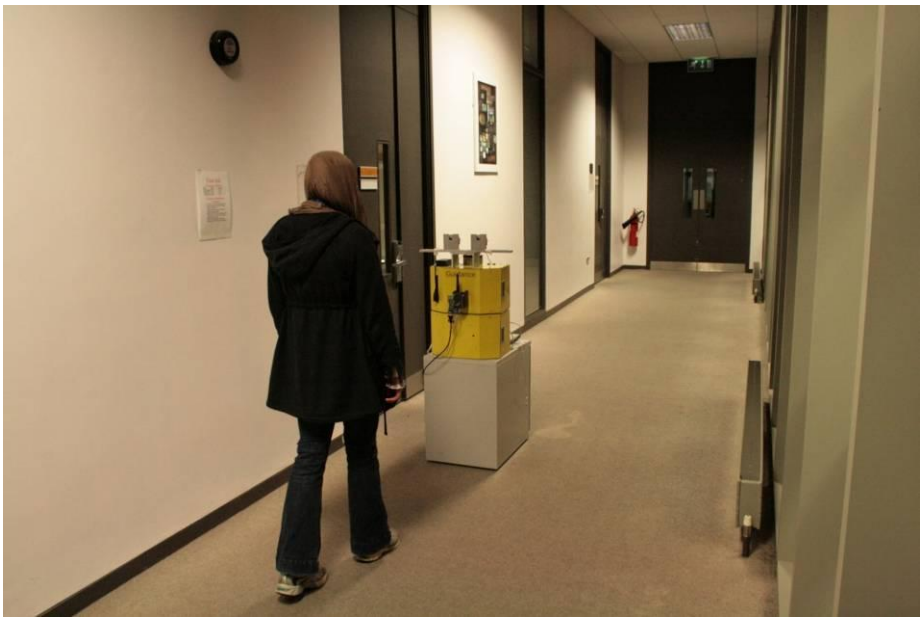

Figure 4-57: Multisensory experiment in a corridor.

4.6.2 Experimental Results

For 2 m distance

In this scenario, the person faced the mobile rig and several readings were taken. Data is presented in Table 4-19. It can be seen that all three sensors successfully recorded their distance data at this range. For cricket, among 5 readings, the average value was found to be 200.2 cm. Both short and long range RFID tags were founded in every reading and the average stereo distance was recorded as 234.8 cm.

Table 4-19: Multisensory Experiment Data in a Corridor

Distance (m)	Order	Cricket (cm)	RFID	Stereo (cm)	Distance (m)	Order	Cricket (cm)	RFID	Stereo (cm)
2	1	200	85,2	226	6	1	585	2	-
	2	200	85,2	238		2	584	2	-
	3	200	85,2	232		3	584	2	-
	4	201	85,2	239		4	583	2	-
	5	200	85,2	239		5	583	2	-
3	1	288	85,2	347	7	1	687	2	-
	2	288	85,2	355		2	687	2	-
	3	288	85,2	355		3	691	-	-
	4	289	85,2	347		4	688	-	-
	5	291	85,2	355		5	689	-	-
4	1	392	2	484	8	1	794	-	-
	2	390	2	485		2	795	-	-
	3	388	2	469		3	794	-	-
	4	389	85,2	491		4	792	-	-
	5	385	2	471		5	792	-	-
5	1	491	2	-	Cornering	1	209	2,85	-
	2	499	2	-		2	216	2,85	-
	3	494	2	-		3	216	2,85	-
	4	491	2	-		4	216	2,85	-
	5	500	2	-		5	215	2,85	-

For 3 m distance

At this distance, the results were quite similar to the previous one. The average for the cricket readings was 288.8 cm and both RFID tags were detected as predicted. The average stereo reading was 351.8 cm. Here, the average cricket reading was found to be 3.73% less accurate than the actual distance whereas the average stereo reading was 17.26% higher than the actual distance.

For 4 m distance

The average cricket distance was recorded as 388.8 cm with an accuracy rate of 97.2%. The stereo reported an average distance of 480 cm with an accuracy of 96%. This was higher than the previous stereo results. Out of five runs the short range tag ID 85 surprisingly reported only once.

For 5 m distance

While the distance between the mobile rig and the follower was 5 m, the experimental results were as predicted. The stereovision could not detect the person and only the long range RFID tag ID 2 was found in every run. The average cricket reading was recorded as 495 cm with an accuracy of 99%.

Figure 4-58: Multisensory Experiment at cornering

For 6 metre distance

The results were similar to the 5m range. The stereo system did not report any readings and only the long range tag was found in every run. The average cricket reading was found to be 583.8 cm with an accuracy of 97.3%.

For 7 m distance

At this distance, the average cricket reading was found to be 688.4 cm. As predicted, the stereo did not report any result. Similar to the 4 m readings, out of five runs the long range RFID tag was found twice.

For 8 m distance

At this range, only the cricket readings were available with an average of 793.4 cm. As predicted, neither the RFID nor the stereo reported any readings.

Cornering

This experiment was carried out while the mobile rig was passing a corner as shown in Figure 4-58.

Even though the cricket receiver and the beacon were not directly at the line of sight position, the average cricket value was recorded as 2.85 cm. The diagonal distance between the mobile rig and the follower was 2 m. The average value of the cricket readings was slightly higher than the actual distance as the US signals were bouncing back from the nearby wall to the receiver. As the follower was out of the camera's view, the stereo system did not report any readings. Both short and long range RIFD tags were reported uniformly in every run in this scenario.

4.6.3 Summary of Findings

This experiment was carried out to see how each individual sensor performs at similar scenarios. In this experiment, while the distances among the person and the robot were kept in between 0 to 3 m and they were at line of sight, all sensors provided reliable data as predicted from the earlier individual sensor tests in Sections 4.1, 4.2 and 4.3. The Cricket provides readings with 98.08% accuracy whereas the stereo reports 91.3% accuracy in the 0 to 3 m range. RFID readings were found to be very consistent with the chosen wrapping style shields. The PGM control system can reliably make the speed synchronisation decision of whether to speed up or down based on its readings either collectively or individually.

Even when the distance increases to 4 m, both the Cricket (97.2% accuracy) and the stereo (96% accuracy) systems still provide results that are very reliable. Surprisingly, on a few occasions the RFID system reported the presence of the short range Tag ID 85 along with the long range tag ID 2. This could be because of the unreliable nature of the radio frequency signal as discussed earlier.

From distances of 5 m and onwards the short range tags were not detected at any occurrences. Similar unpredictable behaviour of RFID readings was also observed at

7 m range. The long range tag ID 2 was not expected to be present at this range but it was visible on a few occasions. The long range tag ID 2 was not detected by the system afterwards at all. The highest range of the stereo system was found up to 4 m and cricket system consistently reported data up to 8 m distance with reliable accuracy.

Although the RFID range seems somewhat of +/-1 m difference from the predicted one, its importance was observed while the experiment was carried out in the 'cornering' scenario. Due to not having line of sight, the stereo readings were not available and the cricket reported only 57.5 % accuracy results. Thanks to the RFID, a person's presence was consistently ensured to the system.

4.7 Chapter Summary

In this chapter all the selected sensors: Cricket, RFID and stereovision were tested at different conditions and their results were discussed. Finally, multisensory experiments (while all three above sensors were running in parallel) were carried out and their results were analysed. The next chapter describes the hardware development of the PGM.

Chapter 5 Hardware Design and Implementation

5.1 Introduction

This chapter describes the hardware implementation of the PGM. Section 5.2 describes the module boxes and the hardware associated with it. Section 5.3 describes how the power-save mode is enabled in the PGM. Section 5.4 presents electric block diagrams of all PGM's hardware.

5.2 Module Box Design

Since all module boxes need to fit into the robots' superstructures, the box specification was developed by the developers of the robot bases (Newcastle University). In line with the modular design concept of the IWARD project, the module box for PGM was made from 1.5 mm thick aluminium sheet metal .The rectangular-shaped box has an overall outside dimension of 392 mm X 225 mm X 232 mm.

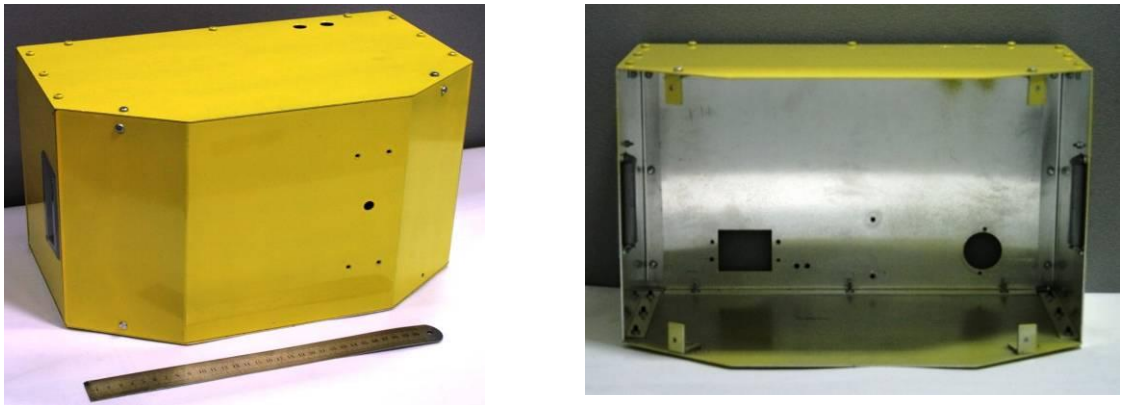

Figure 5-1: Front side of the Module Box (left); Empty space inside (right).

The front side is folded to provide a shape to the robot's body as shown in Figure 5-1 (left). This module can be connected to any IWARD robot module bay using quick-change mechanical connections and standard electrical connections. The empty space inside the module box is shown in Figure 5-1 (right). Figure 5-2 shows the back side of the module box that indicates:

- Power connector (+5V DC, +12V DC).
- Box catching part: used to provide a temporary fixture before locking the box by the robot's locking system.
- Guiding block: used by the robot's locking system.
- Internet connector (using a ceep connector for easier insertion of the box).

Figure 5-2: Module Box (backside).

The following important factors must be considered prior to purchase any hardware for PGM:

- It should be small in size to get an easy fit into the module.
- It should be a low-cost hardware in order to minimise the cost of the overall system and to make it affordable to hospitals.
- The hardware needs to be Linux compatible to integrate with the base robot's on-board computer.
- The power specification should ideally be +5V or 12V DC.

5.2.1 Locking system

In order to lock the module box to the Module bays (superstructure) a Push-to-Close and Pull-to-Open type catching mechanism from Southco [275], Model number C3-803 is used. The 'keeper' part is attached at the back of the module (as shown in Figure 5-3) and the mechanical grabber 'catch' part is attached at the superstructure. This catching block provides temporary fixture of the box in the drawer until the robot locks the box to its superstructure. A microswitch is integrated with the grabber catch so that 'Hardware manager' has full control over it. (There is no microswitch in the catch!!!)

As soon as any module box is attached the ‘Hardware manager’ becomes aware of it. ’Hardware Manager’ needs to send signal in case the module box needs to detach from the robot’s body. This will prevent unauthorised and accidental removal of the module box.

Figure 5-3: Southco C3 screw mount grabber with heavy duty catch [275].

5.2.2 Power Connector

The module is powered through a Strix P72 [276] cordless interface system that is usually used in electric kettles.

Figure 5-4: The strix P72 cordless interface [276].

The interface consists of a male contact housing and a female adaptor which are both cylindrical in shape (Figure 5-4). The female adaptor is mounted on the back of the module box (as shown in Figure 5-2) and the male contact housing sits in the

superstructure. This Strix hot plug supplies power which is required for the electrical devices present inside the module box, drawn from the robot's main power supply unit.

5.2.3 Data Connector

The rectangular Ceep connector from CEEP Ltd., as shown in Figure 5-5, is used to implement an Ethernet connection between the module on-board computer and the robot's computer for data communication. The male part is attached at the back of the module box (Figure 5-2) and the female part is attached to the robot's superstructure.

Figure 5-5: Rectangular Ceep Connector [277].

5.2.4 Computing hardware

Rather than relying on the base robot computer, all module computing (including the guidance module) needs to be performed by the module itself (each module should be self-contained). Based on the IWARD system specification and the sensory requirements of the PGM, the following are the main requirements when selecting the module computing hardware:

- Embedded computer
- Low cost
- Low energy consumption
- Linux platform
- Available serial and USB port, internet connection
- On-board memory

The Gumstix embedded computer fulfils all these requirements. It is the world's smallest Linux computer-on-module [278] which is perfectly suitable given the overall dimensions of the module box. Furthermore, it comes with a Linux kernel installed in it. The Gumstix verdex pro series starter pack kit (KIT0020) is used in the IWARD module development as shown in Figure 5-6. It has an on-board memory, three serial ports, one mini-B USB port, and it is powered by 5V DC power.

Figure 5-6: Gumstix verdex pro series starter pack tool kit [278].

All module computing is performed by this computer such as plug and play of the module, drivers for sensors and actuators, communication of the module with the robot's computer. All module software is cross-compiled–for the Gumstix XScale processor. The Gumstix is powered up automatically once the module box is inserted into the robot.

5.2.5 Module Box Positions on the Robots

As shown in Figure 5-7, the base platform of the Nubot robot (developed by IWARD partner Newcastle University) has 4 drawers and the pioneer has 2 drawers where the functional modules are plugged and unplugged while the robot is running.

The modular design of IWARD means that all drawers and module boxes are identical. Although theoretically any functional modules can be inserted into any drawer on any robot, there are some limitations. In order to operate correctly the guidance module has to be plugged in the top-rear drawer of the base robots (so that the sensors can face the guided person), whereas the cleaning module should be at in the front-bottom drawer.

For example, it is not possible to capture the full upper body of the follower by the stereo camera if it's plugged in at the bottom drawer. Similarly, the cleaning module needs to be plugged at the bottom drawer so that the vacuum pipe can be easily connected to the cleaning module box (shown in Figure 5-8).

Due to this requirement a plug and play mechanism is developed using the rectangular 'Ceep' connector. It is already discussed earlier that this connector is used to implement an Ethernet connection between the module on-board computer and the robot's computer for data communication. Four pins of the 'Ethernet' connector (which are not used for communication purposes) are used to define into which drawer the module box has been inserted. When a module box is inserted into a drawer of the robot the +5V voltage from the robot's power connector is fed to the module's power connector.

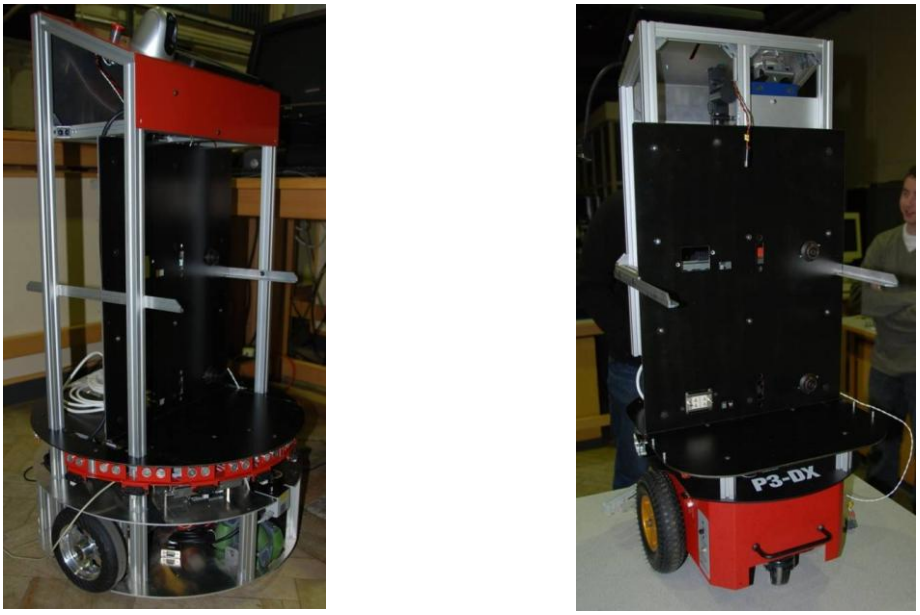

Figure 5-7: Nubot platform with 4 drawers (left) and Pioneer Robot platform with 2 drawers in the front side (right)

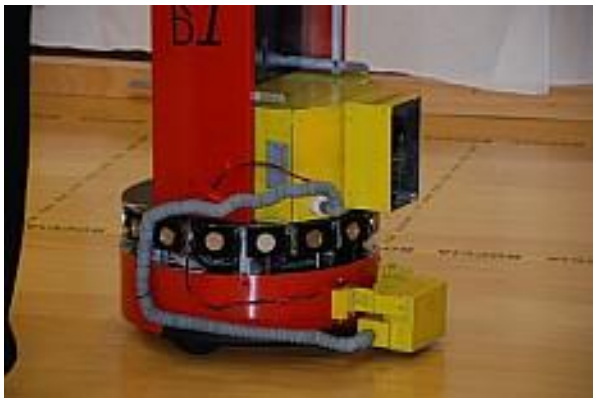

Figure 5-8: Cleaning module connected at the bottom drawer of Nubot.

From there through one of the unused pins of the module's 'Ethernet' connector it is fed back to the same connector at the robot. The three other (unused) pins of this connector are connected to either this +5V voltage or to the Ground, giving a digital code of the drawer of the robot into which the module has been inserted (110 in the picture).

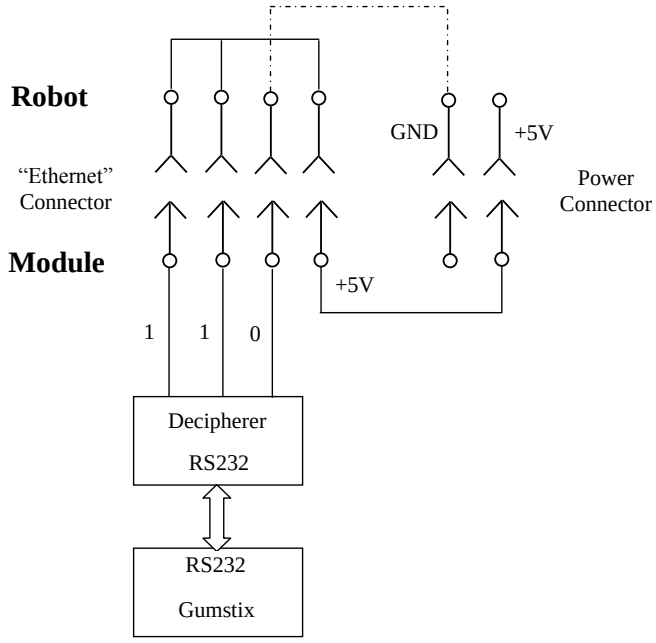

Figure 5-9: Plug-and-play mechanism of a module box using the unused pins of the Ethernet connector.

This code is fed back to the module to a decipherer (PIC-based) which communicates the code through RS232 to the Gumstix computer of the module. The process is shown in Figure 5-9. The Gumstix decides if the module has been inserted into the correct drawer and if yes informs the robot to lock the module to the robot base. Once the module is locked, the hardware manager of the robot's computer is updated with the newly inserted module.

5.3 Power Saving Mode

To save battery power of the robot, all the module sensors that draw power from the robot's main power supply through the Strix hot plug are required to go on standby power-saving mode when they are not in operation. This was implemented by controlling a Solid State Relay (SSR) with the one of the Gumstix serial ports. A SSR requires very little power, which makes it a good solution for the module box. The Gumstix control-vx has three RS-232 ports with miniDIN8 connectors. Pin 6- RTS (request to send) can be used to control a relay. This port doesn't actually send data but

it is used to send the signal to the other devices to convey when to send data. This pin can be set to high or low. When the serial port is open, it sets as high and it can go to about +12 volts. When the serial port is closed, it sets as low and goes to about -12 volts. This voltage swing can be used to control a SSR.

Hardware

The hardware consists of a solid state relay, a diode, a fuse, an 8 pin mini din plug and a number of cables.

Bill of Materials

- SSR, Radionics part # 241-3975(as shown in Figure 5-10)
- 1N4148 diode
- Resistor
- 8 pin mini din plug
- Fuse
- Cables

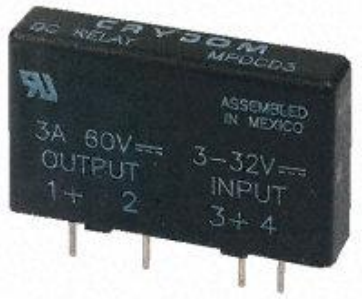

Figure 5-10: Solid State Relay, 3A 3-60Vdc, normally open [279].

Wiring Diagram

The wiring diagram is shown in Figure 5-11. The diagram only shows the wiring of one mains wire.

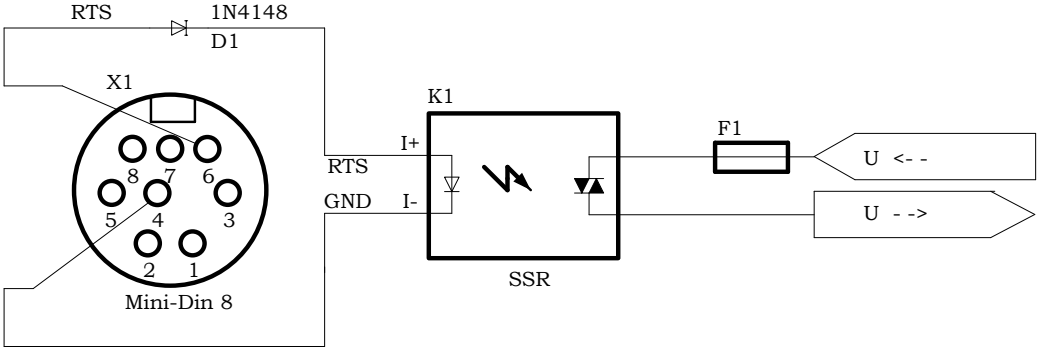

Figure 5-11: Mini-Din 8 port to zero or positive.

When there is a positive voltage between the control terminals, the load will be connected. The SSR works on 3 to 60 volts which is feasible for being driven by the RS-232 port. RS-232 signals normally are either negative or positive. To protect the SSR from negative control voltage a diode is added in series. It limits the voltage from RS-232 port to zero or positive. The SSR that used here can drive up to 3A of continuous load. It is not advisable to draw more than 5mA through the RS-232 port. A fuse is necessary to ensure that the solid state relay does not get destroyed in the event of a short circuit.

Software

The programme to control the SSR through the RS232 port is written using C++ for Linux platform. More details about the software development can be found on Chapter 6.

5.4 Hardware Implementation of the PGM

All PGM's main hardware implementation is shown in Figure 5-12. The completed assembly of the PGM box's exterior and interior are shown in Figure 5-13 and Figure 5-14 respectively.

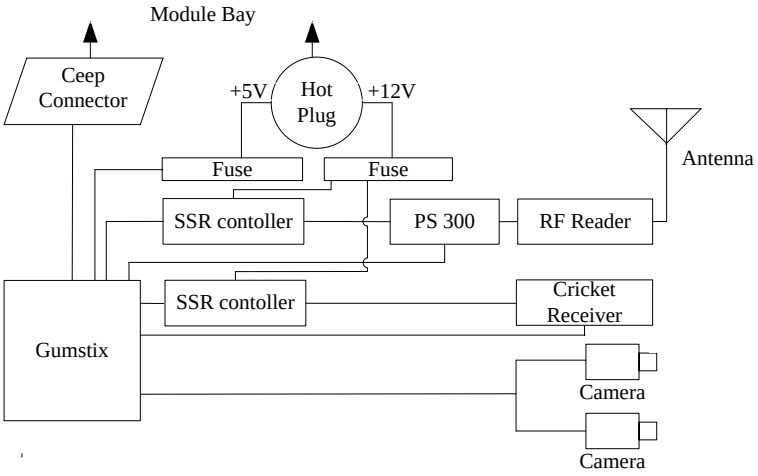

Figure 5-12: PGM hardware implementation.

As soon as the module is plugged into the module bay, the Gumstix gets powered up. It draws power from the robot's batteries through the hot plug. Gumstix's Ethernet port is connected to the Ceep connector for Ethernet data communication. The detail of the

sub-assembly block diagram is presented in the next subsection. Two fuses (for 5V and 12V) are added at the power outlets of the hot plug to protect all the hardware in case of short circuit.

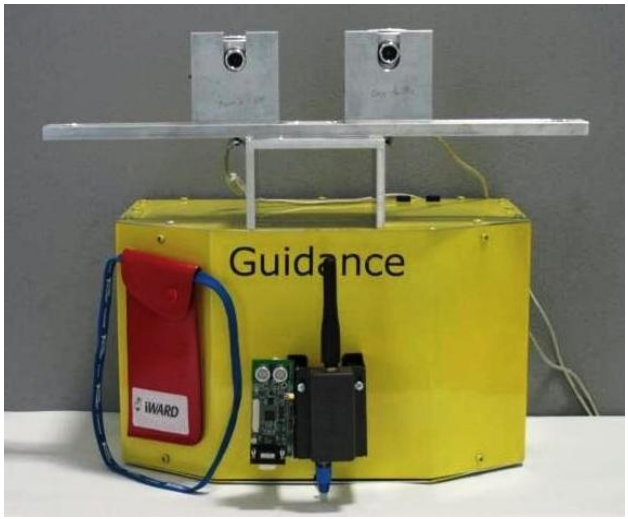

Figure 5-13: Final PGM Hardware Assembly (Exterior).

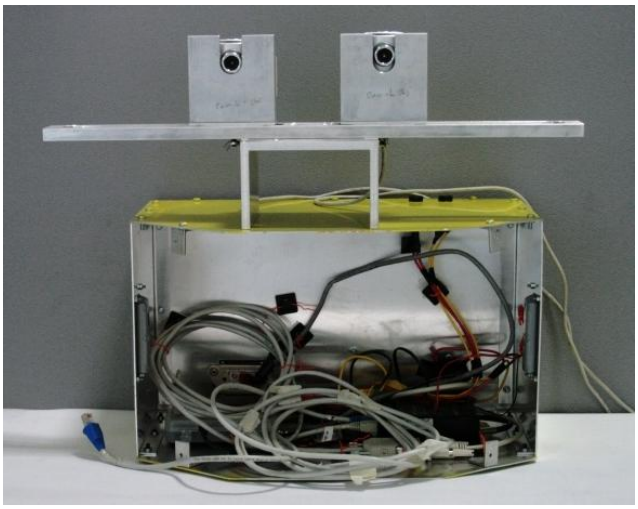

Figure 5-14: Final PGM Hardware Assembly (Interior).

5.4.1 RFID module

The electrical block diagram of the RFID system in the PGM is shown in Figure 5-15. The L-AN200 stub antenna and the L-RX201 RFID reader are attached to the outside of the front plate. A CAT5 connector cable is connected in between the reader and to the 'Net OUT' port of the PS300 Power supply unit. Another CAT 5 connects the 'Net IN' port of the PS 300 unit to the Gumstix serial port. As the Gumstix serial port is of mini-DIN 8 type a null modem adapter and mini gender changer is required before it is

connected to the Gumstix's serial port. The SSR Power controller as discussed in section 5.3 controls the power supply to the PS 300 unit.

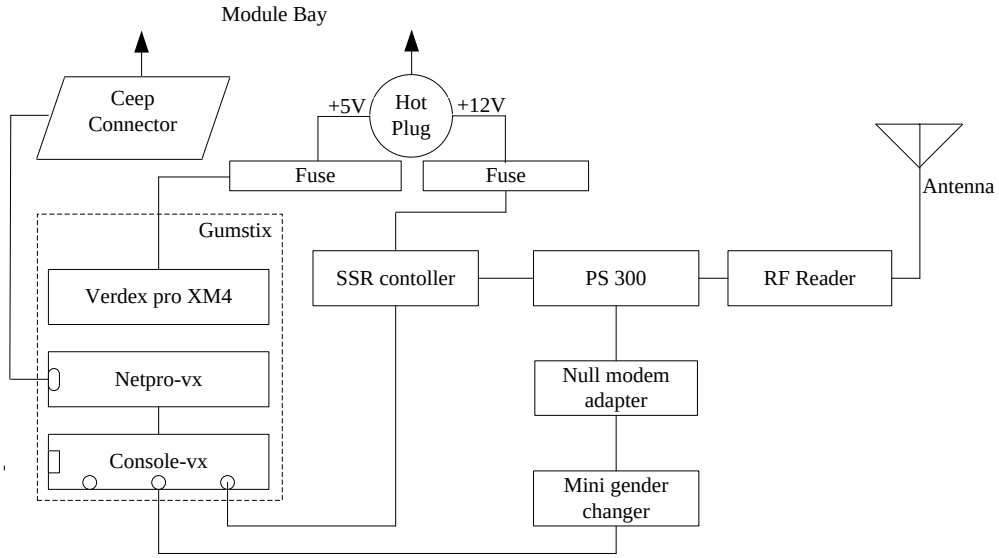

Figure 5-15: Electrical Block diagram of RFID system in PGM Module.

5.4.2 Cricket System

The cricket system in the module box mainly consists of the receiver part. The electrical block diagram is shown in Figure 5-16. Similar to the L-RX201 the cricket receiver is attached to the front side of the module box. The Cricket's power supply is controlled by an SSR controller.

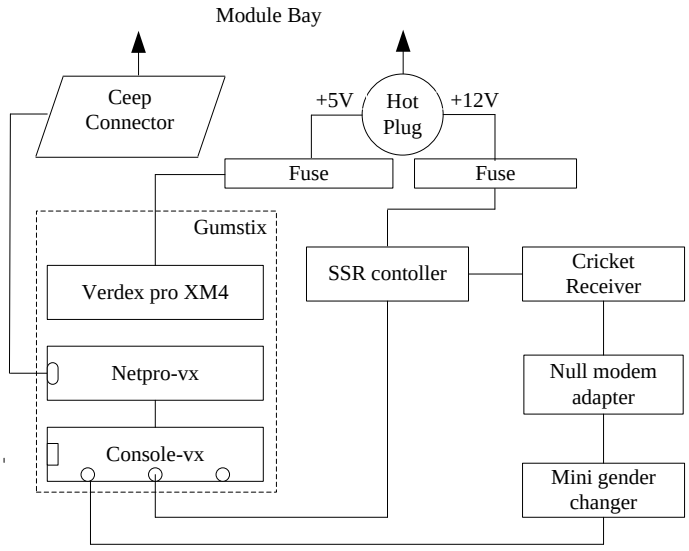

Figure 5-16: Electrical Block diagram of Cricket system in PGM Module

For sending and receiving signals the RS-232 port of Cricket is connected to the

Gumstix's serial port via a 'Null Modem Adapter' and a 'Mini Gender Changer'. The SSR Power controller controls the power supply to the Cricket receiver.

5.4.3 Stereo Vision

The electrical block diagram for stereo vision is shown in Figure 5-17. Two Philips PCVC840K ToUcam PRO II webcam are mounted at the front side of the module box. As the Gumstix Console-vx module has only one USB mini-B connector, a USB hub is required. Furthermore a USB to USB mini-B converter is required before it goes to the Console-vx. Since the cameras are powered directly by the USB port of Gumstix, no SSR controller is required here.

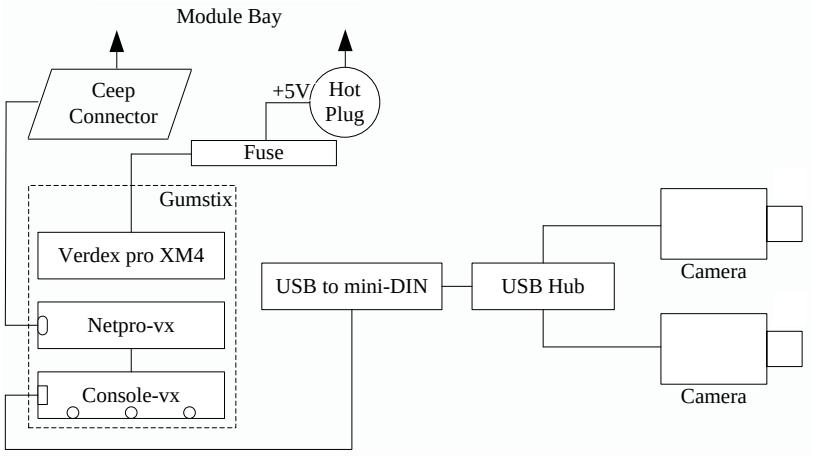

Figure 5-17: Electrical Block diagram of stereovision system in PGM Module

5.5 Chapter Summary

This chapter described how all module hardware was implemented in the module box. The next chapter will describe the software development of this project.

Chapter 6 Software Development

6.1 Introduction

In chapter 2 the general structure of the IWARD software architecture was reported. This chapter gives detailed information about how the software was developed for the PGM. Section 6.2 presents the device drivers that were developed for the RFID reader, cricket transceiver and Philips camera. Algorithms for the PGM's application software are presented in section 6.3. Local communication between software components of one robot is discussed in section 6.4. The software approach for accessing hot-pluggable modules is presented in section 6.5. Finally section 6.6 summarises the chapter.

6.2 Device drivers

Higher-level user application programme access hardware functionality through a device driver. Device drivers are software programmes that simplify programming by acting as a translator between hardware and the application that uses them.

Almost all the PGM hardwares are shipped with a Windows driver. Considering that most robotic development tools are based on Linux, this was the selected Operating System for IWARD (in order to simplify development between different project-partners, Ubuntu Linux was the preferred choice). Device drivers are hardware dependent and operating-system-specific. Therefore, separate device drivers for all PGM hardware are developed. At the development stage, all drivers were designed for Linux 2.6 kernel on X86 platform. Later they were cross-compiled for the gumstix XScale processor.

6.2.1 RFID Driver

Wavetrend provides only a Windows based device driver and executable sample demo application software for the L-RX201 RFID reader. They do not provide any source code to their clients. A Linux device driver is developed for interfacing the L-RX201 RFID reader unit with the PGM application programme. Figure 6-1 presents the architecture for the RFID device driver that is developed for IWARD project. This driver can be accessed also by any other application programme if required.

The L-RX201 reader comprises of a RF Module (RF Receiver and Demodulator) and a network communications module that includes a Micro-controller. The proprietary RFID protocol stack is already implemented by Wavetrend on onboard firmware of this Micro-controller. The Micro-controller communicates directly with the RF Receiver module and connects to the outside world via serial interfaces. Data can be sent independently to and from the 2 x RS485 ports of the L-RX201 reader and is simultaneously represented on the RS232 port. The RFID driver, interfaced with the serial port driver will access this data from the RS232 port of the host (PC, Gumstix etc.) through the serial driver interface of the kernel. The user application programme does not have to know the underlying protocols and addressing techniques, reader settings for configuration, specific packet format for sending commands and receiving responses, and how to decipher the Tag data from the incoming packets. Rather, it needs to invoke a routine in the driver and the driver will issue commands to the device. Once the device sends data back to the driver, the driver will invoke routines in the original calling programme. This also complies with the modular IWARD software architecture requirement as set by the consortium. Thus, writing a higher-level application code will become easier for the programmer. Furthermore, this modular architecture will also protect the system from crash if any programme is coded erroneously [280].

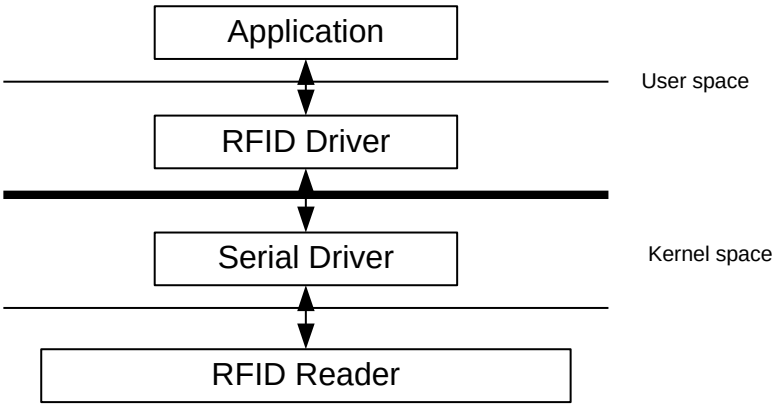

Figure 6-1: Architecture for the RFID device driver in Linux.

The RFID device driver is written in C using POSIX (Portable Standard for UNIX) terminal (serial) control functions. Serial I/O under UNIX is implemented as part of the terminal I/O capabilities of UNIX [280]. There is no separate serial-I/O API in UNIX. Routines that need to control certain terminal I/O characteristics do so by using the 'termios' structure as defined in the header <*termios.h*>. The POSIX "termios" structures are at the centre of serial-port I/O control. This RFID driver is actually a

wrapper around the ‘termios’ structure. The RFID device driver controls the designated serial port through the serial command interface parameters for the L-RX201 (given in Table 6-1).

Table 6-1: Serial command interface for L-RX201.

Transmission speed	115200bits/second
Parity	None
Start bit	1
Stop bit	1
Data bits	8

The application programme invokes the RFID driver using the provided interface. The driver opens the serial port, configures it for communication and passes the associated write command to the serial interface. The serial driver then writes these commands using system calls to the serial interface. The driver then issues a read command and if any data is presented at the serial port, the serial interface passes the response data back to the driver. The driver then deciphers the response data and returns the abstract data to the calling programme. Wavetrend has specific format of the ‘Write’ command and the response data. Due to the confidentiality agreement with Wavetrend Technologies Ltd. these are not disclosed here.

6.2.2 Cricket Driver

The Cricket driver is developed similarly, using a serial port. The cricket’s onboard embedded software is based on TinyOS 1.1.6 and pre installed by the manufacturer. The host device (to which the listener is attached) must run a software to process the data obtained [244].The cricket driver processes the information obtained over the serial interface and passes it to the user application programme. The cricket device driver is written in C using POSIX terminal control functions. The Cricket listener provides data in ASCII format to the cricket device driver running on the attached host over an RS232 interface. The serial command interface parameters for cricket are given in Table 6-2.

Table 6-2: Serial command interface for Cricket.

Transmission speed	115200bits/second
Data format	8 bits, no parity
Flow control	Xon/Xoff(“software”)
Stop bits	1

The application programme invokes the cricket driver using the provided interface. The driver opens the serial port, configures it for communication. If the listener and beacons

are both turned on, every time the listener hears from the beacon it provides output data in ASCII format (as shown in Figure 6-2) to the serial port interface. The serial driver reads the data using standard UNIX system calls *read(2)* and passes it to the cricket driver.

```
VR=2.0,ID=01:dd:be:be:09:00:00:95,SP=MIT-2,DB=224,DR=6479,TM=6789,TS=455424
```

Figure 6-2: Cricket output Data format

From the many fields of the output, the "DB" field gives the distance to the beacon. The default units are centimetres. The driver deciphers the distance results and passes it to the application programme.

6.2.3 Camera Driver

The Philips ToUcam PRO II USB camera only has driver for Windows OS. In Linux, one can use the OpenCV library for grabbing images from the USB connected Philips cameras. OpenCV has an interface for Video4Linux2 (v4l2) API which is included by default in the 2.6 kernel series. Unfortunately, v4l2 API was intended for TV grabber cards and not for webcams. It does not support all the features that Philips webcams have. For example, the settings for frame rate, shutter speed and automatic gain control can not be changed. Allowing a webcam to automatically adjust those features may work well for video conferences but these lighting variations are undesired effects in any image processing operation such as tracking or colour segmentation etc. Such kind of image processing operations requires the above features to be fixed. Fortunately, Pwc Wrapper [281] provides API and can be interfaced with OpenCV in order to gain full features of Philips webcams. A Linux device driver for Philips ToUcam PRO II camera was developed by combining the OpenCV library with Pwc Wrapper functions.

6.3 Module software

6.3.1 Scenario: Guiding a patient from a pick-up point to a specified location

In this scenario a staff member instructs a robot to guide a patient from a start point (nurses' station or reception) to a specified location in the hospital. The steps involved in this scenario are presented in Table 6-3 .The user can request a guidance service using the touch screen or PDA or a mobile phone. The IWARD visual interface was shown in Figure 2-3 in Section 2.5 in Chapter 2. The request service (known as

'mission' within the IWARD system) is transferred to the temporary "Mission Controller" (MC). The MC sends the best suitable robot to the pick-up point.

Table 6-3: Steps in a guiding operation.

Step	Notes
Staff member (nurse, doctor, receptionist) enters HRI	
HRI requests identification (whether the person is authorised to order guidance of patients)	
Staff member identifies herself to HRI	Identification is software based only; login/password (no I-Button)
Staff member requests a patient guidance robot using the control interface, by specifying the start and end location	All locations are nodes on the location graph
Robot generates order number	
Robot sends order number to 'Mission Controller'	
'Mission Controller' selects suitable robot	
'Mission Controller' sends robot to start point	
Robot moves to start point, arrives at start point	
Robot notifies arrival by emitting sound and displaying order number	
Staff member authenticates herself to the robot using IButton	IButton reader is on the robot
On successful identification robot identifies signal from the wearable distance measurement device (the patient's ID is linked to this unit and the robot only guides a patient with this unit)	Wearable distance measurement device consists of RFID Tags, Cricket receiver and concentric badge
Staff member instructs robot to move to specified location using user interface	
Robot moves to destination; patient follows robot with 'virtual elastic band' (PGM measures distance between robot and patient. Speed of robot adjusted according to following distance)	
Robot announces arrival by emitting sound and displaying message (asking patient to wait until received by authorised person) and task information to authorised person	It is assumed that an authorised person at destination receives the patient
Authorised person identifies herself to robot using IButton	
On successful identification authorised person receives patient, notifies robot about completion of task using touch screen on robot, collects Wearable distance measurement device from patient	
PGM switches off distance measurement and identification systems	
Robot informs Mission Controller about completion of task	

The patient follows the robot using an electronic (virtual) rubber band consisting of identification and distance measurement. The distance measurement device worn by a patient consists of RFID Tags, a Cricket receiver and a concentric badge as shown at Figure 4-56 in Chapter 4. The PGM measures the distance between the robot and the patient. If the distance is too large, the robot slows down or stops. If after a long period the patient is still not within a certain range, the robot notifies the mission controller that the patient is lost. The identification system ensures that the robot only guides the specified patient. Upon arrival, the robot notifies the patient and the robot management system.

6.3.2 Zones for Robot Speed Control

Inspired by the proxemics theory discussed in section 3.3 in Chapter 3, the space between the robot and the person during guidance is divided into 3 distinct zones (Figure 6-3):

- ***0-4 meters:*** The robot keeps the human walking speed
- ***4-6 meters:*** the robot slows down: in order to avoid permanent change of speed, the full speed range of the robot is divided into several intervals and speed control is maintained in a step-like manner. If speed reduction is needed, the robot's speed is reduced to the next step below the current one.
- ***6+ meters:*** the robot stops and waits for the tag to come in its range. If after a pre-defined time period the patient does not get into range, the PGM informs the robot management system that the patient is lost.

Speed synchronisation according to these zones ensures that the robot will not chaotically speed up and down and confuse the follower while guiding.

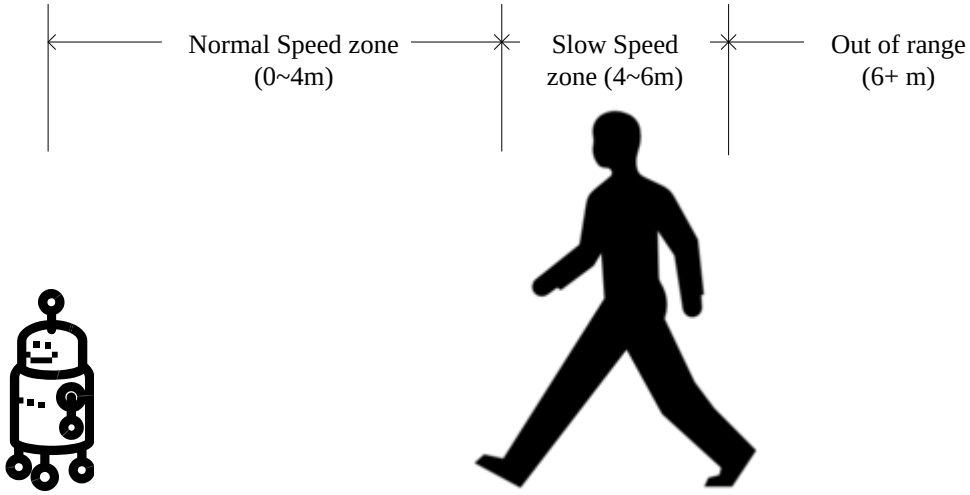

Figure 6-3: Dividing the space behind the robot according to zones for speed control

Speed control requires constant communication between the PGM application software and the robot base's motor control software.

6.3.3 PGM Algorithm

When the 'mission control' receives a guidance mission request, it assigns the task to the most suitable robot through the Orca interface. More details about Orca interfaces

are discussed in details later in this report. Figure 6-3 presents the overall PGM's flow chart.

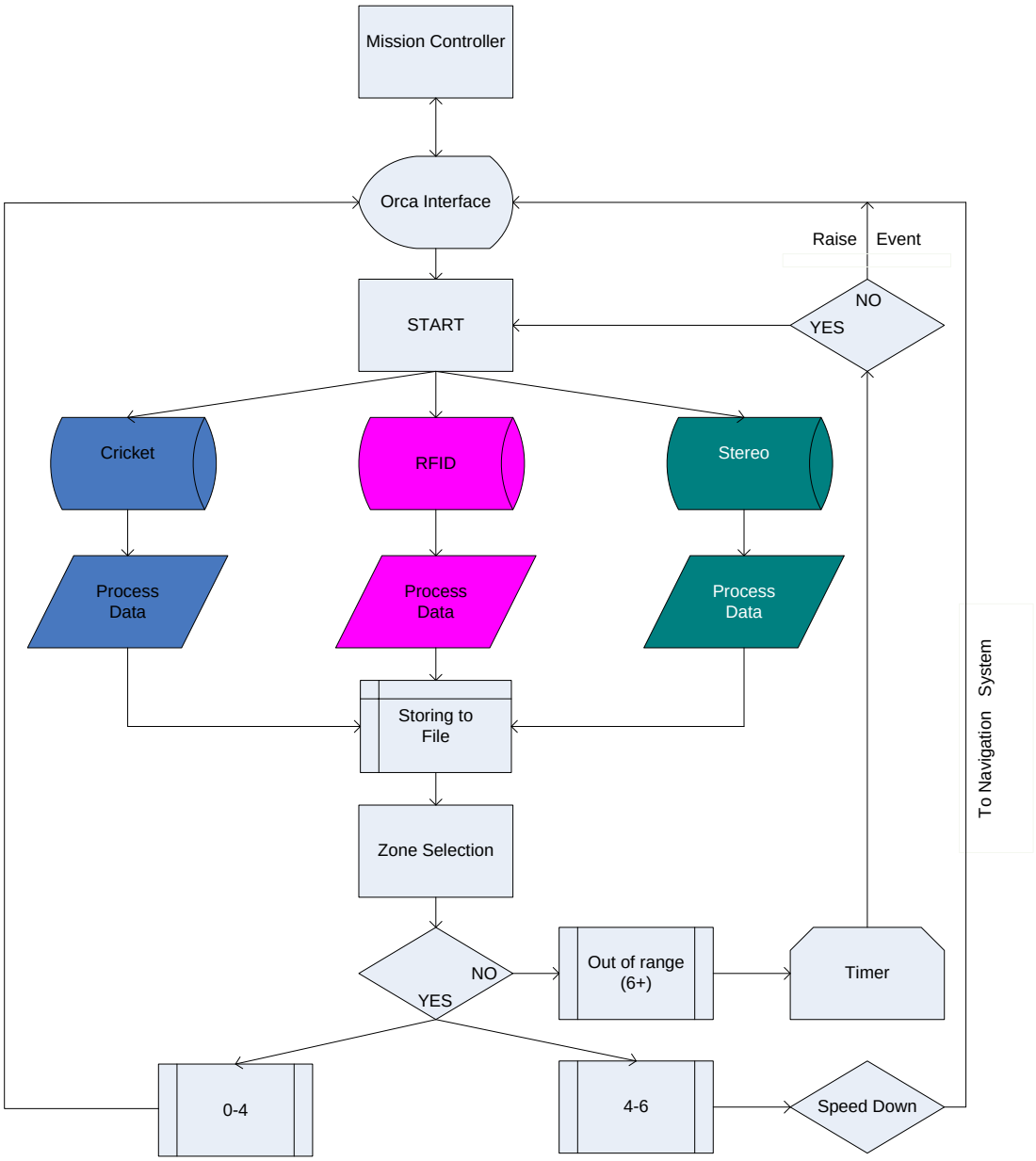

Figure 6-4: Overall Flowchart of the PGM

The robot initiates the PGM. First, it turns on all the module sensors (RFID, Cricket and stereo). Upon successful authentication of the sensors worn by the followers, the robot starts moving towards its destination with its default (normal) speed. At the same time it continuously authenticates and measures data from the sensors carried by the follower. Successful measurements are continuously processed and saved in a file. Based on these

saved measurements, the PGM periodically makes decisions at which zone the follower is currently located at. Decisions are made according to the following manner:

- Data are collected for predefined time.
- Priorities are set according to:
  1. Cricket
  2. Stereo
  3. RFID
- Since Cricket provides higher accuracy than the other two (based on the sensor testing experiments discussed at Chapter 4, the PGM first makes decision based on the latest cricket's data that was stored in the file.
- If cricket's results are unavailable, then the PGM relies on stereo readings for decisions.

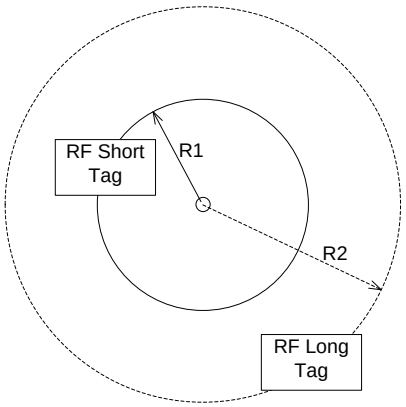

Figure 6-5: Distance calculation technique using two RFID tags

- If first the two sensors on the priority list are unavailable, then it takes decision solely on RFID readings. This follows the protocol below:
  - If the system detects both tags, then it considers that the follower is within the normal speed zone (Figure 6-5).
  - If it detects the Long Tag but no Short Tag, then the follower is in between 4 to 6 m.
  - Finally, if neither tag is detected then the follower is out of range.

If the PGM decides that the follower is in the normal speed zone, then it simply starts the loop again until it receives any other commands from the Orca interface. If the PGM decides that the follower is in the slow speed zone, then it sends a command to the navigation module to step down the robot's speed via the Orca interface. If the PGM

decides that the follower is out of range, then it runs the programme again for a further predefined interval prior to send an emergency STOP command to the navigation module (in case the follower is lagging behind). It will then further wait for a predefined time for detecting the follower. If that fails, the system raises an ‘event’ to the IWARD system that the patient is lost. Once the event has been raised the PGM does NOT continue waiting for the patient any more. Figure 6-6 to Figure 6-8, are showing the individual RFID, Cricket, and stereovision flow charts respectively.

6.3.4 Cricket Programme

The Cricket receiver is turned on as soon as the ORCA interface initiates the START command (Figure 6-6). The programme then opens the corresponding serial port and configures it for communication. If the connection is opened, the programme returns “true”, otherwise it returns “false” and raises an “event” (hardware failure) and passes it to the Orca interface.

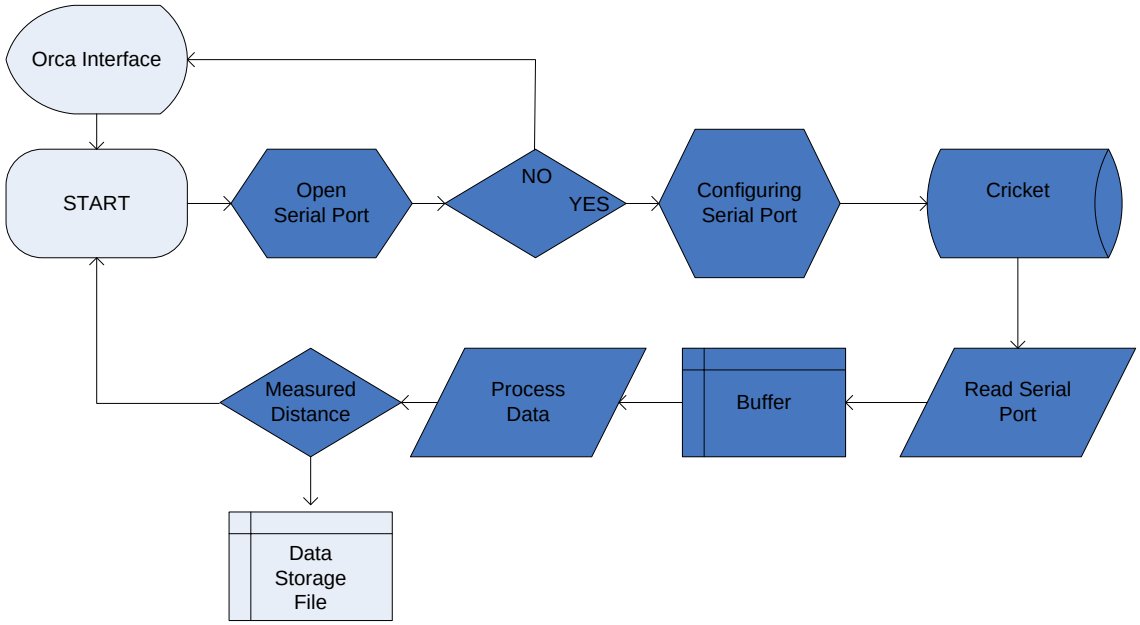

Figure 6-6: Flow chart for Cricket Operation

On successful opening, the programme reads the serial port regardless of whether there is data present or not and stores them into a buffer for further processing. Distance readings from this buffer are extracted and stored into the storage file for decision making. Once finished communicating with the cricket device, the serial port is closed to end the communications session. This programme continues until it receives a terminate command from the Orca interface.

6.3.5 RFID Programme

Similarly to Cricket, the RFID programme is initiated by the Orca interface. It then opens and configures the corresponding serial port. On successful opening, the programme asynchronously reads the tag ID, which is actually a specific hexadecimal string.

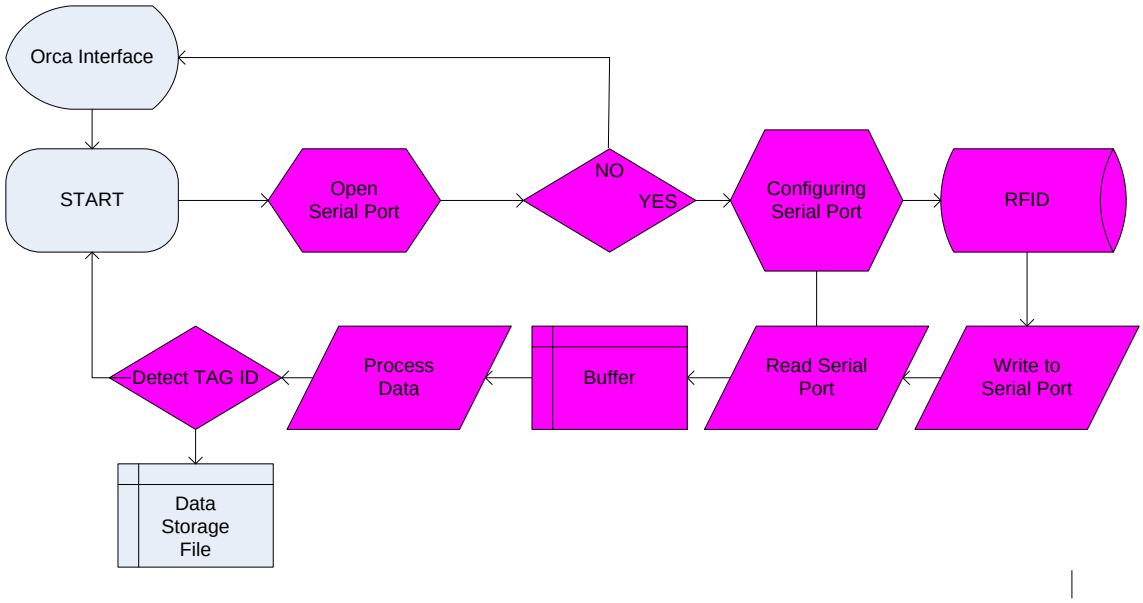

Figure 6-7: Flow chart for the RFID Programme

Then it waits for a predefined time and reads the incoming data and stores them into a buffer. The tag readings are extracted from the buffer and stored into a file similar to the cricket programme. Similarly, the serial port is closed and the programme continues unless it receives the terminate command from the Orca interface.

6.3.6 Stereovision Programme

The main steps in distance calculation using stereo image pairs using a flow chart is given in Figure 6-8. Intel's open source computer vision library, OpenCV is used for all image analysis performed in this thesis. The steps are discussed below:

- At first the programme is initiated by the Orca interface and opens its left and right USB connected stereo camera for capturing images.
- The programme then retrieves images from both cameras and calls *faceDetection()* for detecting the follower's face in the images. Here

OpenCV's Haar Cascades Classifier for detection of frontal faces is used. If the function finds a face, it draws a circle around it. The face detection function also draws a rectangle designating the upper body of the follower (Images in the second row in Figure 6-9). This is done in order to select the ROI for badge detection. The rectangle's height and width is always kept at '4' times the size of the face radius.

- If the *faceDetection()* function successfully detects and draws faces and upper bodies, pointing the possible ROI for badge location in the image pairs, then it calls the *badgeDetection()* function.
- The *badgeDetection()* function at first converts the supplied image (by face detection) into grayscale which is then equalised in order to minimise the effect of differences in lighting conditions (as shown in the third row in Figure 6-9). Furthermore, the equalised images are thresholded using an adaptive thresholding technique. Threshold levels are selected according to the average light intensity of the image.
- In the next step the *badgeDetection()* function performs contour analysis and searches the upper body (ROI selected by the face detection function) and draws a circle if it finds any concentric circles among all the contours. Detection of a concentric badge (carried by the follower) using contour analysis has been recently developed by another IWARD member in DCU.
- Once the badge is successfully found in both left and right image pairs, then the program calls the *distanceCalculation()* function and sends the corresponding coordinates of the centre of the circle found by contour analysis.
- *distanceCalculation()* uses the intrinsic and extrinsic parameters (saved in the stereo calibration experiment) to undistort these axis points using the function *CvUndistortPoints ().*
- The disparity among these points is calculated and transformed into three-dimensional space using the *cvPerspectiveTransform()* function. The 'Z' value after this transformation is the distance of a badge from the stereo rig.
- This value is then saved into a file for PGM decision making and the whole stereo distance calculation program starts again from the beginning again unless it receives a terminate call form the Orca interface.

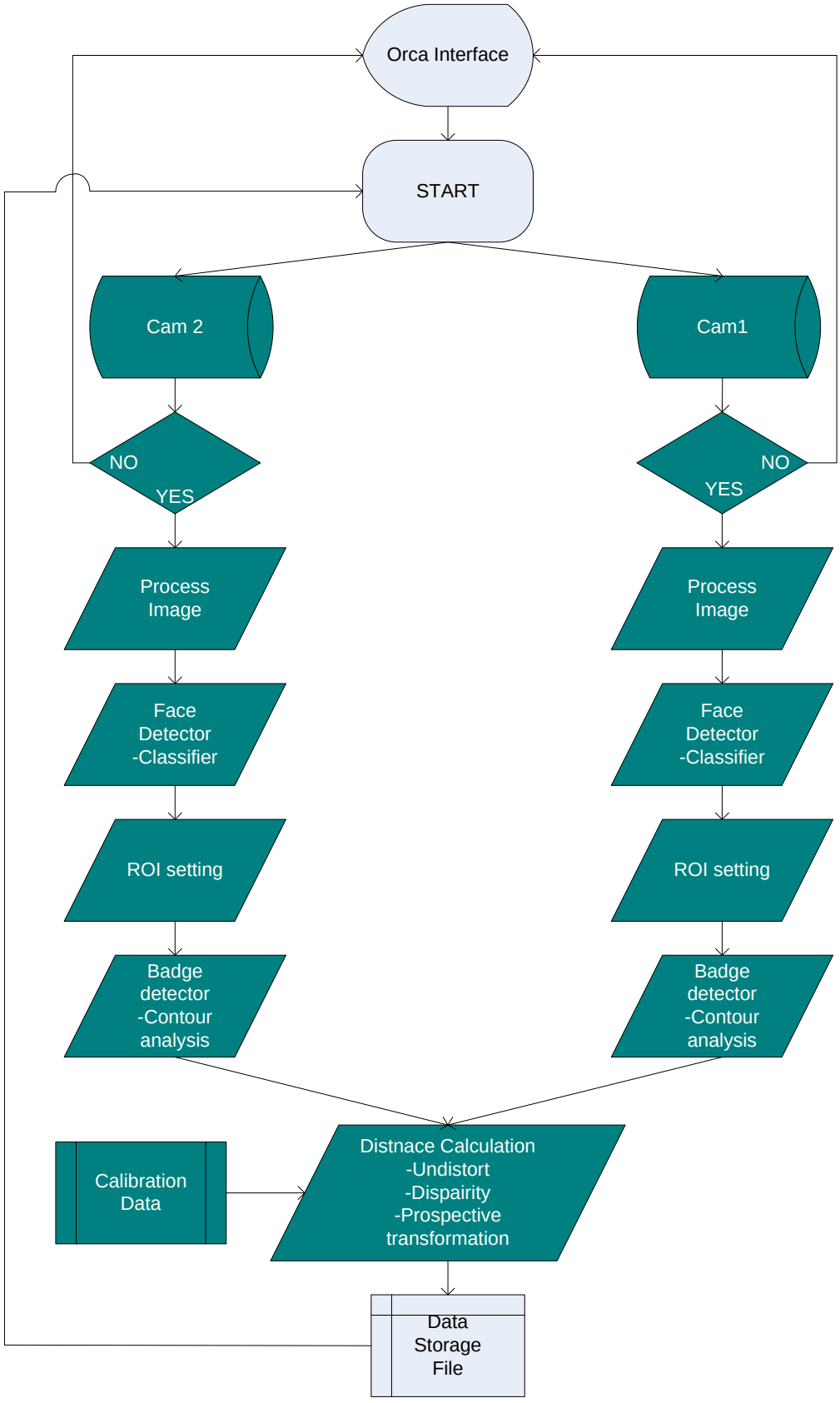

Figure 6-8: Flow chart of the stereo distance calculation programme.

Figure 6-9: Images captured from the stereo distance calculation programme. Left column showing images from the left camera and right column showing images from the right camera.

Stereo calibration

Stereo calibration is the first step for calculating the distance using the stereo pair images. OpenCV's Stereo calibration program is used for calibrating the stereo rig developed in the IWARD project. The calibration process starts with capturing multiple

images of a chessboard viewing from both the left and right cameras as shown in the top images in Figure 6-10. Afterwards it finds all the chessboard corners shown in the bottom images in Figure 6-10 to pair the left and right camera images. The program then calls *cvStereoCalibrate()* to calibrate the stereo rig. This calibration gives the camera matrix_M and the distortion vector_D for the two cameras; it also yields the rotation matrix_R, the translation vector_T, the essential matrix_E, and the fundamental matrix _F. The calibration programme saves this as a YML file as shown in Appendix C. These files are then accessed by the stereo distance calculation programme.

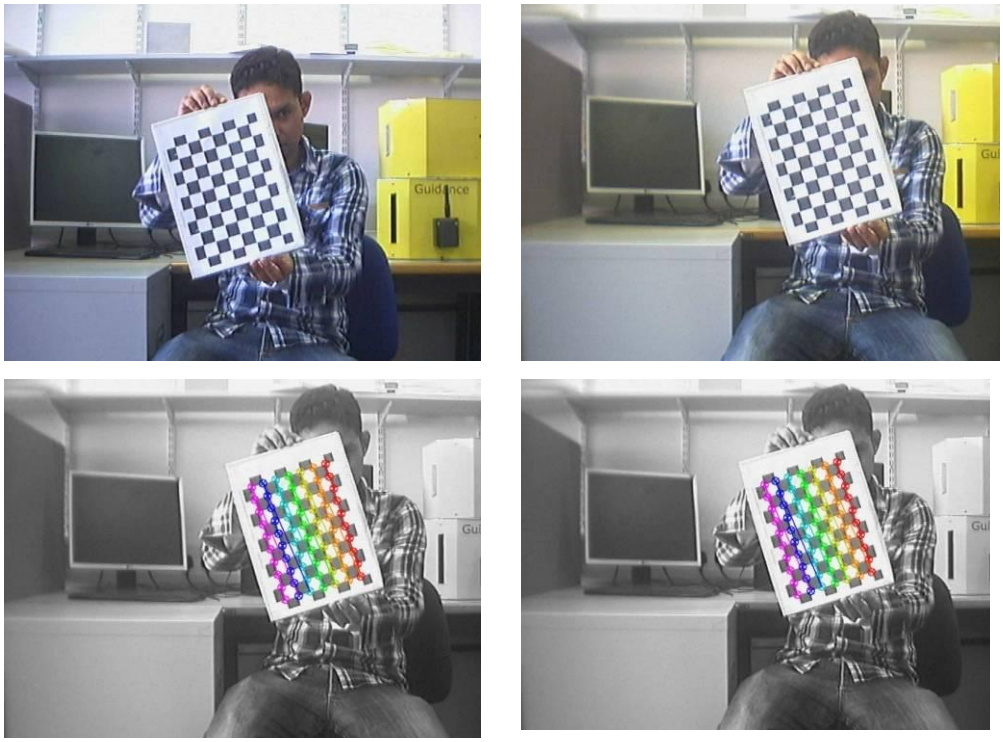

Figure 6-10: Stereo calibration process using multiple view of a plane chess board.

6.4 Module Communications

Following the software architecture specified in Chapter 2, all software modules are developed as Orca2 components. Orca2 considers a system as a set of components which run asynchronously, communicating with one another over a set of well-defined interfaces. In order to define the set of interfaces which make possible the connection between different software components, Orca2 relies on the Internet Communications Engine, or Ice, an object-oriented middleware that provides object-oriented remote procedure call, grid computing, and publish/subscribe functionality [282]. The basic

idea is to have components responsible for dedicated tasks communicate via the Ice middleware (and specifically in Ice's interface definition language, called Slice).

6.4.1 Interfaces and Communication between components

In the IWARD software system, two basic communication concepts between components of a single robot system (local communication) are used:

1. Remote Procedure Calls (RPC). RPCs are directly supported by the Ice middleware. Components provide operations like *start(), initiate()* etc. to trigger a certain action at a component. Other operations, like *setConfiguration()* change the way a component behaves while/when running.
2. Ice Storm/Icebox Events. Ice Storm is a service provided by the Ice framework. It supports components to register a topic at the Ice Storm service. This topic can have several subscribers that get notified in case the topic gets updated.

Thus, it is possible to have synchronous communication (1.) and asynchronous communication (2.).

6.4.2 Components in IWARD

In Figure 6-11, an overview of all components of the IWARD system can be found. The major components of the system are the *RouteManager* (manages the route of each robot), *Peer* (responsible for robot-to-robot communication), *SwarmControl* (responsible for handling swarm level reasoning), *DecisionFInder* (for handling the autonomy level reasoning), *MissionScheduler* (responsible for the execution of a dedicated mission), *HWManager* (keeps track of the status of the robot's hardware and makes it accessible for other components), *InteractionManager* (provides interface to the user), several components that manage robot navigation, and the components of the robot service modules (the PGM is one of them). The various components and the interfaces that they provide were developed by the IWARD partners. The component for the PGM and its interface was developed as part of this thesis. Guidance Component The guidance component controls the guidance module. The interface provides operations to start and stop the guidance functionality. Since the operation of the PGM is initiated by external components (the Mission scheduler through the Hardware Manager), the Guidance component needs to provide an interface through which the internal function of the PGM become available for external components. Once started, the guidance module takes over the control of the robot's speed and is responsible to

keep the guided person in close distance to the robot until guidance gets stopped. For this, it uses the functions of the navigation components (using their interfaces).
Interfaces required: velocitycontrol2d
Interfaces provided: MIGuidance

6.4.3 SCI – interface description language

The IWARD Software Architecture is based on the Orca framework, which at the same time extensively uses services shipped with Ice:

1. IceGrid Registry - centralised registry (naming service)
2. IceGrid Node - sophisticated software activation service
3. IceBox - application server
4. IceStorm - event service with publish/subscribe semantics. It's an object-oriented publish-and-subscribe framework that also supports federation and quality-of-service. Unlike other publish-subscribe frameworks such as TIBCOs' Rendezvous or SmartSockets, message content consist of objects of well defined classes rather than of structured text.
5. IcePatch2 - software distribution service

In the context of the IWARD project, mainly IceGrid Registry and IceStorm are used.

The Simple Component Interface (SCI) is a system developed by Fatronik to reduce complexity of developing interfaces for Orca. Orca has many useful features but there is an issue that makes the development very hard and slow: interface implementation and maintenance. The idea behind developing sci framework was to provide the suitable tools to automatically create all the repetitive code needed to set up the communication among components.

Defining Interfaces

SCI makes use of well defined Extensible Markup Language (XML) files to define interfaces. All the code generation is based on those XML files, whose syntax is specially designed to make easier the generation of the needed code. To define an interface a special XML file has to be written. The interface definition file for the guidance component ("miguidance.sci") is attached in Appendix D. The generic structure of these types of files is as below (SLICE snippets presented here are taken from miguidance.sci):

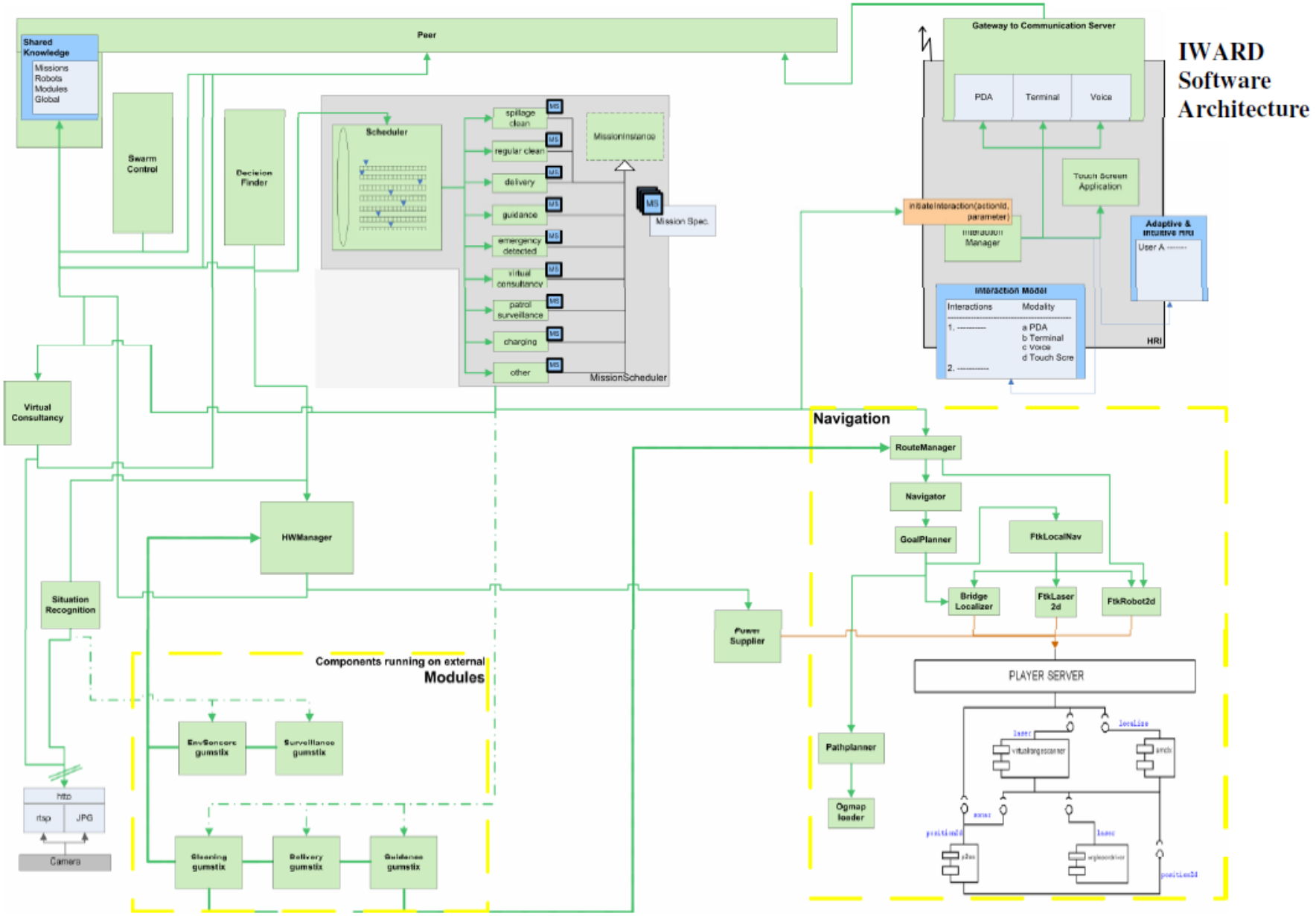

Figure 6-11: Software Components in IWARD System [19]

- At the beginning a header is defined which does not have any effect on code generation but can be useful to tag the files written.
- The SLICE definition is the most important parts of the file. Classes and data types used in the interface can be defined here, using SLICE syntax directly. SLICE snippet for the definition of miguidance.sci is shown below:

```
<definitions type="slice">
    <![CDATA[
        #include <orca/orca.ice>
            module iward
            {
                  enum GuideEventType {lostguidedperson };

                  class GuideEvent extends orca::OrcaObject
                  {
                        GuideEventType type;
                        string eventId;
                        string result;
                  };
            };
    ]]>
      </definitions>
```

To summarize, a GuideEvent class is defined which derives from orca::OrcaObject variables. These data types will be used later in the subscriptions and operations.

- Next step is to define the different mechanisms to communicate. At first the interface name is defined, then the module where its data types are defined and whether it is lockable. Next in the Subscription tag the name of the data type (derived from orca::OrcaObject) to whom it wants to subscribe is given.
- Two operations startGuidance and stopGuidance are also defined in this interface. For each operation its name and its mode (default: normal; options: normal, nonmutating and idempotent) has to be provided.

```
<interface name="MIGuidance" module="iward" lockable="true">

            <subscription type="GuideEvent" />

                  <operation name="startGuidance">

                  </operation>
                        <operation name="stopGuidance">

                        </operation>
</interface>
```

- If required the parameters of the operation, as well as the return value type (if we do not define any return value type, the operation will not return anything) needs to be defined as well. These are not required for miguidance.sci

SCI defines one interface per XML file. Both interface name and XML file name have to be the same (case-insensitive). There is also a restriction: SLICE allows interfaces to derive from another interface (using the keyword 'extends'). SCI also allows interface extensions, but it only supports it whenever the extended interface is also defined by using SCI. The SCI system is fully integrated in the Orca build system, defining interfaces with SCI does not have any effect from the user point of view. That means that when a user writes the .sci file in the suitable directory, it is enough to compile everything as usual to generate all the code needed.

6.4.4 Basic Module

Certain interface functions are common to all functional modules hence they are defined in an abstract module named as "Basic module". The interface definition file for basicmodule.sci is attached in Appendix C. This interface is implemented in PGM along with miguidance.sci (the interface definition file of the PGM) as it must be implemented by all components providing access to a hardware module. This interface subscribes to "ModuleErrorEvent". Two operations, "shutdown" and "reset" are defined as default. The"Shutdown" operation implements shutting down the module completely; this is required before removing the module from the robot base. The "Reset" function restarts a module; normally used if the module has a failure and the embedded computer needs to be re-booted.

6.4.5 Implementing Components with the Interfaces

Once the interface is defined the components that will use them are implemented. Each interface has two sides: sever side and client side. All the code snippets provided here are extracted from the guidance component that is already implemented in the IWARD project.

Client Side

First of all a proxy object has been declared to have remote access to the server. All these codes belong to the *mainthread.cpp* file. Each component has such a file, where the behaviour of the component is implemented. A proxy object for the guidance client is declared as:

```
iward::MIGuidancePrx guidePrx;
```

Subscription to the MIGuidance is defined below:

```
consumerGuide = new
scifaceimpl::iward::MemberNotifyingMIGuidanceConsumerImpl<MainTh
read>::Type(context_);
consumerGuide->subscribeWithTag(TAG_GUIDANCECLIENT, this,
subsysName());
```

MemberNotifying consumer handles the subscription. MemberNotifying consumer saves the value of the data type to whom it is subscribed. The “startGuidance” and “stopGuidance” operations that were defined in the MIGuidance interface can be used in the following way:

```
guidePrx->startGuidance();
guidePrx->stopGuidance();
```

Server Side

Similar to the client, all code lines provided here belong to the mainthread.cpp file. Servers have to implement the operations defined in the interfaces. An example for how two the operations “startGuidance” and “stopGuidance” are implemented in the mainthread.cpp file of guidance server are shown below:

```
void MainThread::MIGuidance_startGuidance()
{
  .......
    return;
  }

void MainThread::MIGuidance_stopGuidance(){
{
.......
    return;
  }
```

The other important function of the servers is to publish data. As discussed before, the IceStorm service is used for these purposes, which uses the “localSetAndSend” method. An example for raising an event if the patient is lost while guiding is shown below:

```
iward::GuideEventPtr myEvent = new iward::GuideEvent();
myEvent->type = iward::lostguidedperson;
myEvent->eventId = "";
myEvent->result = "Patient lost";
scifaceimpl::iward::MIGuidanceImpl::localSetAndSend(myEvent);
```

6.5 Connecting Functional Modules using Plug and Play (PnP)

Following the IWARD modular design, the robot modules are designed to be able to get plugged and unplugged while the robot is running (hot-plug mechanism) .This requires special handling concerning the hardware as well as software aspects.

6.5.1 Module Hardware Interface

The hardware aspects have been initially described in Chapter 5. The modules (drawers) are connected to the platform by only two interfaces.

- A power connection providing 5V and 12V
- Ethernet connection for communication between the module and robot platform

6.5.2 Software Interface

All IWARD modules are equipped with a Gumstix embedded computer. These computers run a special LINUX distribution and this enables them to have Orca components running directly on the module’s computer hardware. After powering a module the Gumstix automatically boots and starts the onboard module component. This component is thereafter responsible to handle the module hardware and provide orca interfaces for it – accessible for the components of the robot system. The second task of the module components is to register the component at the hardware manager to make the modules interfaces accessible. The operation sequence of the registration process after plugging the module and starting the onboard Orca component (Figure 6-12) are:

1. Register the Send type and ID of the module as well as the endpoint address to HWManager

   Example: register (guidanceBox, 10.0.1.3/guidanceBoxDriver)
2. Fire Icestorm Event: ConfigurationEvent (module added)
3. HWManager updates the Shared Knowledge

Access to module components is provided by the HWManager. When a third component needs to access an operation on a module component, it firsts retrieves the current endpoint of the required module. If the module actually is equipped, the HWManager returns the requested endpoint address. Now the component is able to directly communicate with the module. (Figure 6-13 and Figure 6-14). Before removing the module it needs to unregister at the HWManager. Then a Configuration event gets fired to update potential users of the module that the module will power down now. After this the shutdown operation on the module is called by the HWManager and the module is ready to get removed. The process is shown in Figure 6-15.

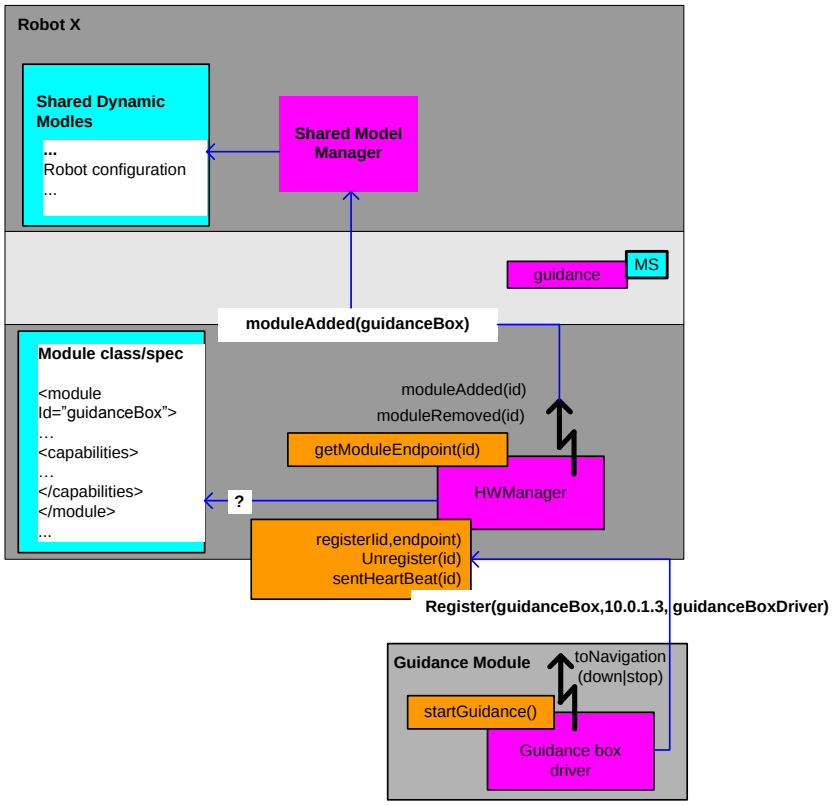

Figure 6-12: Registering the guidance module with the hardware manager

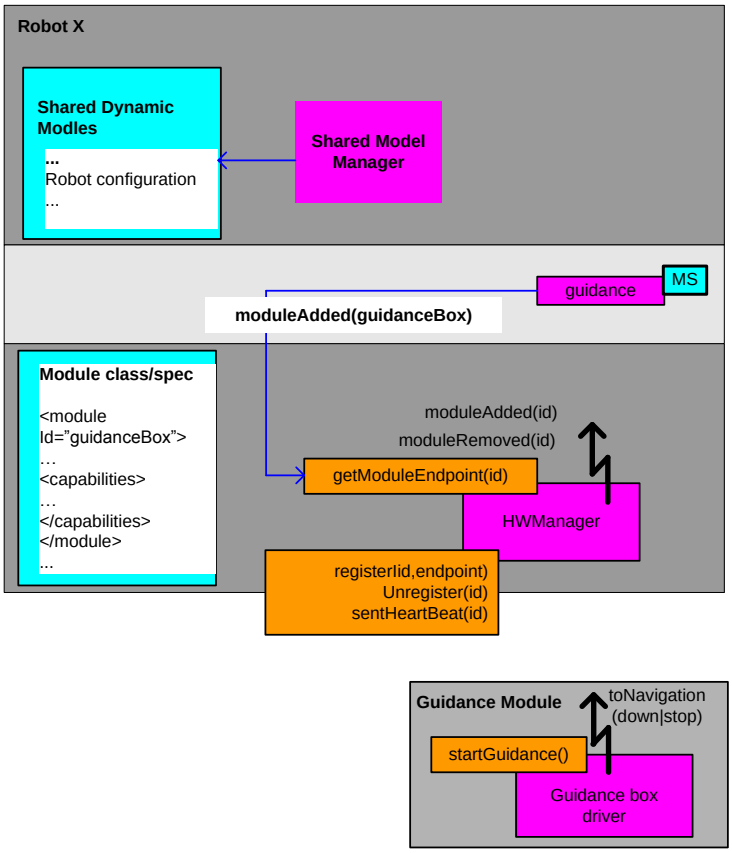

Figure 6-13: Guidance component wants to access the module; it first requests the endpoint at the HWManager

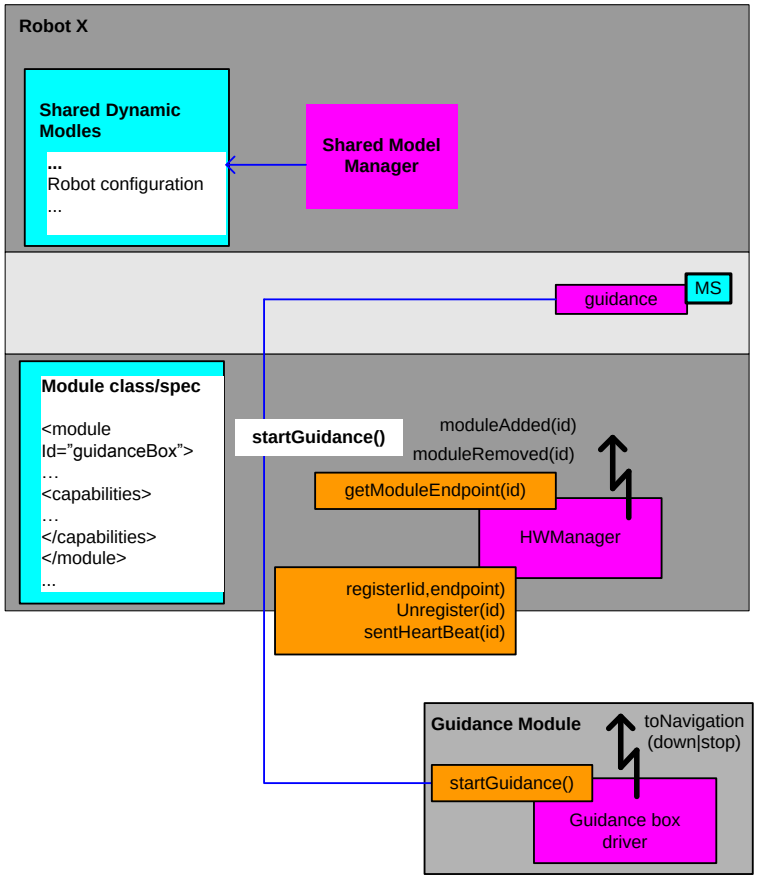

Figure 6-14: The Guidance component is able to contact the module interfaces directly

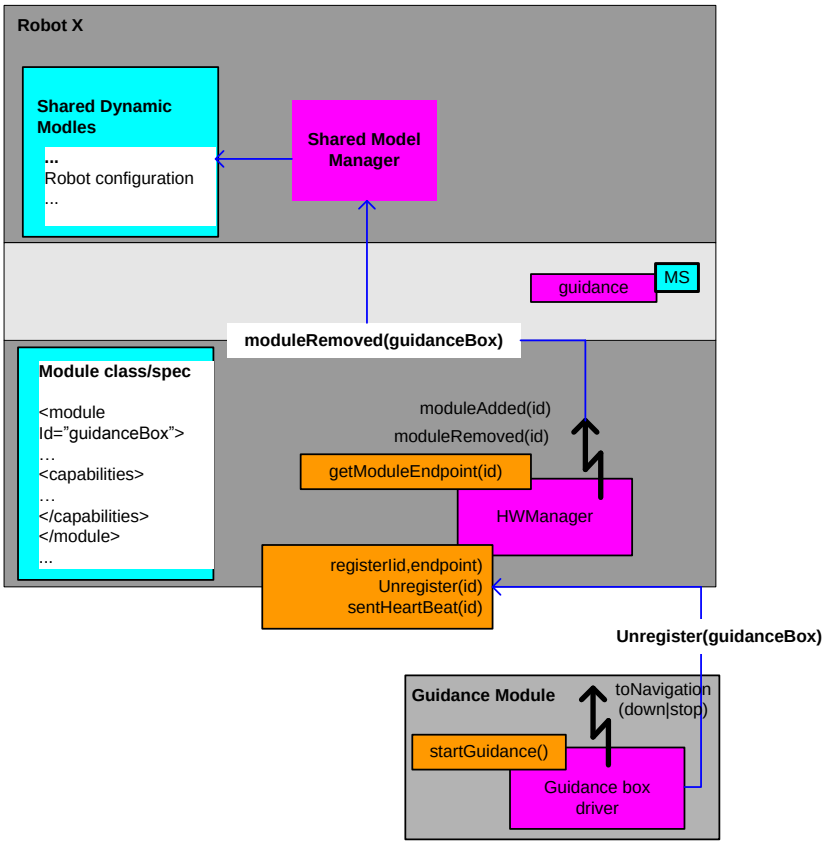

Figure 6-15: Before removing the module it unregisters from the HWManager

6.6 Chapter Summery

In this chapter the software development for the PGM in line with the IWARD software architecture has been presented. The device drivers' development for all PGM sensors is discussed. Software algorithms for PGM are explained in detail. General descriptions of the different Orca components that are involved in the PGM operation are discussed. Furthermore, the local communication process of these components based on the ICE middleware is discussed. Finally, the software approach for accessing hot-pluggable PGM modules is presented.

Chapter 7 Experiments, Results and Discussion

7.1 Introduction

This chapter evaluates the results from the deployment of the Patient Guidance Module (PGM) in the IWARD system. Results from the hospital environment are presented in section 7.2. Section 7.3 presents results from the Final IWARD review meeting. After the IWARD project ended, research and further development of the PGM were continued. Test results from this improved module are presented in section 7.4. Finally, section 7.5 summarizes the chapter.

7.2 Tests in Hospital Environment

To evaluate the usability of the IWARD robots in actual hospital environments, two events were hosted. The first event took place in October 2009 in Newcastle Nursing Training Institute. The second event took place in November 2009 at the Matia hospital in San Sebastian. Nearly thirty healthcare professionals attended these events. These professionals consisted of nurses, nursing lecturers and healthcare assistants. Each scenario of the IWARD robot system was evaluated by these professionals. Images from the Guidance mission conducted in Newcastle are presented in Figure 7-1.

In this scenario, an authorised person requested a guidance service using the GUI of a mobile device, specifying the starting (ward A) and ending position (Doctor's chamber). After these two evaluation events, the general consensus was that the IWARD system is easy to use and all functional modules (including the PGM) function properly according to the expectation. The mission execution (from left to right and top to bottom) is:

- Authorised person is requesting Guidance service from a PDA interface
- Specifying the starting location as ward 'A'
- Specifying the finishing location as Doctor's chamber;
- Nurse helping the follower to wear the pouch (with RFID Tags);
- Robot guiding the follower;
- Mission is complete and the follower is handing over the pouch.

Figure 7-1: Testing of the Guidance Mission at Newcastle Hospital.

7.3 Tests during the IWARD Review Meeting

Within the time span of the IWARD project (January 2007 – March 2011), developers from the IWARD consortium gathered periodically in order to analyse the development progress of the project.

Apart from these periodical meetings, annual review meetings also took place in the presence of two EU project reviewers. Their task was to assess and critically evaluate the IWARD robot system at each stage of its development. The final review meeting took place in San Sebastian in February 2011. At this final meeting all aspects of the IWARD robot system (including the PGM) were demonstrated. The evaluation by the EU reviewers acknowledged the project as a success. Figure 7-2 presents the testing of

the IWARD robots during the final project review meeting. For this review meeting, the PGM was demonstrated using the RFID sensor system.

Figure 7-2: Testing of IWARD robots in San Sebastian during the final review meeting in February 2011.

This is because at this stage only the RFID components were ready. The other two PGM sensors, cricket and stereovision, were still at developing stage.

For this review meeting, two RFID Tags were shielded in such a way that they could only be detected from a range of about 4m. The pouch carrying the RFID tags can be

seen in Figure 7-2. If the PGM detected at least one of the tags, it considered the follower to be in the 'normal speed zone' (0 - 4 m) and if it could not detect any tag then it considered the patient to be out of range (4 m+). The block diagram using such arrangement is presented in Figure 7-3. The second RFID tag was added only to increase the probability of detection.

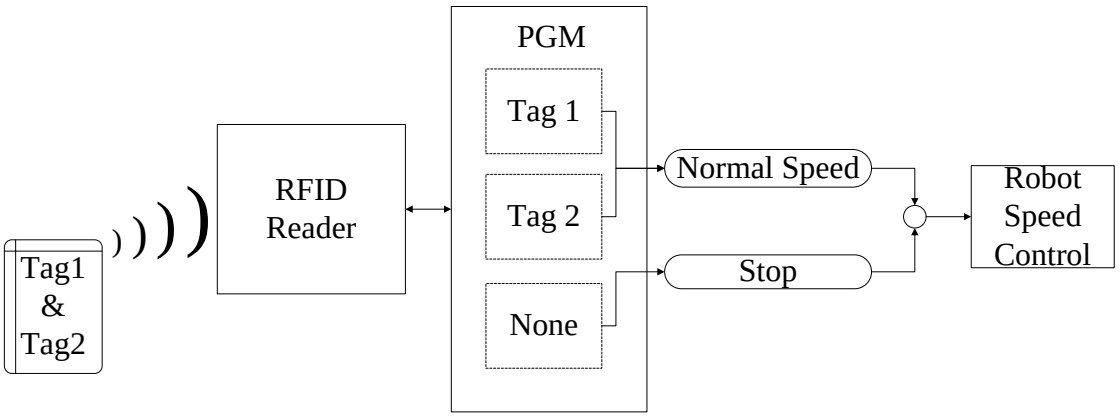

Figure 7-3: Block diagram of the PGM operation using the stand-alone RFID module during the Final Review meeting.

For this demonstration the algorithm was used as follows:

- Once the guidance mission starts, the PGM continuously detects RFID tags until it receives the stop/terminate command from the mission controller. If it finds at least one tag it considers the follower to be in 'zone 1' (0 – 4 m) and it continues moving towards its destination.
- If it can not find any tag, it considers the follower to be in 'zone 2' (outside the 4 m range). At this stage, the PGM waits for a predefined time (T_{temp}) without stopping the robot movement to see whether the detection programme can detect any tag at all.
- If it detects any tag within T_{temp}, then the PGM considers that the follower is back to zone 1 again and the robot continues moving with its current speed.
- If the system can not find any tag during the above T_{temp} interval then the PGM sends a message to the navigation component to stop the robot movement. At this stage, the system still searches for tags for another predefined time (T_{stop}). During this period, if it finds any tag then it considers that the follower is back to 'zone 1' and the robot resumes moving again with its default speed.

- If the system cannot detect any tag within the T_{stop} period, it waits for another predefined period ($T_{emergency}$) and if the follower does not come back then it raises a 'Patient Lost' event to the system.
- The guidance mission was successfully demonstrated several times in the final review meeting in San Sebastian. All events were saved in a log file during this demonstration. Part of this is shown in Figure 7-4.

```
Global Variables Initialised.     Time: Mon Feb 16 17:51:58 2011
Guidance Parameters Obtained.     Time: Mon Feb 16 17:51:58 2011
Serial Port Name:   /dev/ttyS1
Guidance Log File:  Guidance_Logfile.txt
Logfile Max Length: 40000.000000 characters
Operation Mode:  1  (0:LIMITED; 1:FULL_ORCA; 2:SIMULATION)
Print Mode:      1  (1: print to display; 0: do NOT print)
Error Log Mode:  1  (1: log errors to local file; 0: do NOT log)
Process Log Mode:1  (1: log processes to local file; 0: do NOT log)
Event Log Mode:  1  (1: log events to local file; 0: do NOT log)
Tags: 86 88
Comeback timeout from Zone2: 3 sec
Timeout for Wait after Stop: 7 sec
Timeout for Reading Tags:    10 sec
Number of tag measurements:  225
Pause length before reading RFID: 100000.000000 microsec
Power Save Mode: 0  (0:OFF; 1:ON)

Starting guiding patient ....                          Time: Mon Feb 16 17:55:12 2011
Equipment is connected.                                Time: Mon Feb 16 17:55:12 2011
Serial port is open ...                                Time: Mon Feb 16 17:55:12 2011
Patient status not yet known.                          Time: Mon Feb 16 17:55:12 2011
Patient is in Zone 1.                                  Time: Mon Feb 16 17:55:12 2011
Patient is in Zone 2 temporarily.                      Time: Mon Feb 16 17:56:01 2011
Patient is back to Zone 1.                             Time: Mon Feb 16 17:56:03 2011
Patient is in Zone 2 temporarily.                      Time: Mon Feb 16 17:56:20 2011
Patient is in Zone 2, Robot Stopped.                   Time: Mon Feb 16 17:56:23 2011
Robot stopped to wait for patient                      Time: Mon Feb 16 17:56:23 2011
Patient is close to robot again, Robot resumed moving.  Time: Mon Feb 16 17:56:28 2011
Patient is back to Zone 1.                             Time: Mon Feb 16 17:56:28 2011
Patient is in Zone 2 temporarily.                      Time: Mon Feb 16 17:56:45 2011
Patient is back to Zone 1.                             Time: Mon Feb 16 17:56:47 2011
Serial port is Closed                                  Time: Mon Feb 16 17:57:01 2011
Equipment is disconnected.                             Time: Mon Feb 16 17:57:01 2011
Module is in STANDBY mode.                             Time: Mon Feb 16 17:57:01 2011
.............
```

Figure 7-4: Portion of the log file for the guidance mission generated during the demonstration in San Sebastian in February 2011.

7.4 Post-IWARD development tests

After the IWARD project was completed, research and further development of the PGM were continued. The final version of the PGM consists of Cricket, Stereovision and RFID modules. This PGM was tested based on the sensor fusion algorithm described in chapter 6. As the IWARD Base robots (2 Pioneers and 1 Nubot) remained with their developers, the major IWARD components (Mission Controller and Hardware Manager) were running in a simulated mode during these tests, and the robot platforms were simulated with a specially designed mobile platform. Also, an Orca client was developed that requested and used the data from the PGM.

7.4.1 Test in the DCU Computing Building

The first test was carried out on the ground floor of the DCU computing building. In this test a person was guided from the LG26 entrance door to the ground floor lift. The map (Figure 7-5) indicates the 'Start' and 'End' points of this guidance mission and Figure 7-6 shows the actual test location. The experimental data is attached in Appendix D. The mobile rig was positioned at point '0' as indicated in Figure 7-5. The description of the different stages during this mission is presented in Table 7-1.

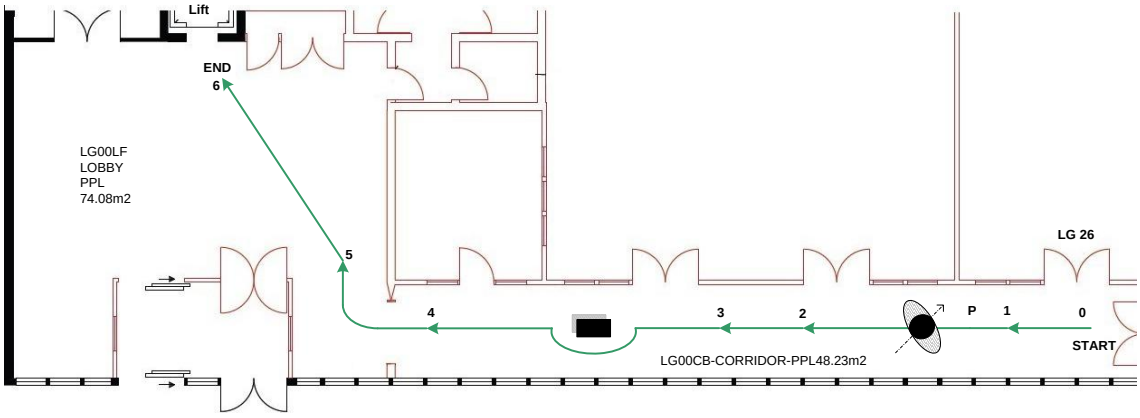

Figure 7-5:Map showing the 'Start' and 'End' positions for the guidance mission on the ground floor of the DCU Computing building.

Table 7-1: Stages of the guidance mission in the DCU Computing Building

Stage	Description
0-1	Normal speed in straight line
1-2	Pedestrians cross from the front
2-3	Slow speed in straight line
3-4	Static obstacle avoidance
4-5	Cornering
5-6	Normal speed in diagonal line

At first all the sensors measured the follower's distance for about 3 seconds. At this stage both cricket and stereo reported the distance readings which ranged from 92 ~ 141 cm. Both short and long range RFID tags detected at this point. The mobile rig reached point '1' in 6 seconds and the PGM System issued the message 'Normal Speed' as the follower was always within the 'Normal Speed Zone' range (0 ~ 4 m). While travelling from point'1' to '2', a few pedestrians crossed the line of sight path between the rig and the follower (marked as point 'P' in Figure 7-5).

Figure 7-6: Test Locations at DCU computing building; long Corridor (left), corner (middle) and wide area at the end (right).

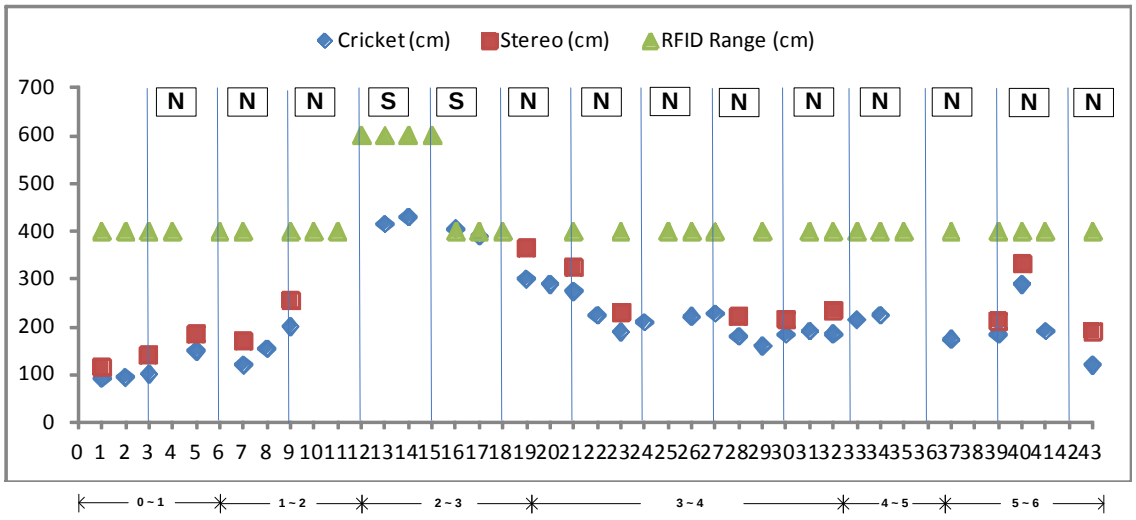

Figure 7-7: Graph for the Computer building Test. The X-axis contains time in seconds and the Y-axis is for distance in cm. N- means' Normal Speed' and S- means 'Slow speed'.

For this reason the cricket and the stereo did not report any distance readings between the time period of 10 ~ 12 seconds. But the RFID system detected both short and long range tags and the rig moved at a normal speed while the follower stood still at point 'P'. Consequently, while travelling from point '2' to '3' the system message was 'slow speed' (as shown in the graph in Figure 7-7) as prior to that, only the long range RFID tag reported its presence. At a time of 16 seconds , the cricket reading was recorded as

405 cm, which means the follower was in the ‘Slow speed zone’ but the RFID system could detect this small variation as instead of only reporting the long range tag, it reported both tags. The rig reached point ’3’ in 19 seconds. At this time the system detected that the follower was back in the ‘Normal Speed’ zone.

A static obstacle was placed in between points ‘3’ and ‘4’ (as shown in Figure 7-5
The mobile rig took a turn to avoid the obstacle and it can be seen in the graph that the cricket reading suddenly jumped from 190 cm at 23 seconds to 210 cm at 24 seconds. This is due to the US signal bouncing back from the corridor wall. Stereo did not report any distance readings at these points. At 25 and 26 seconds, no readings were received from the cricket and stereo due to this manoeuvring. Both the short and long range RFID tags were detected during this manoeuvring so the rig maintained normal speed.
In between the points of ’4’ and ’5’ the rig performed a cornering. From the 33 second period, the rig reached the corner and started manoeuvring and as a result the cricket reading increased from its previous reading slightly (from 185 cm to 215 cm) at this period. In the next two seconds, cricket and stereo did not report any readings while RFID detected the short tag.

The rig finally reached point ‘6’ and during this phase the follower was always found in the ‘Normal speed zone’. To complete this mission, the mobile rig travelled a 25.5 meter path altogether in 43 seconds. In this mission the PGM successfully detected the follower while the pedestrians blocked (point ‘0’~’1’) the line of sight between the mobile rig and the follower. Furthermore, it slowed down its speed when the follower was found to be in the 4-6 m range (travelling from point ‘2’ to ‘3’) from the mobile rig. Finally, the systems successfully detected the follower’s spatial information while performing cornering (point ‘4’~’5’).

7.4.2 Test in the Reception Area of the DCU Engineering Building

This test was carried out on the ground floor of the engineering building in DCU. The mission was to guide a person from the reception desk to the stairs at the second lobby as shown in Figure 7-8. The map (Figure 7-9) indicates the ‘Start’ and ’End’ points. The experimental data is attached in Appendix D. The stages during this mission are presented in Table 7-2 .The resulting graph is shown in Figure 7-10. The mobile rig was positioned at point ‘0’ as indicated in Figure 7-9.

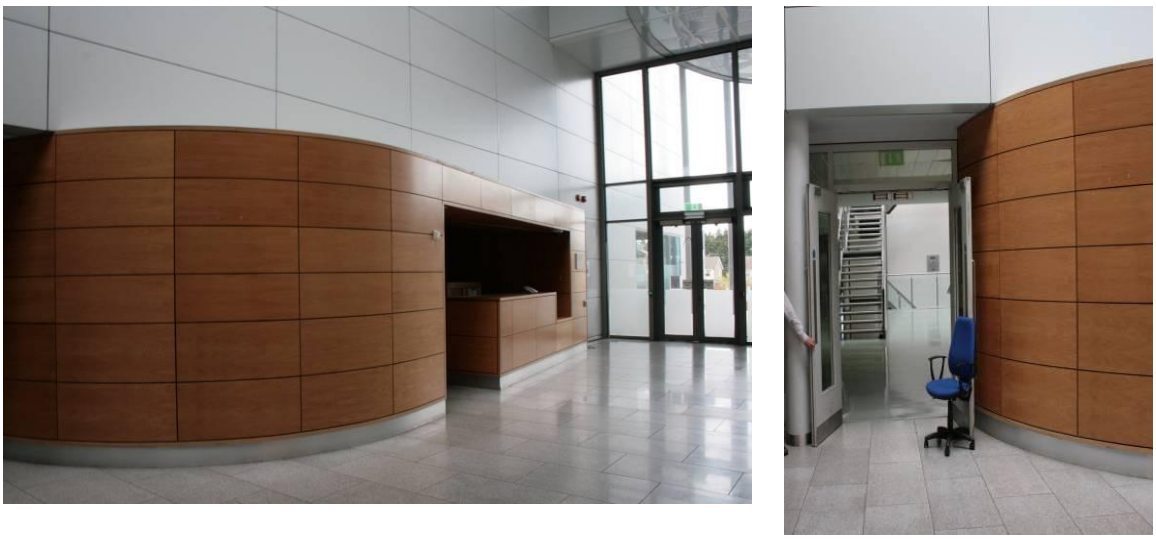

Figure 7-8: Test Locations at the DCU engineering building; reception desk (left) and stairs (right).

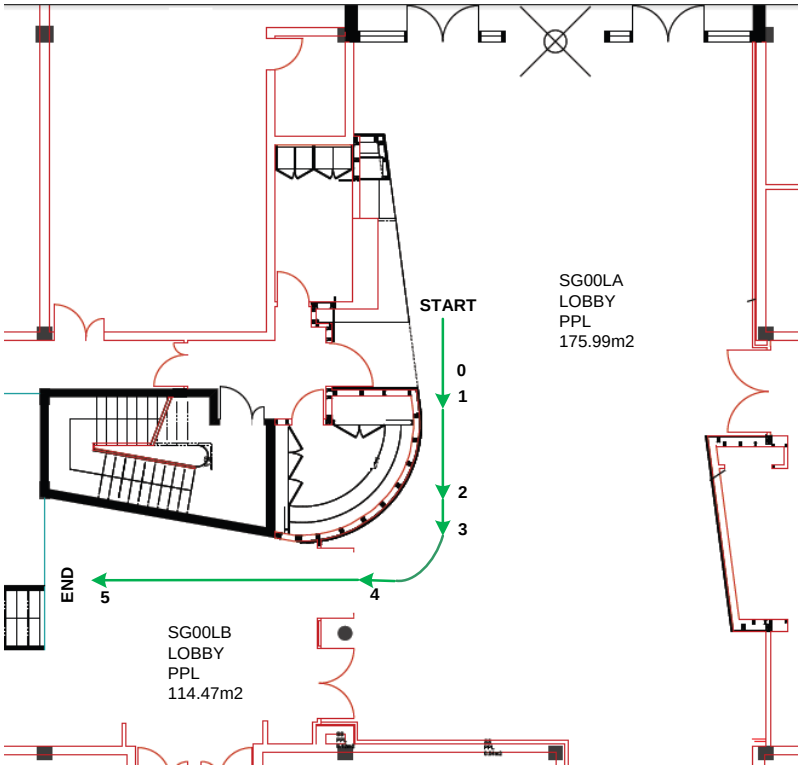

Figure 7-9: Map showing ‘Start’ and ‘End’ for the guidance mission on the ground floor of the DCU Engineering building.

Table 7-2: Stages of the guidance mission in the DCU Engineering Building.

Stage	Description
0-1	Normal speed in straight line
1-2	Slow speed in straight line
2-3	Emergency stop
3-4	Cornering
4-5	Raise ‘patient lost’ event

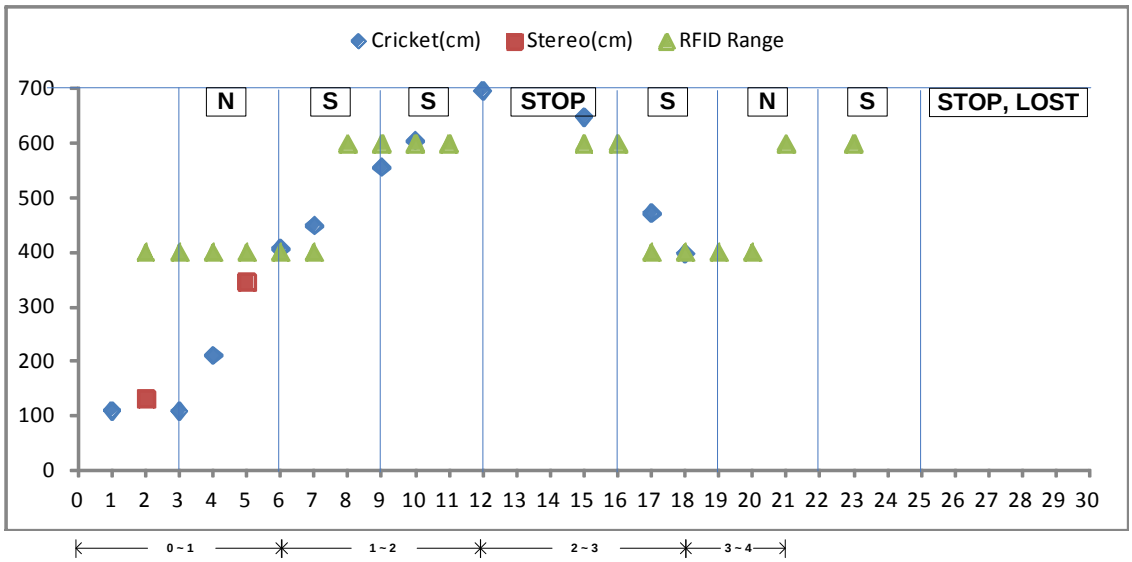

Figure 7-10: Graph for the Engineering building Test. The X-axis contains time in seconds and the Y-axis is for distance in cm. N- means' Normal Speed' and S- means 'Slow speed'.

At first all the sensors measured the follower's distance. The person was intentionally asked to stand still at the starting location to investigate whether the rig would stop as the distance became more than 6 m. The mobile rig reached point '1' in 6 seconds with 'Normal Speed' as the follower was always within the 'Normal Speed Zone' range (0 ~ 4 m). When the rig reached point '1', the cricket reported a 407 cm distance reading whereas the RFID detected both short and long range tags. The PGM instructed the platform to go slowly. The rig reached point '2' at slow speed and the distance readings increased as the person stood still at the starting location. At this point the cricket reported the person to be far away from the 'slow speed' zone and it instructed the rig to stop and wait for the follower. The person was asked to start moving towards the rig and the cricket readings were found to decrease as the person moved towards the rig. At 15 seconds, the RFID system first detected the long range tag. Although cricket reading was 649 cm at this point the RFID system again could not differentiate this small difference. The system instructed the platform to go slow at 16 seconds. The rig reached point '3' with this slow speed in 18 seconds.

Both cricket and RFID detected that the person is in Normal speed zone whereas the stereo could not detect anything. The rig started to take turn right at this point. Unlike in the previous test in the corridor area, while turning the cricket could not detect any readings. Since the nearby walls were far away at that time, the US signal could not bounce back to the receiver. The rig completed its cornering in 21 seconds and reached

position ‘4’. The person was again asked to stay still to investigate how the system detects when it lost the patient for good. At this point the system only could detect the long range RFID tag. At 25 seconds the PGM instructed to stop the robot as it could not find distance readings from any system. It waited for next 5 seconds and then raised an ‘Event’ that the follower was lost.

7.4.3 Test in the Nursing hall in DCU

This last test was carried out on the ground floor in the DCU Nursing hall. The mission was to guide a person form the waiting area lobby to the HG 19 class room. The map (Figure 7-11) indicates the ‘Start’ and End ‘points’ and Figure 7-13 shows the actual test location. The experimental data is attached in Appendix D. The stages of this mission are presented in Table 7-3. Unlike in previous tests, no tests were carried out in this arena before. The person following the rig was asked to move frequently during this guiding mission, i.e. there was no predetermined scenario. The mobile platform was positioned at point ‘0’ as indicated in Figure 7-13.

At first, all the sensors measured the follower’s distance for 5 seconds. At this stage both cricket and stereo reported distance readings. The cricket readings varied from 109 to 211 cm whereas the stereo readings varied from 131 to 345 cm. Both short and long range RFID tags were detected at this point. The rig started moving at ‘Normal Speed’ after these initial readings and reached point ‘1’ in 7 seconds. During this period the PGM System message was ‘Normal Speed’ as the follower was always within the ‘Normal Speed Zone’ range (0 to 4 m). At this point the rig started taking the left and the rig reached point ‘2’. During this time (12 to 17 seconds) the PGM could not detect any readings from the follower. This is due to the large lobby area where the US signal from the cricket listener could not bounce back to the receiver. Meanwhile, the person also took some time to take left with the rig as well. At this period the system messaged ’slow speed’ (as shown in graph in Figure 7-13).

The ‘rig’ reached point ‘3’ at 19 seconds with a slow speed. At this point the PGM again found that the follower was again in the ‘normal speed’ zone. At the time of 23 seconds the rig had to ‘stop’ as a few people came too close to the rig while passing it from the front. At this time the distance readings were decreasing as the follower came

closer to the ‘rig’. The ‘rig started moving again at 30 seconds with ‘normal speed’ and reached point ‘4’ in the next 5 seconds. At this point the rig started turning left again.

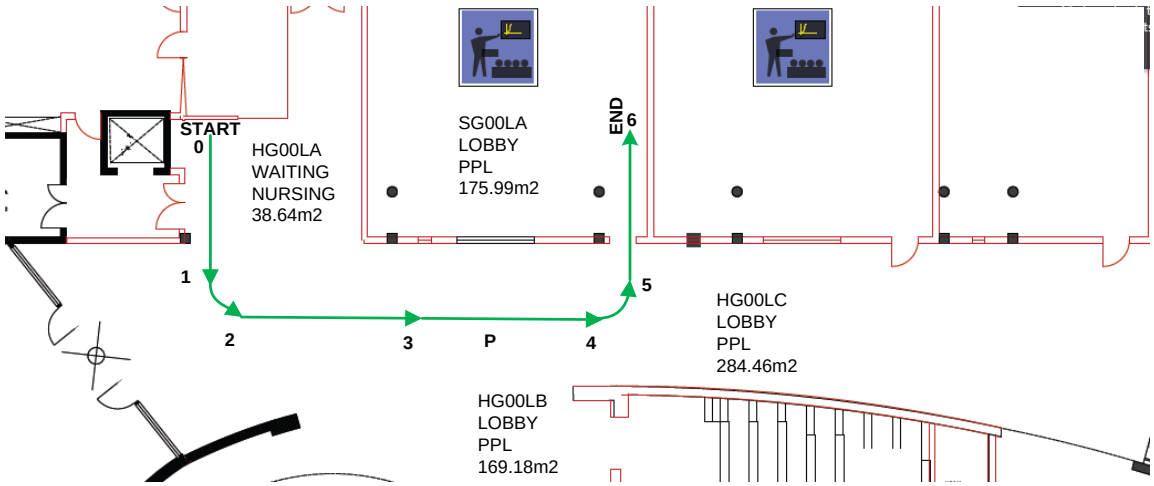

Figure 7-11: Map showing ‘Start’ and ‘End’ for the guidance mission on the ground floor of the DCU nursing building.

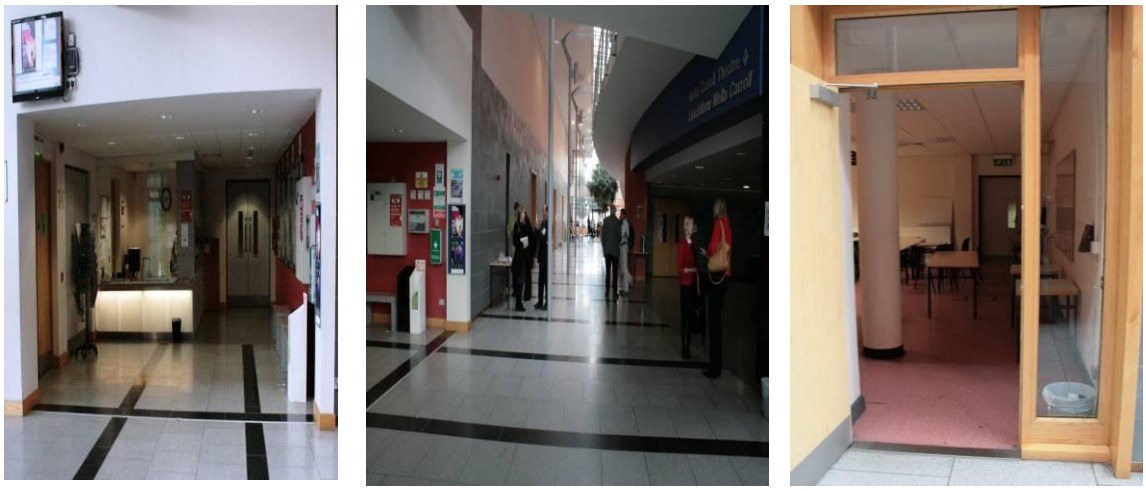

Figure 7-12: Test Locations in the DCU nursing building; reception area (left), wide lobby (middle) and class room at the end (right).

Table 7-3: Stages of the guidance mission in the DCU Nursing Building.

Stage	Description
0-1	Normal speed in straight line
1-2	Cornering
2-3	Slow speed in straight line
3-4	Pedestrian crossing from the front
4-5	Cornering
5-6	Normal speed in straight line

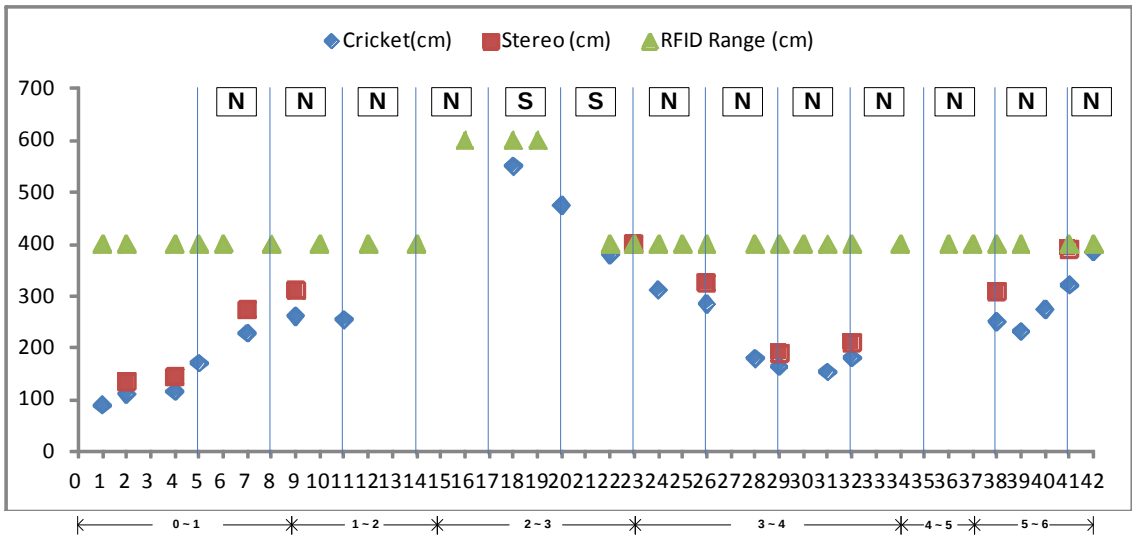

Figure 7-13: Graph for the Nursing building Test. X-axis contains time in seconds and the Y-axis is for distance in cm. N- means' Normal Speed' and S- means 'Slow speed'.

Cricket and stereo readings were again missing during this manoeuvring. But RFID could detect the short range tag all the way so the rig maintained the 'normal speed' and reached point '5'. The rig entered the destination class room and reached point '6' in the next 5 seconds. It took 42 seconds for the mobile rig to travel this 25 meter path. In this mission the PGM successfully detected the follower while it was turning left and slowed down its speed when the person was lagging behind (points '2' to '3').

7.5 Chapter Summary

The results from the actual deployment of the Patient Guidance Module (PGM) in the complete IWARD system are discussed in this chapter. The pre and post IWARD tests prove that the developed PGM can successfully guide a person in various scenarios. The next chapter will present the final conclusions to this thesis.

Chapter 8 Conclusions and Future Work

This dissertation described the design, development, implementation and evaluation of the Person Guidance Module (PGM) for IWARD hospital robots. The plug-and-play PGM is easy to deploy, scalable, and enables an IWARD robot to guide patients and visitors within the hospital's periphery without compromising their comfort.

This chapter summarises the conclusions drawn from the PGM development and the contributions made in this dissertation. Finally, possible future directions for improving and extending the functionality of the PGM are discussed.

8.1 Conclusions

The following main conclusions can be drawn from developing the PGM for IWARD robots:

- Stable human sensing in an unconstructed, busy, crowded public place while relying solely on onboard sensors is a challenging endeavour but stands as a fundamental pre-requisite for the IWARD robots. It is not acceptable to retrofit the whole hospital area with external sensors. Instead, the PGM relies on its own sensor system.
- Speed adaptation is an ambitious task as normal walking speed of people can vary widely. Human motion cannot be modelled as a smooth linear function, as people may stop or change direction abruptly. Moreover, in a hospital environment patients with various physical abilities may require guiding assistance from the robot. Also, a patient may be temporarily hindered from following the robot due to obstacles, people and other robots in the hospital. The developed PGM is able to maintain a pre-defined distance between the robot and the guided person in all guidance scenarios.
- In order to fit into the modular design concept of the IWARD project, all PGM sensors have to be lightweight and small in size to get an easy fit into the rectangular-shaped module box. At the same time, it has to consist of low-cost hardware in order to minimise the cost of the overall system and to make it

affordable to hospitals. All three sensory systems of the PGM fulfil this requirement.

- ‘Power Save Mode’ had to be incorporated to save battery power of the robot. Furthermore, the power supply specification of each sensor should not exceed more than 12 VDC. Finally, all hardware has to be Linux compatible to integrate with the base robot’s on-board computer. The developed PGM uses two DC power sources only (5 VDC and 12 VDC), and all computing and sensor hardware is Linux compatible.
- A plug-and-play technology is essential so that nurses without any prior knowledge of robotics could easily insert and remove the module from the base robot on demand while the robot is in operation. The developed PGM incorporates plug-and-play features and has proven to be reliable.
- Most of the PGM hardware was shipped with Windows drivers. In contrast, the operating system for the IWARD robots is Linux. As device drivers are hardware-dependent and operating system-specific, separate device drivers had to be developed from scratch and cross-compiled for the Gumstix XScale processor. The Linux-compatible device drivers developed for the PGM are fully functional and operational.
- Following the IWARD software architecture, all software modules had to be developed as orca2 components. The developed interfaces for inter-module communication through Ice have been tested and are functioning properly.
- Research on the development of relative location systems based on infrared and/or radio sensors/emitters is a rather unexplored area. Radio propagation in indoor environments is subject to numerous problems, such as severe multipath, rare line-of sight (LOS) path, absorption, diffraction, and reflection due to the presence of obstacles and people. The wave strength is reduced not only by the distance, but also by the scattering and reflection of the wave. This makes it difficult to measure signals precisely. For these reasons, it is not possible to locate an RFID tag from a single RFID reader, particularly in cluttered or dynamically changing environments. The PGM employs multiple tags for multi-zone speed control. However, it still does not allow precise localisation of the guided person.
- The performance of Stereo-based approaches heavily depends on the lighting conditions, viewing angle, distance to persons, and variability of human’s

appearance in video streams. Detecting people across multiple image frames as well as robustly identifying them solely with visual features is not reliable enough in a hospital environment.

- The downside of cricket sensors is that they require optical line of sight between the beacon and the receiver. All the existing tests with cricket, found in literature, were carried out in a controlled environment that did not provide enough information about whether it would be feasible for the IWARD project or not. According to the IWARD patient guidance scenario, the robot needs to perform its guidance task in a crowded hospital environment. The line of sight path between the beacon and the listener may not be maintained during guiding. It is unknown how a follower carrying a beacon would orient himself toward the listener (on the robot). Moreover, during obstacle avoidance, cornering etc. the beacon and receiver would certainly disorient from each other which may cause the sound to reach the listener after reflection and/or refraction. All this means that the cricket system alone is not capable of providing reliable guidance information in all guiding scenarios.
- Although none of the individual sensor systems is robust enough to fulfil all requirements of all guiding scenarios, the sensor fusion arrangement provides sufficient data for reliable guidance.
- Having robots working in a hospital, safety and reliability are features of superior importance. This requires that the PGM operates robustly in any condition, which includes the potential breakdown of any device of the system. The built-in self-diagnosis and messaging system of the PGM fulfils the above requirements.

8.2 Contributions

This dissertation presents a PGM that was developed for the IWARD hospital robots. This PGM enables authorised hospital personnel to instruct a robot to lead a person to any place known to the system using a speed appropriate for them. The PGM features a non-hierarchical sensor fusion of Active RFID, Cricket and Stereo Vision systems. While the guiding task is operational, the non-hierarchical framework is used to continuously measure the distance between the robot and the guided person, regardless of their position and orientation. The speed of the robot is constantly adjusted based on

the calculated distance. This simulates a virtual electronic rubber-band between the robot and the follower. Besides the distance measurements, the PGM is also continuously identifying the follower in order to ensure that the robot only guides the appropriate person. If for some reason the robot loses track of the person, it automatically notifies the authorised hospital personnel.

This dissertation makes the following contributions, while meeting the above challenges:

- The PGM features a reliable and comprehensive solution of human sensing: detection, identification, and tracking with the implementation of speed adaptation measures in one unified platform. Furthermore, it can perform these in any unconstructed environment solely using the robot's on-board sensors. Until now, this has remained elusive in existing literature.
- The fail-safe, non-hierarchical sensor fusion of Active RFID, Cricket and Stereo Vision systems ensures robust sensing of a follower in every possible scenario. If one sensor fails, the non-hierarchical framework ensures that others can still perform the sensing tasks. Such a comprehensive sensor fusion arrangement is new in hospital robot development.
- As opposed to the large, stand alone, individual and single purpose guide robots that are currently available on the market, the development cost of the PGM is much lower. This makes it affordable to hospitals. The IWARD robot swarm is based on smaller robots and heavily relies on low-cost, small, lightweight, standard components and plug-and-play sensors. This should cause less interference with persons and objects in the hospital.
- The PGM module can be plugged and unplugged while the robot is running (hot-plug mechanism). A quick-fix mechanism is provided for attaching and detaching the modules on the base robot on demand. Nurses without any prior knowledge of robotics can easily insert and remove the module from the base robot. Additionally, if any sensor in the PGM fails, the PGM can be taken out for troubleshooting without hampering the general operation of the system. The PGM is also equipped with self-diagnostic tools.
- The developed Plug and play technology ensures that as soon as the PGM is connected, the application software recognises the module and enables the corresponding software. This Plug and play technology was incorporated into

other IWARD service modules as well. Furthermore, the module software ensures that the service modules are connected to the right drawers on the robots.

- A standby power-saving mode has been implemented by controlling a Solid State Relay controlled by the Gumstix serial ports. This prevents the sensors to draw power from the main power supply when they are not in operation.
- The guidance module software is developed as orca2 components that promote decentralisation of software development by the adoption of a Component-Based Software Engineering approach. Advantages of such component based frameworks are that individual components can be developed independently and replaced. Moreover, orca2 is unencumbered by licensing costs and available for free download which significantly reduces the development costs for the PGM.
- To investigate the significant factors that have considerable effects on cricket distance performance measurement in real indoor environments, a robust DOE analysis has been performed. This can also be used for future development.
- The ranges of the Active RFID tags have been tuned according to the PGM requirement through aluminium shielding. To investigate the suitable shield size, an effective qualitative analysis has been conducted.
- An inexpensive stereo rig has been developed using two Philips PCVC840K ToUcam PRO II webcams. The algorithm for the distance calculation using stereo image pairs has been successfully developed and tested.
- Existing human sensing solutions from various disciplines have been summarised in the literature survey part of this dissertation. This can guide researchers in creating new systems in the future.

Finally, the research project, as a whole, has achieved its major goals. The evaluation by the EU reviewers acknowledged the project as a success. Furthermore, during the post-IWARD development phase, this has been further extended and tested successfully.

8.3 Future Directions

Although the developed PGM is fully functional at its current stage, it could further be improved in future research in the following areas:

- The Philips web cameras could be replaced with a higher quality camera. This would increase the accuracy and the range for the stereo distance calculation.

- If a person’s head tilts towards one shoulder or turns towards profile view, the frontal face detector no longer works. Therefore, a pan-tilt stereo could also be incorporated to extend its field of view. Other classifiers for full body, lower body, upper body, or even hands can be investigated and if necessary added to the current algorithm.
- Currently, the guided person needs to carry an RFID tag pouch, a cricket beacon and a concentric circular badge. For ease of use, more research can be conducted to blend these three into a small light-weight wearable platform. This has a potential to be a profitable commercial product as it can be widely used by other developers for their guide robots and many other applications.

References

[1] Hospital staff shortages 'cause 500 deaths a year' - Health News - Health & Families - The Independent , [online], http://www.independent.co.uk/life-style/health-and-families/health-news/hospital-staff-shortages-cause-500-deaths-a-year-2351018.html (Accessed 6/19/2012).

[2] Shortage puts hospitals on critical list - The Irish Times - Tue, Jan 18, 2011, [online], http://www.irishtimes.com/newspaper/health/2011/0118/1224287749080.html (Accessed 11/23/2011).

[3] WHO | The World Health Report 2006 - working together for health , [online], http://www.who.int/whr/2006/en/ (Accessed 11/23/2011).

[4] Health-EU Newsletter, [online], http://ec.europa.eu/health-eu/newsletter/54/newsletter_en.htm (Accessed 11/23/2011).

[5] Szecsi, T. Robonurse leads the way. DCUTIMES, University Magazine 2007 Summer:49.

[6] Thiel, S., Schlegel, T. and Häbe, D., (2010), "Cooperative Robot Teams Performing in a Hospital", *VIMation Journal*, Vol.1 (1), pp. 13.

[7] IWARD-Project - IWARD Approach , [online], http://www.iward.eu/ (Accessed 11/24/2011).

[8] IWARD-Project - IWARD Modular Design, [online], http://www.iward.eu/ (Accessed 11/24/2011).

[9] Hasan, MK. and T. Szecsi 2008, "Developing a patient guidance module for hospital robots", *E. E. E. D.T.Pham A.J.Soroka, ed., Innovative Production Machines and system, 1-14 July 2008,*: Whittles Publishing Scotland,UK, 585.

[10] Simmons, R., et al., (2000), "Lessons learned from Xavier", *Robotics & Automation Magazine, IEEE*, Vol.7 (2), pp. 33-39.

[11] Burgard, W., et al., (1999), "Experiences with an interactive museum tour-guide robot", *Artif.Intell.*, Vol.114 (1-2), pp. 3-55.

[12] Thrun, S., et al., 1999, "MINERVA: a second-generation museum tour-guide robot", *Robotics and Automation, 1999. Proceedings. 1999 IEEE International Conference on,*Vol.3, 1999-2005 vol.3.

[13] Montemerlo, M., et al., 2002, "Experiences with a mobile robotic guide for the elderly", *14th Innovative Applications of Artificial Intelligence Conference (IAAI-02), July 28, 2002 - August 1, 2002,*: American Association for Artificial Intelligence Edmonton, Alta., Canada, 587-592.

[14] Kanda, T., et al., 2002, "Development and evaluation of an interactive humanoid robot "Robovie"", *Robotics and Automation, 2002. Proceedings. ICRA '02. IEEE International Conference on,*Vol.2, 1848-1855 vol.2.

[15] Hasan, M. K., ASM Hoque and T. Szecsi 2010, "Application of a Plug-and-Play Guidance Module for Hospital Robots", *International Conference on Industrial Engineering and Operations Management,*Vol.1, *9-10 January 2010,* Dhaka, Bangladesh,.

[16] Thiel, S., D. Habe and M. Block 2009, "Co-operative robot teams in a hospital environment", *Intelligent Computing and Intelligent Systems, 2009. ICIS 2009. IEEE International Conference on,*Vol.2, 843-847.

[17] IWARD-Project - IWARD at a glance, [online], http://www.iward.eu/ (Accessed 12/14/2011).

[18] Szecsi, T., et al., (2010), "Hospital Robot Module Development in the iWARD Project", *VIMation Journal,* (1), pp. 6.

[19] IWARD-Project - Home, [online], http://www.iward.eu/cms/index.php (Accessed 12/15/2011).

[20] Baalbaki, H., M. Lamiri and Xiaolan Xie 2008, "Joint location and configuration of mobile service robots for hospitals", *Automation Science and Engineering, 2008. CASE 2008. IEEE International Conference on,* 615-620.

[21] Adept MobileRobots Pioneer 3-DX (P3DX) differential drive robot for research and education , [online], http://www.mobilerobots.com/ResearchRobots/ResearchRobots/PioneerP3DX.aspx (Accessed 12/15/2011).

[22] Te, R., et al., (2010), "Human Robot Interface Design for Hospital Robot Swarm", (1), pp. 21.

[23] Baalbaki, H. and X. Xie 2009, "A decision framework for operaon management of reconfigurable mobile service robots in hospitals.", *The 13th IFAC Symposium on Informaon Control Problems in Manufacturing, INCOM '09, June 3-5, 2009,* Moscow,.

[24] Orca Robotics , [online], http://orca-robotics.sourceforge.net/ (Accessed 12/16/2011).

[25] Brugali, D., (2007), *Software engineering for experimental robotics,* , Springer Verlag,.

[26] Jin, J. S., J. W. Park and J. M. Lee 2001, "Design and Implementation of a Service Robot for the Hospital", *2nd International workshop on human-friendly welfare robotic systems, January 15-16, 2001,* KAIST, Korea, 118-123.

[27] Montemerlo, M., et al., 2002, "Experiences with a mobile robotic guide for the elderly", , *Proceedings of the National Conference on Artificial Intelligence,*: Menlo Park, CA; Cambridge, MA; London; AAAI Press; MIT Press; 1999 587-592.

[28] Thrun, S., et al., 1999, "Experiences with two deployed interactive tour-guide robots", *Proceedings of the International Conference on Field and Service Robotics (FSR'99), Pittsburgh, PA,*: Citeseer.

[29] Siegwart, R., et al., (2003), "Robox at Expo.02: A large-scale installation of personal robots", *Robotics and Autonomous Systems,* Vol.42 (3-4), pp. 203-222.

[30] Rodriguez-Losada, D., et al., 2002, "Blacky, an interactive mobile robot at a trade fair", *Robotics and Automation, 2002. Proceedings. ICRA '02. IEEE International Conference on,*Vol.4, 3930-3935 vol.4.

[31] Pacchierotti, E., H. I. Christensen and P. Jensfelt 2006, "Design of an Office-Guide Robot for Social Interaction Studies", *Intelligent Robots and Systems, 2006 IEEE/RSJ International Conference on,* 4965-4970.

[32] Chiu, C. , (2004), "The Bryn Mawr Tour Guide Robot", Bachelor, Citeseer, Bryn Mawr, PA USA.

[33] Gross, H., et al., 2009, "TOOMAS: Interactive Shopping Guide robots in everyday use - final implementation and experiences from long-term field trials", *Intelligent Robots and Systems, 2009. IROS 2009. IEEE/RSJ International Conference on,* 2005-2012.

[34] Horswill, I. , (1995), "Specialization of perceptual processes", PhD, MIT, Cambridge, MA, USA.

[35] Schulte, J., C. Rosenberg and S. Thrun 1999, "Spontaneous, short-term interaction with mobile robots", *Robotics and Automation, 1999. Proceedings. 1999 IEEE International Conference on,*Vol.1, 658-663 vol.1.

[36] Martin, C., H. J. Bohme and H. M. Gross 2004, "Conception and realization of a multi-sensory interactive mobile office guide", *Systems, Man and Cybernetics, 2004 IEEE International Conference on,*Vol.6, 5368-5373 vol.6.

[37] SALIDO, J., V. FELIÚ and A. ADÁN 2002, "An Autonomous Tour-Guide Robot for Public Places", *2002 WSEAS International Conferences, June 12-16, 2002,* 2071-2076.

[38] Gunhee Kim, et al., 2004, "The autonomous tour-guide robot Jinny", "The autonomous tour-guide robot Jinny", *Intelligent Robots and Systems, 2004. (IROS 2004). Proceedings. 2004 IEEE/RSJ International Conference on,*Vol.4, 3450-3455 vol.4.

[39] Clodic, A., et al., 2006, "Rackham: An Interactive Robot-Guide", *Robot and Human Interactive Communication, 2006. ROMAN 2006. The 15th IEEE International Symposium on,* 502-509.

[40] Koide, Y., et al., 2004, "An approach to integrating an interactive guide robot with ubiquitous sensors", *Intelligent Robots and Systems, 2004. (IROS 2004). Proceedings. 2004 IEEE/RSJ International Conference on,*Vol.3, 2500-2505 vol.3.

[41] Bellotto, N.and Hu, H., (2005), "Multisensor integration for human-robot interaction", *The IEEE Journal of Intelligent Cybernetic Systems,* Vol.1 .

[42] Imai, M., T. Ono and T. Etani 1999, "Agent migration: communications between a human and robot", *Systems, Man, and Cybernetics, 1999. IEEE SMC '99 Conference Proceedings. 1999 IEEE International Conference on,*Vol.4, 1044-1048 vol.4.

[43] Shiomi, M., et al., (2007), "Interactive Humanoid Robots for a Science Museum", *Intelligent Systems, IEEE,* Vol.22 (2), pp. 25-32.

[44] Kanda, T., et al., (2010), "A Communication Robot in a Shopping Mall", *Robotics, IEEE Transactions on,* Vol.26 (5), pp. 897-913.

[45] Glas, D. F., et al., 2009, "Simultaneous people tracking and localization for social robots using external laser range finders", *Intelligent Robots and Systems, 2009. IROS 2009. IEEE/RSJ International Conference on,* 846-853.

[46] Sviestins, E., et al., 2007, "Speed adaptation for a robot walking with a human", *HRI 2007: 2007 ACM/IEEE Conference on Human-Robot Interaction - Robot as Team Member, March 8, 2007 - March 11, 2007,*: Association for Computing Machinery Arlington, VA, United states, 349-356.

[47] Gross, H., et al., 2008, "ShopBot: Progress in developing an interactive mobile shopping assistant for everyday use", *Systems, Man and Cybernetics, 2008. SMC 2008. IEEE International Conference on,* 3471-3478.

[48] Müller, S., et al., 2007, "Are you still following me", "Are you still following me", *Proccedings of the 3rd European Conference on Mobile Robots ECMR, Germany,* 211-216.

[49] DimitriosVogiatzis, C. D., et al., 2008, "An Affective Robot Guide to Museums", "An Affective Robot Guide to Museums", *th International Workshop on Human-Computer Conversation, October, 2008,*: Citeseer.

[50] Arras, K. O., et al., 2008, "Efficient people tracking in laser range data using a multi-hypothesis leg-tracker with adaptive occlusion probabilities", *Robotics and Automation, 2008. ICRA 2008. IEEE International Conference on,* 1710-1715.

[51] INDIGO agenda, G. Georgiadis, [online], http://www.ics.forth.gr/indigo/description.html (Accessed 04 May 2011).

[52] TOYOTA: News Releases , [online], http://www.toyota.co.jp/en/news/07/0822.html (Accessed 5/4/2011).

[53] Service Robot enon from Fujitsu Acts as Visitors' Guide at Museum of Best-Selling Mystery Novelist : FUJITSU FRONTECH , [online], http://www.frontech.fujitsu.com/en/release/20070920.html (Accessed 5/4/2011).

[54] Rodriguez-Losada, D., et al., 2008, "Urbano, an interactive mobile tour-guide robot", "Urbano, an interactive mobile tour-guide robot", 229-252.

[55] Lee, S., et al. 2004, "Butler: A Visitor Guide Robot", *Proceedings of International Conference on Automation and Robotics in Construction, Korea.*

[56] Hall, E.T., (1966), *The hidden dimension* . (1st ed.), Doubleday & Co, New York, US.

[57] Nakauchi, Y. and R. Simmons 2000, "A social robot that stands in line", *Intelligent Robots and Systems, 2000. (IROS 2000). Proceedings. 2000 IEEE/RSJ International Conference on,*Vol.1, 357-364 vol.1.

[58] Gockley, R., J. Forlizzi and R. Simmons 2007, "Natural person-following behavior for social robots", *Proceedings of the ACM/IEEE international conference on Human-robot interaction,*: ACM 17-24.

[59] PANDEY, A. K. 2009, "A social robot which guides a person while supporting the persons activity", *Congress EDSYS 14 -15 May, 2009,*.

[60] Sunkyung Oh , [online], http://sunkyungoh.wordpress.com/page/4/ (Accessed 6/21/2012).

[61] Yoda, M. and Y. Shiota 1997, "The mobile robot which passes a man", *Robot and Human Communication, 1997. RO-MAN '97. Proceedings., 6th IEEE International Workshop on,* 112-117.

[62] Pacchierotti, E., H. I. Christensen and P. Jensfelt 2005, "Human-robot embodied interaction in hallway settings: a pilot user study", *Robot and Human Interactive Communication, 2005. ROMAN 2005. IEEE International Workshop on,* 164-171.

[63] Michalowski, M. P., S. Sabanovic and R. Simmons 2006, "A spatial model of engagement for a social robot", *Advanced Motion Control, 2006. 9th IEEE International Workshop on,* 762-767.

[64] Mitsunaga, N., et al., 2005, "Robot behavior adaptation for human-robot interaction based on policy gradient reinforcement learning", *Intelligent Robots and Systems, 2005. (IROS 2005). 2005 IEEE/RSJ International Conference on,* 218-225.

[65] Pandey, A. K. and R. Alami 2009, "Towards a sociable robot guide which respects and supports the human activity", *Automation Science and Engineering, 2009. CASE 2009. IEEE International Conference on,* 262-267.

[66] Teixeira, T., Dublon, G.and Savvides, A., (2010), "A Survey of Human-Sensing: Methods for Detecting Presence, Count, Location, Track, and Identity", *ACM Computing Surveys*, .

[67] Aslam, J., et al., 2003, "Tracking a moving object with a binary sensor network", *Proceedings of the 1st international conference on Embedded networked sensor systems,*: ACM 150-161.

[68] Kim, W., et al., 2005, "On target tracking with binary proximity sensors", *Information Processing in Sensor Networks, 2005. IPSN 2005. Fourth International Symposium on,*: IEEE 301-308.

[69] Xiangqian, L., Gang, Z.and Xiaoli, M., (2009), "Target localization and tracking in noisy binary sensor networks with known spatial topology", *Wireless Communications and Mobile Computing,* Vol.9 (8), pp. 1028-1039.

[70] Oh, S. and S. Sastry 2005, "Tracking on a graph", "Tracking on a graph", *Information Processing in Sensor Networks, 2005. IPSN 2005. Fourth International Symposium on,*: IEEE 195-202.

[71] Shrivastava, N., R. M. U. Madhow and S. Suri 2006, "Target tracking with binary proximity sensors: fundamental limits, minimal descriptions, and algorithms", *Proceedings of the 4th international conference on Embedded networked sensor systems,*: ACM 251-264.

[72] Song, B., H. Choi and H. S. Lee 2008, "Surveillance tracking system using passive infrared motion sensors in wireless sensor network", *Information Networking, 2008. ICOIN 2008. International Conference on,*: IEEE 1-5.

[73] Sekmen, A.S., Wilkes, M.and Kawamura, K., (2002), "An application of passive human-robot interaction: human tracking based on attention distraction", *Systems, Man and Cybernetics, Part A: Systems and Humans, IEEE Transactions on,* Vol.32 (2), pp. 248-259.

[74] Hosokawa, T. and M. Kudo 2005, "Person tracking with infrared sensors", "Person tracking with infrared sensors", *Knowledge-Based Intelligent Information and Engineering Systems,*: Springer 682-688.

[75] Schiff, J. and K. Goldberg 2006, "Automated intruder tracking using particle filtering and a network of binary motion sensors", *Automation Science and Engineering, 2006. CASE'06. IEEE International Conference on,*: IEEE 580-587.

[76] Lee, S., Ha, K.N.and Lee, K.C., (2006), "A pyroelectric infrared sensor-based indoor location-aware system for the smart home", *Consumer Electronics, IEEE Transactions on,* Vol.52 (4), pp. 1311-1317.

[77] Luo, X., et al., 2009, "Human tracking using ceiling pyroelectric infrared sensors", *Control and Automation, 2009. ICCA 2009. IEEE International Conference on,*: IEEE 1716-1721.

[78] Nithya, V., et al., 2010, "Model based target tracking in a wireless network of passive infrared sensor nodes", *Signal Processing and Communications (SPCOM), 2010 International Conference on,*: IEEE 1-5.

[79] Hao, Q., et al., (2006), "Real-time walker recognition using pyroelectric sensors", *IEEE Sensors Journal, submitted,* .

[80] Shankar, M., et al., (2006), "Human-tracking systems using pyroelectric infrared detectors", *Optical Engineering,* Vol.45 pp. 106401.

[81] Fang, J.S., et al., (2006), "Path-dependent human identification using a pyroelectric infrared sensor and Fresnel lens arrays", *Opt.Express,* Vol.14 (2), pp. 609-624.

[82] Hao, Q., et al., (2006), "Tracking and identifying multiple humans with wireless geometric pyroelectric sensors", *IEEE Trans.Syst., Man, Cybern.A,* .

[83] Fang, J.S., et al., (2006), "Real-time human identification using a pyroelectric infrared detector array and hidden Markov models", *Opt.Express,* Vol.14 pp. 6643-6658.

[84] Fang, J.S., et al., (2007), "A pyroelectric infrared biometric system for real-time walker recognition by use of a maximum likelihood principal components estimation (MLPCE) method", *Opt.Express,* Vol.15 (6), pp. 3271-3284.

[85] Liu, T., et al., 2010, "Distributed infrared biometric sensing for lightweight human identification systems", *Intelligent Control and Automation (WCICA), 2010 8th World Congress on,*: IEEE 6969-6974.

[86] Pinkston, R.F. (1994), "A touch sensitive dance floor/MIDI controller", *J.Acoust.Soc.Am.,* Vol.96 pp. 3302.

[87] Murakita, T., Ikeda, T.and Ishiguro, H., (2004), "Human tracking using floor sensors based on the Markov chain Monte Carlo method", *Pattern Recognit,* Vol.4 pp. 917-920.

[88] Addlesee, M.D., et al., (1997), "The ORL active floor", *IEEE Personal Communications,* Vol.4 pp. 35-41.

[89] Orr, R. J. and G. D. Abowd 2000, ""The smart floor: a mechanism for natural user identification and tracking", *CHI'00 extended abstracts on Human factors in computing systems,*: ACM 275-276.

[90] Middleton, L., et al., (2005), "A floor sensor system for gait recognition", .

[91] Future-Shape, [online], http://www.future-shape.com/en/index.html (Accessed 24.04.2011).

[92] Henry, R., L. Matti and S. Raimo 2008, "Human tracking using near field imaging", *Pervasive Computing Technologies for Healthcare, 2008. PervasiveHealth 2008. Second International Conference on,*: IEEE 148-151.

[93] Valtonen, M. and J. Vanhala 2009, "Human tracking using electric fields", *Pervasive Computing and Communications, 2009. PerCom 2009. IEEE International Conference on,*: IEEE 1-3.

[94] Pakhomov, A., et al., 2003, "Seismic footstep signal characterization", *Proceedings of SPIE,*Vol.5071, 297-305.

[95] Audette, W.E., et al., (2009), "Improved Intruder Detection Using Seismic Sensors and Adaptive Noise Cancellation", .

[96] Diermaier, J., et al., (2008), "Distributed Accelerometers as a Main Component in Detecting Activities of Daily Living", *Computers Helping People with Special Needs*, pp. 1042-1049.

[97] Potamitis, I., Chen, H.and Tremoulis, G., (2004), "Tracking of multiple moving speakers with multiple microphone arrays", *Speech and Audio Processing, IEEE Transactions on*, Vol.12 (5), pp. 520-529.

[98] Zetik, R., et al., 2006, "Detection and localization of persons behind obstacles using M-sequence through-the-wall radar", *Proc. SPIE,*Vol.6201,: Citeseer.

[99] Chang, S. H., M. Wolf and J. W. Burdick 2009, "An MHT algorithm for UWB radar-based multiple human target tracking", *Ultra-Wideband, 2009. ICUWB 2009. IEEE International Conference on,*: IEEE 459-463.

[100] Wan, E. A. and A. S. Paul 2010, "A tag-free solution to unobtrusive indoor tracking using wall-mounted ultrasonic transducers", *Indoor Positioning and Indoor Navigation (IPIN), 2010 International Conference on, 15-17 SEPTEMBER 2010,*: IEEE 1-10.

[101] Trahanias, P., et al., (2005), "TOURBOT and WebFAIR: Web-operated mobile robots for tele-presence in populated exhibitions", *Robotics & Automation Magazine, IEEE*, Vol.12 (2), pp. 77-89.

[102] Schulz, D., et al., 2001, "Tracking multiple moving targets with a mobile robot using particle filters and statistical data association", *Robotics and Automation, 2001. Proceedings 2001 ICRA. IEEE International Conference on,*Vol.2, 1665-1670 vol.2.

[103] Schulz, D., et al., (2003), "People tracking with mobile robots using sample-based joint probabilistic data association filters", *Int.J.Robotics Res.*, Vol.22 (2), pp. 99-116.

[104] Topp, E. A. and H. I. Christensen 2005, "Tracking for following and passing persons", *Intelligent Robots and Systems, 2005. (IROS 2005). 2005 IEEE/RSJ International Conference on*, 2321-2327.

[105] Hashimoto, M., et al., 2006, "A Laser Based Multi-Target Tracking for Mobile Robot", "A Laser Based Multi-Target Tracking for Mobile Robot", *Intelligent Autonomous Systems,*Vol.9, 135-144.

[106] Nishimura, H., et al., 2007, "People tracking with multiple laser range sensors", *Minoru Sasaki, et al., eds.*, Vol.6794,: SPIE 679410.

[107] Fod, A., A. Howard and M. A. J. Mataric 2002, "A laser-based people tracker", *Robotics and Automation, 2002. Proceedings. ICRA '02. IEEE International Conference on,*Vol.3, 3024-3029.

[108] Frank, O., et al., 2003, "Multiple Target Tracking using Sequential Monte Carlo Methods and Statistical Data Association", *2003 IEEE/RSJ International Conference on Intelligent Robots and Systems, October 27, 2003 - October 31,*Vol.3, *2003,*: Institute of Electrical and Electronics Engineers Inc Las Vegas, NV, United states, 2718-2723.

[109] Lindstrom, M. and J. -O Eklundh 2001, "Detecting and tracking moving objects from a mobile platform using a laser range scanner", *Intelligent Robots and Systems, 2001. Proceedings. 2001 IEEE/RSJ International Conference on,*Vol.3, 1364-1369 vol.3.

[110] Kluge, B. 2002, "Tracking multiple moving objects in populated, public environments", *Selected Revised Papers, 15-20 Oct. 2000,*: Springer-Verlag Berlin, Germany, 25-38.

[111] Topp, E. A., et al., 2004, "An interactive interface for service robots", "An interactive interface for service robots", *Proceedings- 2004 IEEE International Conference on Robotics and Automation, April 26, 2004 - May 1,*Vol.2004, *2004,*: Institute of Electrical and Electronics Engineers Inc New Orleans, LA, United states, 3469-3474.

[112] Kawata, H., et al., 2009, "Adaptive sensing system for human detecting with dynamic disposition", *2009 IEEE/RSJ International Conference on Intelligent Robots and Systems, IROS 2009, October 11, 2009 - October 15, 2009,*: IEEE Computer Society St. Louis, MO, United states, 2168-2173.

[113] Jinshi Cui, et al., 2006, "Robust Tracking of Multiple People in Crowds Using Laser Range Scanners", *Pattern Recognition, 2006. ICPR 2006. 18th International Conference on,*Vol.4, 857-860.

[114] ifm Vision Sensors Offer Smarter Inspection and Error-Proofing , [online], http://www.ifm.com/ifmus/web/app_vision.htm (Accessed 5/5/2011).

[115] Schöler, F., et al., "Person Tracking in Three-Dimensional Laser Range Data with Explicit Occlusion Adaption", .

[116] Petrovskaya, A.and Thrun, S., (2009), "Model based vehicle detection and tracking for autonomous urban driving", *Auton.Robots,* Vol.26 (2-3), pp. 123-139.

[117] Luo, X., O'Brien, W.J.and Julien, C.L., (2011), "Comparative evaluation of Received Signal-Strength Index (RSSI) based indoor localization techniques for construction jobsites", *Advanced Engineering Informatics,* Vol.25 (2), pp. 355-363.

[118] Geisheimer, J. L., W. S. Marshall and E. Greneker 2001, "A continuous-wave (CW) radar for gait analysis", *Signals, Systems and Computers, 2001. Conference Record of the Thirty-Fifth Asilomar Conference on,*Vol.1,: IEEE 834-838 vol. 1.

[119] Geisheimer, J. L., E. F. Greneker III and W. S. Marshall 2002, "High-resolution Doppler model of the human gait", *Proceedings of SPIE,*Vol.4744, 8.

[120] Gurbuz, S., W. Melvin and D. Williams 2007, "Detection and Identification of Human Targets in Radar Data", *In Proceedings of SPIE. April 9-13,*.

[121] Van Dorp, P. and FCA Groen 2003, "Human walking estimation with radar", *Radar, Sonar and Navigation, IEE Proceedings*-,Vol.150,: IET 356-365.

[122] Chen, V. C. 2000, "Analysis of radar micro-Doppler with time-frequency transform", *Statistical Signal and Array Processing, 2000. Proceedings of the Tenth IEEE Workshop on,*: IEEE 463-466.

[123] Smith, G. E., K. Woodbridge and C. J. Baker 2008, "Multistatic micro-Doppler signature of personnel", *Radar Conference, 2008. RADAR'08. IEEE,*: IEEE 1-6.

[124] Orovic, I., Stankovic, S.and Amin, M., (2010), "A new approach for classification of human gait based on time-frequency feature representations", *Signal Process,* .

[125] Tivive, F.H.C., Bouzerdoum, A.and Amin, M.G., (2010), "A human gait classification method based on radar Doppler spectrograms", *EURASIP Journal on Advances in Signal Processing,* Vol.2010 pp. 10.

[126] Ram, S. R. and H. Ling 2009, "MicroDoppler Signatures of Anomalies in Human Gait", *International Symposium on Electromagnetic Compatibility, July 20-24,* Ram,S.S. ; Ling,H.

[127] Kalgaonkar, K. and B. Raj 2007, "Acoustic Doppler sonar for gait recogination", *Advanced Video and Signal Based Surveillance, 2007. AVSS 2007. IEEE Conference on,* 27-32.

[128] Lin, A.and Ling, H., (2006), "Three-dimensional tracking of humans using very low-complexity radar", *Electronics Letters,* Vol.42 (18), pp. 1062-1063.

[129] Kubo, H., T. Mori and T. Sato 2009, "Human location estimation with multiple microwave Doppler sensors in home environment", *Networked Sensing Systems (INSS), 2009 Sixth International Conference on,* 1-6.

[130] Yarovoy, A.G., et al., (2006), "UWB Radar for Human Being Detection", *Aerospace and Electronic Systems Magazine, IEEE,* Vol.21 (11), pp. 22-26.

[131] Cambridge Consultants, [online], http://www.cambridgeconsultants.com/prism_200.html (Accessed 27-04-2011).

[132] Time Domain, [online], http://www.timedomain.com/products.php (Accessed 24-04-2011).

[133] Camero-Tech, [online], http://www.camero-tech.com/ (Accessed 24-04-2011).

[134] Wilson, J.and Patwari, N., (2010), "Radio Tomographic Imaging with Wireless Networks", *Mobile Computing, IEEE Transactions on,* Vol.9 (5), pp. 621-632.

[135] Griffiths, H.and Baker, C., (2006), "Fundamentals of tomography and radar", *Advances in Sensing with Security Applications,* pp. 171-187.

[136] Coetzee, S., CJ Baker and HD Griffiths 2006, "Narrow band high resolution radar imaging", *Radar, 2006 IEEE Conference on,*: IEEE 4 pp.

[137] Wicks, M. C., et al., 2005, "Ultra narrow band adaptive tomographic radar", *Computational Advances in Multi-Sensor Adaptive Processing, 2005 1st IEEE International Workshop on,* 36-39.

[138] Songmin Jia, Jinbuo Sheng and K. Takase 2008, "Human recognition using RFID system with multi-antenna", *Advanced Intelligent Mechatronics, 2008. AIM 2008. IEEE/ASME International Conference on,* 1213-1218.

[139] Gerónimo, D., et al., (2010), "Survey of Pedestrian Detection for Advanced Driver Assistance Systems", *Pattern Analysis and Machine Intelligence, IEEE Transactions on,* Vol.32 (7), pp. 1239-1258.

[140] Snidaro, L., Micheloni, C.and Chiavedale, C., (2005), "Video security for ambient intelligence", *Systems, Man and Cybernetics, Part A: Systems and Humans, IEEE Transactions on,* Vol.35 (1), pp. 133-144.

[141] Bradski, G. and Kaehler, A., (2008), *Learning OpenCV,* (First ed.), O'Reilly Media, Inc., Sebastopol, USA.

[142] Barnich, O. and M. Van Droogenbroeck 2009, "ViBE: A powerful random technique to estimate the background in video sequences", *Acoustics, Speech and Signal Processing, 2009. ICASSP 2009. IEEE International Conference on,* 945-948.

[143] Li, L., et al., 2003, "Foreground object detection from videos containing complex background", *In MULTIMEDIA '03: Proceedings of the eleventh ACM international conference on Multimedia,*: ACM Press 2-10.

[144] Javed, O., K. Shafique and M. Shah 2002, ""A hierarchical approach to robust background subtraction using color and gradient information", *Motion and Video Computing, 2002. Proceedings. Workshop on,* 22-27.

[145] Rother, C., V. Kolmogorov and A. Blake 2004, ""GrabCut" - interactive foreground extraction using iterated graph cuts", *ACM SIGGRAPH 2004,*Vol.23, *08,*: ACM USA, 309-14.

[146] Lowe, D.G. (2004), "Distinctive image features from scale-invariant keypoints", *International Journal of Computer Vision,* Vol.60 (2), pp. 91-110.

[147] Dalal, N. and B. Triggs 2005, "Histograms of oriented gradients for human detection", *Computer Vision and Pattern Recognition, 2005. CVPR 2005. IEEE Computer Society Conference on,*Vol.1, 886-893 vol. 1.

[148] Turk, M. A. and A. P. Pentland 1991, "Face recognition using eigenfaces", *Computer Vision and Pattern Recognition, 1991. Proceedings CVPR '91., IEEE Computer Society Conference on,* 586-591.

[149] Viola, P.and Jones, M., (2002), "Robust real-time object detection", *International Journal of Computer Vision,* Vol.57 (2), pp. 137-154.

[150] Rowley, H.A., Baluja, S.and Kanade, T., (1998), "Neural network-based face detection", *Pattern Analysis and Machine Intelligence, IEEE Transactions on,* Vol.20 (1), pp. 23-38.

[151] Gerónimo, D., et al., (2010), "2D-3D-based on-board pedestrian detection system", *Comput.Vision Image Understanding,* Vol.114 (5), pp. 583-595.

[152] Calisi, D., L. Iocchi and R. Leone 2007, "Person following through appearance models and stereo vision using a mobile robot", *1st International Workshop on Robot Vision, 8-11 March 2007,*: INSTICC Press Setubal, Portugal, 46-56.

[153] Gavrila, D.M.and Munder, S., (2007), "Multi-cue pedestrian detection and tracking from a moving vehicle", *International Journal of Computer Vision,* Vol.73 (1), pp. 41-59.

[154] Nickel, K., et al., 2005, "A joint particle filter for audio-visual speaker tracking", *Proceedings of the 7th international conference on Multimodal interfaces,*: ACM New York, NY, USA, 61-68.

[155] Cielniak, G., T. Duckett and A. J. Lilienthal 2007, "Improved data association and occlusion handling for vision-based people tracking by mobile robots", *Intelligent Robots and Systems, 2007. IROS 2007. IEEE/RSJ International Conference on,* 3436-3441.

[156] Stogdale, N., et al., 2003, "Array-based infra-red detection: an enabling technology for people counting, sensing, tracking, and intelligent detection.", *In Proceedings of SPIE,*Vol.5071. 465.,.

[157] Bertozzi, M., et al., (2007), "Pedestrian detection by means of far-infrared stereo vision", *Comput.Vision Image Understanding,* Vol.106 (2-3), pp. 194-204.

[158] FLIR Infrared Cameras & Thermal Imaging , [online], http://www.flir.com/thermography/ (Accessed 5/5/2011).

[159] Yilmaz, A., Javed, O.and Shah, M., (2006), "Object tracking: A survey", *ACM Comput.Surv.,* Vol.38 (4),.

[160] Reid, D. (1979), "An algorithm for tracking multiple targets", *Automatic Control, IEEE Transactions on,* Vol.24 (6), pp. 843-854.

[161] Bar-Shalom, Y.and Tse, E., (1975), "Tracking in a cluttered environment with probabilistic data association", *Automatica,* Vol.11 (5), pp. 451-460.

[162] Isard, M.and Blake, A., (1998), "CONDENSATION - conditional density propagation for visual tracking", *International Journal of Computer Vision,* Vol.29 pp. 5-28.

[163] Wiskott, L., et al., (1997), "Face recognition by elastic bunch graph matching", *Pattern Analysis and Machine Intelligence, IEEE Transactions on,* Vol.19 (7), pp. 775-779.

[164] Kale, A., et al., 2003, "Gait analysis for human identification", *Audio-and Video-Based Biometric Person Authentication,*: Springer 1058-1058.

[165] Liang Wang, et al., (2003), "Silhouette analysis-based gait recognition for human identification", *Pattern Analysis and Machine Intelligence, IEEE Transactions on,* Vol.25 (12), pp. 1505-1518.

[166] Dacheng Tao, et al., (2007), "General Tensor Discriminant Analysis and Gabor Features for Gait Recognition", *Pattern Analysis and Machine Intelligence, IEEE Transactions on,* Vol.29 (10), pp. 1700-1715.

[167] Yanying Gu, Lo, A.and Niemegeers, I., (2009), "A survey of indoor positioning systems for wireless personal networks", *Communications Surveys & Tutorials, IEEE,* Vol.11 (1), pp. 13-32.

[168] Da Zhang, et al., 2010, "Localization Technologies for Indoor Human Tracking", *Future Information Technology (FutureTech), 2010 5th International Conference on,* 1-6.

[169] Yun, J., SungBu Kim and JangMyung Lee 2006, "Robust positioning a mobile robot with active beacon sensors", *10th International Conference on Knowledge-Based Intelligent Information and Engineering Systems, KES 2006, October 9, 2006 - October 11,*Vol.4251 LNAI - I, *2006,*: Springer Verlag Bournemouth, United kingdom, 890-897.

[170] Gezici, S. (2008), "A survey on wireless position estimation", *Wireless Personal Communications,* Vol.44 (3), pp. 263-282.

[171] Werb, J.and Lanzl, C., (1998), "Designing a positioning system for finding things and people indoors", *Spectrum, IEEE,* Vol.35 (9), pp. 71-78.

[172] Amundson, I. and Xenofon D. Koutsoukos 2009, "A survey on localization for mobile wireless sensor networks", *2nd International Workshop on Mobile Entity Localization and Tracking in GPS-less Environments, MELT 2009, September 30, 2009 - September 30,*Vol.5801 LNCS, *2009,*: Springer Verlag Orlando, FL, United states, 235-254.

[173] Want, R., et al., (1992), "Active badge location system", *ACM Transactions on Information Systems,* Vol.10 (1), pp. 91-102.

[174] Gesture Central - Firefly , [online], http://www.gesturecentral.com/firefly/ (Accessed 5/9/2011).

[175] Accurate Measurement Solutions for Medical, Industrial, and Life Sciences Applications | NDI , [online], http://www.ndigital.com/ (Accessed 5/9/2011).

[176] Ni, L. M., et al., 2003, "LANDMARC: Indoor location sensing using active RFID", *1st IEEE International Conference on Pervasive Computing and Communications, PerCom 2003, March 23, 2003 - March 26, 2003,*: IEEE Computer Society Fort Worth, TX, United states, 407-415.

[177] Bouet, M. and Aldri L. Dos Santos 2008, "RFID tags: Positioning principles and localization techniques", *2008 1st IFIP Wireless Days, WD 2008, November 24, 2008 - November 27, 2008,*: Inst. of Elec. and Elec. Eng. Computer Society Dubai, United arab emirates,.

[178] Seco, F., et al., 2010, "Improving RFID-based indoor positioning accuracy using Gaussian processes", *Indoor Positioning and Indoor Navigation (IPIN), 2010 International Conference on,* 1-8.

[179] Harter, A., et al., (2002), "The anatomy of a context-aware application", *Wireless Networks,* Vol.8 (2-3), pp. 187-197.

[180] Priyantha, N. B., Anit Chakraborty and Hari Balakrishnan 2000, "Cricket location-support system", *6th Annual International Conference on Mobile Computing and Networking (MOBICOM 2000), August 6, 2000 - August 11, 2000,*: ACM Boston, MA, USA, 32-43.

[181] WhereNet ISO 24730 Real Time Location Tracking Sytem , [online], http://www.zebra.com/ (Accessed 5/9/2011).

[182] King, T., et al., 2006, "COMPASS: A probabilistic indoor positioning system based on 802.11 and digital compasses", *WiNTECH 2006 - First ACM International Workshop on Wireless Network Testbeds, Experimental Evaluation and Characterization, September 29, 2006 - September 29,*Vol.2006, *2006,*: Association for Computing Machinery Los Angeles, CA, United states, 34-40.

[183] Indoor Location, People and Asset Tracking, Positioning , [online], http://www.tadlys.co.il/ (Accessed 5/9/2011).

[184] - Ubisense , [online], http://www.ubisense.net/en/ (Accessed 5/9/2011).

[185] Aitenbichler, E. and M. Muhlhauser 2003, "An IR local positioning system for smart items and devices", *Proceedings 23rd International Conference on Distributed Computing Systems Workshops, 19-22 May 2003,*: IEEE Piscataway, NJ, USA, 334-9.

[186] Sonitor - Home , [online], http://www.sonitor.com/ (Accessed 5/9/2011).

[187] Ascension MotionStar Wireless 2 from Inition , [online], http://www.inition.co.uk/ (Accessed 5/9/2011).

[188] de Ipina, D.L., Mendonca, P.R.S.and Hopper, A., (2002), "TRIP: a low-cost vision-based location system for ubiquitous computing", *Personal and Ubiquitous Computing,* Vol.6 (3), pp. 206-19.

[189] Mandal, A., et al., 2005, "Beep: 3D indoor positioning using audible sound", *Consumer Communications and Networking Conference, 2005. CCNC. 2005 Second IEEE,* 348-353.

[190] Krumm, J., et al., 2000, "Multi-camera multi-person tracking for EasyLiving", *Visual Surveillance, 2000. Proceedings. Third IEEE International Workshop on,* 3-10.

[191] Javed, O., et al., 2003, "KNIGHT™: a real time surveillance system for multiple and non-overlapping cameras", *Multimedia and Expo, 2003. ICME '03. Proceedings. 2003 International Conference on,*Vol.1, I-649-52 vol.1.

[192] Stillman, S., R. Tanawongsuwan and I. Essa 1999, "A system for tracking and recognizing multiple people with multiple cameras", *Proceedings of the Second International Conference on Audio-Vision-based Person Authentication,*: Citeseer.

[193] Rekimoto, J. and Yuji Ayatsuka 2000, "CyberCode: Designing Augmented Reality Environments with Visual Tags", 1-10.

[194] Nagumo, Y. and A. Ohya 2001, "Human following behavior of an autonomous mobile robot using light-emitting device", *Robot and Human Interactive Communication, 2001. Proceedings. 10th IEEE International Workshop on,* 225-230.

[195] Ohya, A. 2002, "Human robot interaction in mobile robot applications", *Robot and Human Interactive Communication, 2002. Proceedings. 11th IEEE International Workshop on,* 5-10.

[196] Gigliotta, O., et al., 2005, "Toward a person-follower robot", "Toward a person-follower robot", *Proceedings of the Second RoboCare Workshop,*: Citeseer.

[197] Ohya, A., Y. Nagumo and M. Takahata 2002, "Intelligent escort robot moving together with human-human following behavior", *12th International Symposium on Measurement and Control in Robotics, June,*.

[198] Ohya, A., Y. Nagumo and Y. Gibo 2002, "Intelligent escort robot moving together with human-methods for human position recognition", *Joint 1st International Conference on Soft Computing and Intelligent Systems and 3rd International Symposium on Advanced Intelligent Systems (SCIS & ISIS 2002), 24B5-2,*.

[199] Nuñez, C., et al., 2010, "Electronic Luggage Follower", *Florida Conference on Recent Advances in Robotics, FCRAR,* 20-21.

[200] Getting, I.A. (1993), "Perspective/navigation-The Global Positioning System", *Spectrum, IEEE,* Vol.30 (12), pp. 36-38, 43-47.

[201] Hasan, M. K. and T. Szecsi 2008, "Developing a patient guidance module for hospital robots", *4th IPROMS Virtual International Conference Innovative Production Machines and Systems, 1-14 July 2008,*: Whittles Publishing Dunbeath, UK, 6.

[202] Kim, M., T. Takeuchi and N. Y. Chong 2004, "A 3-axis orthogonal antenna for indoor localization", *First international workshop on networked sensing systems,* 59-62.

[203] Luo, R. C., Jhu Yi-Huei and Ogst Chen 2008, "Robotics human tracking system through wireless pyroelectric sensor system", *Advanced robotics and Its Social Impacts, 2008. ARSO 2008. IEEE Workshop on,* 1-6.

[204] RFID-radar - A new identification technology , [online], http://www.rfid-radar.com/ (Accessed 5/9/2011).

[205] Popa, V., Coca, E.and Dimian, M., "Applications of RFID Systems-Localization and Speed Measurement", .

[206] Kim, M.and Nak, Y.C., (2007), "RFID-based mobile robot guidance to a stationary target", *Mechatronics,* Vol.17 (4-5), pp. 217-29.

[207] Kim, M., Wook Kim Hyung and Young Chong Nak 2007, "Automated robot docking using direction sensing RFID", *2007 IEEE International Conference on Robotics and Automation, 10-14 April 2007,*: IEEE Piscataway, NJ, USA, 6.

[208] Kim, M.and Chong, N.Y., (2009), "Direction sensing RFID reader for mobile robot navigation", *IEEE Transactions on Automation Science and Engineering,* Vol.6 (1), pp. 44-54.

[209] Kim, M., Kim, K.and Chong, N., (2010), "RFID based collision-free robot docking in cluttered environment", *Progress in Electromagnetics Research,* Vol.110 pp. 199-218.

[210] Kanda, T., et al., 2003, "Person identification and interaction of social robots by using wireless tags", *Intelligent Robots and Systems, 2003. (IROS 2003). Proceedings. 2003 IEEE/RSJ International Conference on,*Vol.2, 1657-1664 vol.2.

[211] Hori, T., et al., 2008, "A Multi-Sensing-Range Method for Position Estimation of Passive RFID Tags", *Networking and Communications, 2008. WIMOB '08. IEEE International Conference on Wireless and Mobile Computing,* 208-213.

[212] Grejner-Brzezinska, D. A., C. K. Toth and Y. Yi 2001, "Bridging GPS Gaps in Urban Canyons: Can ZUPT Really Help?", *Proceedings of the 58th Annual Meeting of The Institute of Navigation and CIGTF 21st Guidance Test Symposium,* 231-240.

[213] Ojeda, L. and J. Borenstein 2007, "Personal Dead-reckoning System for GPS-denied Environments", *Safety, Security and Rescue Robotics, 2007. SSRR 2007. IEEE International Workshop on*, 1-6.

[214] Foxlin, E. (2005), "Pedestrian tracking with shoe-mounted inertial sensors", *Computer Graphics and Applications, IEEE,* Vol.25 (6), pp. 38-46.

[215] Chia-How Lin, et al., 2008, "A new design on multi-modal robotic focus attention", *Robot and Human Interactive Communication, 2008. RO-MAN 2008. The 17th IEEE International Symposium on,* 598-603.

[216] Tse Min Chen and R. C. Luo 2000, "Multilevel multi-agent based team decision fusion for mobile robot behavior control", *Intelligent Control and Automation, 2000. Proceedings of the 3rd World Congress on,*Vol.1, 489-494 vol.1.

[217] Wilhelm, T., Böhme, H.-.and Gross, H.-., (2004), "A multi-modal system for tracking and analyzing faces on a mobile robot", *Robotics and Autonomous Systems,* Vol.48 (1), pp. 31-40.

[218] Schaffernicht, E., et al., 2005, "A probabilistic multimodal sensor aggregation scheme applied for a mobile robot", *Proceedings, 11-14 Sept. 2005,*: Springer-Verlag Berlin, Germany, 320-34.

[219] Nakadai, K., et al. Real-Time Auditory and Visual Multiple-Object Tracking for Humanoids. 2001.

[220] Okuno, H. G., et al., 2001, "Human-robot interaction through real-time auditory and visual multiple-talker tracking", *Intelligent Robots and Systems, 2001. Proceedings. 2001 IEEE/RSJ International Conference on,*Vol.3, 1402-1409 vol.3.

[221] Hyun-Don Kim, et al., 2007, "Auditory and visual integration based localization and tracking of humans in daily-life environments", *Intelligent Robots and Systems, 2007. IROS 2007. IEEE/RSJ International Conference on,* 2021-2027.

[222] Bellotto, N.and Huosheng Hu., (2009), "Multisensor-Based Human Detection and Tracking for Mobile Service Robots", *Systems, Man, and Cybernetics, Part B: Cybernetics, IEEE Transactions on,* Vol.39 (1), pp. 167-181.

[223] Brooks, A. and Stefan Williams 2004, "Tracking People with Networks of Heterogeneous Sensors", *In proceeding of the Australian conference on robotics and automation,* 1-7.

[224] Kleinehagenbrock, M., et al., 2002, "Person tracking with a mobile robot based on multi-modal anchoring", *Robot and Human Interactive Communication, 2002. Proceedings. 11th IEEE International Workshop on,* 423-429.

[225] Fritsch, J., et al., 2004, "Audiovisual Person Tracking with a Mobile Robot", *In Proc. Int. Conf. on Intelligent Autonomous Systems,*: IOS Press 898-906.

[226] Scheidig, A., et al., 2006, "Generating Persons Movement Trajectories on a Mobile Robot", *Robot and Human Interactive Communication, 2006. ROMAN 2006. The 15th IEEE International Symposium on*, 747-752.

[227] Itoh, K., et al., 2006, "Development of a Person Following Mobile Robot in Complicated Background by Using Distance and Color Information", *IEEE Industrial Electronics, IECON 2006 - 32nd Annual Conference on*, 3839-3844.

[228] Germa, T., et al., (2010), "Vision and RFID data fusion for tracking people in crowds by a mobile robot", *Comput.Vision Image Understanding*, Vol.114 (6), pp. 641-51.

[229] Ching-Chih Tsai, et al., 2009, "Human-robot interaction of an active mobile robotic assistant in intelligent space environments", *Systems, Man and Cybernetics, 2009. SMC 2009. IEEE International Conference on*, 1953-1958.

[230] Morioka, K., Joo-Ho Leeand Hashimoto, H., (2004), "Human-following mobile robot in a distributed intelligent sensor network", *Industrial Electronics, IEEE Transactions on*, Vol.51 (1), pp. 229-237.

[231] Tae-Seok Jin, Jang-Myung Leeand Hashimoto, H., (2006), "Position control of mobile robot for human-following in intelligent space with distributed sensors", *International Journal of Control, Automation, and Systems*, Vol.4 (2), pp. 204-16.

[232] Ergen, E., Akinci, B.and Sacks, R., (2007), "Tracking and locating components in a precast storage yard utilizing radio frequency identification technology and GPS", *Autom.Constr.*, Vol.16 (3), pp. 354-367.

[233] Ruiz, A. R. J., et al., 2010, ""Pedestrian indoor navigation by aiding a foot-mounted IMU with RFID Signal Strength measurements", *2010 International Conference on Indoor Positioning and Indoor Navigation (IPIN 2010), 15-17 Sept. 2010,*: IEEE Piscataway, NJ, USA, 7.

[234] Luo, R. C., O. Chen and Wei Lin Cheng 2010, "Indoor human monitoring system using wireless and pyroelectric sensory fusion system", *2010 IEEE/RSJ International Conference on Intelligent Robots and Systems (IROS 2010), 18-22 Oct. 2010,*: IEEE Piscataway, NJ, USA, 1507-12.

[235] Nohara, K., et al., 2008, "Integrating passive RFID tag and person tracking for social interaction in daily life", *2008 RO-MAN: The 17th IEEE International Symposium on Robot and Human Interactive Communication, 1-3 Aug. 2008,*: IEEE Piscataway, NJ, USA, 545-52.

[236] Chang, H., et al., 2006, "Reliable Position Estimation Method of The Mobile Robot By Laser Scanner and Indoor GPS System", *Proceedings of the 23rd International Symposium on Automation and Robotics in Construction 2006 (ISARC 2006),*.

[237] Schulz, D., Fox, D.and Hightower, J. People Tracking with Anonymous and ID-Sensors Using Rao-Blackwellised Particle Filters. 2003.

[238] Kim, D., et al., 2008, "Distance correction system for localization based on linear regression and smoothing in ambient intelligence display", *Engineering in Medicine and Biology Society, 2008. EMBS 2008. 30th Annual International Conference of the IEEE*, 1443-1446.

[239] Li, H., et al., 2009, "Networked ultrasonic sensors for target tracking: An experimental study", *2009 IEEE Global Telecommunications Conference, GLOBECOM 2009, November 30, 2009 - December 4, 2009,*: Institute of Electrical and Electronics Engineers Inc Honolulu, HI, United states,.

[240] Teixeira, T., et al., 2009, "Identifying people in camera networks using wearable accelerometers", *2nd International Conference on PErvasive Technologies Related to Assistive Environments, PETRA 2009, June 9, 2009 - June 13, 2009,*: Association for Computing Machinery Corfu, Greece,.

[241] Germa, T., Lerasle, F.and Simon, T., (2009), "Video-based face recognition and tracking from a robot companion", *Int.J.Pat.Recognit.Artif.Intell.*, Vol.23 (3), pp. 591-616.

[242] Zajdel, W., Z. Zivkovic and B. J. A. Krose 2005, "Keeping Track of Humans: Have I Seen This Person Before?", *Robotics and Automation, 2005. ICRA 2005. Proceedings of the 2005 IEEE International Conference on*, 2081-2086.

[243] Morishita, H., R. Fukui and T. Sato 2002, ""High resolution pressure sensor distributed floor for future human-robot symbiosis environments", *Intelligent Robots and Systems, 2002. IEEE/RSJ International Conference on,*Vol.2,: IEEE 1246-1251 vol. 2.

[244] *Cricket v2 User Manual*, (2004), MIT Computer Science and Artificial Intelligence Lab, Cambridge, MA 02139.

[245] Al Sabbagh, M. , (2006), "Real-time Tracking for Assisted Living", Distinction Project, The Ohio State University,.

[246] Priyantha, N.B. , (2005), "The cricket indoor location system", PhD thesis, Massachusetts Institute of Technology,.

[247] Doebelin, E.O., (1995), *Engineering experimentation: planning, execution, reporting* , McGraw-Hill College, Singapore.

[248] Experimental Design, [online], http://www.statsoft.com/textbook/experimental-design/#3a (Accessed 9/26/2011).

[249] Stat-Ease, I. Design-Expert. 2009;8.

[250] Design-Expert 8 Help File. 2009.

[251] Human Figure Drawing Proportions , [online], http://realcolorwheel.com/human.htm (Accessed 9/26/2011).

[252] Montgomery, D.C., (1984), *Design and analysis of experiments*, (2nd Edition ed.), John Wiley & Sons Inc, New York.

[253] Miller, I. and Freund, J.E., (1985), *Probability and Statistics for Engineers*, (3rd Edition ed.), Prentice-Hall, Inc., New Jersey.

[254] Finkenzeller, K., (2010), *RFID Handbook: Fundamentals and applications in contactless smart cards, radio frequency identification and near-field communication*, (2nd ed.), Wiley, UK.

[255] Ouyang, D. , (2008), "Identification of Car Passengers with RFID for Automatic Crash Notification", MSc, Blekinge Institute of Technology, Sweden.

[256] Amanna, A., Ambuj Agrawal and Majid Manteghi 2010, "Active RFID for enhanced railway operations", *ASME 2010 Rail Transportation Division Fall Technical Conference, RTDF2010, October 12, 2010 - October 13, 2010,*: American Society of Mechanical Engineers Roanoke, VA, United states, 31-37.

[257] Lien, T.H. , (2011), "Automatic Identification Technology: Tracking Weapons and Ammunition for the Norwegian Armed Forces", MBA, Naval Postgraduate School, Monterey, CA USA.

[258] Types of RFID , [online], http://www.controlelectric.com/RFID/Types_of_RFID.html (Accessed 11/17/2011).

[259] Maloni, M.and Dewolf, F. Understanding Radio Frequency Identification (RFID) and Its Impact on the Supply Chain. 2006.

[260] Wavetrend. Active RFID Manual.

[261] IAF - ISM 433/868 , [online], http://iaf-bs.de/projects/ (Accessed 11/17/2011).

[262] Wavetrend. Information sheet for AN200 Stub Antenna.

[263] Cheng, H. , (2006), "Heterogenenous Sensor Networks Design for Aged Care", Undergraduate, The University of Western Australia, Perth, Australia.

[264] Benkic, K., et al., 2008, "Using RSSI value for distance estimation in wireless sensor networks based on ZigBee", *Systems, Signals and Image Processing, 2008. IWSSIP 2008. 15th International Conference on*, 303-306.

[265] Kitsos, P. and Zhang, Y., (2008), *RFID security: techniques, protocols and system-on-chip design*, , Springer Verlag,.

[266] Green, A. Shielding Magnetic Fields. The Industrial Physicist 2001:24.

[267] Hitchcock, R.T. and Patterson, R.M., (1995), *Radio-frequency and ELF electromagnetic energies: A handbook for health professionals*, , Wiley,.

[268] Stereo Vision and Applications , [online], http://www.vision.deis.unibo.it/smatt/stereo.htm (Accessed 1/17/2012).

[269] Trucco, E. and Verry, A., (1998), *Introductory Techniques for 3-D Computer Vision*, (First ed.), Prentice Hall, New Jersey.

[270] Hartley, R.I. Theory and Practice of Projective Rectification. 1998.

[271] Konolige, K. 1998, "Small vision systems: Hardware and implementation", "Small vision systems: Hardware and implementation", *Robotics Research-International Symposium-*,Vol.8,: MIT PRESS 203-212.

[272] Welcome - OpenCV Wiki , [online], http://opencv.willowgarage.com/wiki/ (Accessed 1/17/2012).

[273] Elmenreich, W. , (2002), "Sensor fusion in time-triggered systems", DSc, Technische Universität Wien, Austria.

[274] Mirabadi, A., N. Mort and F. Schmid 1996, "Application of sensor fusion to railway systems", *Multisensor Fusion and Integration for Intelligent Systems, 1996. IEEE/SICE/RSJ International Conference on*, 185-192.

[275] C3-803 :: C3 - Grabber Catch Latches | Southco , [online], http://www.southco.com/products/c3-grabber-catch-latches/c3-803.html (Accessed 1/10/2012).

[276] S T R I X , [online], http://www.strix.com/product/prodp72.php (Accessed 1/10/2012).

[277] CEEP - Rectangular Connectors , [online], http://www.ceep.co.uk/rectangular-connectors.aspx (Accessed 1/10/2012).

[278] Gumstix small open source hardware , [online], http://www.gumstix.com/ (Accessed 1/10/2012).

[279] Buy PCB Solid State Relays (SSR) SIL solid state relay,3A 3-60Vdc,SPST-NO Crydom MPDCD3 online from RS for next day delivery. , [online], http://radionics.rs-online.com/web/p/products/2413975/ (Accessed 1/10/2012).

[280] Serial Programming/Serial Linux - Wikibooks, open books for an open world , [online], http://en.wikibooks.org/wiki/Serial_Programming/Serial_Linux (Accessed 3/15/2012).

[281] Using Philips webcam features with OpenCV and pwc , [online], http://rainsoft.de/projects/pwc.html (Accessed 3/15/2012).

[282] ZeroC - The Internet Communications Engine (Ice) , [online], http://www.zeroc.com/ice.html (Accessed 3/15/2012).

Appendix A : Cricket Experiments

Table A-1: Data Sheet for Cricket Accuracy Model of Corridor.

		Factor 1	Factor 2	Factor 3	Factor 4	Response
Std	Run	A:	B:	C:	D:	Accuracy
		cm	cm	*cm*	*cm*	*%*
45	1	150	150	80	400	99,125
70	2	0	150	80	600	97,3333
10	3	0	0	80	200	100
5	4	75	75	60	200	100
58	5	0	75	60	600	99,6667
66	6	150	0	80	600	96,9167
32	7	75	75	60	400	99,125
71	8	75	150	80	600	99,75
42	9	150	75	80	400	99
76	10	0	75	100	600	99,9167
17	11	75	150	80	200	93,5
49	12	0	75	100	400	98,625
47	13	75	0	100	400	98,375
31	14	0	75	60	400	99,125
41	15	75	75	80	400	99
7	16	0	150	60	200	73,25
67	17	0	75	80	600	100
73	18	0	0	100	600	99,9167
35	19	75	150	60	400	99,125
61	20	0	150	60	600	97,0667
64	21	0	0	80	600	99,2917
75	22	150	0	100	600	97,0667
28	23	0	0	60	400	99,375
15	24	150	75	80	200	93,75
14	25	75	75	80	200	100
24	26	150	75	100	200	92,75
12	27	150	0	80	200	72,25
3	28	150	0	60	200	73
4	29	0	75	60	200	92,75
50	30	75	75	100	400	99,5
48	31	150	0	100	400	92,375
22	32	0	75	100	200	91
30	33	150	0	60	400	92,625
46	34	0	0	100	400	99,75
29	35	75	0	60	400	99
43	36	0	150	80	400	99,125
72	37	150	150	80	600	99,5
9	38	150	150	60	200	99,5
27	39	150	150	100	200	98,75
74	40	75	0	100	600	99,4167

56	41	75	0	60	600	97.4167
68	42	75	75	80	600	99.5
57	43	150	0	60	600	97.3333
53	44	75	150	100	400	98.75
52	45	0	150	100	400	92.75
11	46	75	0	80	200	92.75
34	47	0	150	60	400	93.125
6	48	150	75	60	200	94.5
65	49	75	0	80	600	99.5833
79	50	0	150	100	600	97
80	51	75	150	100	600	99.5833
8	52	75	150	60	200	93.75
33	53	150	75	60	400	99.25
55	54	0	0	60	600	99.76
78	55	150	75	100	600	99.6667
37	56	0	0	80	400	99.25
54	57	150	150	100	400	99.375
16	58	0	150	80	200	73.75
1	59	0	0	60	200	99.75
38	60	75	0	80	400	98.875
13	61	0	75	80	200	93
18	62	150	150	80	200	100
69	63	150	75	80	600	99.6667
21	64	150	0	100	200	71.25
19	65	0	0	100	200	98.25
59	66	75	75	60	600	99.4167
20	67	75	0	100	200	91.75
60	68	150	75	60	600	99.75
62	69	75	150	60	600	99.5833
51	70	150	75	100	400	98.75
40	71	0	75	80	400	99.25
23	72	75	75	100	200	98.25
26	73	75	150	100	200	91.75
77	74	75	75	100	600	99.4167
39	75	150	0	80	400	92.625
25	76	0	150	100	200	72.5
81	77	150	150	100	600	99.5833
36	78	150	150	60	400	99.375
2	79	75	0	60	200	93
44	80	75	150	80	400	99.25
63	81	150	150	60	600	99.5833

Table A-2: ANOVA Report for Corridor.

Response 1		**Accuracy**							
ANOVA for Response Surface Reduced Cubic Model									
Analysis of variance table [Partial sum of squares - Type III]									
	Sum of		**Mean**	**F**	**p-value**				
Source	**Squares**	**df**	**Square**	**Value**	**Prob > F**				
Model	3058.486	7	436.9265	32.23294	< 0.0001				
A-Receiver Horizontal Displacement	0.976094	1	0.976094	0.072008	0.7892				
B-Beacon Horizontal Displacement	4.046107	1	4.046107	0.298489	0.5865				
D-Distance	962.1195	1	962.1195	70.97748	< 0.0001				
AB	1210.962	1	1210.962	89.3351	< 0.0001				
AD	0.15802	1	0.15802	0.011657	0.9143				
BD	0.169277	1	0.169277	0.012488	0.9113				
ABD	880.0543	1	880.0543	64.92336	< 0.0001				
Residual	989.5354	73	13.55528						
Cor Total	4048.021	80							
Std. Dev.	3.681749		R-Squarec	0.755551					
Mean	95.81864		Adj R-Squ	0.73211					
C.V. %	3.842414		Pred R-Sq	0.680809					
PRESS	1292.093		Adeq Prec	21.08375					
	Coefficient		**Standard**	**95% CI**	**95% CI**				
Factor	**Estimate**	**df**	**Error**	**Low**	**High**	**VIF**			
Intercept	95.81864	1	0.409083	95.00334	96.63395				
A-Receiver Horizontal Displacement	-0.13445	1	0.501023	-1.13298	0.86409	1			
B-Beacon Horizontal Displacement	0.27373	1	0.501023	-0.72481	1.272266	1			
D-Distance	4.221022	1	0.501023	3.222486	5.219559	1			
AB	5.799814	1	0.613625	4.576861	7.022767	1			
AD	-0.06625	1	0.613625	-1.28921	1.1567	1			
BD	-0.06857	1	0.613625	-1.29152	1.15438	1			
ABD	-6.05549	1	0.751534	-7.55329	-4.55768	1			
Final Equation in Terms of Coded Factors:									
	Accuracy	=							
	95.81864								
	-0.13445	* A							
	0.27373	* B							
	4.221022	* D							
	5.799814	* A * B							
	-0.06625	* A * D							
	-0.06857	* B * D							
	-6.05549	* A * B * D							
Final Equation in Terms of Actual Factors:									
	Accuracy	=							
	104.8785								
	-0.23884	* Receiver Horizontal Displacement							
	-0.23333	* Beacon Horizontal Displacement							
	-0.0085	* Distance							
	0.003184	* Receiver Horizontal Displacement * Beacon Horizontal Displacement							
	0.000399	* Receiver Horizontal Displacement * Distance							
	0.000399	* Beacon Horizontal Displacement * Distance							
	-5.4E-06	* Receiver Horizontal Displacement * Beacon Horizontal Displacement * Distance							

Table A-3: Data Sheet for Cricket Accuracy Model of Reception Area.

		Factor 1	Factor 2	Factor 3	Factor 4	Response
Std	Run	A:	B:	C:	D:	Accuracy
		cm	cm	cm	cm	%
41	1	75	75	80	400	98.75
77	2	75	75	100	600	99.5
30	3	150	0	60	400	85.75
26	4	75	150	100	200	92
34	5	0	150	60	400	86.5
37	6	0	0	80	400	98.5
39	7	150	0	80	400	85.5
81	8	150	150	100	600	99.25
42	9	150	75	80	400	97.75
31	10	0	75	60	400	98.5
48	11	150	0	100	400	85
71	12	75	150	80	600	98.5
28	13	0	0	60	400	98.5
38	14	75	0	80	400	98
17	15	75	150	80	200	93
21	16	150	0	100	200	71.25
73	17	0	0	100	600	99.75
40	18	0	75	80	400	98.25
24	19	150	75	100	200	91.5
44	20	75	150	80	400	97.75
6	21	150	75	60	200	93
22	22	0	75	100	200	92
12	23	150	0	80	200	72.25
29	24	75	0	60	400	97.75
70	25	0	150	80	600	91.75
74	26	75	0	100	600	98.25
18	27	150	150	80	200	95
78	28	150	75	100	600	98.25
64	29	0	0	80	600	99.25
36	30	150	150	60	400	98.5
16	31	0	150	80	200	73.5
67	32	0	75	80	600	98.75
19	33	0	0	100	200	98.25
62	34	75	150	60	600	98.75
61	35	0	150	60	600	91.75
49	36	0	75	100	400	97.5
76	37	0	75	100	600	99
5	38	75	75	60	200	99.75
46	39	0	0	100	400	99.25
51	40	150	75	100	400	96.75

60	41	150	75	60	600	98.25
7	42	0	150	60	200	73.75
80	43	75	150	100	600	98.75
3	44	150	0	60	200	72.25
35	45	75	150	60	400	98
43	46	0	150	80	400	86
47	47	75	0	100	400	97
13	48	0	75	80	200	93
56	49	75	0	60	600	98.5
52	50	0	150	100	400	85.5
4	51	0	75	60	200	93.75
50	52	75	75	100	400	99.25
58	53	0	75	60	600	99.25
57	54	150	0	60	600	90.085
69	55	150	75	80	600	98.75
25	56	0	150	100	200	72.25
1	57	0	0	60	200	99.5
45	58	150	150	80	400	98.75
63	59	150	150	60	600	99
75	60	150	0	100	600	89.75
2	61	75	0	60	200	93
65	62	75	0	80	600	98
9	63	150	150	60	200	100
66	64	150	0	80	600	90.5
8	65	75	150	60	200	93.5
55	66	0	0	60	600	98.75
53	67	75	150	100	400	97.25
10	68	0	0	80	200	99.5
72	69	150	150	80	600	99
20	70	75	0	100	200	91
15	71	150	75	80	200	92.5
33	72	150	75	60	400	97.75
27	73	150	150	100	200	98.5
14	74	75	75	80	200	99.75
11	75	75	0	80	200	92.25
54	76	150	150	100	400	99.25
68	77	75	75	80	600	99
32	78	75	75	60	400	98.5
79	79	0	150	100	600	91.25
23	80	75	75	100	200	98.5
59	81	75	75	60	600	98.75

Table A-4: ANOVA Report for Reception.

Response	**1**	**Accuracy**							
ANOVA for Response Surface Reduced Cubic Model									
Analysis of variance table [Partial sum of squares - Type III]									
	Sum of		**Mean**	**F**	**p-value**				
Source	**Squares**	**df**	**Square**	**Value**	**Prob > F**				
Model	3352.274	7	478.8963	34.59934	< 0.0001				
A-Receiv	6.980412	1	6.980412	0.504321	0.4799				
B-Beacon	1.729856	1	1.729856	0.124979	0.7247				
D-Distanc	639.5305	1	639.5305	46.20485	< 0.0001				
AB	2239.104	1	2239.104	161.7709	< 0.0001				
AD	0.185617	1	0.185617	0.01341	0.9081				
BD	0.236034	1	0.236034	0.017053	0.8965				
ABD	464.508	1	464.508	33.55981	< 0.0001				
Residual	1010.407	73	13.8412						
Cor Total	4362.681	80							
Std. Dev.	3.720376		R-Squared	0.768398					
Mean	94.20475		Adj R-Squ	0.746189					
C.V. %	3.949244		Pred R-Sq	0.702884					
PRESS	1296.222		Adeq Prec	21.75373					
	Coefficient		**Standard**	**95% CI**	**95% CI**				
Factor	**Estimate**	**df**	**Error**	**Low**	**High**	**VIF**			
Intercept	94.20475	1	0.413375	93.3809	95.02861				
A-Receive	-0.35954	1	0.506279	-1.36855	0.649476	1			
B-Beacon	0.178981	1	0.506279	-0.83003	1.187994	1			
D-Distanc	3.441389	1	0.506279	2.432376	4.450402	1			
AB	7.886528	1	0.620063	6.650745	9.122311	1			
AD	0.071806	1	0.620063	-1.16398	1.307589	1			
BD	0.080972	1	0.620063	-1.15481	1.316755	1			
ABD	-4.39938	1	0.759419	-5.91289	-2.88586	1			
Final Equation in Terms of Coded Factors:									
	Accuracy	=							
	94.20475								
	-0.35954	* A							
	0.178981	* B							
	3.441389	* D							
	7.886528	* A * B							
	0.071806	* A * D							
	0.080972	* B * D							
	-4.39938	* A * B * D							
Final Equation in Terms of Actual Factors:									
	Accuracy	=							
	104.4934								
	-0.22918	* Receiver Horizontal Displacement							
	-0.22224	* Beacon Horizontal Displacement							
	-0.00555	* Distance							
	0.002966	* Receiver Horizontal Displacement * Beacon Horizontal Displacement							
	0.000298	* Receiver Horizontal Displacement * Distance							
	0.000299	* Beacon Horizontal Displacement * Distance							
	-3.9E-06	* Receiver Horizontal Displacement * Beacon Horizontal Displacement * Distance							

Appendix B : RFID Experiments

Table B-1: Data for Corridor area.

Tag 068	**Low Gain**																				
Distnace	Full Wrap	No Wrap	style 1	**style 2**	style 3	style 4	style 5	style 6	style 7	style 8	style 9	style 10	style 11	style 12	style 13	style 14	style 15	style 16	style 17	style 18	style 19
1	X	98.5	71.5	77	100	97.5	X	74	95	X	78	89	96.5	X	72.5	83	89.5	X	X	X	X
2	X	91.5	X	X	71	91	72	79	90.5	X	X	82	94	X	X	80.5	89	X	X	X	71
3	X	92	X	70	79.5	93	68	75.5	93	X	73.5	84.5	94.5	X	X	74	82.5	X	X	X	69
4	X	99.5	X	79	94.5	100	72	84.5	97	X	75	90.5	97.5	X	X	83.5	89.5	X	X	X	70.5
5	X	79.5	X	72	82.5	87	X	X	80	X	71	69	74.5	X	X	X	X	X	X	X	X
6	X	73.5	X	X	80	76	X	X	73.5	X	X	X	70.5	X	X	X	X	X	X	X	X
7	X	84.5	X	X	79	89.5	X	69.5	87	X	X	75.5	88	X	X	X	X	X	X	X	X
8	X	66	X	X	79.5	80.5	X	X	78.5	X	X	75.5	82	X	X	X	X	X	X	X	X
Tag 631	**Low Gain**																				
Distnace	Full Wrap	No Wrap	style 1	style 2	style 3	style 4	style 5	style 6	style 7	style 8	style 9	style 10	style 11	style 12	style 13	style 14	style 15	style 16	style 17	style 18	style 19
1	X	100	X	80	78	97.5	X	76.5	90	X	74	84	86	X	X	75	73.5	X	X	X	X
2	X	69.5	X	X	69	75	X	X	70	X	X	X	72.5	X	X	X	X	X	X	X	X
3	X	78	X	X	73.5	81.5	X	X	93.5	X	X	X	76	X	X	X	X	X	X	X	X
4	X	92	X	X	80	91	X	76	87	X	X	77.5	85.5	X	X	70	73	X	X	X	X
5	X	81.5	X	X	X	82	X	69.5	78.5	X	X	71	77	X	X	X	X	X	X	X	X
6	X	76	X	X	X	74.5	X	X	71.5	X	X	X	68	X	X	X	X	X	X	X	X
7	X	74	X	X	70	79	X	X	72.5	X	X	X	73.5	X	X	X	X	X	X	X	X
8	X	69.5	X	X	X	76	X	X	73	X	X	X	74.5	X	X	X	X	X	X	X	X
Tag 068	**High Gain**																				
Distnace	Full Wrap	No Wrap	style 1	**style 2**	style 3	style 4	style 5	style 6	style 7	style 8	style 9	style 10	style 11	style 12	style 13	style 14	style 15	style 16	style 17	style 18	style 19
1	X	109	70	**83.5**	97	98.5	71	92.5	99.5	69.5	71.5	80	89.5	X	X	71	81	X	X	69.5	73
2	X	96.5	X	**75**	88.5	95.5	72	83	93.5	72	72	78.5	89.5	X	68	76.5	84	X	X	X	X
3	X	97.5	X	**79.5**	71.5	93	X	87.5	98.5	X	69.5	79.5	98	X	X	77.5	80.5	X	X	X	X
4	X	94	X	**75**	90.5	98	71	83	94.5	X	75	86.5	98	X	70.5	71.5	86	X	X	X	X
5	X	85	X	**X**	73.5	X	X	70.5	72.5	X	71	X	80.5	X	X	X	78.5	X	X	X	X
6	X	81.5	X	**X**	72	77.5	X	X	72.5	X	68	69	X	X	X	71	68.5	X	X	X	X
7	X	93.5	X	**X**	80.5	91	X	80	89.5	X	X	72.5	92.5	X	X	70	X	X	X	X	X
8	X	82.5	X	**X**	81.5	87	X	75	83	X	X	77.5	85.5	X	X	72.5	X	X	X	X	X
Tag 631	**High Gain**																				
Distnace	Full Wrap	No Wrap	style 1	style 2	style 3	**style 4**	style 5	style 6	style 7	style 8	style 9	style 10	style 11	style 12	style 13	style 14	style 15	style 16	style 17	style 18	style 19
1	X	100	X	69.5	86	**87.5**	X	71.5	90.5	X	X	75	81.5	X	X	X	X	X	X	X	X
2	X	87.5	X	X	78.5	**85.5**	X	X	X	X	X	66	77	X	X	X	X	X	X	X	X
3	X	78	X	X	79.5	**89**	X	X	77.5	X	X	X	78	X	X	X	X	X	X	X	X
4	X	86	X	X	76	**X**	X	84.5	86.5	X	X	X	86	X	X	X	X	X	X	X	X
5	X	73	X	X	X	**X**	X	X	X	X	X	X	X	X	X	X	X	X	X	X	X
6	X	68.5	X	X	X	**X**	X	X	X	X	X	X	X	X	X	X	X	X	X	X	X
7	X	82.5	X	X	X	**X**	X	X	78.5	X	X	X	77	X	X	X	X	X	X	X	X
8	X	74	X	X	X	**X**	X	X	73.5	X	X	X	74.5	X	X	X	X	X	X	X	X

Table B-2: Data for Reception area.

Tag 068	Low Gain																				
Distnace	Full Wrap	No Wrap	style 1	style 2	style 3	style 4	style 5	style 6	style 7	style 8	style 9	style 10	style 11	style 12	style 13	style 14	style 15	style 16	style 17	style 18	style 19
1	X	91	X	84.5	82	90.5	X	83.5	82	X	73.5	79.5	85.5	X	X	69	77.5	X	X	X	X
2	X	79.5	X	77	X	78.5	X	X	70.5	X	X	X	76.5	X	X	X	69	X	X	X	X
3	X	72	X	X	X	73.5	X	X	X	X	X	X	X	X	X	X	X	X	X	X	X
4	X	73.5	X	X	73.5	75	X	70	77	X	X	X	77	X	X	X	X	X	X	X	X
5	X	88	X	X	75.5	75	X	70.5	78.5	X	X	X	83.5	X	X	X	X	X	X	X	X
6	X	72	X	X	76.5	79.5	X	68	79	X	X	X	79	X	X	X	X	X	X	X	X
7	X	86	X	X	77	87.5	X	69.5	79.5	X	X	X	88	X	X	X	X	X	X	X	X
8	X	75.5	X	X	X	X	X	X	73.5	X	X	X	74	X	X	X	X	X	X	X	X
Tag 631	Low Gain																				
Distnace	Full Wrap	No Wrap	style 1	style 2	style 3	style 4	style 5	style 6	style 7	style 8	style 9	style 10	style 11	style 12	style 13	style 14	style 15	style 16	style 17	style 18	style 19
1	X	89.5	X	74.5	80.5	88.5	X	77.5	87	X	X	70.5	84	X	X	X	75	X	X	X	X
2	X	81.5	X	70	71	84.5	X	X	79	X	X	X	75.5	X	X	X	X	X	X	X	X
3	X	70.5	X	X	X	X	X	X	X	X	X	X	X	X	X	X	X	X	X	X	X
4	X	81	X	X	74	79	X	X	71.5	X	X	X	74.5	X	X	X	X	X	X	X	X
5	X	82.5	X	X	74.5	82.5	X	X	79.5	X	X	X	76	X	X	X	X	X	X	X	X
6	X	73	X	X	X	X	X	X	X	X	X	X	X	X	X	X	X	X	X	X	X
7	X	73	X	X	X	77.5	X	X	X	X	X	X	X	X	X	X	X	X	X	X	X
8	X	X	X	X	X	X	X	X	74	X	X	X	X	X	X	X	X	X	X	X	X
Tag 068	High Gain																				
Distnace	Full Wrap	No Wrap	style 1	style 2	style 3	style 4	style 5	style 6	style 7	style 8	style 9	style 10	style 11	style 12	style 13	style 14	style 15	style 16	style 17	style 18	style 19
1	X	80.5	X	68	75.5	87	75	89.5	100	71	76	83	91	70	X	70.5	72	X	X	X	X
2	X	74.5	X	72.5	70	82	X	75	91.5	69	77.5	89.5	98.5	X	69	74	80.5	X	X	X	X
3	X	75.5	X	70	69	82.5	X	X	72.5	70.5	69	73.5	79.5	X	X	X	78	X	X	X	X
4	X	74.5	X	77.5	70.5	75.5	X	81	87.5	71	69	81.5	91.5	X	X	71.5	76	X	X	X	X
5	X	84.5	X	75	77.5	83.5	X	77.5	86.5	70	68.5	75.5	86.5	X	X	69	73	X	X	X	X
6	X	80	X	71	73	69.5	X	70	79	70	67.5	73	88	X	X	71	71	X	X	X	X
7	X	85.5	X	72	74	87	X	71.5	81	68.5	X	73.5	82.5	X	X	70.5	70.5	X	X	X	X
8	X	75	X	X	X	75.5	X	X	68.5	70	X	67	74.5	X	X	X	X	X	X	X	X
Tag 631	High Gain																				
Distnace	Full Wrap	No Wrap	style 1	style 2	style 3	style 4	style 5	style 6	style 7	style 8	style 9	style 10	style 11	style 12	style 13	style 14	style 15	style 16	style 17	style 18	style 19
1	X	84	X	X	75	82	X	X	73.5	X	X	67	76.5	X	X	X	68	X	X	X	X
2	X	75	X	X	X	76.5	X	X	X	X	X	68	79.5	X	X	X	X	X	X	X	X
3	X	69.5	X	X	X	72	X	X	X	X	X	X	69.5	X	X	X	X	X	X	X	X
4	X	76	X	X	X	X	X	X	X	X	X	X	72	X	X	X	X	X	X	X	X
5	X	76	X	X	X	X	X	X	X	X	X	X	70.5	X	X	X	X	X	X	X	X
6	X	X	X	X	X	X	X	X	X	X	X	X	73	X	X	X	X	X	X	X	X
7	X	85	X	X	X	X	X	X	X	X	X	X	70.5	X	X	X	X	X	X	X	X
8	X	X	X	X	X	X	X	X	X	X	X	X	X	X	X	X	X	X	X	X	X

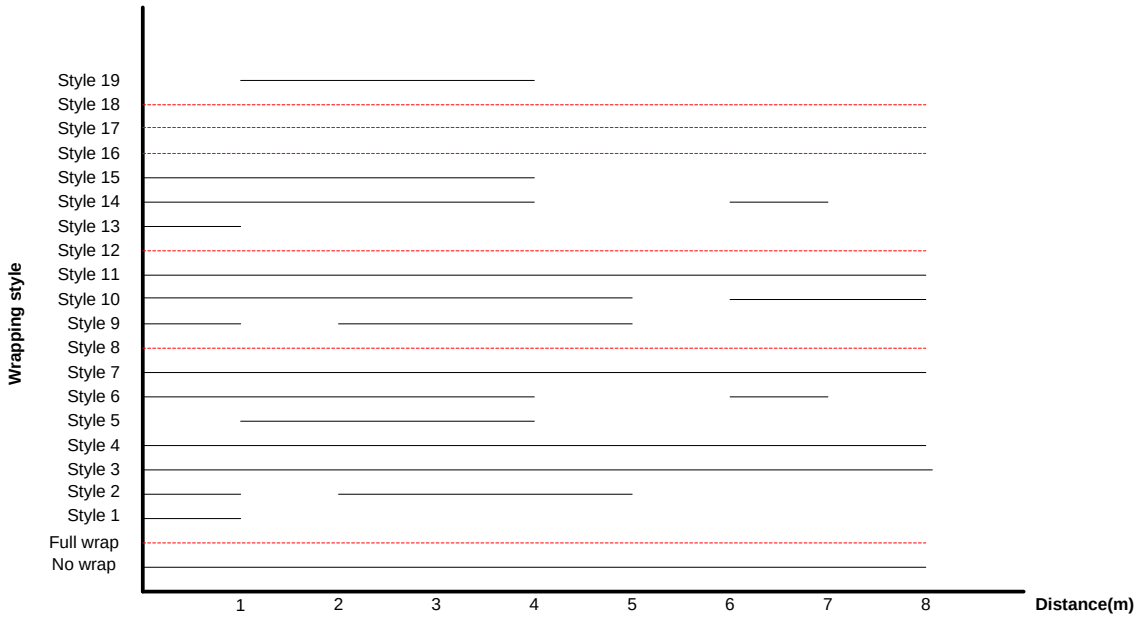

Figure B-1: Detection graph of Tag068 at Low gain mode in Corridor.

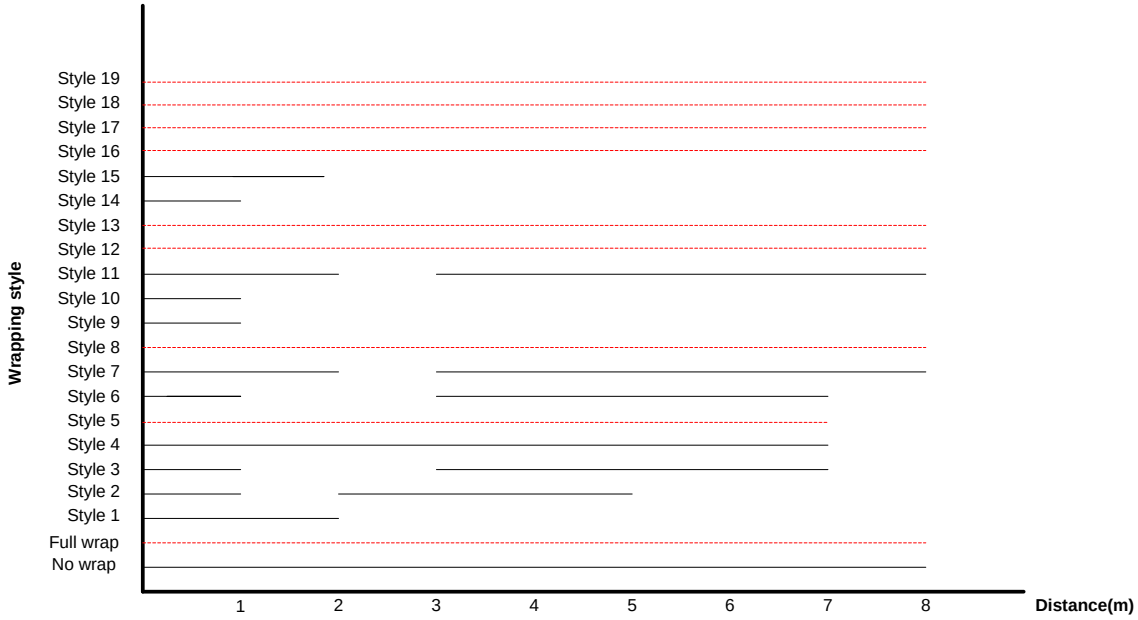

Figure B-2: Detection graph of Tag068 at Low gain mode in Reception.

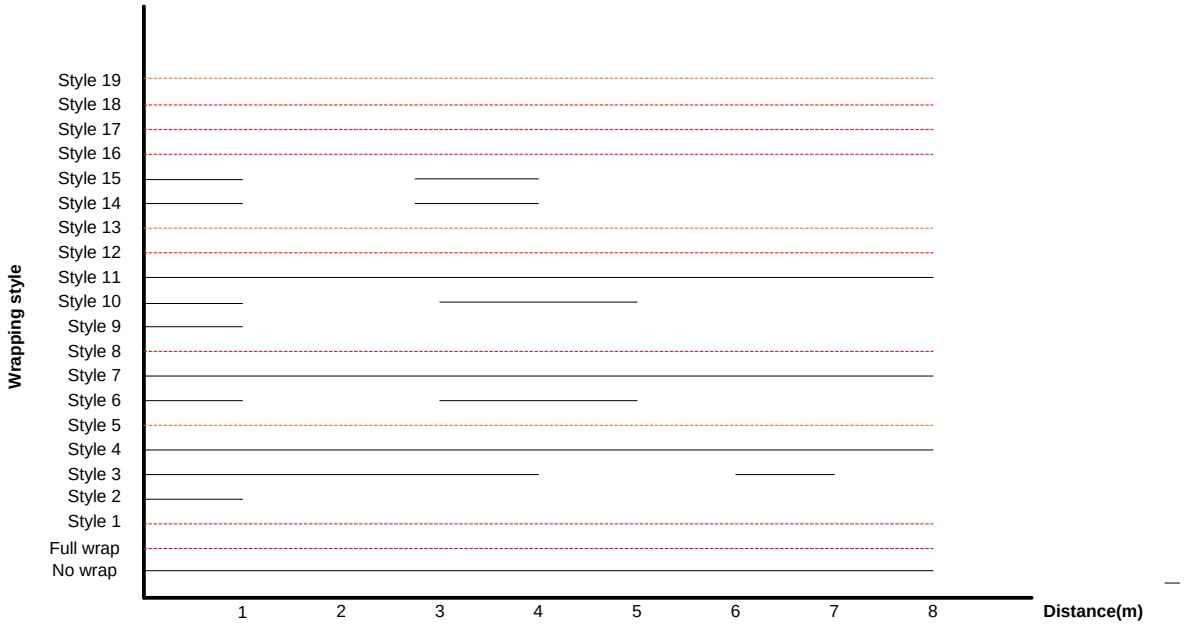

Figure B-3: Detection graph of Tag631 at Low gain mode in Corridor.

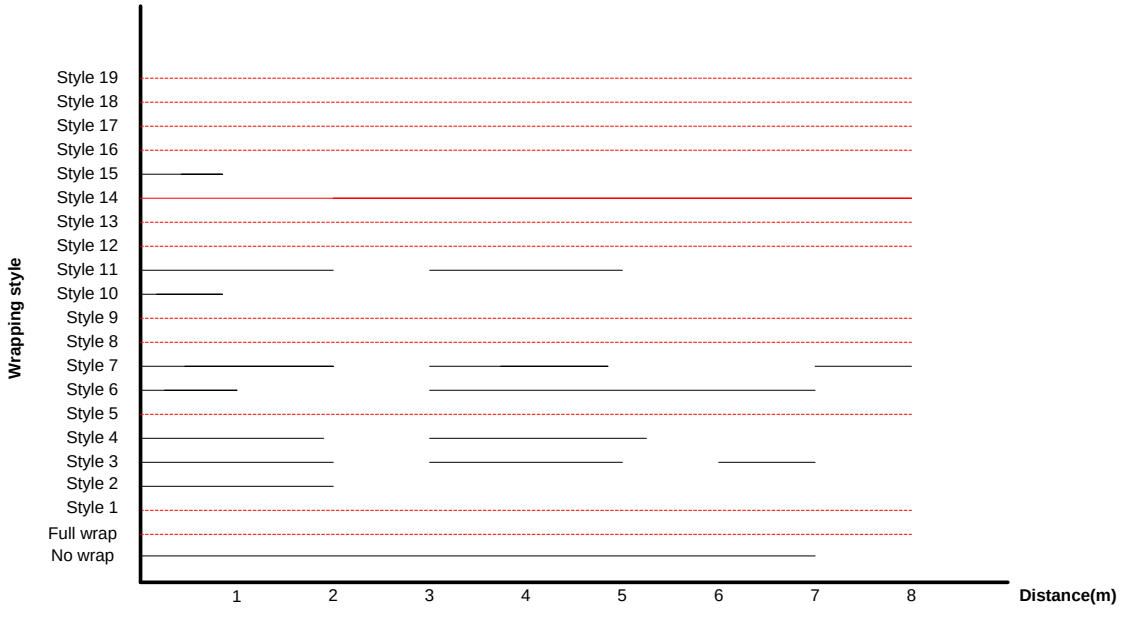

Figure B-4: Detection graph of Tag631 at Low gain mode in Reception.

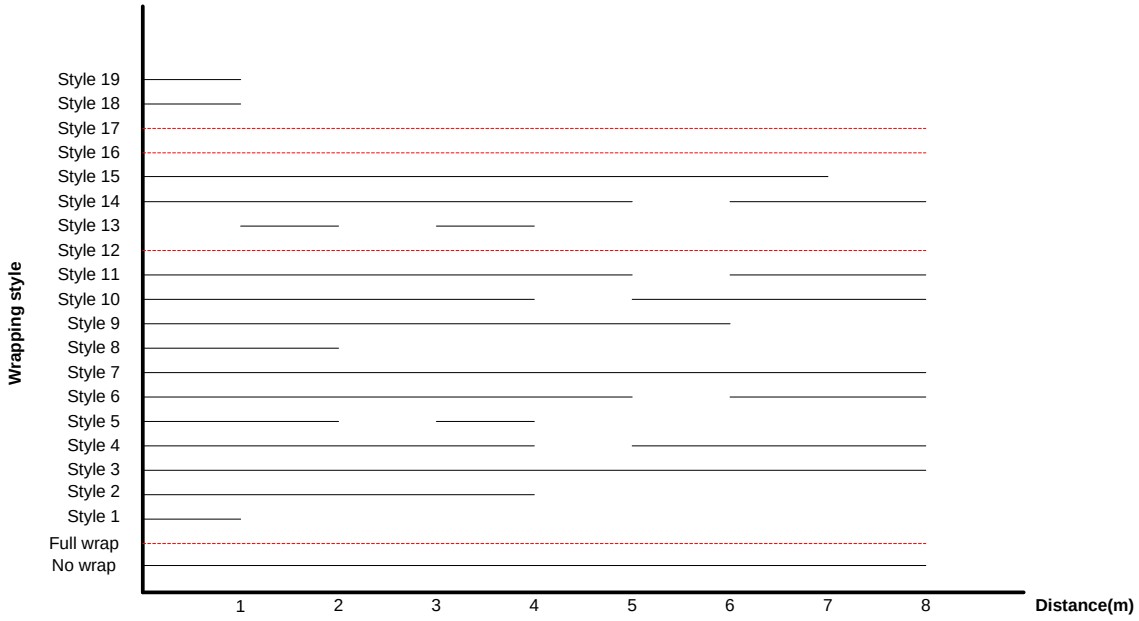

Figure B-5: Detection graph of Tag 068 at High gain mode in Corridor.

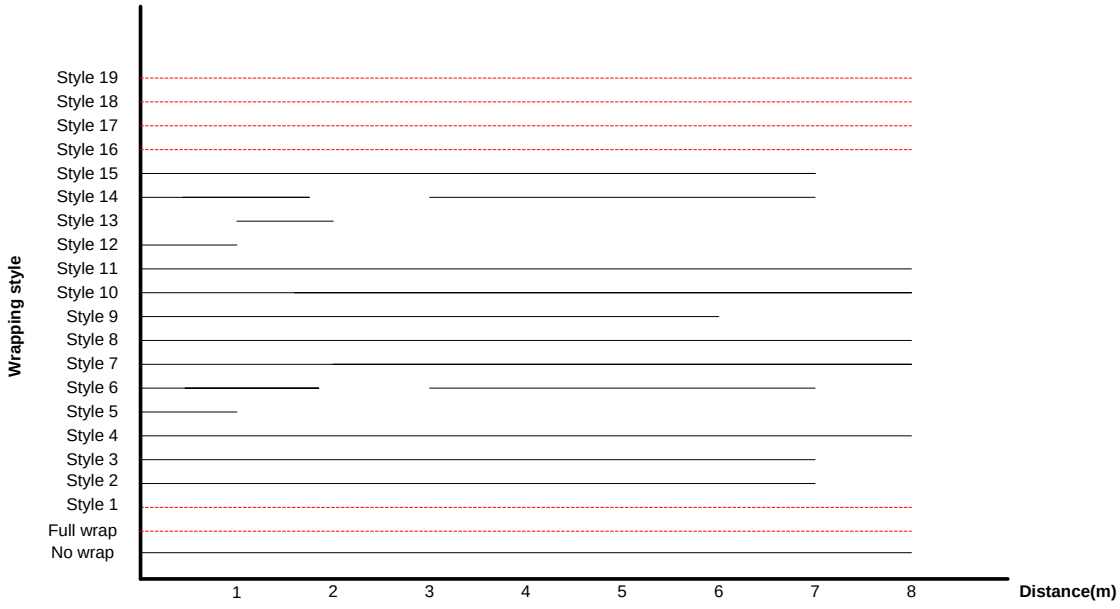

Figure B-6: Detection graph of Tag 068 at High gain mode in Reception.

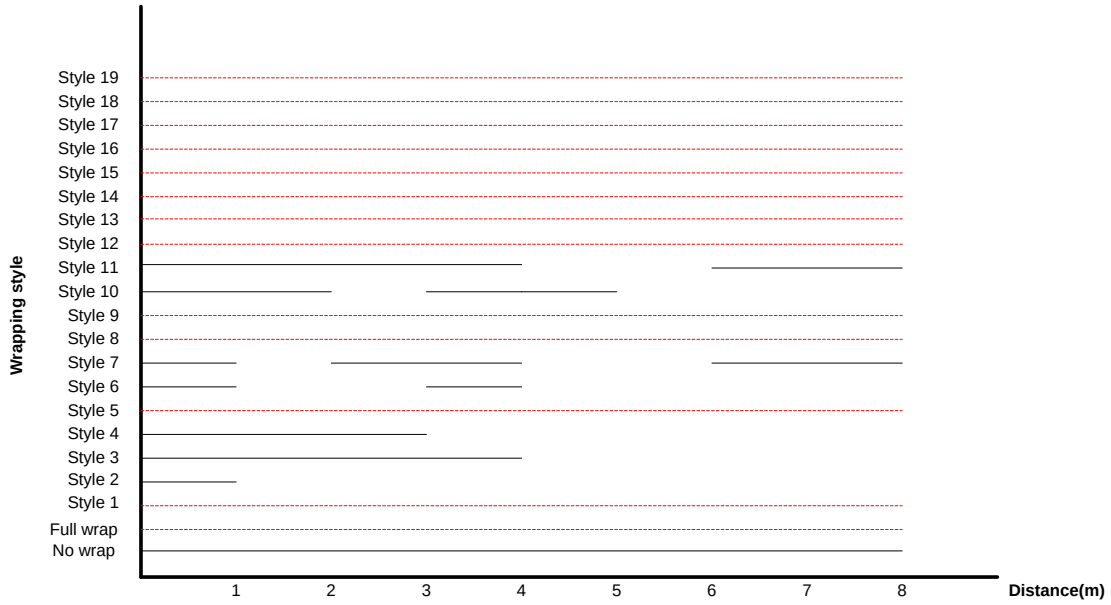

Figure B-7: Detection graph of Tag 631 at High gain mode in Corridor.

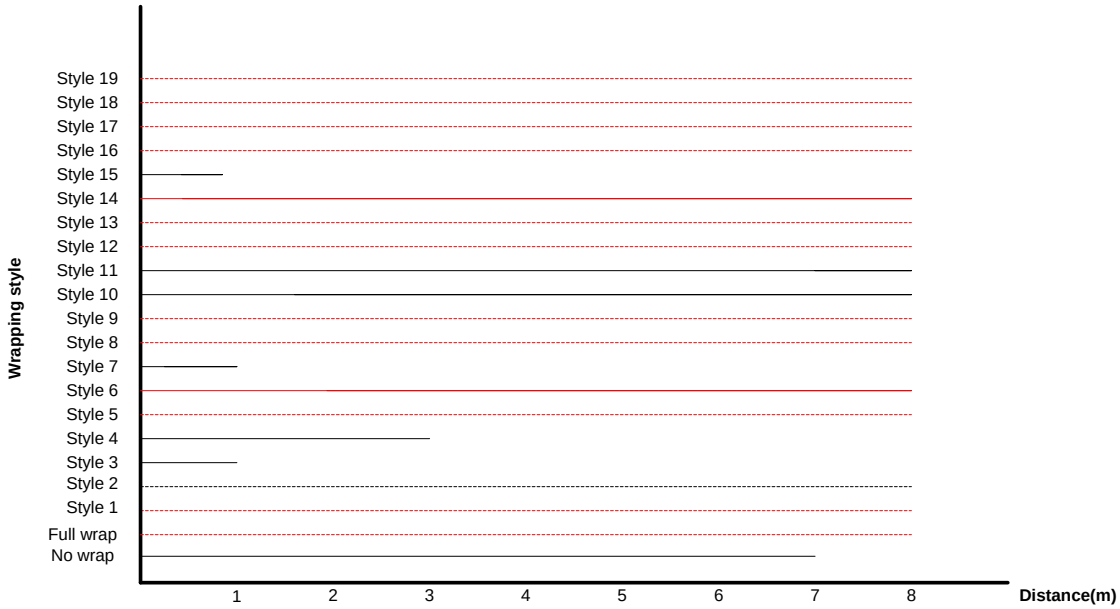

Figure B-8: Detection graph of Tag 631 at High gain mode in Reception.

Appendix C：Software Development

Table C-1：Stereo Calibration results generated in YML format.

INTRINSIC
%YAML:1.0
M1: !!opencv-matrix
rows: 3
cols: 3
dt: d
data: [1.0824975411053115e+03, 0., 381.4820352846707578, 0.,
1.0824975411053115e+03, 198.9328361324868126, 0., 0., 1.]
D1: !!opencv-matrix
rows: 1
cols: 5
dt: d
data: [-0.1629466545984846, -0.0621399735092692, 0., 0., 0.]
M2: !!opencv-matrix
rows: 3
cols: 3
dt: d
data: [1.0824975411053115e+03, 0., 392.7139953863228925, 0.,
1.0824975411053115e+03, 201.3454642100354590, 0., 0., 1.]
D2: !!opencv-matrix
rows: 1
cols: 5
dt: d
data: [-0.5562549892148734, 4.6530644908412899, 0., 0., 0.]

EXTRINSIC

%YAML:1.0
R: !!opencv-matrix
rows: 3
cols: 3
dt: d
data: [0.9999866997495215, 2.8818577239738729e-03,
-4.2772912128052794e-03, -2.9867786592157469e-03,
0.9996897166025979, -0.0247295303687394, 4.2046970522526973e-03,
0.0247419767819049, 0.9996850279501152]
T: !!opencv-matrix
rows: 3
cols: 1
dt: d
data: [20.7121422806134952, 0.0597940090725704, -1.6201716775019064]
R1: !!opencv-matrix
rows: 3
cols: 3
dt: d
data: [0.9966006411567846, 3.8207819788370640e-03,
-0.0822955871900571, -4.8429883056217114e-03, 0.9999135421885258,
-0.0122251221779957, 0.0822417625671878, 0.0125821211671762,
0.9965329812488781]
R2: !!opencv-matrix
rows: 3
cols: 3
dt: d
data: [0.9969503992606282, 2.8781021494859059e-03,
-0.0779847289031092, -1.9090249201347545e-03, 0.9999200720818275,
0.0124982027398845, 0.0780144668502491, -0.0123112134207021,
0.9968762094594199]
P1: !!opencv-matrix
rows: 3
cols: 4
dt: d
data: [1.0002795268421999e+03, 0., 471.2984352111816406, 0., 0.,
1.0002795268421999e+03, 202.7818794250488281, 0., 0., 0., 1., 0.]
P2: !!opencv-matrix
rows: 3
cols: 4
dt: d
data: [1.0002795268421999e+03, 0., 465.1339569091796875,
2.0714352348476768e+04, 0., 1.0002795268421999e+03,
202.7818794250488281, 0., 0., 0., 1., 0.]
Q: !!opencv-matrix
rows: 4
cols: 4
dt: d
data: [1., 0., 0., -471.2984352111816406, 0., 1., 0.,
-202.7818794250488281, 0., 0., 0., 1.0002795268421999e+03, 0., 0.,
0.0482892011304305, 0.2976777325895469]

Table C-2: Sci file for miGuidance.

```
<?xml version="1.0" ?>
<sci xmlns="http://www.fatronik.com/sci" version="1.0">
        <header>
                <author>IWARD</author>
                <date>2008-10-29</date>
        </header>
        <definitions type="slice">
    <![CDATA[
         #include <orca/orca.ice>
                module iward
                {
                        enum GuideEventType { lostguidedperson };

                        class GuideEvent extends orca::OrcaObject
                        {
                                GuideEventType type;
                                string eventId;
                                string result;
                        };
                };
    ]]>
        </definitions>
        <interface name="MIGuidance" module="iward" lockable="true">
                <doc>
                        Provides access to the guidance module.The guidance module doesn't
                        know where the patient will be guided to. It just increases and
                        decreases the robots velocity to keep the patient "in range
                </doc>
                <subscription type="GuideEvent" />

                <operation name="startGuidance">
                <doc>
                        This commands starts the guidance process. It's normaly initiated
                        by a person pressing the start guidance button on the touchscreen.
                        While the mission orders the navigation to reach the target of
                        guidance, the module is responsible for keeping the ordered person
                        in range.
                </doc>
                </operation>
                <operation name="stopGuidance">
                <doc>
                         This operation tells the guidance module that guidance is
                         finished (the target has been reached) or aborted. So it stops
                         controlling the robots speed and switches of the guidance
                         sensors.

                </doc>
                </operation>
        </interface>
</sci>
```

Table C-3: Sci file for basic module.

```
<?xml version="1.0" ?>
<sci xmlns="http://www.fatronik.com/sci" version="1.0">
       <header>
              <author>IWARD</author>
              <date>2008-11-12</date>
       </header>
       <definitions type="slice">
    <![CDATA[
        #include <orca/orca.ice>

  module iward
  {
    enum ModuleErrortype {MODULEHARDWARE, MODULEFILEIO, MODULESOFTWARE, MODULEOTHER};
    enum    ModuleActionRequestType    {MODULESHUTDOWN,    MODULERESET,    MODULECONTINUE,
MODULERETRY};
    enum ModuleHWtype {MODULEPORT, MODULESENSOR, MODULECAMERA, MODULEAUXDEVICE};
    enum    ModuleFILEIOtype    {MODULEFILEOPEN,    MODULEFILECLOSE,    MODULEFILEAPPEND,
MODULEFILEDELETE};

    class ModuleErrorEvent  extends orca::OrcaObject
    {
      ModuleErrortype failType;
      string errormessage;
      ModuleActionRequestType actionRequest;
    };

    class HardwareModuleErrorEvent extends ModuleErrorEvent
    {
      ModuleHWtype HWFailType;
      string HWname;
    };

    class FileIOModuleErrorEvent extends ModuleErrorEvent
    {
      ModuleFILEIOtype fileiofailtype;
      string filename;
    };

    class SoftwareModuleErrorEvent extends ModuleErrorEvent
    {
      string functionname; //Example: "CalcConeDistance()"
    };

  };
  ]]>
       </definitions>
       <interface name="BasicModule" module="iward" lockable="true">
                <doc>
               This interface must be implemented by all components providing access to
a hardware module. The               interface provides access to basic behaviour that
is required for all modules. The subscription will be              raised,  in  case  a
module dependent error occurs.
               </doc>
               <subscription type="ModuleErrorEvent" />
               <operation name="shutdown">
               <doc>
               The module is ordered to shut down
               </doc>
               <return type="int"/>
               </operation>
               <operation name="reset">
               <doc>
                      Reset the module
              </doc>
             <return type="int"/>
              </operation>
       </interface>
</sci>
```

Appendix D : Final Experiments

Table D-1: Data for the Test in the corridor in the DCU Computing Building.

Point	Time (sec)	Cricket (cm)	Stereo (cm)	Short RFID	Long RFID	RF Zone	Comments
0	1	92	224	Yes	Yes	Zone 1	*Rig at '0', no movement*
	2	95		Yes	Yes	Zone 1	
	3	101	236	Yes	Yes	Zone 1	
	4			Yes	Yes	Zone 1	*Rig started moving at Normal speed*
	5	150					
1	6		136	Yes	Yes	Zone 1	*Reached at '1', rig travelled first 2 m in 3s*
	7	121		Yes	Yes	Zone 1	*PGM instructed Normal speed*
	8	155					
	9	201	255	Yes	Yes	Zone 1	
	10			Yes	Yes	Zone 1	*Pedestrians cross; Normal Speed*
	11						
2	12			No	Yes	Zone2	*Rig reached at '2'; moving with Normal Speed*
	13				Yes	Zone2	*PGM instructed Slow speed; Follower in Zone 2*
	14			No	Yes	Zone 2	
	15			No	Yes	Zone 2	
	16	405		Yes	Yes	Zone 1	*PGM instructed slow speed; RFID Tag Error*
	17	390	445	Yes	Yes	zone1	
	18			Yes	Yes	Zone 1	
3	19	301	365				*Rig reached at '3';Normal speed*
	20	290					
	21	275		Yes	Yes	Zone 1	*Rig stopped for obstacle*
	22	225					
	23	190		yes	yes	Zone 1	
	24	210					*Rig started moving around obstacle*
	25			yes	yes	Zone 1	
	26	222		yes	yes	Zone 1	
	27	228		yes	yes	Zone 1	
	28	180					*Rig straight again*
	29	160		yes	yes	Zone 1	
	30	184	216				
	31	191		yes	yes	Zone 1	
4	32	185	235	yes	yes	Zone 1	*Rig reached at '4'*
	33	215		yes	yes	Zone 1	*Started cornering*
	34	225		yes	yes	Zone 1	
	35			yes	yes	Zone 1	
	36						
5	37	174		yes	yes	Zone 1	*Rig finished cornering and reached at '5'*
	38						
	39	185	212	yes	yes	Zone 1	
	40	290	331	yes	yes	Zone 1	
	41	191		yes	yes	Zone 1	
	42						
6	43	121	191	yes	yes	Zone 1	*Rig reached at '6'*

Table D-2: Data for the Test in Reception Area in the DCU Engineering Building.

Point	Time (sec)	Cricket (cm)	Stereo (cm)	Short RFID	Long RFID	RF Zone	Comments
0	1	110		Yes	Yes	Zone 1	*Rig at '0', no movement*
	2		131	Yes	Yes	Zone 1	
	3	109		Yes	Yes	Zone 1	*Rig started moving at Normal speed*
	4	211		Yes	Yes	Zone 1	
	5		345	Yes	Yes	Zone 1	
1	6	407		Yes	Yes	Zone 1	*Rig reached at '1';PGM instructed Slow speed*
	7	*449*		Yes	Yes	Zone 1	
	8			No	Yes	Zone 2	
	9	*556*		No	Yes	Zone 2	PGM instructed Slow speed
	10	*605*		No	Yes	Zone 2	
	11			No	Yes	Zone 2	
2	12	*697*		No	No		PGM instructed to STOP
	13			No	No		
	14	*712*		No	No		
	15	*649*		No	Yes	Zone 2	PGM detected again
	16			No	Yes	Zone 2	PGM instructed Slow speed
	17	*472*		Yes	No	Zone 1	
3	18	*398*		Yes	Yes	Zone 1	Rig reached at '3'; Normal speed
	19			No	Yes	Zone 1	Robot turning right
	20			No	Yes	Zone 2	
4	21						Finished turning
	22				Yes	Zone 2	PGM instructed to go slow
	23						
	24						
	25						PGM instructed to stop
	26						
	27						
	28						
	29						
	30						PGM raised an even; Follower lost

Table D-3: Data for the Test in Reception Area in the DCU Nursing Building.

Point	Time (sec)	Cricket (cm)	Stereo (cm)	Short RFID	Long RFID	RF Zone	Comments
0	1	90		Yes	Yes	Zone 1	*Rig at '0', no movement*
	2	111	136	Yes	Yes	Zone 1	
	3						
	4	116	145	Yes	Yes	Zone 1	
	5	171		Yes	Yes	Zone 1	*Rig started moving at Normal speed*
	6			Yes	Yes	Zone 1	
	7	229	274				
	8			Yes	Yes	Zone 1	
	9	262	311				
	10			Yes	Yes	Zone 1	
1	11	255					*Reached at '1',started turning left*
	12			Yes	Yes	Zone 1	
	13						
	14			Yes	Yes	Zone 1	
2	15						*Finished cornering, reached at '2'*
	16			No	Yes	Zone 2	
	17						
	18	551		No	Yes	Zone 2	
	19			No	Yes	Zone 2	*Reached at '3';*
	20	475					
	21						
	22	380		Yes	Yes	Zone 1	
3	23		*402*	Yes	Yes	Zone 1	
	24	312		Yes	Yes	Zone 1	
	25			Yes	Yes	Zone 1	
	26	285	327	Yes	Yes	Zone 1	*Rig stopped*
	27						
	28	180		Yes	Yes	Zone 1	
	29	165	191	Yes	Yes	Zone 1	
	30			Yes	Yes	Zone 1	*Rig started again*
	31	154		Yes	Yes	Zone 1	
	32	181	210				
	33			Yes	Yes	Zone 1	
4	34						*Rig reached at '4'*
	35			Yes	Yes	Zone 1	
	36			Yes	Yes	Zone 1	
5	37			Yes	Yes	Zone 1	*Rig finish cornering and reached at '5'*
	38	251	310	Yes	Yes	Zone	

						1	
	39	232					
	40	275		Yes	Yes	Zone 1	
	41	321	391	Yes	Yes	Zone 1	
6	42	385		Yes	Yes	Zone 1	*Rig reached at '6'*

Glossary

A

AC Alternating Current

Adj R-Squared Adjusted R-Squared (Adj R-Squared)

AOA Angle of Arrival

ARC Agent-Oriented Robot Control

C

cm Centimeter

CPU Central Processing Unit

CW Continuous Wave

D

DCU Dublin City University

DOA Direction of Arrivals

DOE Design of Experiment

DR Dead Reckoning

E

EBGM Elastic Bunch Graph Matching

EC European Commission

EF electric field

ELF Electronic Luggage Follower

EU European Union

F

FOV Field of View

fps Frame Per Second

FP6 Sixth Framework Programme

FSRs Force Sensing Resistors

G

gm gram

GND Ground

GRGP Guide Robot for Guests and Patients

GUI Graphical User Interface

H

HF High Frequency

HMMs Hidden Markov models

HoG Histograms of Oriented Gradients

HRI Human-Robot Interface

HWManager Hardware Manager

I

ICE Internet Communications Engine

ID Identification

IMU Inertial Measurement Unit

IP Internet Protocol (IP)

IR Infrared

IWARD Intelligent Robot Swarm for Attendance, Recognition, Cleaning and Delivery

J

JPDAF Joint Probabilistic Data Association Filter

L

LED Light-emitting diode

LF Low Frequency

LOS Line-of Sight

Ltd. Limited

M

m Meter

MC Mission Controller

MCMC Markov Chain Monte Carlo method

MEMS Microelectromechanical systems

MIT Massachusetts Institute of Technology

MHT Multiple Hypothesis Tracking

MS Mercury Switch

P

PCA Principal Component Analysis

PC Personal Computer

PDA Personal digital assistant (PDA)

PGM Person Guidance Module

PIR (Passive Infra-Red)

Pred R-Squared Predicted R-squared
Prob Probability

R

RF Radio Frequency
RFID Radio-frequency identification
ROI Region of Interest
RPC Remote Procedure Call
RSS Received Signal Strength
RSS Radio Signal Strength
RSS Relative Signal Strength
RSSI Received Signal Strength Indicator
RTI Radio Tomographic Imaging
RTS Ready to send

S

s Second
SCI Simple Component Interface
SIFT Scale-invariant feature transform
Slice Specification Language for Ice
SSR Solid State Relay

T

TDOA Time Delay of Arrival
TOA Time of Arrival

U

UHF Ultra High Frequency
UK United Kingdom
UKF Unscented Kalman Filter
UNB Ultra-narrowband
US Ultrasound
USB Universal Serial Bus
UWB Ultra Wideband

W

WHO World Health Organization
WLAN Wireless Local Area Network

X

XML Extensible Markup Language

Z

ZUPT Zero Velocity Update